Aston University

Some pages of this thesis may have been removed for copyright restrictions.

If you have discovered material in Aston Research Explorer which is unlawful e.g. breaches copyright, (either yours or that of a third party) or any other law, including but not limited to those relating to patent, trademark, confidentiality, data protection, obscenity, defamation, libel, then please read our Takedown policy and contact the service immediately (openaccess@aston.ac.uk)

DEVELOPMENT OF A CONCEPTUAL MODEL OF THE SOIL-MOISTURE-PLANT SUB-SYSTEM OF THE HYDROLOGICAL CYCLE

VOL 1

DARRYN ANDREW EVANS

Doctor of Philosophy

THE UNIVERSITY OF ASTON IN BIRMINGHAM

October 1990

The copy of the thesis has been supplied on condition that anyone who consults it is understood to recognise that its copyright rests with its author and that no quotation from the thesis and no information derived from it may be published without the author's prior, written consent.

The University of Aston in Birmingham

DEVELOPMENT OF A CONCEPTUAL MODEL OF THE SOIL-MOISTURE-PLANT SUB-SYSTEM OF THE HYDROLOGICAL CYCLE

DARRYN ANDREW EVANS

Doctor of Philosophy
1990

SUMMARY

The soil-plant-moisture subsystem is an important component of the hydrological cycle. Over the last 20 or so years a number of computer models of varying complexity have represented this subsystem with differing degrees of success. The aim of this present work has been to improve and extend an existing model.

The new model is less site specific than the existing model thus allowing for the simulation of a wide range of soil types and profiles. Several processes, not included in the original model, are simulated by the inclusion of new algorithms, including: macropore flow; hysteresis and plant growth. Changes have also been made to the infiltration, water uptake and water flow algorithms.

Using field data from various sources, regression equations have been derived which relate parameters in the suction-conductivity-moisture content relationships to easily measured soil properties such as particle-size distribution data. Independent tests have been performed on laboratory data produced at Aston University. The parameters found by regression anaysis for the suction relationships were then used in equations describing the infiltration and macropore processes.

An extensive literature review produced a new model for calculating plant growth from actual transpiration, which was itself partly determined by the root densities and leaf area indices derived by the plant growth model. The new infiltration model uses intensity/duration curves to disaggregate daily rainfall inputs into hourly amounts.

The final model has been calibrated and tested against field data, and its performance compared to that of the original model. Simulations have also been carried out to investigate the effects of various parameters on infiltration, macropore flow, actual transpiration and plant growth. Qualitatively comparisons have been made between these results and data given in the literature.

Keywords:-
Soil Moisture, Crop Growth, Hydrological Modelling, Irrigation Monitoring, Simulation

ACKNOWLEDGEMENTS

I would like to express my sincere gratitude to my supervisor, Mr W J Walley, for his advice and guidance throughout the project.

I would also like to thank the following members of the Department of Civil Engineering for their assistance: Dr J Elgy, Dr D Just, Mr D Hall, Mr R Neale and Mr T Hewings and special thanks to Dr P D Hedges whose door seems eternally open for advice both professionally and personally.

My final thanks are reserved for my friends and colleagues who have helped me in accomplishing this goal these include Mike, various Pauls, Andy, Denis, Fungus, Cormac, Martin, Brian, Jane, Nicky, Guiness and Bass to name but a few. Special thanks are also due to Cimar the inspiration behind me doing a PhD.

CONTENTS

Volume 1

List of Tables 9

List of Figures 13

Notations 20

1. INTRODUCTION 25

1.1 Origins of the Project 26

1.2 Aims and Objectives 27

1.3 Structure of the Thesis 29

2. SOIL-MOISTURE-PLANT MODELS 31

2.1 Introduction 31

2.2 Models 32

2.2.1 MORECS 32

2.2.2 SPAW 34

2.2.3 SWATR 37

2.3 Hussein's Model 38

2.3.1 Structure of the Model 39

2.3.2 Plant Factors 41

2.3.3 Soil Factors 42

2.3.4 Hydrometeorological Factors 44

2.3.5 Model Applications 45

2.4 Conclusion 46

3. SOIL PROCESSES 48

3.1 Introduction 48

3.2 Movement of Water in the Unsaturated Zone 48

3.2.1 Suction 54

3.2.1.1 Equations Describing the Moisture Characteristic Curve 55

3.2.1.2 Genuchten's Equation 57

3.2.2 Conductivity 81

3.2.3 Soil Water Movement Equations 88

3.3 Infiltration 94

3.3.1 Factors Affecting Infiltration 95

3.3.2 The Infiltration Model 101

3.4 Macropores 106

3.4.1 Macropore Formation and Characteristics 107

3.4.2 Flow in Macropores 109

3.4.3 Macropore Model 110

3.5 Summary 117

4. PLANT FACTORS 118

4.1 Introduction 118

4.2 Plant Growth 119

4.2.1 General 119

4.2.2 Roots and Root Growth 123

4.2.3 Above Ground Development 127

4.2.4 Plant Growth Model 127

4.3 Plant Water Uptake 137
4.3.1 General 137
4.3.2 Plant Water Uptake Model 141
4.4 Summary 144

5. ATMOSPHERIC PROCESSES 145
5.1 Introduction 145
5.2 Rainfall 145
5.3 Evaporation 157
5.4 Summary 159

6. THE SOIL-MOISTURE-PLANT MODEL 160
6.1 Introduction 160
6.2 Model Structure 160
6.3 Model Operation and Program 163
6.4 Input Algorithms 170
6.5 Determination of the Timestep 175
6.6 Rainfall Algorithms 177
6.7 Infiltration Algorithms 177
6.8 Macropores 181
6.9 Percolation 184
6.10 Plant Routines 190
6.11 Summary 190

7. THE SOIL-MOISTURE-PLANT MODEL SIMULATIONS 191
7.1 Testing the Soil-Moisture-Plant Model 192
7.1.1 Model Input Data 192
7.1.1.1 Hussein's Data 192

7.1.1.2 Additional Data Required 195
7.1.2 Determination of the Parameter Values 200
7.1.3 Results and Discussion 206
7.2 Plant Water Uptake 225
7.2.1 Spreadsheet Analysis 226
7.2.2 Simulation Analysis 234
7.2.3 Conclusions 244
7.3 Infiltration 245
7.3.1 Method 246
7.3.2 Results and Discussion 247
7.4 Plant Growth 267
7.4.1 Method 267
7.4.2 Results 270
7.4.3 Discussion 286
7.5 Summary 292

8. CONCLUSIONS 294
8.1 Objectives 295
8.2 Further Work 303
8.3 Summation 305

REFERENCES 306

Volume 2

APPENDIX 1 USDA-SCS Particle-Size Ranges 333

APPENDIX 2 Program Listings 334

APPENDIX 3 Input Data 408

LIST OF TABLES

3.1 Descriptive Statistics of Soil Properties 63

a) SCS-USDA (1974)

b) Cassel (1974)

c) Long et al (1969)

3.2 Correlation Coefficients Achieved Between Individual Soil Properties and the Parameters of Genuchten's Equation 69

a) SCS-USDA (1974)

b) Cassel (1974)

c) Long et al (1969)

3.3 Correlation Coefficients for Several Soil Properties for Bar 15 and Bar 1/3 From SCS-USDA (1974) and Long et al (1969) 74

3.4 Multiple Regression Coefficients to Determine Parameters a and n from SCS-USDA (1974) 74

3.5 Multiple Regression Coefficients to Determine Bar 15 and Bar 1/3 Moisture Content Values from SCS-USDA (1974) and Long et al (1969) 75

3.6 Correlation Between Experimental Moisture Contents (Hedges 1990) and Calculated Moisture Contents Using Tables 3.4 and 3.5 75

3.7 Comparison of the Parameter a obtained for the Drying (a_d) and Wetting (a_w) Curves for Several Soils Obtained from Mualem (1976b) 79

3.8 Correlation Coefficients for Calculated K and Observed K for 5 Soils Given by Mualem (1976b) 87

3.9 Correlation Coefficients for Calculated and Observed Drainage Rates from Nine Soil Columns (Hedges 1990) 87

4.1 Differences Between Monocotyledons and Dicotyledons 121

5.1 Example of Rainfall Data Obtained from the Tipping Bucket Rain Gauges 148

5.2 Summary of Site Data Acquired from STWA PDL5 Tipping Bucket (0.5mm) Rain Gauges 149

5.3 Summary of Size of Rainfall Events for 6 Sites Acquired from STWA PDL5 Tipping Bucket (0.5mm) Rain Gauges 150

5.4 Rainfall Event Data for Days of 20mm or More 152

5.5 Correlation Values Obtained Between Rain Magnitude and the Intensity/Duration Equation 154

Parameters a,b and c

7.1 Results of Analysis of Soils from Preston Vale Farm 198

7.2 Calibration Equations Derived for Aston's Neutron Probe 198

7.3 Model Parameter Values not Determined by Calibration 205

7.4 Model Parameter Values Determined by Calibration 205

7.5 Particle-Size (%), Bulk Density (g/cc) and Saturated Moisture Content (cc/cc) for the 20 Soils Used in the Evapotranspiration Simulations 227

7.6 Upward Moisture Movement for Several Soils and Evaporative Demands Produced by Evapotranspiration Simulations 239

7.7 Upward Moisture Movement for Soil 15 240

7.8 Particle-Size (%), Bulk Density (g/cc) and Saturated Moisture Content (cc/cc) for the 5 Soils Used in the Infiltration Simulations 248

7.9 Initial Conditions for the 21 Simulations Run for Infiltration Model 249

7.10 Summary of the Ten Irrigation Simulations. Particle-Size (%), Bulk Density (g/cc) and Saturated Moisture Content (cc/cc) for the Soil Used in the Irrigation Simulations. Initial Plant and Soil Conditions are Also Given as well as Irrigation Frequencies and Amounts 271

7.11 Potential and Actual Water Use Results From Irrigation Simulations 273

LIST OF FIGURES

2.1 Computational Sequence of the SPAW Model 35

2.2 Structure of Hussein's Model 40

3.1 The Soil Moisture Characteristic Curve 52

3.2 Soil Moisture Characteristic Curve Showing Significance of Genuchten's Equation Parameters 52

3.3 Comparison of Curves Obtained by Fitting the Parameter tr or Determining it Statistically from Table 3.3 67

3.4 Comparison of Calculated Moisture Contents to Experimentally Derived Values for Soil Columns from Hedges (1989). 77

3.5 Comparison of Calculated Conductivity-Moisture Content Values with those Observed by Mualem (1976b) for Silt Mont Cenis 85

3.6 Comparison of Calculated Conductivity-Moisture Content Values with those Observed by Mualem (1976b) for Several Soils 86

3.7 Flow Diagram of the Model Simulating Drainage from Soil Columns 90

3.8 Comparison of Calculated Drainage Rates to Observed (Hedges 1989) Rates for Several Soil Columns 92

3.9 'Typical' Infiltration Rate Curve 98

3.10 Movement of a Wetting Front Down the Profile 98

4.1 Differences betweem Monocotyledons and Dicotyledons 121

4.2 The Plant Model Parameter Determination Curves 132

a) Growth Units/Potential Transpiration

b) Partitioning of Growth Units to LAI

c) Actual LAI/Potential LAI

5.1 Values of Curve Parameters Obtained Against Daily Rainfall Amount 155

a) Parameter a

b) Parameter b

c) Parameter c

d) Daily Rainfall Duration (hrs) for Particular Rain Magnitudes

5.2 Intensity Duration Curves Formulated for After Each Daily Rainfall Class 156

6.1 Structure of Soil-Moisture-Plant Model 162

a) Without Wetting Fronts

b) With Wetting Fronts

6.2 Flowchart of Soil-Moisture-Plant Model 164

6.3 Flowchart for Varying Timestep 169

6.4 Flowchart for Infiltration Subroutine 179

6.5 Flowchart for Macropore Routines 182

6.6 a) Flowchart for Percolation Subroutine 185

b) Flowchart of Redist-Percolation Subroutine 186

7.1 Location Maps 193

a) Preston Vale Farm

b) Location of Probe Tubes at Preston Vale Farm

7.2 Apparatus for Determining Saturated Conductivity 199

7.3 Calculated Suction-Moisture Content Curves for Soils at Preston Vale Farm 201

7.4 Calculated Relative Conductivity-Moisture Content Curves for Soils at Preston Vale Farm 201

7.5 Calculated and Observed Soil Moisture Deficits for each Soil Layer 207

7.6 Calculated and Observed Total Soil Moisture Deficit 208

7.7 Water Uptake From Each Layer 215

7.8 Calculated and Observed Soil Moisture Deficit for each Soil Layer when Surface Layer Ks =0.5E-05 218

7.9 Calculated and Observed Soil Moisture Deficit for each Soil Layer when Surface Layer Ks =0.5E-06 219

7.10 Comparison of Calculated Soil Moisture Deficits for each layer from the New Model to Hussein's (1979) Model 221

7.11 Comparison of the Calculated Total Soil Moisture Deficit from the New Model to Hussein's (1979) Model 224

7.12 Relative Transpiration/Soil Suction for a Fine Soil 229

7.13 Relative Transpiration/Soil Suction for a Coarse Soil 229

7.14 The Effect of Increasing 'n' on Relative Transpiration/Soil Suction for Soil No. 14 231

a) n =1.0

b) n =5.0

7.15 The Effect of Increasing 'a' on Relative Transpiration/Soil Suction for Soil No. 14 232

a) a =0.0001

b) a =0.1

7.16 The Effect of Increasing 'tr' on Relative Transpiration/Soil Suction for Soil No. 14 233

a) tr =0.01

b) tr =0.15

7.17 Fall in Actual Evaporation Rate with Time for Several Potential Evaporation Rates 236

a) Soil No. 5

b) Soil No. 18

7.18 Decline from the Relative Transpiration Rate with Time for Several Potential Rates 237

a) Soil No. 5

b) Soil No. 18

7.19 Decline from Potential Rate Over Time for Several Potential Rates in a Soil with Limited Capillary-Rise 240

a) Transpiration Rate

b) Relative Transpiration Rate

7.20 The Effect of Increasing Root Density on the 242

Transpiration Rate for Soil No. 17

7.21 The Effect of Decreasing Root Density on the Transpiration Rate for Soil No. 17 243

7.22 Infiltration Characteristics of Soil No. 19 251

a) Depth of Ponding

b) Depth of Wetting Front

c) Infiltration Rate Over Time

d) Cumulative Infiltration Rate Over Time

7.23 Infiltration Characteristics of Soils 1-3 254

a) Depth of Ponding

b) Depth of Wetting Front

c) Infiltration Rate Over Time

d) Cumulative Infiltration Rate Over Time

7.24 Infiltration Characteristics of Soil No. 7 255

a) Depth of Ponding

b) Depth of Wetting Front

c) Infiltration Rate Over Time

d) Cumulative Infiltration Rate Over Time

7.25 Infiltration Characteristics of Soils 20 & 21 257

a) Depth of Ponding

b) Depth of Wetting Front

c) Infiltration Rate Over Time

d) Cumulative Infiltration Over Time

7.26 Infiltration Characteristics of Soils 8 & 9 258

a) Depth of Ponding

b) Depth of Wetting Front

7.27 Effect of Macropores on Infiltration Characteristics for Soils 11 & 12 259

a) Depth of Wetting Front

b) Infiltration Rate Over Time

c) Cumulative Infiltration Rate Over Time

7.28 Infiltration Rates for Soils 8 & 9 261

a) Soils 8 & 9

b) Soil 9

7.29 Effect of Macropores on Infiltration 262

Characteristics for Soils 13-15

a) Total Infiltration Rate Over Time

b) Infiltration Rates Over Time for Soil 13

c) Infiltration Rates Over Time for Soil 14

d) Infiltration Rates Over Time for Soil 15

e) Depth of Ponding

f) Depth of Wetting Front

g) Total Cumulative Infiltration Over Time

7.30 Effect of Macropores on Infiltration 265

Characteristics for Soils 16-18

a) Total Infiltration Rates Over Time

b) Infiltration Rates Over Time for Soil 16

c) Infiltration Rates Over Time for Soil 17

d) Infiltration Rates Over Time for Soil 18

e) Depth of Ponding

f) Depth of Wetting Front

g) Total Cumulative Infiltration

7.31 Growth Unit Partitioning Curves for Plant A & B 274

7.32 Water Uptake Over Time for Plant A 276

a) Run No. 2 T7

b) Run No. 7 T7

7.33 Water Uptake Over Time for Plant B 277

a) Run No. 5 T7

b) Run No. 9 T7

7.34 The Effect of Plant Strategy and Evaporative 279
Demand Rate on Relative Transpiration Curves

a) Run No. 1 T0

b) Run No. 4 T0

c) Run No. 9 T0

7.35 The Effect of a Number of Factors on Water 280
Uptake from Different Layers

a) The Effect of the Amount of the Irrigation Application (Run 1 T7 & Run 3 T7)

b) The Effect of Irrigation Frequency (Run 2 T7 & Run 2 T14)

c) The Effect of Plant Strategy (Run 2 T14 & Run 5 T14)

7.36 The Effect of the Amount of the Evaporative 287
Demand on the Depth of the Water Table

a) Run No. 3

b) Run No. 8

7.37 The Effect of the Amount of the Evaporative 288
Demand on the Leaf Area Index

a) Run No. 1

b) Run No. 8

LIST OF NOTATIONS

a	1) dimensionless empirical parameter used in Genchten's suction equation (equation 3.3).	
	2) dimensionless empirical parameter denoting the maximum possible number of growth units	
	3) dimensionless empirical parameter	
A	area	cm^2
a1	dimensionless empirical parameter	
actlai	actual leaf area index	
a_d	value of parameter a in Genuchten's suction equation for the drying curve	
a_n	number of macropores for group n	m^2
a_t	total number of macropores	m^2
a_w	value of parameter a in Genuchten's suction equation for the wetting curve	
AT	actual transpiration	cm
b	dimensionless empirical parameter	
b1	dimensionless empirical parameter	
b2	dimensionless empirical parameter	
c	1) clay content	(%)
	2) dimensionless empirical parameter	
Cg	dimensionless empirical parameter partitioning root growth between layers	
Cp	fraction of growth units partitioned to the leaves	
Cr	fraction of growth units partitioned to the	

	roots	
D	depth of layer	cm
dayno	number of days since the plant emerged	
dgl	thickness of the basal soil layer	cm
d_n	layer into which macropores of class n extend	
dwt	distance from the top of the base layer down to the water table	
e	porosity	(%)
ED	potential evaporative demand	cm d^{-1}
EDS	potential evaporative demand from the soil	cm d^{-1}
ES	actual soil evaporation	cm d^{-1}
emerg	number of days after the start of the simulation before the plant emerges	
f	matching factor for determining conductivity	cm s^{-1}
F	infiltration rate	cm s^{-1}
Fa	sum of water infiltrated	cm
Fs	water depth infiltrated before ponding occurs	cm
Gr	plant growth units (dimensionless)	
h	suction	cm
harv	number of days from the start of the simulation to the crop's harvest	
h_b	suction at air entry as used by Brooks and Corey	cm
Hf	suction at the wetting front	cm
I	rainfall intensity	cm s^{-1}

K	unsaturated conductivity	cm s^{-1}
Kf	conductivity within the wetting front	cm s^{-1}
Kr	relative conductivity (dimensionless)	
Ks	saturated conductivity	cm s^{-1}
L	1) length of wetting front	cm
	2) length	cm
	3) dimensionless empirical parameter	
LAI	leaf area index -the fraction of the ground surface covered by the leaves.	
Lc	empirical parameter converts Gr into increased leaf area index	
Lp	increase in root density in a soil layer	
m	dimensionless empirical parameter used in Genuchten's suction equation	
m1	dimensionless empirical parameter	
maxlai	maximum possibe leaf area index	
Md	moisture difference across the wetting front	cm^3 cm^{-3}
mr	minimum fraction of growth units allocated to the leaves	
Mr	maximum fraction of growth units allocated to the leaves	
n	1) dimensionless empirical parameter used in Genuchten's suction equation	
	2) dimensionless empirical parameter	
n1	dimensionless empirical parameter	
p_b	dry bulk density	g/cc
potlai	potential leaf area index	

Pn	surface area of the nth macropore class	(%)
PR	plant resistance	d^{-1}
p_s	particle density	g/cc
PT	potential transpiration	cm
q	pore-size distribution index used in the Brooks and Corey suction equation (dimensionless)	
r	radius of macropore channel	cm
R	rainfall	mm hr^{-1}
Rc	empirical parameter converts Gr into additional root density	cm cm^{-1}
Rcrit	the amount of rainfall needed before the total distributed hourly by the intensity/ duration curve method.	
Rd	root density	cm cm^{-1}
rgrow	total increase in root density	cm cm^{-1}
Rt	total daily rainfall	mm
Rw	radius of macropore wetting front minus the radius of the macropore	cm
s	soil shrinkage	(%)
S	plant stress index	
Sc	leaf crown suction	cm
Sca	actual leaf crown suction	cm
Scp	potential leaf crown suction	cm
Se	relative moisture content	cm^3 cm^{-3}
Ss	soil suction	cm
sv	maximum soil shrinkage between 0.05 bars and 15 bars	(%)

t	1) time	
	2) moisture content	$cm^3\ cm^{-3}$
tint	initial moisture content	$cm^3\ cm^{-3}$
tf	moisture content at 0.05 bars	$cm^3\ cm^{-3}$
tr	residual moisture content	$cm^3\ cm^{-3}$
ts	saturated moisture content	$cm^3\ cm^{-3}$
U	plant water uptake	$cm\ d^{-1}$
V	water flux	$cm\ s^{-1}$
w	width	cm
z	height above a datum	cm

CHAPTER 1 INTRODUCTION

> "There are many physical factors which should receive considerably more attention from computer-orientated hydrological scientists, both parametric and stochastic. Of these, the plant-soil-water relationships and their time-space distribution in the hydrological system are probably most amenable and most important. Few watersheds yield as high as 30% of the precipitation as runoff. Many yield 5% or less. Virtually all the remaining water is returned to the atmosphere by evapotranspiration of the plant-soil-water system."

Hall (1969) above realised the potential of using computer simulations to aid in the understanding and prediction of an important sub-system of the hydrological cycle. The ability to realise this potential has important consequences in agriculture, flood control, groundwater management and water resources planning and control.

In one area in particular, that of agriculture, the benefits to be gained by having an accurate method of predicting the water contents of soils is large. Numerous authors have pointed out the limiting effect the supply of water has on crop yields (e.g Hansen 1979, Nielsen et al 1986, Stern 1979). Random irrigation of crops though is not the answer as this may waterlog the soil, cause the upward migration of harmful substances and increase capital costs. A method therefore is required to predict when crops need

water (i.e when the soil has a water deficit) and how much. As Monteith (1981) states in regard to the Meterological Offices model (MORECS) for predicting the water deficit:-

> "Farmers are not interested in the rate of evaporation from crops but in how fast they grow, how much they yield and what profit they produce. When we start to consider the agricultural and horticultural uses of a scheme like MORECS, we have to remember that growers want to know when to irrigate, how much water to apply and what increase of yield can be expected per unit of applied water."

The present work aims to produce a model to calculate the size and occurence of soil water deficits on field-size scales, and to analyse how different processes within the plant-soil-water system interact. The model consists of a number of routines arranged so as to allow individual processes to be examined and also to allow the model, if required, to be incorporated into catchment models analysing resource potentials and flood evaluations.

1.1 ORIGINS OF THE PROJECT

In 1975 Mr W. J. Walley of the Department of Civil Engineering at Aston University set up a research project on the economic feasibility of a network of neutron probe stations for determining soil moisture deficits on a farm by farm basis. It was later decided to include a general purpose soil-moisture-plant model (Hussein 1979, Walley and

Hussein 1982). Walley (1983), following on from the results of this work, suggested several areas in which further work was required before a more comprehensive and reliable model could be used on a farm basis. These points included work on:-

a) the need to represent drainage from macropores as well as from micropores;
b) to incorporate the soil-moisture hysteresis effect;
c) the need to represent faster acting processes such as infiltration with a smaller timestep than the overall time interval;
d) the incorporation of crop development algorithms, especially in relation to root and leaf development, which requires a data bank of typical values to be compiled;
e) the need to improve the calculation of bare soil evaporation;
f) the need to relate soil water retention and conductivity curves to some index of soil type.

These requirements formed the basis of this project which was initiated in the autumn of 1986.

1.2 AIMS AND OBJECTIVES

The original aim of the project, as stated by Evans (1986), is to

Improve and extend an existing computer-based model of the soil-moisture-plant sub-system, and to increase its flexibility in terms of allowing variation in soil type and the number of layers.

The existing model being that developed by Walley and Hussein (Hussein 1979, Walley and Hussein 1982).

To achieve this aim several objectives were defined:

a) the development of new algorithms to simulate the effects of macropore flow, plant growth, hysteresis and lateral flow;
b) to relate the soil-moisture characteristic curve and conductivity relationships to the soil's physical properties;
c) to derive an algorithm which treats the process of infiltration in a more realistic manner, this incorporates the need to develop an algorithm for distributing daily rainfall totals into hourly amounts;
d) to incorporate into the evapotranspiration algorithm the effects of interception and the surface roughness of plants on the potential demand calculations;
e) to allow the model to work on different time intervals depending on the rapidity of the

process under consideration.

1.3 STRUCTURE OF THE THESIS

The following chapter describes previous soil-moisture-plant models used in the field and lists their advantages and disadvantages. It then proceeds to describe in more detail Walley and Husseins' (1982) model and areas in which it is to be altered.

The next three chapters describe the development of the routines to be used within the soil-moisture-plant model. Chapter 3 deals with the soil component describing the retention and conductivity curves and movement of water through the soil and includes experimental results as well as theory. The chapter also includes the development of macropore and infiltration algorithms. Chapter 4 deals with plant development and water uptake. Both Chapters 3 and 4 include comprehensive literature reviews before detailing the theories inherent in each component of the model. Chapter 5 shows how atmospheric data input into the model is dealt with.

Chapter 6 describes how the model is arranged, how it runs and its basic structure.

Chapter 7 describes the results for various simulations

run using either parts or the whole of the model. Hypothetical simulations are undertaken to test how the model performs in calculating plant development, infiltration and evapotranspiration, these are then compared qualitatively to data provided in the literature. The whole model is subsequently tested against data previously collected by Hussein (1979).

Chapter 8 assesses the performance of the model in meeting the projects original aims and suggests areas in which future work may be appropriate.

CHAPTER 2 SOIL-MOISTURE-PLANT MODELS

2.1 INTRODUCTION

The chapter starts by describing several models available in the literature. The chapter then continues by describing the model formulated by Walley and Hussein (1982) in greater detail and suggesting improvements consistent with the aims and objectives discussed in Section 1.2.

Hussein's (1979) thesis described a soil moisture monitoring network using neutron probes. It used data obtained from a field study to investigate the spatial and temporal variability of soil moisture between and within experimental sites. It compared these with variations estimated by the Meteorological Office and the Ministry of Agriculture, Fisheries and Food. The cost-effectiveness of such monitoring networks was also discussed. In addition to this work, Hussein developed a soil-moisture-plant model to simulate the principal physical processes involved within the soil-moisture-plant subsystem of the hydrological cycle. Using data derived from neutron probe observations a relatively simple model was formulated and tested. The results of this work showed that the model simulated the processes well at Preston Vale Farm.

2.2 MODELS

The following section considers several well known soil-moisture-plant models. These models have been formulated to be used not only for research purposes but also to provide data for irrigation scheduling and crop yields. The models attempt to describe in detail the processes operating within the soil profile. Three such models are described in the following subsections: MORECS, SWATR and SPAW.

A number of simpler models have also been developed which have been used extensively for hydrological and agricultural purposes (Walley, 1983). These models generally assume all water inputs infiltrate into the ground and that evapotranspiration continues at the potential rate up to some critical value of moisture deficit. The decline from potential then follows one of a variety of methods, which are described by Calder et al (1983). Such models have proved useful because they describe rainfall and evapotranspiration, the two factors dominating soil moisture change, reasonably accurately (Walley, 1983)

2.2.1 MORECS

MORECS, a system developed by the Meteorological Office, produces soil moisture deficit predictions based on

input and output data for 40Km x 40Km grid squares for the whole of mainland Britain.

The model consists of two main parts: the calculation of daily potential evapotranspiration and soil moisture extraction. Potential evapotranspiration is calculated using a modified version of the Penman-Monteith combination equation (Institute of Hydrology, 1981). Walley (1983) considers this part of the model to be well developed with much to be commended.

The soil moisture component consists of two layers: the upper layer containing the rooting zone. Within these two layers a Zero-Flux-Plane (ZFP) occurs which is defined as the plane across which no water passes up or down. The ZFP tends to move downwards as the soil moisture deficit increases. The model uses the concept of field capacity which it defines as the water content the profile returns to 48 hours after receiving excess water. If the water content is greater than field capacity this water is assumed to drain away immediately so negating the need for an unsaturated flow algorithm.

A number of criticisms can be made of MORECS. As has been noted, it ignores the movement of water within the profile this may lead to a false representation of soil moisture status (Bell, 1981). Bell (1981) showed that the use of field capacity was only valid in two extreme cases -

soils with high conductivity; and soils of low conductivity where drainage was governed by macropores. The inclusion of a ZFP ignores bypass flow (Bell, 1981). The model is restricted to three soil types: coarse, medium and fine, and only takes into account different crop varieties by specifying the maximum possible deficits for the three soil types. MORECS does not simulate runoff. Furthermore there is no indication in what part of the root profile the moisture deficit occurs - it is averaged.

Despite these limitations, according to Gardner (1981) MORECS estimates the relative changes in soil moisture deficit well but tends to over-estimate the absolute values.

2.2.2 SPAW

The Soil-Plant-Air-Water (SPAW) model was originally developed by Saxton et al (1974). It has been subsequently further modified and is described in detail by Saxton (1983) and Jong and Zentner (1985). The model being essentially developed for use in semi-arid areas. Figure 2.1 illustrates the computational sequence of the SPAW model.

The model begins by assigning all intercepted water to evaporation, the remaining evaporative demand being assigned to soil evaporation and transpiration according to crop cover. The actual amount of evaporation from the soil is

FIGURE 2.1 Computational Sequence of the SPAW Model (extracted from Saxton, K. E., 1983)

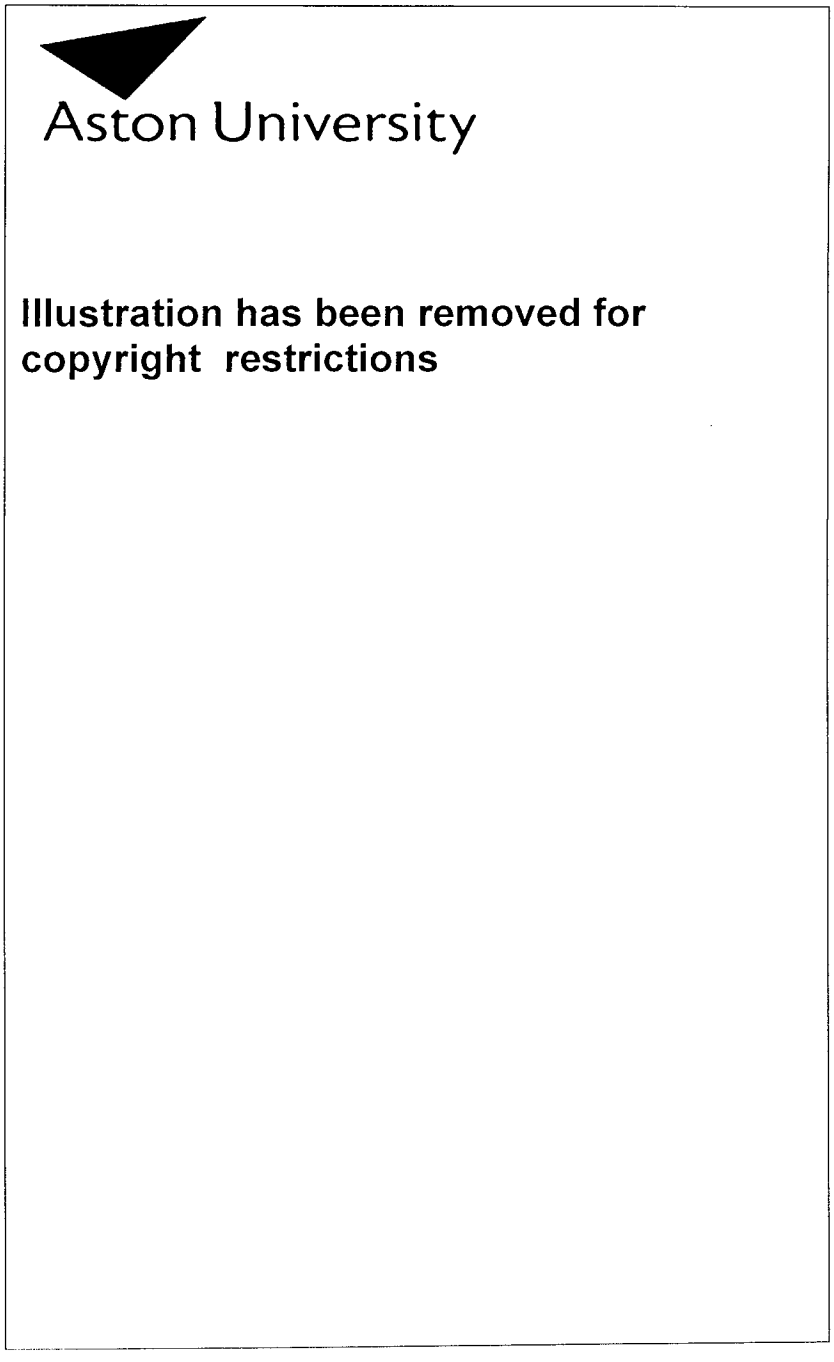

limited by the soil's hydraulic properties. Any remaining demand is transferred to the transpiration routine. The amount of reduction of transpiration from the potential rate is dictated by the development stage of the crop and the amount of available water left for transpiration. Subsequently using a crop water stress function, which is based on a function of the relationship between actual and potential transpiration, and a yield susceptibility curve (i.e. which expresses the sensitivity of the crop to stress at its present stage of development) the effect of the daily transpiration calculations on the eventual crop yield is determined.

The amount of water available for infiltration is calculated by subtracting canopy interception values from precipitation. The water is then distributed to the top soil layer until 90% of storage is reached, when this is exceeded water is passed on to the layer below and so on until enough storage space is found. No consideration is given to surface runoff. Flow between the layers is calculated from suction-conductivity-moisture content relationships in a general flow equation. A mirror layer (i.e. a layer of the same soil type as the basal layer of the real profile) is used to define the base of the profile where, if the moisture content exceeds field capacity, the excess water is lost to the profile, and if it is drier than the layer above water moves up due to capillary-rise.

A number of points about assumptions within the model may be made. In the calculation of actual transpiration SPAW relates moisture uptake to the percentage of available water in the soil rather than to the soil suction which is a better indicator of how easy the water is to remove from the soil. The model neither attempts to simulate root development nor considers how plant-water stresses, in addition to affecting yield, influence crop development and hence the future development of soil suction. Infiltration is treated in a very simplistic manner and ignores totally the effects of macropore flow.

Jong and Zentner (1985) show the model to produce good results for wheat grown in the semi-arid zone of Saskatchewan, Canada, despite minimal local calibration and the limitations of the model noted above.

2.2.3 SWATR

The Soil-Water-Actual-Transpiration-Rate (SWATR) model was developed by Feddes et al (1978). The model can be used in conjunction with CROPR (Feddes et al, 1978) which calculates crop yield.

Potential evapotranspiration is calculated using a modified Penman equation and then divided between soil evaporation and transpiration. The soil is divided into two

layers, with the upper layer containing the roots. This upper layer may increase in depth with the crop's development over the season. Within this framework up to 25 nodal points can be assigned for calculation. Actual transpiration is the sum of the uptake of water from each of the nodes within the root layer. Actual transpiration varies from the potential rate depending on the soil suction. Water flow between nodal points is achieved by use of a hydraulic flow equation.

The use of suction as the only criteria for determining uptake ignores the effect of transpirational demand and plant factors such as root density. SWATR also neglects crop development, although it does allow rooting depth to increase with time. Macropore flow is not simulated and the model also requires suction-conductivity-moisture content relationships to be determined in the field.

Feddes et al (1978), with results gained from two field experiments, concluded "that the rather simple model SWATR can provide a useful tool in solving actual flow problems in the field".

2.3 HUSSEIN'S MODEL

Hussein's model was developed as part of a comprehensive study of soil moisture monitoring systems

(Hussein 1979) and was further developed by Walley and Hussein (1982).

The following sections outline the structure of the original model and describe the plant, soil and meteorological factors incorporated in it. In each of these sections, those aspects of the model amenable to improvement in accordance with the aims and objectives in Sections 1.1 and 1.2 are discussed.

2.3.1 STRUCTURE OF THE MODEL

The model works as a one-dimensional soil column, with all fluxes considered to take place in the vertical plane. As shown in Figure 2.2, the profile is split into four layers: the top three incorporate the root zone, the fourth, the basal layer includes the groundwater table. The model works on the concept of moisture stores, which means that the moisture profile produced is discrete. The model operates on a daily timestep in response to inputs of daily values of rainfall and potential evapotranspiration.

As Walley (1983) pointed out the inclusion of a timestep of one day restricted the model's potential. With regard to the more rapid soil water processes (e.g infiltration). If these are to be successfully modelled shorter timesteps are required.

FIGURE 2.2 Structure of Husseins Model

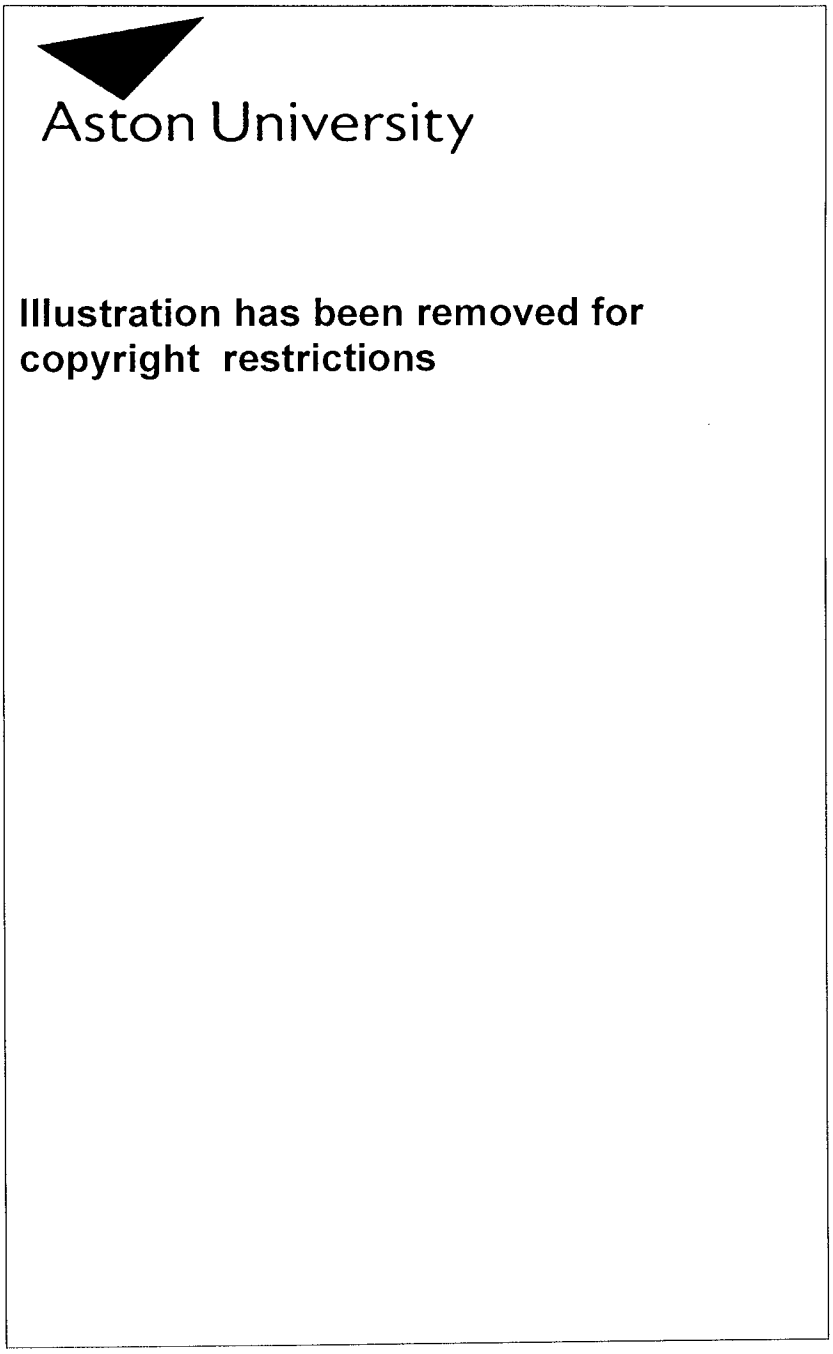

It was with this in mind that a routine was developed which, by reducing the timestep, enabled those processes involving the rapid movement of water to be simulated more accurately (see Section 6.3). An additional alteration allowed the model to incorporate as many layers as required plus the groundwater layer. The ability to include extra layers increases the models flexibility and its applicability to sites other than Preston Vale Farm.

2.3.2 PLANT FACTORS

In Hussein's model the simulation of vegetation within the soil-moisture-plant system is incorporated into two main components: root abstraction and the calculation of actual leaf tension. Using these two components, water flow from the soil to the leaf is treated as a response to potential gradients.

Water uptake into the roots uses Feddes's (1978) relationship, where the flow to the root is treated as comparable to that of radial flow towards a well with soil resistance playing an intergral part in the calculation. Hussein (1979) added an empirical root search function to account for the movement of root hairs towards water. This effectively increases the uptake when the conductivity in the soil close to the root is negligible. The theory, on which the equation formulated by Feddes is based, that soil

resistance is an important factor in determining plant water uptake has recently been questioned by several authors (Section 4.3.1). Bearing this in mind a new relationship was incorporated into the new model (see Section 4.3.2).

Hussein calculated the leaf suction from the potential leaf suction needed to produce the potential transpiration. The result was then modified using the relationship given by Ritjema (1965) to produce an expression relating potential to actual leaf suction. Interception is treated as a delayed store and given an empirical value.

In discussing soil-moisture-plant models Walley (1983) highlighted the fact that the incorporation of a crop development algorithm could simulate the change in plant factors, over time - especially such aspects as percentage canopy cover and root densities. Such an algorithm would allow the idealized plant to react to its environment just as a real plant would, and to generate important feedback for the water uptake and soil evaporation routines. In Section 4.2.4 such a model has been formulated.

2.3.3 SOIL FACTORS

Three algorithms are incorporated into this part of Hussein's model to calculate: the suction, the conductivity and the unsaturated flow between layers. Suction and

conductivity are calculated for each layer, then flow across these layers is simulated by the unsaturated flow equation. If the layer receiving the water becomes oversaturated then the excess is passed back up to the overlying layer (eventually generating overland flow if necessary). Parameter values for the calculation of suction and conductivity were only derived for the three soil types found at Preston Vale Farm using curves for suction given by Hall et al (1977) and curve fitting Gardner's (1958) equation to available data for conductivity. No variation was accounted for within these three soil classes (sand, loamy sand and humus sandy loam). In the case of suction, the function used describes the drying curve only.

To increase the flexibility and applicabiltiy of the model to other sites it was decided that suction-conductivity-moisture content functions should be formulated from easily measured soil parameters, e.g particle-size data. Such relationships would not only allow more soil types to be represented but would also allow parameter values to take into account variations in properties within soil types. A method for determining the wetting curve has also been formulated using parameters from the drying curve. This allows capillary-rise to be more accurately represented (see Section 3.2.1.2).

2.3.4 HYDROMETEOROLOGICAL FACTORS

The Hydrometeorological algorithms are used in Husseins' model to simulate the following factors: infiltration, soil evaporation and the partitioning of evaporative demand.

Infiltration is described as the input into the top layer on a daily basis. If the rainfall is heavy the surplus rain not accommodated by layer 1 is divided between rapid percolation into layers 2 and 3 (firstly into layer 2 until it becomes saturated and then layer 3) and overland flow. The division is calculated using empirical relationships, and the parameters were given values to "produce the desired infiltration characteristics" (Walley and Hussein, 1982) but it is not clear how these were calculated. As suggested by Walley (1983) a more realistic treatment of the process of infiltration is required.

Changes to Husseins' model were made to take this into account (see Section 3.3) and in addition a relatively simple model to simulate the process of bypass flow through macropores was developed (see Section 3.4). For these modifications to be achieved the model was altered so that these processes could run on a smaller timestep (see Section 6.3). Such changes also necessitated the need for distributing the daily rainfall total into smaller timesteps. A simple procedure based upon rain intensity

duration curves has been developed for this purpose (see Section 5.2).

In Husseins' model the potential evaporative demand was distributed to the interception store, bare soil evaporation and potential transpiration. However, in the new model interception is considered as unimportant in the overall water budget and is subsequently neglected (see Section 4.1). Evaporative demand is only partitioned between bare soil evaporation and potential transpiration according to the percentage crop cover (see Section 5.3). Bare soil evaporation is calculated according to the moisture available to the soil surface (see Section 5.3).

2.3.5 MODEL APPLICATIONS

The objective of the model developed by Hussein (1979) was to provide a simple and reliable method of representating the soil-moisture-plant system which could be used in determining irrigation scheduling. The model was tested against data from Preston Vale Farm (see Section 7.1), one of the sites from the moisture monitoring program described earlier in his thesis (Hussein 1979). Hussein (1979) describes the model as providing reliable estimates of soil moisture deficits, and notes that the model has the potential for wider hydrological applications such as flood forecasting.

However, the model was limited in its simulation of several of the processes within the soil-moisture-plant system as discussed in Sections 2.3.1 - 2.3.4. Although the model had a theoretical as well as an empirical basis its parameters were calibrated purely for conditions at Preston Vale Farm. The model could therefore not only be substantially improved but also given wider applicability if a significant number of model parameters could be determined on the basis of soil type and plant type, thus leaving fewer parameters to be found by calibration.

2.4 CONCLUSION

As stated in Section 1.2 the aim of this project has been to extend and improve Hussein's (1979) soil-moisture-plant model. This model was a significant improvement on the three other models described earlier in that transpiration was not calculated by actual/potential transpiration functions, but rather by root abstraction algorithms (Section 2.3.2). Of the other models SPAW has some useful ideas. For example, relating suction-conductivity-moisture content relationships to soil properties by statistical relationships (see Section 3.2.1.2) and the concept of a stress index (see Section 4.2.4), both of which have been incorporated into the new model.

The following chapters describe in greater detail the

development of the new soil-moisture-plant model and its calibration and testing against field data.

CHAPTER 3 SOIL MOISTURE PROCESSES

3.1 INTRODUCTION

The aim of this chapter is to describe the movement of water in the unsaturated zone above the water table. It describes the entry of water into the soil subsystem by infiltration at the surface, either into the soil matrix or into the macropores, and flow between these two domains is simulated using a mathematical expression. Water is also added to this subsystem from the water table by means of capillary rise.

Processes operating within the soil are described by mathematical expressions, whose parameters are derived either by statistical analysis or, in the case of those relating to macropore distribution and sizes, from representative values found in the literature.

3.2 MOVEMENT OF WATER IN THE UNSATURATED ZONE

Water is primarily held in the soil by two processes; surface tension and adsorption. Although adsorption produces layers of water only a few molecules thick, a significant amount of water can be retained by this mechanism,

especially in the finer grained soils where surface areas are large. The effectiveness of these two processes is affected by several factors: salt concentration (Nye and Tinker 1977), temperature (Hopmans and Dane 1986), surface area (Hillel 1971) and electrical charge of the soil particles (Nielsen et al 1986). Water may also be held in the soil by retention in pools on the upper surface of particles. Boushi and Davies (1969) found this to be important where particles have a diameter greater than 100mm. Where particles are less than 30mm in diameter capillary forces (i.e. surface tension) dominate.

Soil moisture energy consists of two forms, kinetic and potential but, since flow velocities are relatively small, Hillel (1971) considered the kinetic component to be negligible. Soil moisture potential equates the total potential energy of the water held in the soil to that of a static column of water held at the same elevation at atmospheric pressure. The total potential energy of the soil comprises the sum of the gravitational, absorptive, osmotic and matric potentials. The gravitational potential refers to the height of a water molecule in relation to a defined datum point, being positive if above and negative if below. The osmotic potential arises from the presence of solutes in the soil, and its effects (except in the case of saline soils) are negligible in relation to that of the matric potential and as such it is generally neglected. In an unsaturated soil, adsorptive and capillary forces lower the

potential energy of the soil water to below that of free water, thus producing a negative potential or tension. The moisture content of the soil may remain at the saturated value even if the potential becomes increasingly negative, until the time when air starts to enter the soil. The potential at which this occurs is known as the air-entry value the actual value being dependant on the soil structure (Philip 1958b).

The removal of water from the soil first takes place from pores in which it is only weakly held, and as the soil dries the remaining water is held in decreasingly smaller pores at increasingly higher tension forces. Thus there is a clear relationship between suction - the modulus of tension as used by soil physicists - and moisture content, which when presented graphically is known as the soil moisture characteristic curve (Childs 1940). However, this relationship is not unique. If the soil is gradually wetted, instead of dried, a slightly different curve is produced, this non-unique behaviour is termed hysteresis. Between these two boundary curves, known as the wetting and drying curves, are an infinite number of possible curves which join the two together. These were termed scansion curves by Carman (1953) but are now generally referred to as scanning curves (Figure 3.1). They describe the suction-moisture content relationship as it switches from drying to wetting or vice versa, though repeated switching can complicate the curves. The cause of this non-unique relationship is not

fully understood, Haines (1930) attributed it to the differing size of the pore neck and centre which result in a greater pressure being needed to fill a pore than to drain it. This theory has been supported by others (Klute 1969, Hillel 1971), but experimental evidence from Foster (1932,1951), Cary (1967), Staple (1965) and Onishchenko (1986) suggest other factors may be at work. Foster (1932) suggested that there is a delay in the formation of the meniscus on wetting, whereas Klute (1969) noted differing interfacial contact angles on wetting and drying.

Water moves within the soil from areas of high potential to areas of low potential in order to gain equilibrium. Darcy's equation (Equation 3.1) describes movement within a saturated soil using this principle (though potentials in this case are positive) and adds an empirically derived proportionality constant K, which is known as the hydraulic conductivity.

$$V = K\left[\frac{dh}{dz} - 1\right] \qquad -3.1$$

where V =water flux (positive upwards) (cm s^{-1})

K =conductivity (cm s^{-1})

h =soil suction (cm)

z =height above reference datum (cm)

1 refers to the unit hydraulic gradient due to gravity.

FIGURE 3.1 The Soil Moisture Characteristic Curve

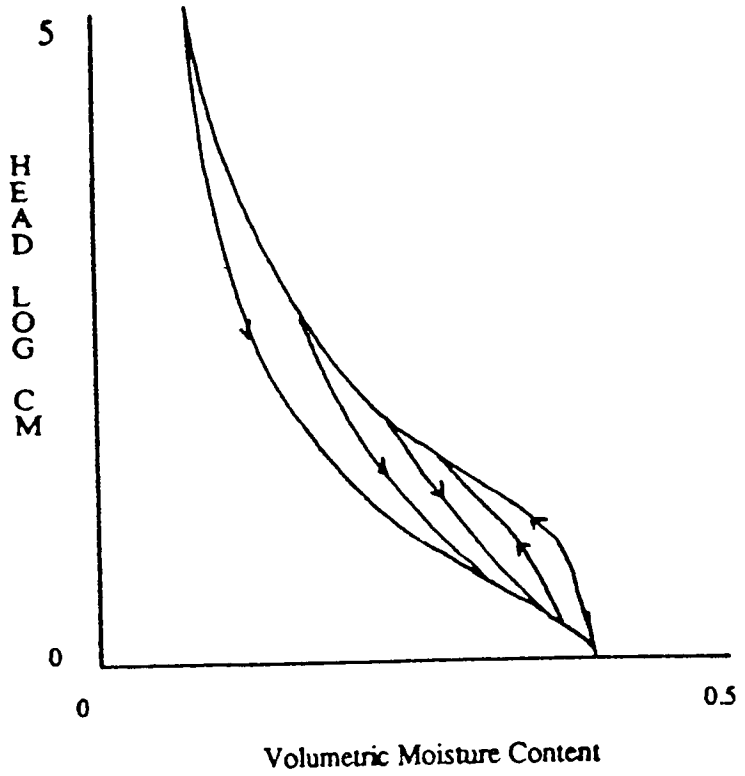

FIGURE 3.2 Soil Moisture Characteristic Curve Showing Significance of Genuchten's Equation Parameters

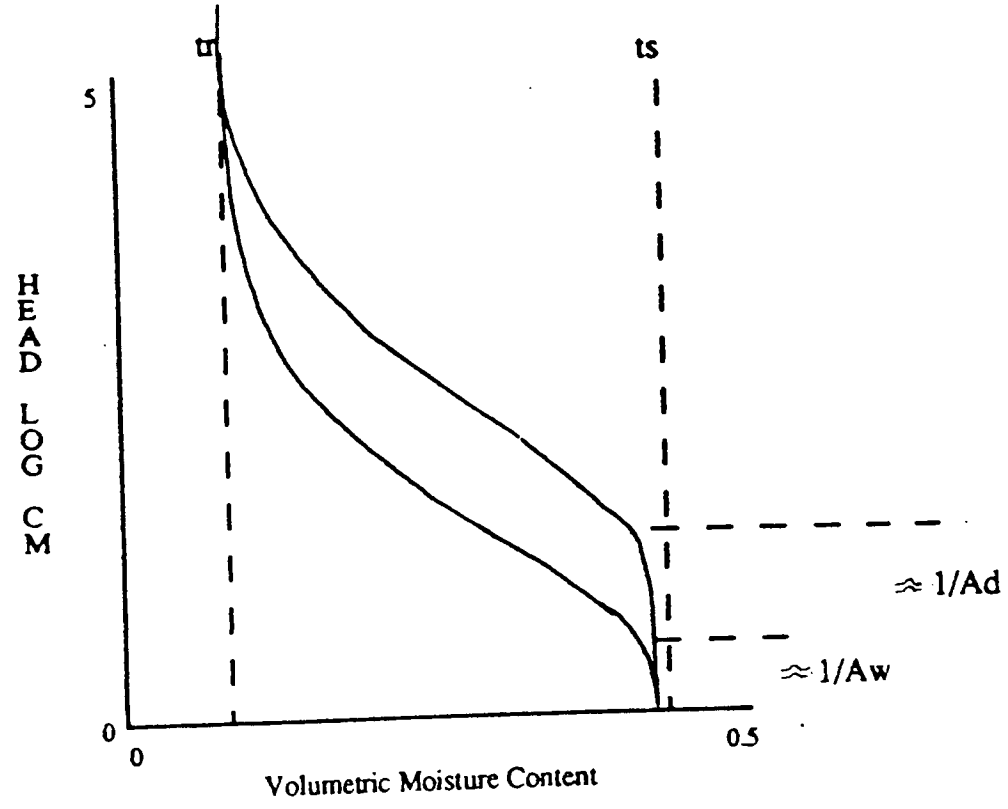

Though originally derived as a semi-empirical equation, Richards (1931) showed that where inertial forces in the fluid are negligible and the main resistance to flow is viscosity the equation is a generalized solution to the Navier-Stokes flow equation (Klute 1969). Richards also showed that the equation could be applied to unsaturated soils with air-filled pores being regarded as solid particles. This leads to hydraulic conductivity no longer being considered a constant value but rather a function of head or moisture content.

Conductivity is affected by several factors:

a) the pore-size distribution of the medium which is itself a function of particle architecture;
b) the type of particle in the medium - clay particles may shrink and swell, reorientate themselves and move within the liquid phase (Nakano et al 1986);
c) the properties of the liquid phase, such as pH, solute composition and temperature (see review by Nielsen et al 1986);
d) the presence of entrapped air.

As mentioned earlier, conductivity is a function of head or water content and the conductivity-head relationship is hysteretic. However, the conductivity-moisture content curve shows little hysteresis (e.g Topp 1969,1971, Talsma 1970 and Vachaud and Thony 1971) although Staple (1965) and Dane and Wierenga (1975) claim to have found significant effects.

However, these are still less than those observed with the conductivity-suction relationship and because of this it was decided that the conductivity-moisture content relationship would be used.

The validity of Darcy's Law has been challenged by numerous authors (see review Swartzendruber 1968), but Bavel (1969) claims that he has yet to find a convincing experiment disproving it and Jensen (1981) suggests that even if Darcy's equation is not strictly correct the errors involved in measuring hydraulic conductivity in the field are probably more significant. However work by several authors has shown certain infiltration (review Hillel 1987b) and macropore processes (review Beven and Germann 1982) where Darcy's law does not hold and these are described later in the chapter.

3.2.1 SUCTION

Due to the prohibitive expense of producing a relationship from actual field data, researchers have sought over recent years to derive empirical methods for producing such curves from less expensively obtained data: e.g soil-type and particle-size data. This section reviews several methods available and then goes on to describe the method adapted for use within the final model.

3.2.1.1 Equations Describing the Moisture Characteristic Curve

Complex methods are available which use particle-size and bulk density data to derive the soil moisture characteristic curve. Ayra and Paris (1981) converted the particle-size data into pore-size distributions using assumptions regarding particle-shape. For each pore-size range calculated, an equivalent moisture content is calculated. As many pore-size classes can be defined as deemed necessary for the particular application. However, the increase in accuracy obtained by the use of more and more points diminshes with the number of points (Ayra and Paris 1982). Another method proposed by Haverkamp and Parlange (1986) produces a soil moisture characteristic based on the shape similarity between it and the cumulative particle-size distribution curve. The method calculates both the wetting and drying curve and can calculate scanning curves. Both methods can be criticized on various points. The Ayra and Paris method is criticized by Haverkamp and Parlange (1982) for the abitrary way in which pore-size classes are defined, in terms of both number and range, leading to ambiguity in the method. The Haverkamp and Parlange method is only applicable to sandy soils without organic matter and the curves produced are not continuous so they can cause problems with computer programming.

Simpler methods are available to describe the soil

moisture characteristic curve. These use regression analysis to calculate specific points on the curve from particle-size and bulk density data. Early statistical analysis indicated that properties such as the percentage of clay within the soil were related to the moisture content at 15 bars (W15) for soils varying from coarse to fine texture (Lund 1959, Kivisaari 1971, Petersen 1968a). Petersen et al (1968b), working with silt loams, found organic content also to be correlated with this value (W15). He also found that the coarser the soil the lower the moisture content at one-third bar ($W^1/_3$). Available Water Capacity ($W^1/_3$-W15) was found to be closely correlated to the silt fraction (Kivisaari 1971 and Jamison and Kroth 1958) for soils containing silt. Following on from this work, it was found that more points could be calculated. Gupta and Larson (1979b) calculated 12 points based on sand, silt, clay and organic matter percentages and bulk density. Rawls et al (1982a) calculated fewer points but improved their own analyses by including two measured points on the curve at 1/3 bar and 15 bars. Comparison with independent data show Rawls et al's method to produce high correlation coefficients, even when the measured points are not included in the analysis. However, Ahuja et al (1985) showed the equations of Rawls et al to have high mean relative errors and high standard deviation of errors. Rawls et al (1982b) tried another approach, using the Brooks and Corey equation (Brooks and Corey 1965), they determined the parameter values in the equation for specific soil types.

The present study follows on from Rawls et al (1982b) by determining parameter values from the data. However, it determines these values based on particle-size data not soil texture, and uses Genuchten's (1978) equation, which is similar to the Brooks and Corey equations but produces a continuous function.

3.2.1.2 Genuchten's Equation

The equation described by Genuchten (1978) was developed as a simple empirical relationship which can be fitted to experimentally derived data points on the suction-moisture content curve in order to produce its characteristic S-shape curve. It is similar to the Brooks and Corey (1965) equation but has the advantage that a continuous function is produced, whereas the Brooks and Corey equation produces two expressions based on the value of suction. At large values of suction (h) the equation reduces to an approximate form of the Brooks and Corey relationship as shown below:-

Brooks and Corey (1965)

$$Se = (h_b/h)^{-q} \qquad h > h_b \qquad -3.2a$$

$$Se = 1 \qquad h <= h_b \qquad -3.2b$$

where Se =relative moisture content i.e. (t-tr)/(ts-tr)

tr =residual moisture content (cm^3/cm^3)

ts =saturated moisture content (cm^3/cm^3)

t =moisture content (cm^3/cm^3)

h =suction (cm)

h_b =curve fitting parameter (cm)

q =curve fitting parameter

Genuchten (1978)

$$Se = 1/(1+(ah)^n)^m \qquad -3.3a$$

At large values of h

$$(1+(ah)^n)^m = (ah)^{nm} \qquad -3.3b$$

Therefore equation 3.3a reduces to

$$Se = (1/ah)^{-nm} \qquad -3.3c$$

Putting

$$a = 1/h_b \qquad -3.3d$$

$$nm = q \qquad -3.3e$$

gives the Brooks and Corey Equation (3.1).

Brooks and Corey (1965) found that the equation parameters 'h_b' and 'q' could be related to certain soil properties. The capillary pressure at which air flow could be first observed was found to closely correspond to 'h_b', and was termed the bubbling head. It was also found that 'q' had a high value where there was a narrow pore-size distribution and a low value where there was a broad pore-size distribution: thus 'q' was termed the pore-size distribution index. The parameter tr as used by Brooks and Corey is also seen to be a curve-fitting parameter (Genuchten and Nielsen 1985). Genuchten (1980b) found problems when defining tr, especially with fine soils, due to the fact that desorption continues at very high suctions. Genuchten (1980b) defined the residual moisture content (tr) as the moisture content where the gradient (dt/dh) becomes zero (excluding the region near ts), but where there are insufficient data at higher suctions the value is obtained by curve-fitting using the available values. Genuchten (1980b) and Genuchten and Nielsen (1985) found this method unsatisfactory and suggested that there should be an independent method for calculating the residual moisture content. Equating tr to the moisture content at 15 bars was suggested. Figure 3.2 presents a typical curve produced by Genuchtens' equation and illustrates several of the points mentioned in the preceding paragraph.

The product 'nm' as can be seen from equation 3.3e can be related to 'q'. Genuchten and Nielsen (1985) tested three

variations of this model by fitting it to real data. The first two models assumed that 'm' was a function of 'n'; the first m =1-1/n was based on Mualem (1976a), the second m =1-2/n was from Burdine's (1953) theory. The final model assumed 'm' and 'n' were independent. A comparison of the results showed that of the two models where 'm' was a function of 'n' it was the first model (i.e Mualems formulation) that performed best. Overall model 3 was the best. However, in several cases model 3 produced values of n < 1, which resulted in the slope of the retention curve near to saturation taking on the unrealistic value of minus infinity.

To date work by several authors (e.g Genuchten 1980, Genuchten and Nielsen 1985, Sakellariou-Makrantonaki et al 1987, Kool and Parker 1987) using this equation has concentrated on fitting the equation to experimentally derived suction-moisture content data for various soils. The object of this study is to take this one step further to see if the parameters 'a' and 'n' can be related to easily measurable soil properties (e.g particle-size data) in order to produce predictive equations. Genuchten (1980) suggested that tr could be equated to some large value of suction i.e. at the permanent wilting point (h =15000cm). This work examines the merits of this against purely finding tr by curve-fitting. Finally it looks at the parameters 'm' and 'n' and examines what happens if 'm' and 'n' are independantly calculated.

To this end three sources of data were used, describing a wide variety of soils:-

a) SCS-USDA (1974) described points on the suction curves from saturation to wilting point;

b) Cassel (1974) described data from near-saturation to around 0.5 bars depending on the available data for each soil, and in effect it described the wet end of the curve;

c) Long et al (1969) described data from 0.1 bars to 15 bars (i.e the dry end of the curve).

A summary of the composition of the soils and their particle-size data is given in Tables 3.1a-c. Genuchten's equation was fitted to each of these soils within the data sets using the NAG library routine E04JAF on Aston University's Vax Cluster. As well as the points on the curve, values for ts and tr had to be input. In the case of ts, only SCS-USDA (1974) gives a measured value. For Cassel (1974), the moisture content at 0.004 bars was deemed adequate for describing ts. This was due to the fact that in most cases with the next data point described , usually 0.01bar, the moisture content had changed little if at all suggesting that desorption was negligible at these small values. For Long et al (1969), porosity was calculated from the bulk density and was then equated to ts, as suggested by Avery and Boscombe (1974), using the relationship below

$$ts = e = 1-(p_b/p_s) \qquad -3.4$$

where e = porosity

p_b = bulk density (g/cc)

p_s = particle density (taken as that of SiO_2 i.e 2.65) (g/cc)

In fine soils where there is swelling, the value of ts calculated by eq. 3.4 was sometimes found to be less than the moisture content at 0.1 bar. These soils were eliminated from the analysis, but in other fine soils where the difference was marginal between ts and moisture content at 0.1 bars the effects of swelling still meant that sometimes there were significant errors in ts calculated from bulk density. In the case of tr for SCS-USDA (1974) and Long et al (1969) the parameters 'a' and 'n' were calculated twice, once for where tr was equated to wilting point and once where tr was fitted. For Cassel (1974) 'a' and 'n' were only calculated once as tr could only be determined by fitting, since no values for moisture content at 15 bars were given. Values of 'm' independent of 'n' were calculated from SCS-USDA (1974) data, the other data sources being used to derive relationships between 'm' and 'n' using Mualems (1976a) theory.

Results of the curve-fitting exercise indicated that fitting tr to the data gave better results than those where tr was equated to the water content at 15 bars, as might be expected. However, the effect was more marked with SCS-USDA (1974) where tr fitted produced a value of 0 for 145 out of

TABLE 3.1a DESCRIPTIVE STATISTICS OF SOIL PROPERTIES TAKEN FROM SCS-USDA (1974)

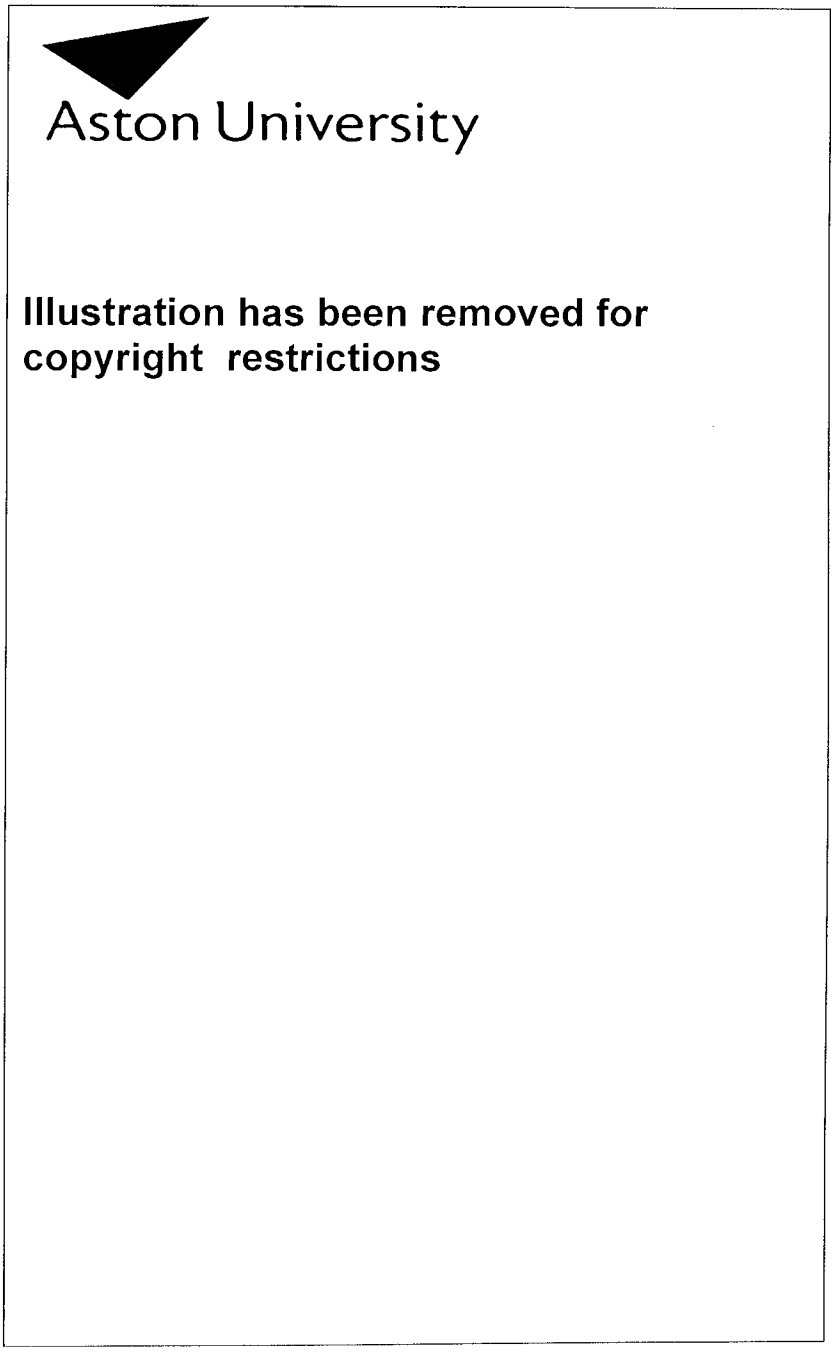

TABLE 3.1b DESCRIPTIVE STATISTICS OF SOIL PROPERTIES TAKEN FROM CASSEL (1974)

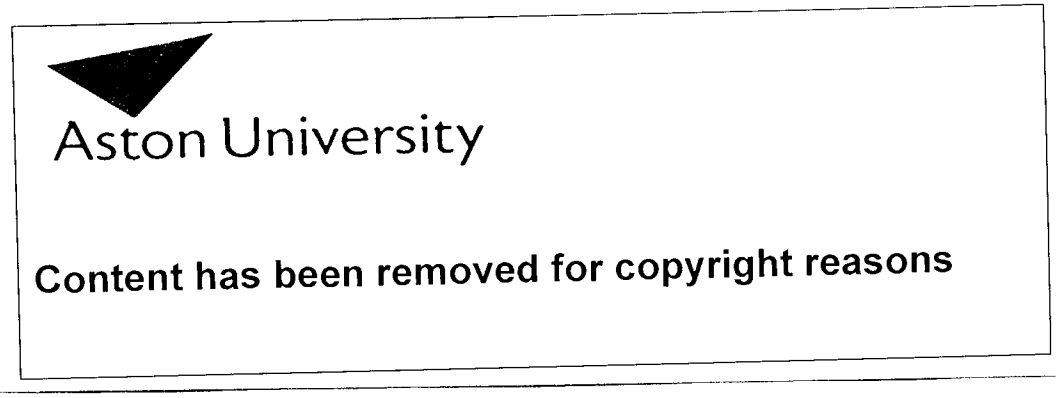

TABLE 3.1c DESCRIPTIVE STATISTICS OF SOIL PROPERTIES TAKEN FROM LONG ET AL (1969)

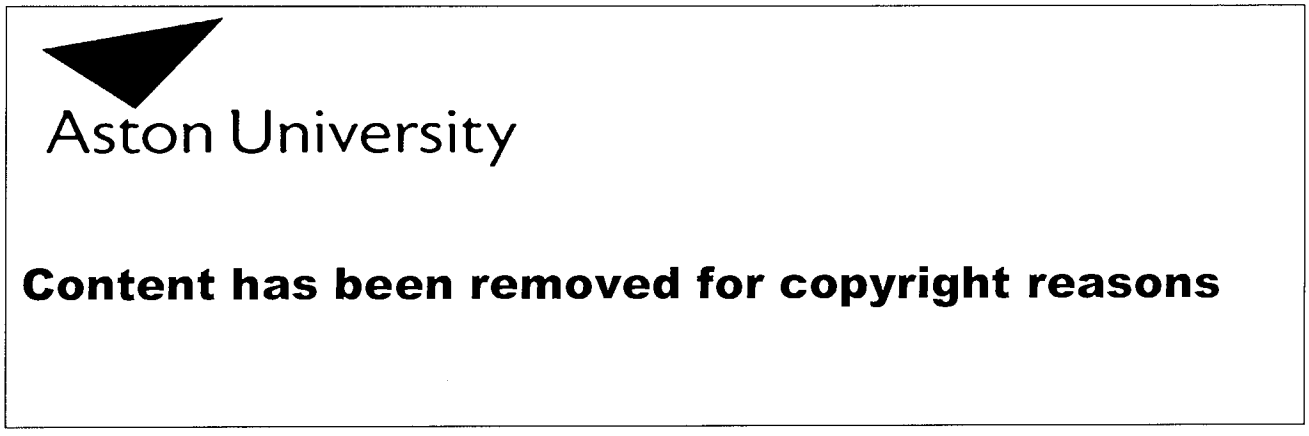

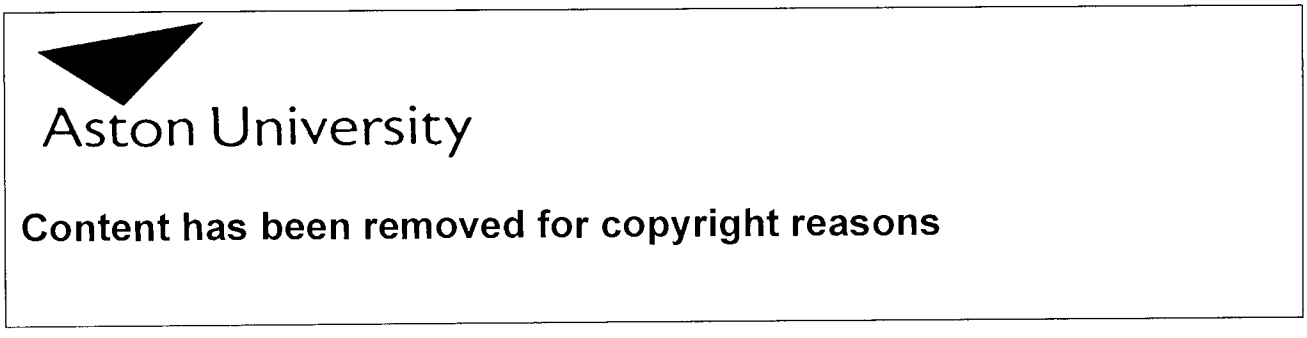

238 soils which ranged from sands to clays. This indicates that the curve-fitting routine is favouring the wet end of the curve where there is a greater number of points and relative errors have a greater absolute value. This was not observed with data from Long et al (1969) where the difference between tr fitted and tr constrained was minimal. This was due to the fact that the curve only had to fit values at the drier end of the moisture characteristic. There were however problems with Long et al (1969), where the coarser soils gave values of 'a' approaching unity, thus producing curves without the characteristic S-shape. Only in the finer soils where the rapid change in dt/dh at the wet end occurred within the range 0.1 - 15 bars did the S-shape occur, hence Long et al (1969) was considered unsuitable as the data did not cover a sufficient range of suction values.

The Cassel (1974) values of tr calculated by the best fit method like SCS-USDA (1974), were considered unrealistic. For the sandy soils on average tr was calculated as 0.101 (SD 0.02). This was considered too high as a look at data from the literature (e.g SCS-USDA 1974 and Mualem 1976b) indicated that these soils show much further desorption. This illustrated the need for an independent method of determing tr, as suggested by Genuchten (1980b) and Genuchten and Nielsen (1985). With this need in mind, SCS-USDA (1974) and Long et al (1969) were used to derive a statistical relationship between certain soil properties and moisture content at 15 bars. Though Long et al (1969) was

considered unsuitable in determining statistical relationships for the shape of the curve it does provide a large set of data describing the moisture content at 15 bars. Equating tr to the moisture content at 15 bars (Table 3.5) it was then possible to use this as an independant input into the curve-fitting algorithm. Figures 3.3 compares for several soils from Cassel (1974) the effect on the moisture characteristic of using values of tr determined using the statistical approach with those derived from curve-fitting. The results illustrated by Figures 3.3 clearly show that where tr is found by curve-fitting, the predicted curves fit the observed data better. However, as with SCS-USDA (1974) and Long et al (1969) when comparing tr determined from moisture content at 15 bars against tr determined from fitting, this is to be expected. The curves produced when tr is added as an independant variable still have 'a' and 'n' determined by curve-fitting and it can be seen from Figure 3.3 that the values nearer saturation are better represented by the curve than the values at the drier end of the suction range examined. However, this method allows tr to be input independently into the equation when no data are available for moisture content at 15 bars, and as such produces a curve which takes into account the drier end of the curve and not just the wet end. The relationship between soil properties and parameter values is fully described below.

In terms of minimizing the sum of squared error varying

Figure 3.3a

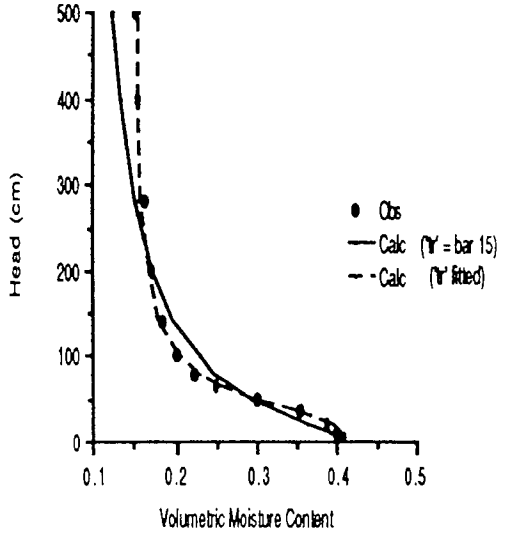

Figure 3.3b

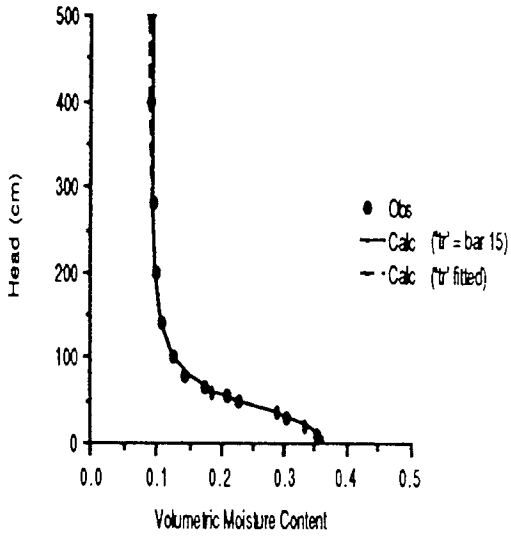

Figure 3.3c

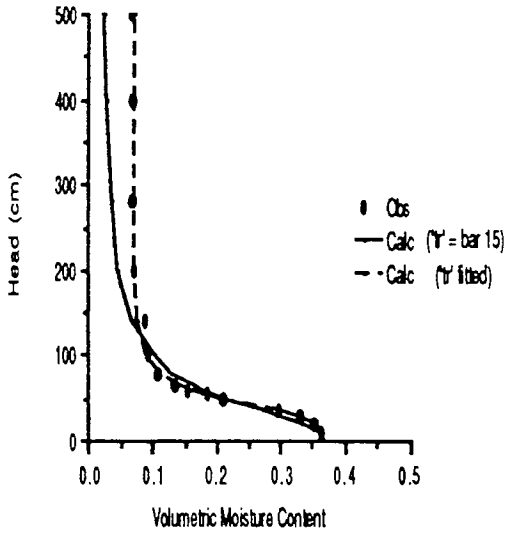

Figure 3.3d

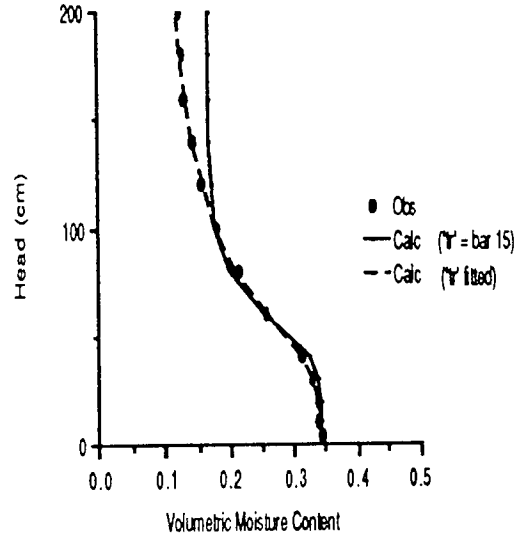

Figure 3.3e

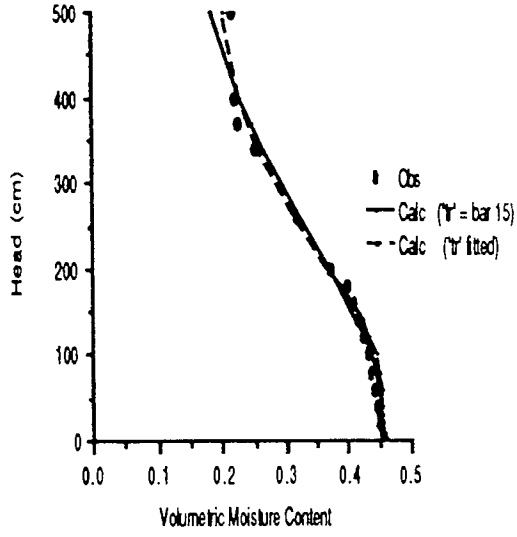

Figure 3.3 Curve-Fitting of Genuchten's Equation to Observed Data Using Two Methods: 1. 'tr' Determined by Curve-Fitting, and 2. 'tr' Determined by Regression Equations.

ASTON UNIVERSITY
LIBRARY AND

'm' and 'n' independently produced better fits to the data than when 'm' was dependent on 'n'. However, in over 50% of the cases 'n' was less than 1 and according to Genuchten and Nielsen (1985) this is unrealistic. For this reason 'm' was assumed to be dependent on 'n' as described by Mualem (1976a).

The next stage in the analysis was to input the calculated values of 'a' and 'n' along with the soil properties into a database. Using these data, equations were derived from multiple regression analysis to calculate 'a' and 'n' from soil properties. For completeness the data from Cassel (1974) and Long et al (1969) were also analysed as was that from SCS-USDA (1974) where tr was determined by curve-fitting. The results of simple linear regression between variables and parameters are shown in Tables 3.2a-c. The rest of this section concentrates on the results from SCS-USDA (1974) where tr was equated to the 15 bar value, as indicated by the preceeding discussion is the reference with the widest range of data points and inputting tr will give the most representative curves. The other results are only referred to where such inclusion aids discussion.

It can be seen in Table 3.2 that the variables 'a' and 'n' are strongly correlated to many soil properties (i.e at the 1% significance level). This was to be expected with such a large set of data. As significance only indicates to what level the event is related by factors other than

TABLE 3.2a CORRELATION COEFFICIENTS ACHIEVED BETWEEN INDIVIDUAL VARIABLES AND THE PARAMETERS OF GENUCHTEN'S EQUATION FOR SCS-USDA (1974)

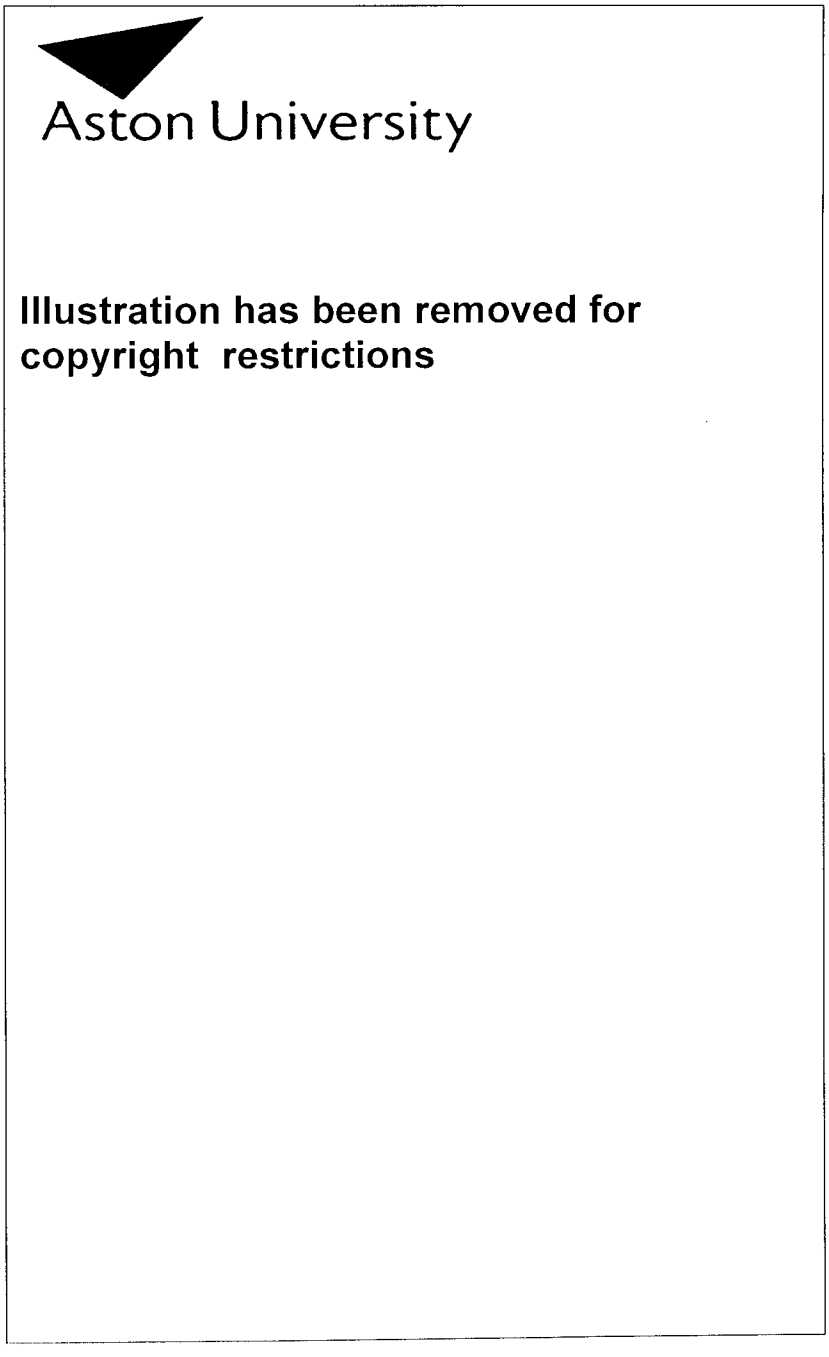

TABLE 3.2b CORRELATION COEFFICIENTS ACHIEVED BETWEEN INDIVIDUAL VARIABLES AND THE PARAMETERS OF GENUCHTEN'S EQUATION FOR CASSEL (1974)

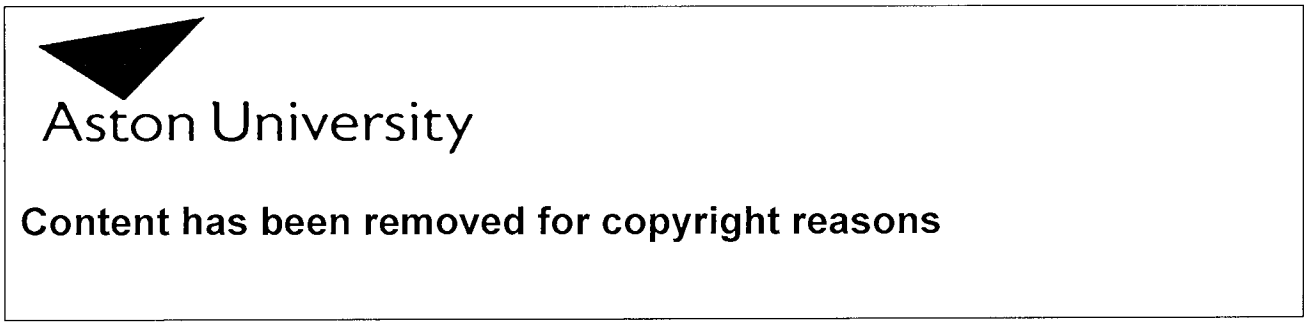

TABLE 3.2c CORRELATION COEFFICIENTS ACHIEVED BETWEEN INDIVIDUAL VARIABLES AND THE PARAMETERS OF GENUCHTEN'S EQUATION FOR LONG ET AL (1969)

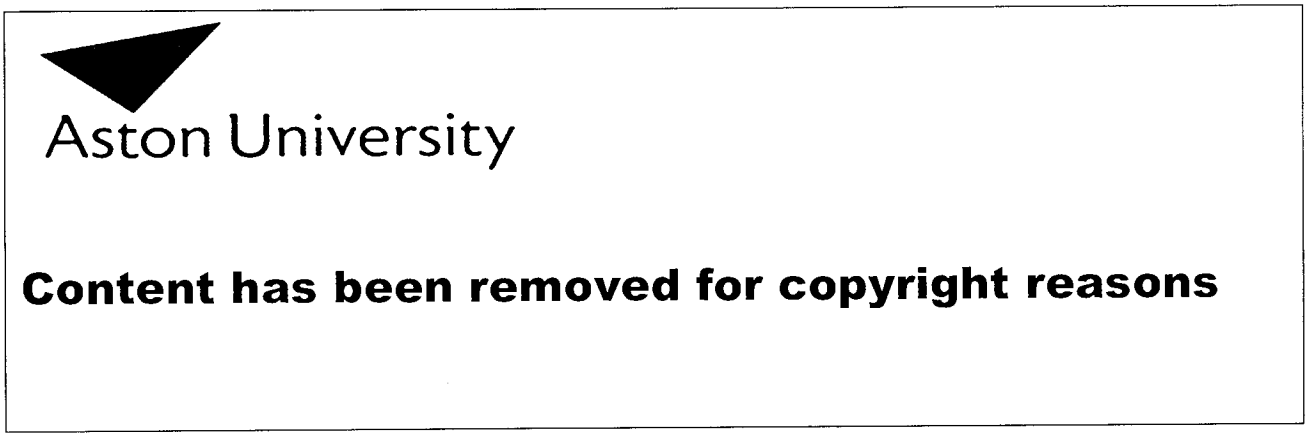

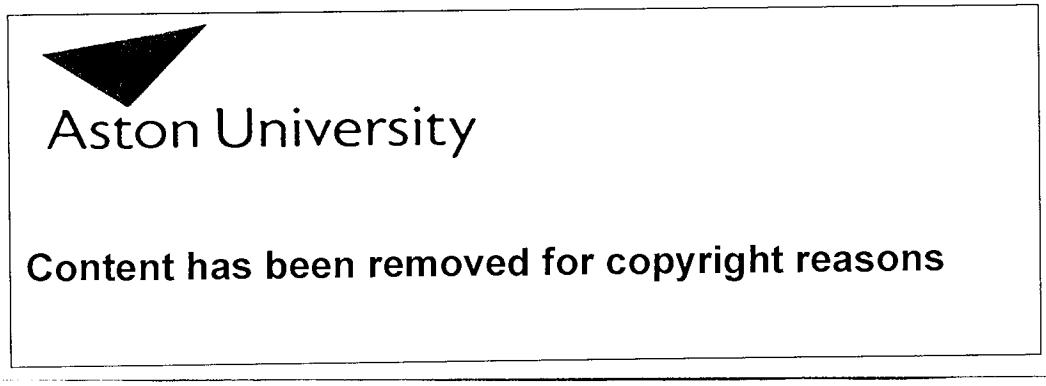

chance, increasing the sample size lowers the probability that a result of a given magnitude occurs by chance alone. The effect of sample size on the amount of variation accounted for by this factor (r^2) though is to give a more accurate indication of the population r^2. Due to these two points variables often show a high level of statistical significance but with little practical significance i.e they do not account for a large amount of the variation. This can be seen with respect to the variables in Tables 3.2a-c where individually none of the soil properties account for a large proportion of the variation as shown by the r^2 value. For SCS-USDA (1974) data the parameter 'n' is more clearly correlated with soil properties when tr is found by curve fitting than when tr is equated to moisture content at 15 bars, but the reverse is true for the parameter 'a'. For SCS-USDA (1974) data the parameter 'n' is more highly correlated with soil properties than 'a', but this is the reverse with Long et al (1969) data due to the fact that 'a' is increasingly overestimated for coarser soil due to the lack of data at the wet end. The moisture content at 15 bars was found to be highly correlated with particle-size data especially clay, and was also significantly correlated with chemical composition, although this was probably due to the strong interaction of these factors with clay. One surprising result of the present work is seen with bulk density. On examination of Tables 3.2a-c it is seen that it is poorly correlated with all of the other soil properties for all three references. The inclusion of measured values

on the retention curve (i.e moisture contents at 1/3 bar and 15 bars) does produce high correlations between these points and parameter values determined for Genuchten's suction-moisture content equation.

Table 3.3 shows the linear correlation coefficients obtained for moisture contents at 1/3 and 15 bars when data is combined from SCS-USDA (1974) and Long et al (1969). The number of soil variables is limited to those that are commonly defined by both references. As tr is equated to the moisture content at 15 bars it can be seen that tr can be related simply to soil properties. The importance of determining the moisture content at 1/3 bar is discussed later in the section when determining parameter 'a', in relation to simulating the suction-moisture content relationships produced by Hedges (1989).

Since individual linear regressions did not describe or account for the variation in Genuchten's equation parameter values, with the exception of tr, multiple regression was tried. In addition certain 'promising' soil variables were squared or cubed, and other soil variables multiplied together, the ultimate aim being to increase the amount of variation accounted for. This approach was justified on the grounds that few natural variables vary linearly owing to the many complex interactions that are involved (see McNeil et al 1975).

Once the data were suitably arranged all the variables were fed into the statistical package, SPSS-PC, and using forward insertion (i.e the computer determines the next parameter to insert into the relationship that increases the significance) expressions were formulated to predict values of 'a' and 'n' from SCS-USDA (1974) with tr equated to the moisture content at 15 bars. The program was stopped when the increase in the amount of variation accounted for was not considered significant enough to justify the inclusion of additional variables. The increase in number of variables also decreases the F -statistic and widens the gap between r^2 and adjusted r^2 (which takes account of the number of variables) and may even reduce adjusted r^2. The coefficients used in the equations formed by this process are shown in Table 3.4. In order to permit the value of tr to be estimated without deriving it experimentally, the data from SCS-USDA (1974) and Long et al (1969) were pooled and using properties common to both, the relationship shown in Table 3.5 was found by using SPSS-PC as has been described before.

When manipulating these equations it was noted that with finer soils the moisture content at wilting point given by the curve was greater than tr, despite tr being set equal to the wilting point value. This was due to the inability of the curve to produce an S-shape within the range of moisture contents, a problem caused by the independent calculation of the parameters. This effect was especially noticeable when values were input for soil properties which were outside the

TABLE 3.3 CORRELATION COEFFICIENTS FOR MOISTURE CONTENTS AT BAR 15 AND BAR 1/3 FROM SCS-USDA (1974) AND LONG ET AL (1969)

Aston University

Content has been removed for copyright reasons

TABLE 3.4 MULTIPLE REGRESSION COEFFICIENTS TO DETERMINE a AND n FROM SCS-USDA (1974)

Aston University

Content has been removed for copyright reasons

Aston University

Content has been removed for copyright reasons

TABLE 3.5 MULTIPLE REGRESSION COEFFICIENTS TO DETERMINE MOISTURE CONTENTS AT BAR15 AND BAR 1/3 FROM SCS-USDA (1974) AND LONG ET AL (1969)

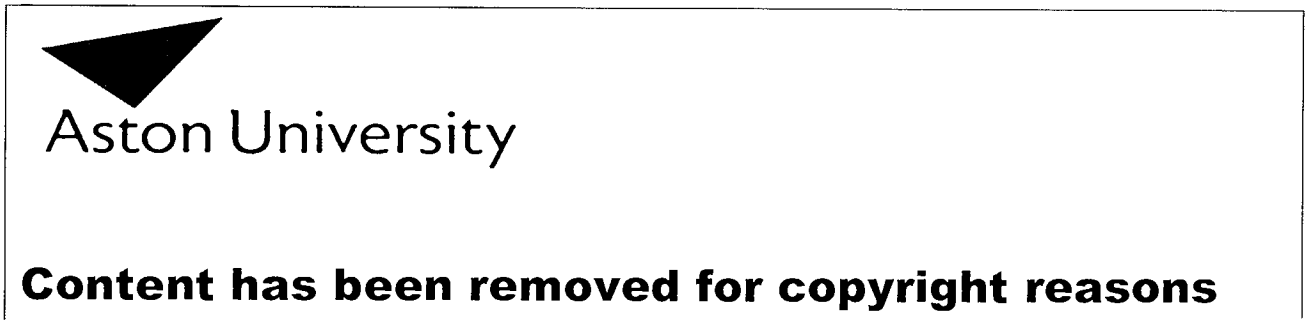

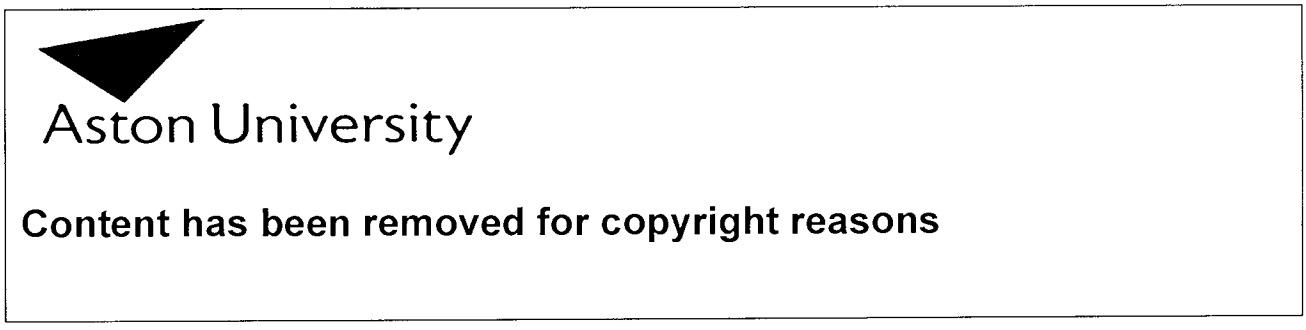

TABLE 3.6 CORRELATION BETWEEN EXPERIMENTAL (HEDGES 1989) AND CALCULATED MOISTURE CONTENTS USING TABLES 3.4 AND 3.5

COLUMN NUMBER	METHOD 1	METHOD 2

** Significant at the

range of those used for the study. This illustrates the pitfalls of extending predictive equations beyond the range of soil values (see Table 3.1a) from which they were originally formulated.

To test the effectiveness of the derived regression equations some independent data were required. These were found in the form of work done by Hedges (1989) on the drainage of 2m high soil columns. The soils within the columns were sands or sandy loams and are described more fully elsewhere (Hedges 1989). The correlation between calculated and observed values of moisture content are shown in Table 3.6 for all 17 soils and for all the values. Two methods were used: method 1 calculated the parameter 'a' using the relationship in Table 3.4, whereas method 2 the moisture content at $^1/_3$ bar, calculated from the expression in Table 3.5, was substituted into Genuchtens equation leaving parameter 'n' as the only unknown, hence it could be then determined. Method 1 consistently produced better results than method 2, giving very high correlation coefficients. However, the four most highly correlated curves (Figure 3.4) clearly show that the curves are not equivalent. This is only to be expected since the curves produced by the predictive equations were meant to be for the whole range of moisture contents and, as the data from Cassel (1974) demonstrated, this requirement was to the detriment of precision at the wet end. Nevertheless, the equations still account for a large amount of the variation.

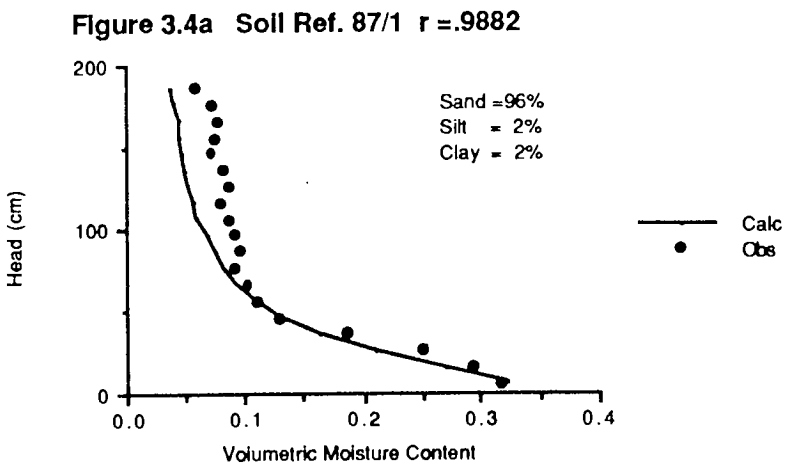

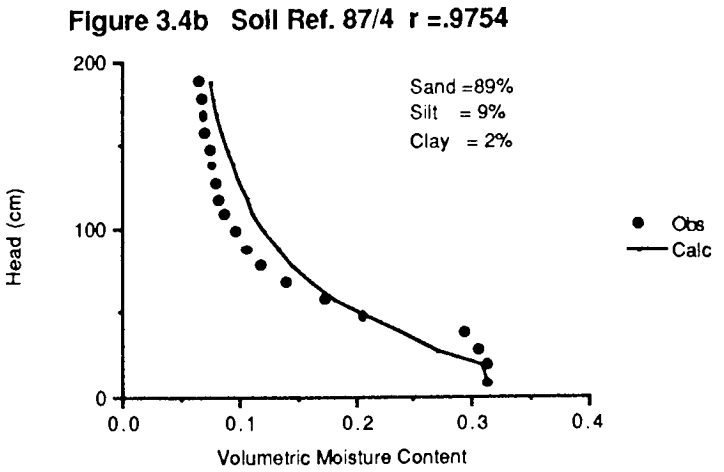

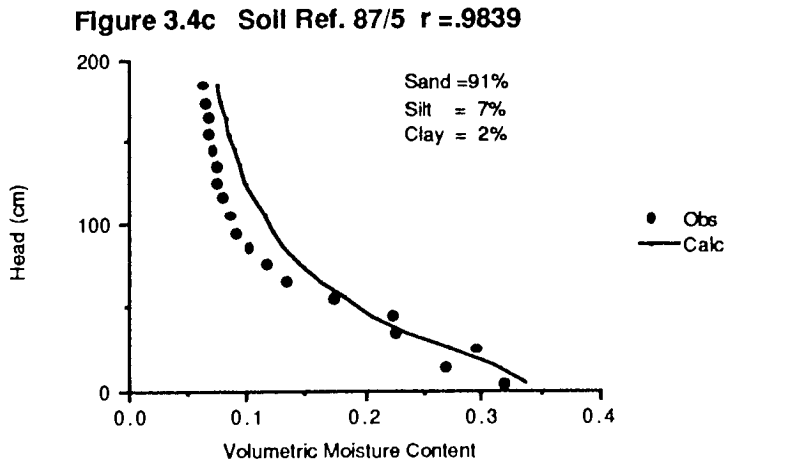

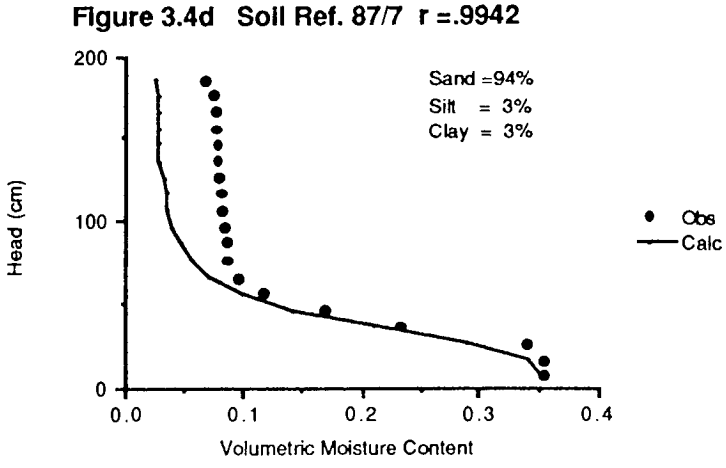

Figure 3.4 Observed and Calculated (Method 1) Soil Moisture Characteristic for Several Soils

This work highlights a number of problems associated with the determination of soil moisture characteristic curves. Firstly the precision of curves and parameters derived by curve-fitting depends on the amount of data available and their distribution along the soil moisture characteristic: e.g around the wet end or the dry end. For field situations, where the range of values required is from 0-15 bars or even higher, a function which only describes one end of the retention curve is of little use. With the data available it was possible to describe the whole curve between 0 and 15 bars provided the characteristic S-shape of the moisture characteristic fell within this suction range. If, as in the case of certain fine soils, significant desorption continued after 15 bars thus not permitting the S-shape to form within the range 0 -15 bars, serious errors could be induced as equating tr to the value of moisture content at 15 bars would not take this into account. Secondly, as Brooks and Corey (1966) point out media in which structure deteriorates on wetting may not follow a typical S-shape (e.g clay), and this was noted when attempting to fit curves to several sets of data.

So far this section has concentrated on determining the drying curve of the hysteresis loop, the remainder is devoted to the wetting curve. Though there are simple methods for calculating the scanning curve (review Jaynes 1984) these are not required within the context of the soil-moisture-plant model being developed. Using the constrained

TABLE 3.7 COMPARISON OF THE PARAMETER a OBTAINED FOR THE DRYING (a_d) AND WETTING (a_w) CURVES FOR SEVERAL SOILS OBTAINED FROM MUALEM (1976b)

model of Kool and Parker (1987) in which the drying and wetting boundary curves are calculated using Genuchtens equation in which only the parameter 'a' is allowed to vary from one curve to the other, the equations were fitted to data from Mualem (1976b). First the equation was fitted to the drying curve then only allowing 'a' to alter it was fitted to the wetting curve. The results shown in Table 3.7 indicate that the value of the parameter 'a' for the drying curve is twice that of the wetting curve. Kool and Parker (1987) using eight of the soils used in this analysis, concluded likewise. Bouwer (1964,1969) suggested a similar relationship but in connection with the Brooks and Corey Equation.

In summary several regression equations have been formulated relating soil variables to the parameter values 'a' (Table 3.4), 'n' (Table 3.4) and tr (which is equated to the moisture content at 15 bars itself derived from the statistical relationship in Table 3.5) in the Genuchten equation. In this study it was concluded that the quality of the data was important. These relationships were then used to produce moisture characteristic curves for several soils and compared with the experimentally derived suction curves for these soils (Hedges 1989) with success. With the drying curve defined it was found that the wetting curve could be described by simply using the parameter values of the drying curve with the exception of parameter a which was halved. The equations produced are only valid for the range

of soil property values summarised in Table 3.1a and especially for sands, loamy sands, sandy loams and loams which make up the majority of the soils used.

3.2.2 CONDUCTIVITY

The measurement of unsaturated conductivity tends to be prohibitive in terms of cost, and is usually only done for fundamental research purposes and in major projects. Results obtained from field data have shown the large spatial variability in conductivity (Carvallo et al 1976, Nielsen et al 1973). With this in mind a number of authors have tried to relate the relationship to other field-derived data such as the retention curve and particle-size distribution.

A number of early equations (Childs and Collis-George 1950, Marshall 1958, Millington and Quirk 1959,1960) were based on the idea that the retention curve reflected the pore-size distribution within the soil. The soil is split into a number of pore-classes the range of which can be calculated from the retention curve. For each class a conductivity value is calculated based on the number of classes still containing water and the size of connecting pores determined in a probabilistic way. Since each class represents a section of the retention curve, a number of points can be plotted on the conductivity-suction [K(h)] curve.

Reviews of these various methods (Jackson et al 1965, Green and Corey 1971 and Gradwell 1974) all indicated good agreement between calculated and observed values of conductivity. The agreement between calculated and observed conductivity-suction (K(h)) curves can be improved by determining a matching coefficient. This was found by equating a point on the calculated curve with the corresponding point on the observed. This is normally the saturated conductivity (Ks) value as this is the most easily obtained. The use of Ks as a matching factor is discussed later in this section. The problem with these relationships is that they calculate the conductivity-suction relationship, and as the suction curve is hysteretic so then will be the conductivity function. The pore-size method though is only suitable for describing the drying curve (Green and Corey 1971). What is needed is a method of describing the conductivity-moisture content relationship.

Jaynes and Tyler (1984) describe a relationship derived statistically between K(h) and particle-size data. However, this has only been formulated for sandy soils and as Schuh and Sweeney (1986) demonstrated it does not work well for finer soils. In addition it describes only the draining portion of the curve.

The most promising methods make use of parameters found in equations describing the retention function as this means the number of parameters needing to be determined are

reduced. Two examples are presented by Laliberte et al (1966) (which utilizes the Brooks and Corey Equation) and by Genuchten (1978) using parameters derived within his paper. Genuchtens equation is used to describe the retention function within this model, the method of determining these parameters based on soil properties has been developed within this chapter. Genuchten (1978,1980) and Genuchten and Nielsen (1985) have also shown it to produce acceptable results. For these reasons it is this method which is to be used to describe the conductivity function. The general form of the relationship is:

$$K_r = Se^{0.5}.[1-(1-Se^{1/m})^m)^2 \qquad -3.5a$$

$$K = f.K_r \qquad -3.5b$$

where K_r = relative conductivity $K_r = K/K_s$

Se = as equation 3.2

m = $1-1/n$ as equation 3.3

K = conductivity ($cm\ s^{-1}$)

f = matching factor ($cm\ s^{-1}$) normally taken as K_s

Genuchten (1978,1980b) has shown this method to adequately describe the shape of the conductivity-moisture content [K(t)] function. The saturated conductivity was used as the matching factor in these examples. However, Genuchten and Nielsen (1985), though realizing the relative ease with which K_s can be measured, suggested that it may be better to

match the curve at some other value. This is due to the fact that at saturation K is ill-defined since it may be influenced by cracks or pores which are unrepresentative of the overall matrix. Carvallo et al (1976) also noted this and matched their curves at lower K(t) values thus reducing the variation between measured and calculated conductivity values.

Genuchten's work involved the determination of parameters for the conductivity equation from actual soil moisture suction data. The present work determines the characteristic curve from particle-size data as this is easier and cheaper to collect from the field. To investigate whether the K(t) relationship can still be adequately described using this approach, a study of several soils was conducted using data from Mualems (1976b) catalogue. Using the particle-size data, the values of parameters tr and 'm' were calculated from the regression equations formulated in Section 3.2.1.2, and thus the K(t) function defined. The derived function was then compared to the relevant observed conductivity data. The two curves were matched by a matching factor. Using Supercalc 3, a spreadsheet package, it was possible to match the derived K(t) function with each point in turn to determine which matching factor gave the minimum difference between the curves as signified by the sum of squares (SSQs). All of the results of the analysis are shown in Figures 3.5 and 3.6.

Figure 3.5 Conductivity/ Moisture Content Relationships

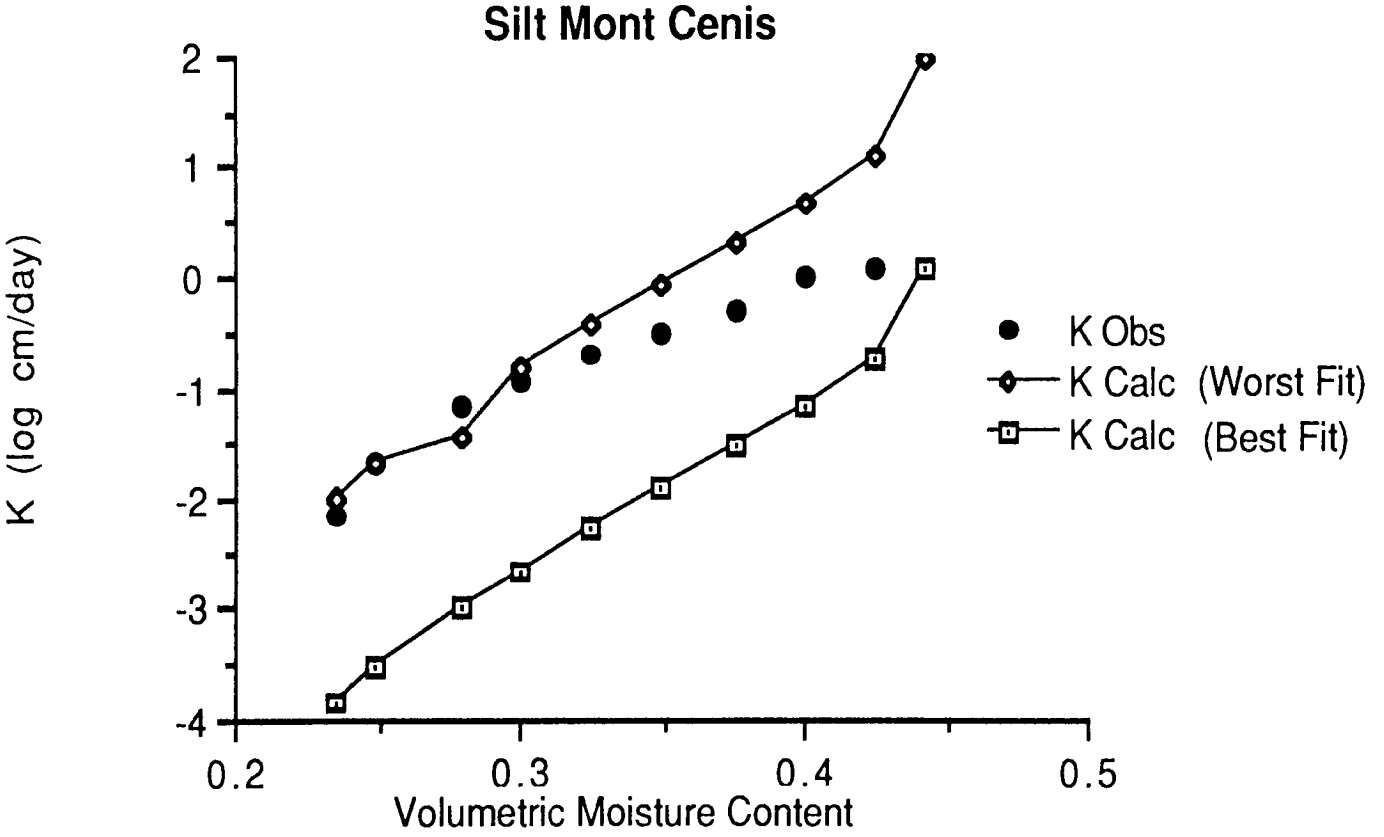

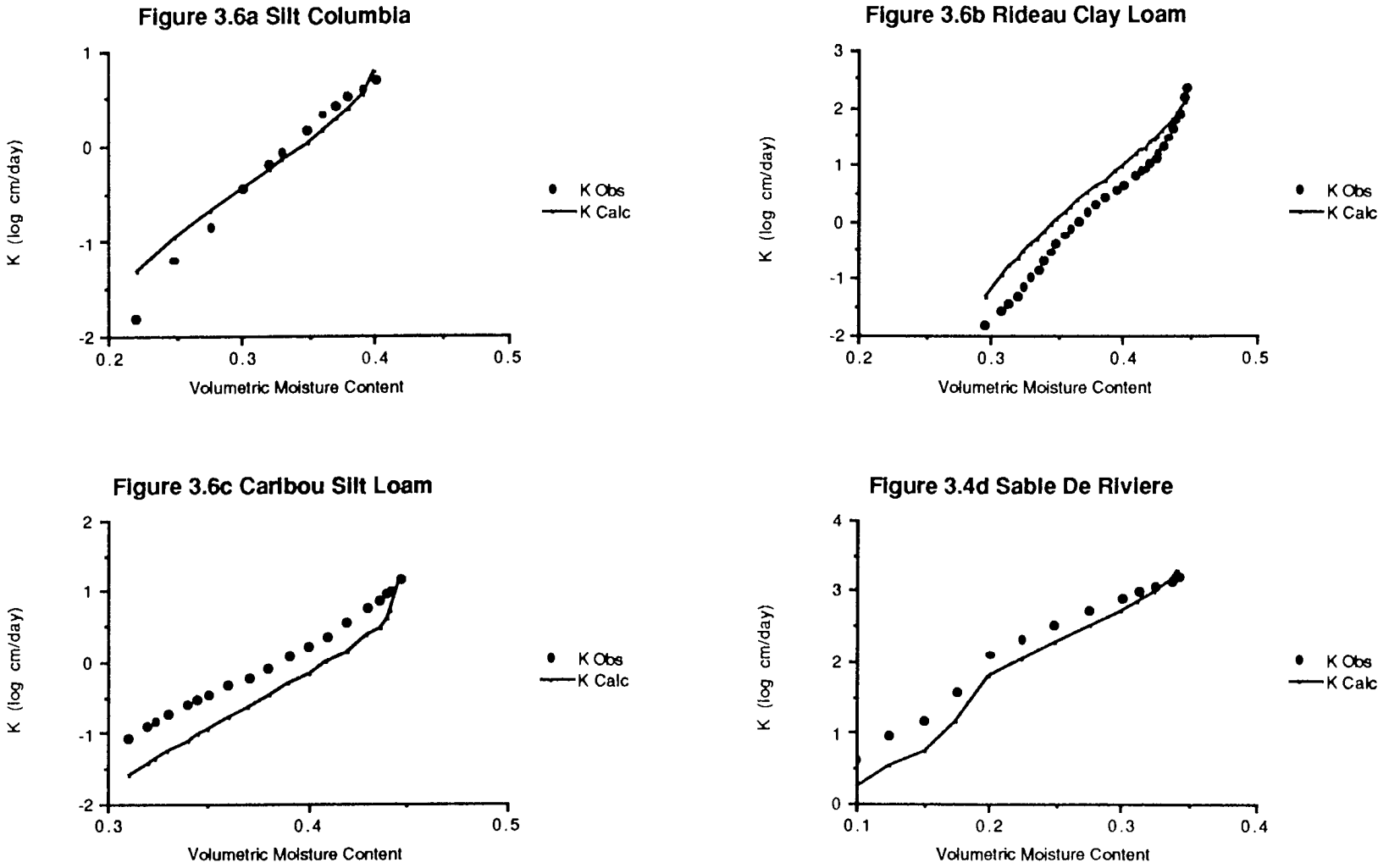

FIGURE 3.6 Comparison of Calculated Relative Conductivity-Moisture Content Values With Those Observed by Mualem (1976b) for Several Soils

TABLE 3.8 CORRELATION COEFFICIENTS FOR CALCULATED K AND OBSERVED K FOR FIVE SOILS GIVEN BY MUALEM (1976b)

Aston University

Content has been removed for copyright reasons

TABLE 3.9 CORRELATION COEFFICIENTS FOR CALCULATED AND OBSERVED DRAINAGE RATES FROM NINE SOIL COLUMNS (HEDGES 1989)

Aston University

Content has been removed for copyright reasons

In two of the soils: Silt Mont Cenis and Silt Colombia the shape of the calculated curve does not adequately represent that of the observed data. In the case of the Silt Mont Cenis the least SSQs is given by matching the saturation point, though looking at Figure 3.5 suggests the worst fit (i.e highest values of SSQs) produces a curve which seems to match the observed curve better. This is because errors near saturation are numerically more significant than those at the drier end of the curve, where errors may be tolerated (Green and Corey 1971). All but two of the curves produced the least SSQs by matching at saturation - Silt Colombia and Sable De Riviere. The latter soil matched at the next wettest value. In both cases the lower SSQs found by this alternative matching point is not significantly less than matching it to the saturation point. Table 3.8 shows that in all cases significant correlations are achieved between measured and observed conductivity.

The above study indicates that the described regressions approximate the K(t) curve reasonably well once a matching factor has been used. In these examples matching at saturation produced the best results.

3.2.3 SOIL WATER MOVEMENT EQUATIONS

Although there have been numerous solutions of the Richards equation using numerical methods (e.g Laat 1976,

Tompson and Gray 1986a,b), the method used in this analysis was that proposed by Hussein (1979) and Walley and Hussein (1982) as shown by equation 3.6:

$$V_i = K_i \cdot \left[\frac{S_{j+1} - S_j}{(D_{j+1} + D_j)/2} + 1 \right] \qquad -3.6$$

where V_i =flow across the ith layer boundary (cm s^{-1})

K_i =conductivity at the ith boundary (cm s^{-1})

S_j =suction head in the jth layer (cm)

D_j =thickness of the jth layer (cm)

In Husseins' (1979) work K_i was calculated from a K(h) relationship, head was determined at the juncture of the two layers from where K_i could be found. However, within the context of the present work, it is K(t) which is calculated for each layer and then K_i is calculated from a weighted harmonic mean (Section 3.3.2). For capillary rise equation 3.6 is used, but with the suction head being calculated from the wetting curve using the altered value of parameter 'a' (Section 3.2.1.2).

To test the above model a number of simulations were run using a model formulated for this purpose (Figure 3.7) and data derived from drainage columns (Hedges 1989). Observed drainage was compared with calculated and the resulting correlation coefficients are given in Table 3.9. Figure 3.8 plots the calculated drainage rate over time

FIGURE 3.7 FLOWCHART FOR PROGRAM COLSIM

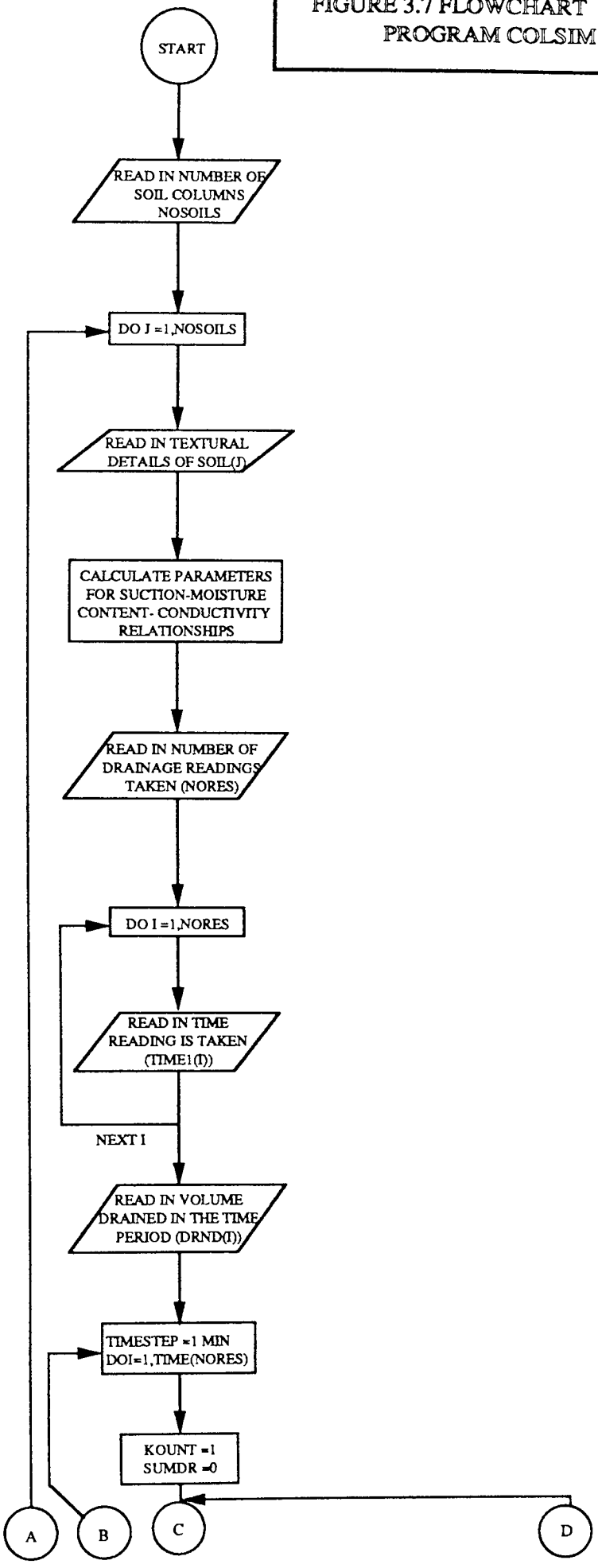

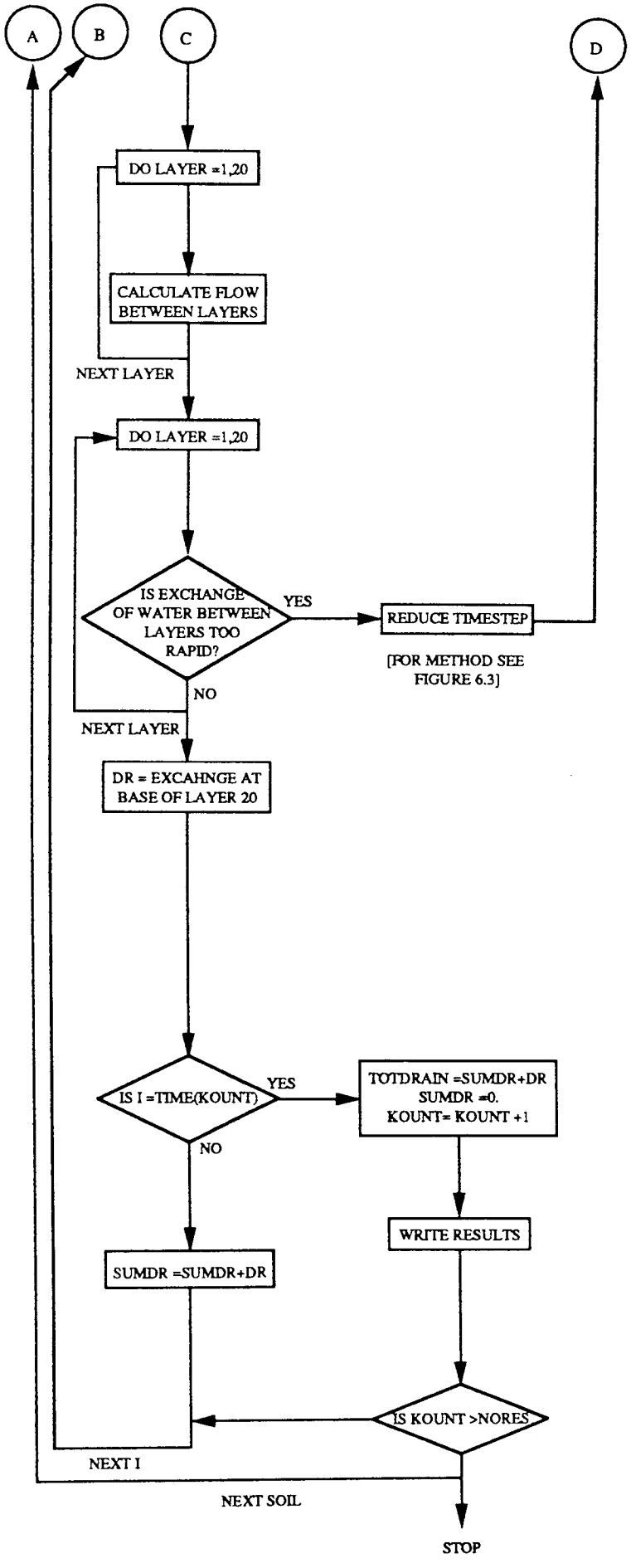
A
B
C
D
DO LAYER =1,20
CALCULATE FLOW BETWEEN LAYERS
NEXT LAYER
DO LAYER =1,20
IS EXCHANGE OF WATER BETWEEN LAYERS TOO RAPID?
YES
REDUCE TIMESTEP
[FOR METHOD SEE FIGURE 6.3]
NO
NEXT LAYER
DR = EXCAHNGE AT BASE OF LAYER 20
IS I =TIME(KOUNT)
YES
TOTDRAIN =SUMDR+DR
SUMDR =0.
KOUNT= KOUNT +1
NO
WRITE RESULTS
SUMDR =SUMDR+DR
IS KOUNT >NORES
NEXT I
NEXT SOIL
STOP

Figure 3.8a Soil Ref. 87/0 r =.9035

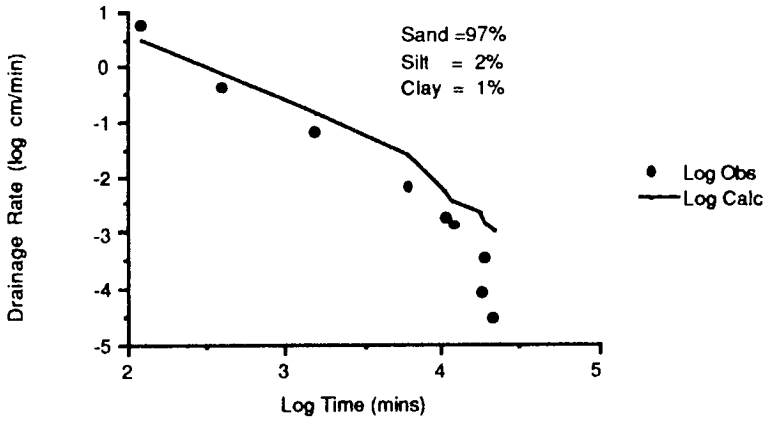

Figure 3.8b Soil Ref. 87/1 r =0.5361

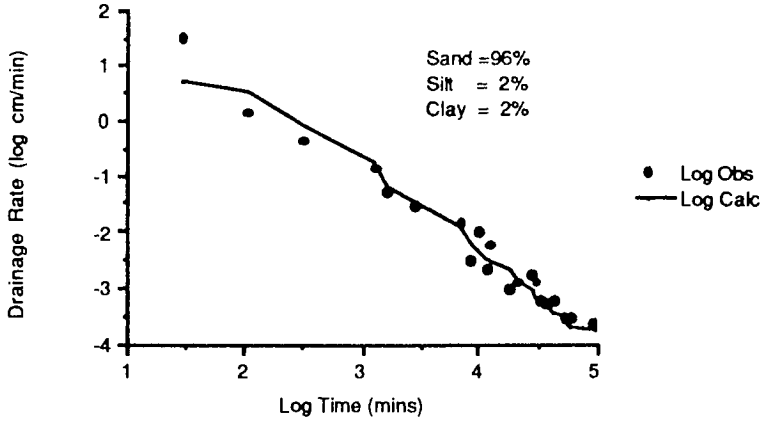

Figure 3.8c Soil Ref. 87/3 r =.9947

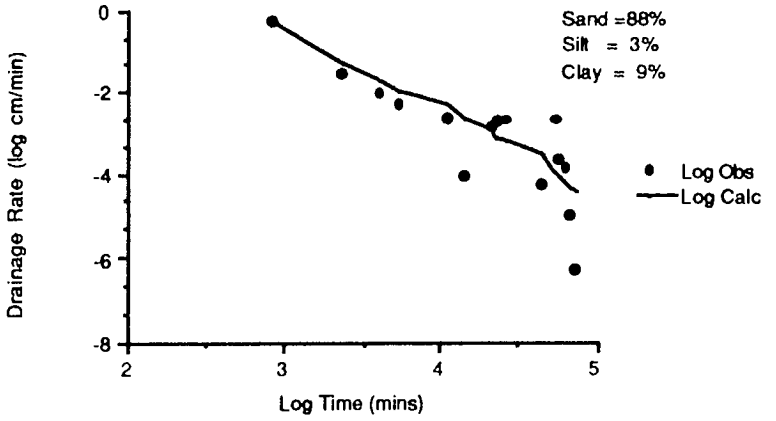

Figure 3.8d Soil Ref. 87/4 r =.84

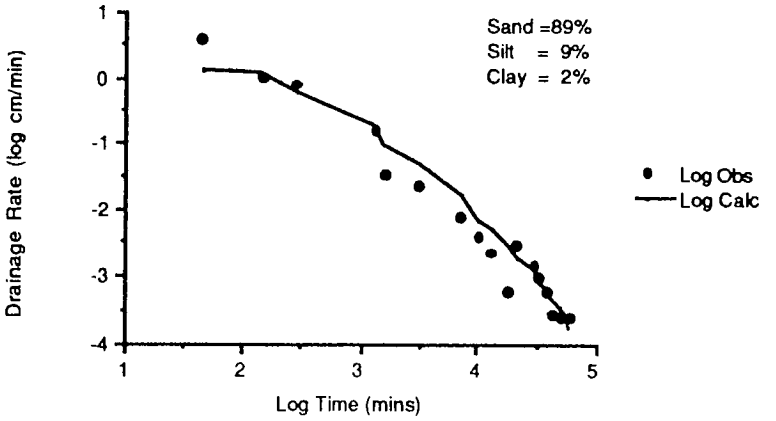

Figure 3.8a-d Comparison of Calculated Drainage Rates to Observed (Hedges 1989) for Several Soil Columns

Figure 3.8e Soil Ref. 87/6 r =.9691

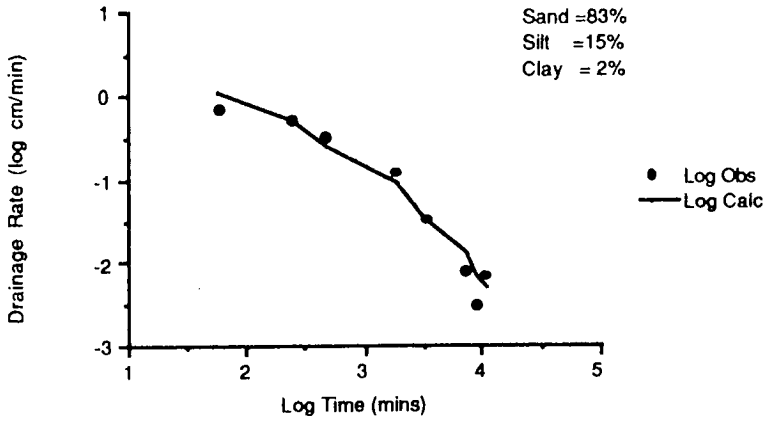

Figure 3.8f Soil Ref. 88/4 r =.9332

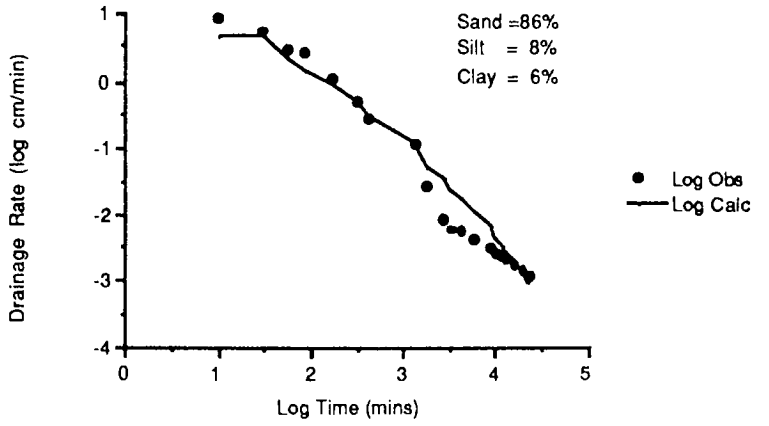

Figure 3.8g Soil Ref. 88/5 r =.8153

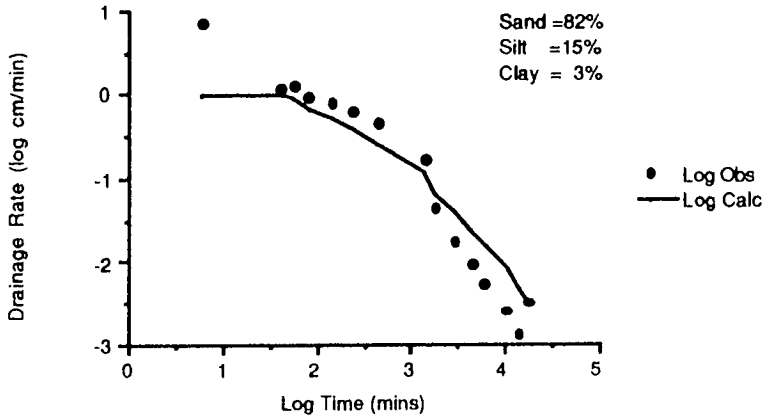

Figure 3.8h Soil Ref. 88/8 r =.9025

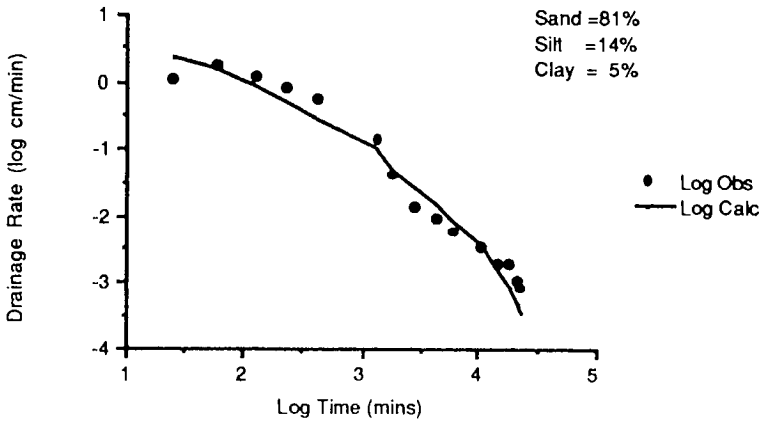

Figure 3.8e-h Comparison of Calculated Drainage Rates to Observed (Hedges 1989) for Several Soil Columns

against the measured rate.

All simulation runs show very significant correlation between observed and calculated drainage. From Figures 3.8 it can be seen that with the exceptions of 87/1, 87/4 and 88/5 the graphs of calculated and observed rates are very similar. In columns 87/1, 87/4 and 88/5 the initial drainage rate of the observed column was much greater than that of the simulated one. The calculated curves are generally smoother especially at lower flows where different degrees of compaction within the actual columns may have retarded flow for a while. This is best seen in columns 87/1, 87/3 and 87/4.

In conclusion it can be noted that equation 3.6, on the evidence of these runs, produces a reasonable prediction of drainage rate, especially considering that neither suction nor conductivity were measured but were predicted from physical soil properties (Sections 3.2.1.2 and 3.2.2). However, it should be pointed out that all the soils studied where of a sand or loamy sand texture and that for soils of finer texture the method of prediction is not proven.

3.3 INFILTRATION

Infiltration is defined by Freeze (1969) as the entry of water into the soil and its subsequent downward flow. The

rate at which it enters the soil (infiltration rate) and the maximum rate at which it can enter (infiltration capacity) are affected by a number of factors. The following two sub-sections describe the processes that influence infiltration and discuss these in relation to the infiltration model used within the present work.

3.3.1 FACTORS AFFECTING INFILTRATION

Horton (1933,1939) considered the condition of the soil surface as the most important factor determining infiltration, relating the decrease in infiltration with the increased compaction of the soil. However, more recently several authors have commented that it is the flow regimes within the soil that have the most profound effects (e.g Gardner 1967, Tricker 1981 and Bonnel and Williams 1986). Though apparently contradictory, both viewpoints are equally valid when considered in the context of the wide variety of soils, vegetation types and climatic regions.

Surface factors affecting infiltration include those of vegetation, soil compaction, mulching and macropores. As Horton hypothesized, the soil becomes more compact as a rainstorm continues due to the energy released by raindrop impact, producing a surface crust. Mc Intyre (1958) when studying fine sandy loams, noted a thin 0.1mm thick skin with no visible pores overlying a 1.5-3.0mm layer of reduced

porosity due to the inwashing of fines. Tarchitsky et al (1984) also found this skin on sands and clays as well as sandy loams, below this was a layer with a higher bulk density than the surrounding soil and of similar size to McIntyre's washed-in zone. Tackett and Pearson (1965) and Moore (1981a) also noticed such seals in clay soils, but observed that these were in the main formed by slaking as opposed to impact. Irrespective of their mode of formation these layers greatly reduce infiltration: McIntyre (1958) noted reductions in permeability of 2000 times in the crust and 200 times in the washed-in region; and Edwards and Larson (1969) and Moore (1981a) noted reductions in infiltration of 50% and 80% respectively. These reductions would be even greater except for the formation of tensions in the soil below the crust which produce movement of water through them in excess of saturated conductivity (Edwards et al 1980).

Moore (1981a) notes that mulching and organic matter have an opposite effect on infiltration to seals and Tricker (1981) observed that litter layers can also increase infiltration. This can be attributed to the fact that they absorb much of the water, in the case of litter up to two to three times their weight, and then release it slowly (Tricker 1981). Vegetation can also have indirect effects. By reducing raindrop impact and acting as a rainfall store, it thus smooths over the effects of an intense storm, although the longer the storm the less is this effect (Ward

1975). The presence of macropores also increases infiltration and may negate the effects of crusts. This latter point is more fully described in Section 3.4.

The flow regimes within the soil play an important role in the absorption of water. The observed pattern of the infiltration curve (i.e declining after a short period to the saturated conductivity of the soil, Figure 3.9) is a function of the transmitting ability of the underlying soil. Even if the surface increased its ability to absorb water it cannot absorb it faster than the rate at which it is transmitted downwards once the surface layers have become saturated. The initial high rate of matrix infiltration is the product of steep suction gradients produced on initial wetting, but these decrease as water is transmitted down the profile. Colman and Bodman (1945) described four major zones of water movement down the profile (Figure 3.10):

1. at the top a saturated region only a few cms thick;
2. a zone where moisture content changes slowly with depth;
3. a zone which is wetting;
4. the wetting front delineating the extent of infiltration.

The initial moisture content affects this pattern, with high values reducing the infiltration rate but increasing the rate of penetration of the wetting front (Gray and Norum 1968, Philip 1957e). Philip (1957e) attributed this to a storage effect. The initial moisture content can also

Figure 3.9 A Typical Infiltration Curve

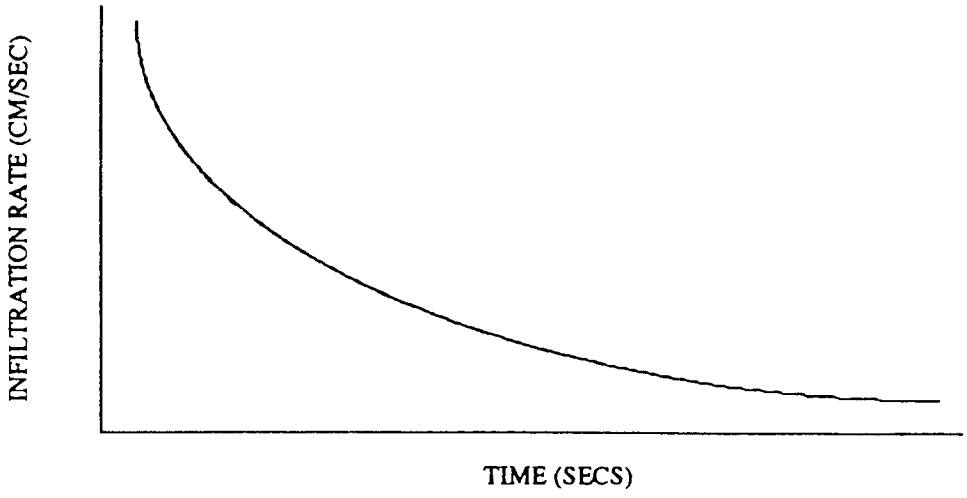

Figure 3.10 Moisture Zones During Infiltration (Adapted from Ward 1975)

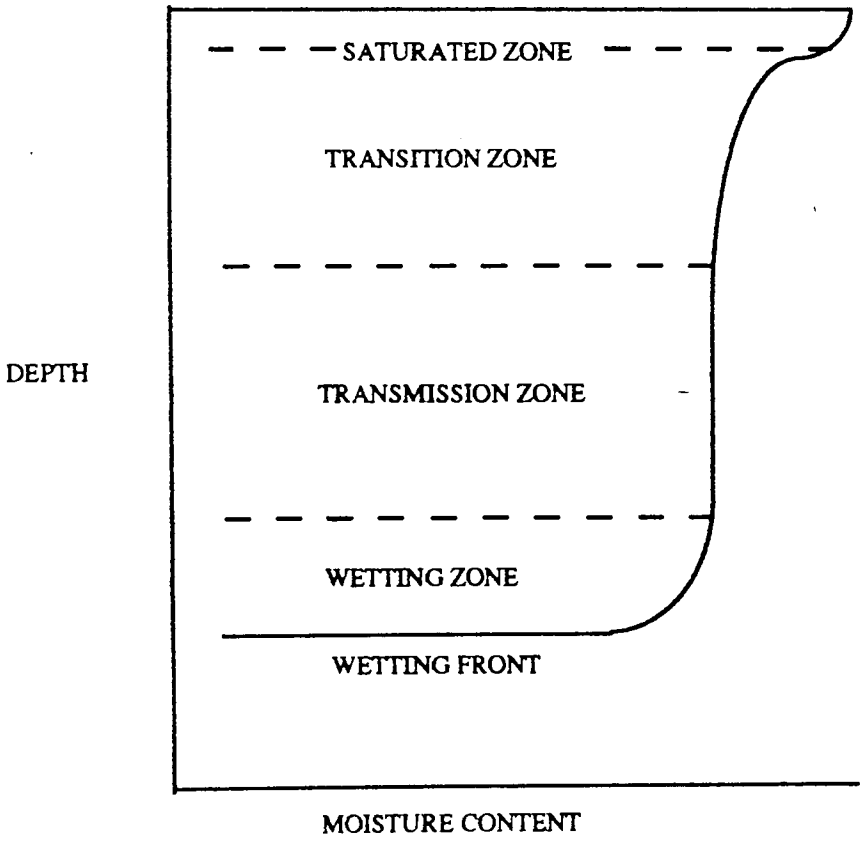

influence the moisture gradient at the wetting front: dry soils produce sharp and distinct fronts.

The preceeding discussion on flow regimes within the soil has referred to homogeneous soils under ponded conditions. In the field this is not normally the situation because soils are non-homogeneous and infiltration takes place under non-ponded conditions (Dunin 1976). Where ponded conditions do not form, water is transmitted freely down the profile. The situation with respect to non-homogeneneous soils is described below.

In non-homogeneous profiles it is the finer layers, or layers of lower conductivity which control the infiltration rate (Colman and Bodman 1945, Childs and Byobordi 1969). This effect is seen most clearly where coarse soils overlie finer (Moore 1981a) and infiltration proceeds in the lower layer at the same rate as if it were at the surface (Colman and Bodman 1945).

Where a fine layer overlies a coarse layer, the coarse layer may actually reduce conductivity to below that of the fine layer. Several authors have observed that there is a build up of moisture above the boundary of the two layers (e.g Stroosnijder et al 1972 and Asseed and Swartzendruber 1975). Aylor and Parlange (1973) suggest this is because the water in the fine layer has to be near saturation before it can enter the underlying coarser layer. Asseed and

Swartzendruber (1975) also show that when the wetting front does enter the coarser layer the moisture content of the transmission zone is less than the value obtained if the coarse layer was above the finer layer. Hillel (1987b) in a review of such boundaries noted the existence on non-Darcian unstable flow conditions at and below the juncture. This occurred in the presence of apparently random pathways propagating downwards, which he termed "fingers". These were unpredictable in their position and occurrence.

Trapped air within the profile may also affect infiltration. Wilson and Luthin (1963) noted that the build-up of pressure ahead of a wetting front may form sufficient head to slow it. Touma et al (1984) observed a decrease of a third in infiltration rate in a soil column due to air pressure. Adrian and Franzini (1966) however, consider this effect to be negligible in the field due to the fact that there is little lateral restraint to air movement.

The preceding discussion on infiltration in homogeneous and non-homogeneous soils has assumed that in the lateral direction the soils and surface cover are constant. In reality this is not the case: indeed there is great spatial variability in factors such as saturated conductivity (e.g Carvallo et al 1976) and the distribution of macropores (Green and Askew 1965).

The importance of surface effects and flow dynamics

(i.e their magnitude, relative dominance and spatial variability) depend on the soil conditions. With bare soil, Morin and Benyamini (1977) showed that it is the formation of a crust which most determines the moisture movement rate, whereas where vegetation is present it is the flow processes within the soil which dominate. Schumm and Lusby (1963) noted that the highest rates of infiltration were in the summer when soil fauna and flora were active, indicating that the above factors vary in magnitude between the seasons.

Macropores vary in size and abundance according to the seasons. Dessication cracks may form in summer due to drying and in winter due to the formation of ice crystals, and both forms of cracks may be destroyed by the swelling of the soil on wetting (Schumm and Lusby 1963). Swelling may also destroy channels formed by the fauna and flora and they may also be destroyed by the reworking of the soil by worms and other burrowing animals, though Green and Askew (1965) suggest macropores formed by fauna may be more permanent, lasting for several hundred years. From the preceeding discussion it can be seen that there is temporal as well as spatial variability in infiltration.

3.3.2 THE INFILTRATION MODEL

A large number of models have been proposed to describe

infiltration. Some based on the solution of the Richards equation (e.g Campbell et al 1985, Jayawardena and Kaluarachiki 1986 and Molen 1986) but there are a number of semi-empirical models (e.g Green and Ampt 1911, Philip 1957a-e, 1958a,b, Holtan 1961 and Horton 1941). These latter equations have been shown to give good results in differing conditions (Watson 1959, Skaggs et al 1969, Gifford 1976 and Bonnel and Williams 1986). In the model adopted in this research the Green and Ampt relationship was chosen due to the ease with which the parameter values could be calculated using the suction-moisture content curve formulated in Section 3.2.1. This therefore reduced the total number of parameters in the soil-moisture-plant model. The model employed is similar in design to that of Mein and Larson (1973) but works for multiple layers.

The model is divided into two modes:

1. when rainfall is less than or equal to the saturated conductivity, of the surface layer. However, in some cases where the wetting front has moved further down the profile it is the saturated conductivity of the layer containing the wetting front which is considered;

2. when rainfall exceeds the saturated conductivity.

In the first instance water is allowed to enter the soil freely. In the second case, the amount of infiltration occurring before ponding occurs is calculated using the expression formulated by Mein and Larson (1973) ;

$$Fs = (Hf.Md)/((I/Ks)-1) \qquad -3.7$$

where Fs = amount of infiltration up to ponding (cm)

Hf = suction at the wetting front (cm)

I = rainfall intensity (cm s^{-1})

Ks = saturated conductivity (cm s^{-1})

Md = moisture difference across the wetting front ($ts-t_{int}$)

ts = saturated moisture content

t_{int} = initial moisture content

Once ponding has occurred equation 3.8 derived from Fok (1970) and Flerchinger (1988) for infiltration into multiple layered soils is used to calculate the infiltration:

$$Fp = \frac{Hf+Ln-Li}{\frac{Ln}{Kfn} + \frac{Li}{Kfi}} \qquad -3.8$$

where Fp = infiltration rate (cm s^{-1})

Kf = conductivity within the transmission zone (cm s^{-1})

L = length of wetting front (cm)

Subscripts i and n refer to the layer the wetting front is in and the sum of the layers above this respectively

Equation 3.8 reduces to 3.9 as given by Mein and Larson (1973), when the surface layer only is involved.

$$Fp = Kf.(1+(Hf/L_1)) \qquad -3.9$$

In both equations 3.8 and 3.9 the parameter L is calculated from equation 3.10 (Mein and Larson 1973).

$$L = Fa/Md \qquad -3.10$$

where Fa =sum of water infiltrated (cm)

Equations 3.8 and 3.9 apply where conductivity decreases with depth, but (as seen in the previous discussion) where a fine layer overlies a coarse layer the wetting front is first halted then becomes unstable. Within the context of the present model it is not possible to predict these or estimate such an effect. Instead it is assumed that the wetting front halts at the boundary and infiltration is then evaluated assuming that the wetting front remains stationary, the infiltrated water being added directly to the layer below the wetting front. This continues until the underlying layer is saturated after which the wetting front is assumed to have moved through the coarser layer. The overlying layer is thus considered to control the infiltration rate, as was stated by Coleman and Bodman (1945).

Careful examination of equation 3.7 shows that conductivity is calculated for a number of layers using the weighted harmonic mean. Bouwer (1969) described parallel

flow (i.e arithmetic mean where the soil properties vary in a horizontal direction) and series flow (i.e harmonic mean where they vary in a vertical direction or in layers), and indicated that in a real soil flow would be a combination of these two types. However, the model under development assumes that the soil is heterogeneous vertically (i.e layered) and that within the layers the properties are homogeneous. So to maintain consistency the harmonic mean is used.

At the start of this section it was noted that this model was used because of the ease with which the parameters in the Green and Ampt relationship can be calculated from the soil moisture characteristic. Rawls et al (1983) describe how the parameter Hf is calculated from the Brooks and Corey equation (equation 3.2). Referring back to Section 3.2.1.2 it can be seen that Genuchten's parameters can be related to those of Brooks and Corey (equations 3.3d & 3.3e). Substituting these into the expressions given by Rawls et al (1983) gives equation 3.11.

$$Hf = (2+3L)/(1+3L).(1/2a) \qquad -3.11$$

where $L = n-1$

n and a are parameters of Genuchtens equation

Bouwer (1969) has shown the other unknown parameter Kf to be approximately half the value of Ks.

Unfortunately insufficient data were found in the literature to allow the infiltration componenet to be tested independently of the larger model.

3.4 MACROPORES

The occurence of large vertically continuous channels within the soil has led to speculation that these features may be instrumental in determining infiltration. Observations by Beven and Germann (1981), who noted greatly reduced conductivities when macropores were drained, and by Scotter (1978), who noted the more rapid transport of nutrients and pollution along these paths than in the surrounding matrix, have borne out this point. Macropores are normally defined either by their size or by the capillary potential at which they drain. Beven and Germann (1982) give the following description of macropores, "the movement of water through the macropores once initiated, may be much faster than the equilibration of potentials in a representative volume of the soil matrix. If this is so, the potential gradients associated with the two systems will be different".

The following sections describe to the best of present knowledge in a poorly understood area, the formation of macropores, their dynamics and importance in infiltration, and finally the modelling of these drainage structures.

3.4.1 MACROPORE FORMATION AND CHARACTERISTICS

A macropore can be generally assigned to one of three groups dependent on its origin. They may be formed by fauna, flora or mechanical means, and owe their characteristics to the method of formation.

Channels formed by fauna, depend on the type of animal for their characteristics. The holes tend to be tubular in shape varying widely in size from those formed by insects (Bryson 1939) and worms, to the burrows of rabbits, prairie dogs and moles (Hole 1981). Green and Askew (1965) noted ant colonies in which greater than 5% of the soil volume consisted of burrows. Edwards and Lofty (1980), Edwards et al (1988) and Ehlers (1975) reported large numbers of earthworms per square metre of plan area in some areas. However, these are greatly reduced if the land is tilled. The burrows of insects tend to be shallow and intertwining (Bryson 1939) as do those of some worms, but deeper burrowing species such as the worm *Lumbriscus terrestris* can reach depths of 2 metres or more (Edwards and Lofty 1972) and are commonly a metre deep (Edwards et al 1988).

Old and decaying roots can also provide channels. The nature of the rooting system will determine the channel pattern. In some plants the roots can form pipes as the inside of the root decays leaving the cork material on the outside of the root still intact. This is especially true of

trees. Water stress can cause the root to shrink (Cole and Alston 1974) allowing water flow along the outside of the root. The importance of roots in channelling water was demonstrated by Beven and Germann (1982), who showed that old and decaying roots of corn channelled water.

Mechanically formed channels owe their origin normally to dessication or thermal cracking, but larger structures such as pipes may be formed by erosive action (Beven and Germann 1982). Gillham and Newson (1980) described such structures in Upland Wales, but these large features are not of relevance to this project. Channels formed by dessication or thermal means tend to form planar cracks several centimetres wide and up to a metre deep (Ritchie and Adams 1974, Reeve et al 1980, Avery 1973). Cracking has been correlated most notably with clay and its mineralogy (Greene-Kelly 1974, McCormack and Wilding 1975, Schafer and Singer 1976 and Reeve et al 1980). The pattern of these planar features is often polygonal with cracks being up to 25cm apart (Reeve et al 1978), but they can follow planes of weakness (White 1986). However, Scott et al (1986) showed the patterns to be the result of random processes. Cracks may form in the same pattern and position during various phases of wetting and drying on bare ground (Virgo 1981), but where plants occur differing crack patterns are seen from cycle to cycle.

3.4.2 FLOW IN MACROPORES

Due to their relatively large size water will not enter macropores until the soil is near to saturation. Scotter (1978) describes channels greater than 0.2mm in diameter and cracks greater than 0.1mm as being air-filled if soil suction is greater than 15cm. Therefore, for most of the time their worth as conduits for bypassing the matrix is not utilized. Bouma et al (1982) and Bouma and Anderson (1977) showed that covering the macropores with a thin layer of soil restricted this preferential flow and Gardner (1962) noted that macropores not connected with the surface were ineffective at transmitting water through the soil. So when are macropores important?

Macropores are of significance when rainfall exceeds infiltration capacity and water is available for flow into the channels connected to the surface. Rain falling directly into the channels is considered insignificant due to the small plan area occupied by the channels (Beven and Germann 1982) - e.g 1.4% of the ground surface area (Edwards et al 1988). When infiltration capacity is exceeded water penetrates deep into the network, though only along channels connected to the surface (Ehlers 1975). It flows along the wall of the macropore, as has been shown by dye-staining techniques (Bouma and Dekker 1978 and Omoti and Wild 1979) and the use tritium tracers (Blake et al 1973). Flow within these channels is rapid and channels such as wormholes may

fill in around one minute (Bouma et al 1982).

3.4.3 MACROPORE MODEL

The model developed distinguishes between 2 divisions of macropore based on their origin, that is: 1) faunal and floral or permanent channels; and, 2) shrinkage or temporary channels. For each of the divisions included in the model a number of classes may be added e.g different species of worms, mixed crops etc. For each of the classes the following parameters are required:

a) layer into which they extend (d_l), it is assumed that the macropore extends to the base of this layer so the depth of the crack can then be calculated;

b) radius (r) or width (w) of the channel;

c) number of macropores per square metre for each class (a_n).

The total number of macropores from all classes per square metre (a_t) is then calculated.

For faunal and floral channels these values stay constant throughout the simulation, as Green and Askew (1965) pointed out that in untilled soils faunal channels are near permanent. With floral channels there is a great deal of uncertainty as to which channels are associated with the flow, since water may flow down the outside of live

roots, within dead hollowed-out roots and also in channels left by decayed roots (Beven and Germann 1982). With present knowledge the inclusion of factors to take account of this would complicate the model and would not be theoretically based.

For the temporary channels cracks may expand and crack further due to shrinkage, or may close due to the swelling of the ped. To simulate dessication cracking it is assumed that the cracks form in a square pattern with a spacing between parallel cracks of 25cm, a commonly observed distribution (Reeve et al 1978) which produces 8 cracks per square metre. Assuming isotropic shrinkage (Jarvis and Leeds-Harrison 1987a,b) the width of the cracks can be calculated provided the shrinkage characteristics are known. Data describing shrinkage relationships are sparse, but Reeve et al (1980) have shown a positive correlation between clay content and shrinkage. They found for a number of soils that shrinkage between 0.05 and 15 bars varied from 5-27% while clay content varied from 26-89%. Assuming that the lower and upper limits of both variables correspond and that the relationship is linear, equation 3.12 was derived:

$$sv = 0.35c - 4.2 \qquad c > 12.0 \qquad -3.12a$$

$$sv = 0.0 \qquad c <= 12.0 \qquad -3.12b$$

where sv =maximum possible shrinkage between 0.05 and 15bar (%)

c =clay content (%)

This relationship is simplistic and assumes all types of clay behave in the same way, but it is adequate for this purpose. Assuming the soil shrinks linearly from 0.05-15bars the shrinkage-moisture content characteristic can be calculated by employing equation 3.13:

For t <= tf

$$s(t) = (1-((t-tr)/(tf-tr))).sv \quad -3.13a$$

For t > tf

$$s(t) = 0. \quad -3.13b$$

where t =volumetric moisture content

tr =volumetric moisture content at 15 bars

tf =volumetric moisture content at 0.05bars

s(t) =shrinkage as a function of moisture content (%)

As s(t) is equivalent to the percentage of a square metre occupied by the plan area of the pores (A), their width can be calculated by equation 3.14:

$$w = (8L-(8L^2-64A)^{0.5})/32 \quad -3.14$$

where w =width (cm)

L =length of crack (cm)

A =surface area of cracks (cm^2)

To simplify the calculations, the cracks were represented by a set of tubular channels of the same area and width (where r =0.5w) using equation 3.15.

$$a_n = (A/\pi(w/2)^2) \qquad -3.15$$

From a knowledge of macropore number and radius for each sub-class, the surface area per square metre for each group can be calculated and expressed as a percentage. The layer into which the cracks extend is input into the model. At present the model is only able to represent cracks in the surface layer as different layers may have different shrinkage characteristics and how these would relate to each other would need to be determined. This may be accommodated by designating different classes however, time did not permit me to investigate this further.

Having determined the macropore characteristics it is necessary to determine when flow occurs into them, and when it does, how the macropore and matrix domains interact.

Water flows into the macropores when infiltration capacity is exceeded and a ponded depth of water forms on the surface (d_p). It was assumed that this volume of water

is equally distributed between the macropores and instantly transferred to their base (Smettem 1986, Beven and Clarke 1986). Infiltration into the macropore walls from water running down the sides was shown by Hoogmoed and Bouma (1980) to be negligible and so has not been considered here, as in Brownijk's (1988) model which considered flow through soil cracks.

The height of water within the macropores of each class (Z_n) is calculated from equation 3.16 below:

$$Z_n = \frac{a_n \cdot d_p}{a_t} \cdot \frac{100}{P_n} \qquad -3.16$$

where P_n = percentege surface area of nth macropore class (equivalent to s(t) for drying cracks)

If a macropore class is filled with water any excess is added to the other classes. If all classes are full, any surplus water is held in a ponded store at the soil surface. Once the height has been calculated, flow from the macropore into the surrounding matrix is calculated using a version of Beven and Clarke's (1986) equation which has been simplified (eq 3.17) so that only horizontal infiltration is accounted for:

$$F_j = \frac{Kf_j . r . (d_1 + Hf)}{Rw^2 + Rw} \qquad -3.17$$

where Kf =conductivity of water within the wetting front (Section 3.3.2) (cm s^{-1})

Hf =suction at the boundary of the wetting front (Section 3.3.2) (cm)

r =radius of the macropore (for cracks equals 0.5w) (cm)

d_1 =height of water above point of infiltration (cm)

Rw =radius of the wetting front from the centre of the macropore minus the radius of the macropore itself (cm)

F_j =amount of infiltration (cm s^{-1})

Horizontal infiltration is only considered, as the inclusion of infiltration from the base of the macropore would greatly complicate this model. As the original intent was to redistribute excess surface water deeper into the profile by bypass methods, this complication is unwarranted. Errors introduced by this assumption may partially be offset by the assumption that all macropores extend to the base of the deepest layer they penetrate.

In the model infiltration from the macropores into the soil layers is calculated for each macropore class and every soil layer in direct contact with the water column. If the column extends up to or beyond the layer height the point of

infiltration is taken as half the layer height, otherwise it is taken as occurring at half the height from the base of the layer to the top of the water column. The amount infiltrated is then distributed over the whole layer. An important assumption is that none of the wetting fronts spreading from the macropores intersect each other. Infiltration from the macropores is halted when the layer becomes saturated and wetting fronts are assumed to have merged and diffused, the water left in the macropore is held in storage until infiltration recommences or in the case of temporary macropores, the end of the day where the water is lost to runoff. If the amount of infiltration calculated is greater than the volume of water within the macropore, preference is given to the deeper layers. Macropores may only infiltrate the amount of water held within them and their share of the ponded store. A macropore classes's share of the ponded store is based on the percentage of the total number of pores it accounts for.

Although there are a number of operational simplifications in this model, it is a substantial improvement on Hussein's model which simply transferred the excess water between deeper layers and runoff by an empirical relationship, taking no account of the processes involved and how these may change in time.

3.5 SUMMARY

The purpose of this chapter has been to describe the movement of water through an unsaturated soil. Flow characteristics within the soil matrix have been correlated with soil physical properties and have been shown (Section 3.2.3) to provide an adequate description of the drainage characteristics of several draining soils. The models when tested against independant data obtained from the literature, yielded high correlations. Using some of these derived relationships models were formulated to describe infiltration (Section 3.3.2), and macropore flow and interaction with the matrix (Section 3.4.3). However, due to the lack of specific experimental data neither of these models could be validated independently of the main model. Other factors affecting soil water movement, such as temperature and solute concentration (see review by Nielsen et al 1986) and unstable flow (Hillel 1987) were considered to be outside the scope of this study.

CHAPTER 4 PLANT FACTORS

4.1 INTRODUCTION

The following discussion relates to vascular or water conducting plants only, though some points may be applicable to non-vascular plant groups. For a more complete discussion of some of the more general points the reader is referred to more general texts such as Weier et al (1982), Hufford (1978) and Russel (1977).

The aim of this chapter is to integrate into the model a plant growth routine designed to calculate actual transpiration from the evaporative demand. Because of limited time, in terms of development and the gathering of information, the model is at present restricted to grasses and cereals. The routine is also used to calculate relative yield using a water use function, but interception loss is not included. This was considered to be of minor importance, since the plant growth model has only been developed for pasture crops and cereals and in these cases increased evapotranspiration loss due to interception is minimal (Gash and Stewart 1977 and Calder 1979). These monocultured stands also have little effect on rainfall redistribution due to stemflow and throughfall (Reynolds 1967), though this effect is noticeable in mixed communities and with bushes and trees

(Specht 1957, Vincent and Clarke 1982 and Miranda 1986). It is therefore felt that interception in terms of the water budget has insignificant effects for this type of simulation.

It should be noted at this stage that many of the following comments regarding plant growth must be viewed with caution due to the high coefficients of variation observed in plant characteristics in the field, especially with respect to root length and root density (Vos and Groenwold 1986 and Noordwijk et al 1985). Many of the effects described by authors are smaller than the sampling variation so conclusions must be regarded as tenuous, though these are at present the best available.

4.2 PLANT GROWTH

4.2.1 GENERAL

Plants grow due to the accumulation of carbohydrates formed from the products of photosynthesis and the uptake of nutrients from the roots. The amount of growth depends on a number of factors including the availability of nutrients, water and the energy available. The roots absorb nutrients and water while the leaves absorb energy and CO_2. Growth in this sense can be defined as the addition of new material. Net growth on the other hand indicates whether and by what

magnitude the addition of biomass exceeds the loss of plant material.

Before the plant comes to depend on the aerial environment for its nutrition and energy requirements (i.e before and just after emergence) it gains its sustenance from the reserves of energy stored within the seed. During this time, as the embryonic stem pushes towards the surface, the roots start to develop. By the time of emergence a root system has formed and the future prospects of the plant depend on the ability of this network to physically support the newly emerged organism and to supply it with water and nutrients. Above ground, embryonic leaves or cotyledons form on the stem. The form of these early leaves separate the vascular plants into two distinct groups: the monocotyledons and the dicotyledons. The differences between the two groups are described in Table 4.1 and Figure 4.1.

After emergence there follows a stage of steady vegetative growth where, given constant environmental conditions, roots and shoots tend to grow at about the same rate. However, prevailing environmental conditions can cause much variation in the distribution of the products of metabolism (Russel 1977). While the roots absorb water and the nutrients needed for assimilation, the leaves absorb the CO_2 and energy required for photosynthesis. A shortage of these components at either interface will cause the plant to become stressed in terms of its optimal growth potential. To

TABLE 4.1 Differences Between Monocotyledon and Dicotyledon Plants

	Monocotyledon	Dicotyledon
Roots	Vascular Cambium generally absent seconday growth absent	Vascular Cambium secondary growth though less in herbaceous than woody plants.
Stems	Vascular Cambium and secondary growth generally absent	Vascular Cambium Secondary Growth
Leaves	In grasses form sheaths around stem parallel veining	net veining. leaves connected to stem by petiole
Cotyledons	One	Two
Flower Parts	Multiples of Three	Whorls of four or five or their multiples

Concluding Remarks: Only the cotyledons and flower parts are characteristic of either group, with the other differences both groups have species which show exceptions.

FIGURE 4.1 Differences Between Monocotyledons and Dicotyledons

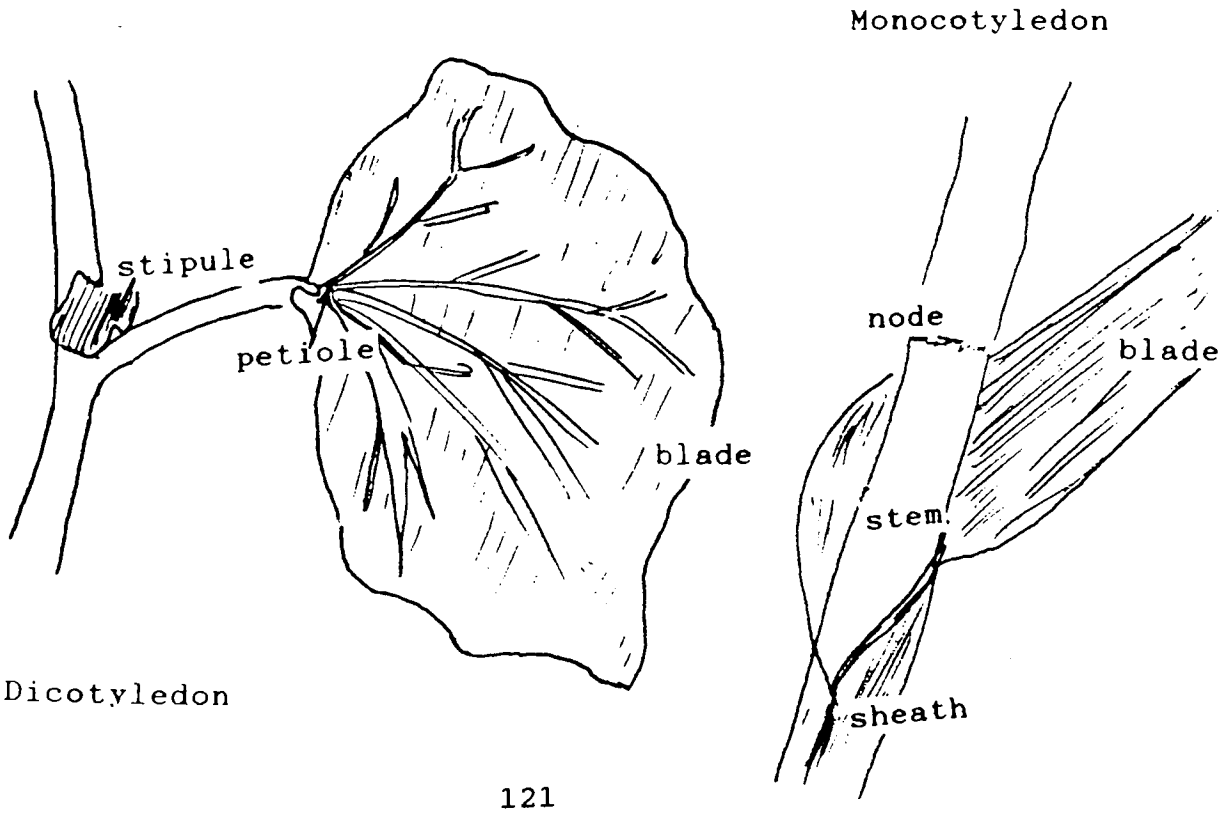

compensate for this a greater proportion of the growth is directed towards the interface limiting the plant's development, so as to increase its absorbing capacity. When the roots cannot supply enough water or nutrients, a greater proportion of the growth occurs within the root zone (Hoogenboom et al 1986,1987, Taylor and Klepper 1974 and Molyneux and Davies 1983), and when water and nutrients are plentiful, leaf growth reaches potential to maximise the plants photosynthetic ability and hence increase its growth and competitive ability (Huck and Hillel 1983).

When assessing the assimilates it must be noted that, as well as being used for growth, they are also needed for respiration, storage (in preparation for seeding) and the structural needs of the plant. Structural and respiration requirements increase as the plant expands. In order to counter this, the plant starts to shed unprofitable areas where assimilate import is greater than export (Huck and Hillel 1983). In the case of leaves this occurs due to mutual shading, but for roots, those parts of the network where uptake is minimal lose the smaller roots. The larger roots remain dormant, thus allowing rapid colonization by finer roots if conditions at a later date become suitable. The way plants communicate and respond to these stresses is controlled by the growth hormones (i.e auxins, cytokins, gibberellins, ethylene and absicisic acid) which provide the software for plant development.

In annual monocotyledons, the vegetative stage is superceded by anthesis, where the plant starts to produce seeds. This is normally accompanied by the loss of leaves and root weight, as the seeds act in a parasitic-like way on the parent plant using up stored assimilates.

4.2.2 ROOTS AND ROOT GROWTH

All roots form due to the division and extension of cells at the apex of the root in a region known as the apical meristem. In monocotyledons roots attain their maximum diameter when the cells are fully expanded, but in dicotyledons they continue to thicken due to progressive cell division tangential to the root axis.

Root growth and extension are affected both by genetic traits, as shown by cotton cultivars (Gorny and Patyna 1984), and by environmental factors, which can inhibit or modify the root structure. Environmental factors may overshadow the genetic differences to such an extent that false conclusions can be drawn about rooting depth and extension rates (Hamblin and Hamblin 1985). The magnitude of these alterations may be determined by the sensitivity of the plant at various growth stages (Hoogenboom et al 1987). Many external factors influence root development (e.g water content, nutrient supply and temperature) while many other factors may indirectly affect it (e.g soil strength,

aeration and acidity). These processes are described more fully below.

The water content of a soil can affect roots in a variety of ways. Low water content encourages root development, because as the plants become stressed more growth is partitioned to the roots. This has been clearly illustrated by irrigation experiments, where well watered crops have produced much smaller rooting systems than infrequent or non-irrigated ones (Myers et al 1984 and Proffitt et al 1985). However, if the plant is too highly stressed the amount of synthates available for partition to the roots will be small as the stomata in the leaves close to reduce water loss, with the result that CO_2 is no longer absorbed. Water also provides a lubricating effect, so when the water content is low it may reduce root penetration (Belford et al 1987 and Ehlers et al 1983). It is not only a low moisture content that affects root growth, a high moisture content may also cause problems due to waterlogging. Under these conditions the roots are starved of oxygen. This is considered to be unimportant in the U.K (Greenwood 1969), though it may cause some restriction in rooting depth (Trouse 1971c).

Nutrients provide the plant with the necessary materials for growth. If adequate nutrients are absorbed, and there is no other limiting factor, shoot growth will be enhanced and thus result in smaller root systems. Nutrient

deficiency on the other hand encourages development of roots (Anderson 1987, Welbank et al 1973). The presence of certain ions can also deter root development by forming acidic or calcic soils (Joost and Hoveland 1986). The addition of nitrate ions has also been shown to both increase and decrease root growth in seperate experiments. This is due to the complex interaction between these ions and other factors, such as phosphate, light intensity (Ennik and Hofman 1983), temperature and water content.

High strength soils have a debilitating effect on root elongation. This has been shown through the latters inverse correlation with penetrometer resistance (Dexter 1986a, Ehlers et al 1983, Pearson et al 1970) and bulk density (Cornish et al 1984 and Yapa et al 1988), both of which are indicators of soil strength. It is the reduction in pore size and pore continuity which reduces the penetration, as roots need to grow into pores of at least equal diameter to the root tip. However, the tip can build up sufficient pressure to push aside some particles. Logsdon et al (1987) describe root thickening at such junctures, and Hettiaratchi and Ferguson (1973) indicate that this process may aid roots to push through soils up to five times stronger than is possible without thickening. However, the more compact the soil, the more difficult this process becomes (Dexter 1986a and Olson 1985). As roots normally occupy less than 5% of the soil volume, there need only be this amount of pore space greater than root diameter for root growth to be

unimpeded (Russel 1977). Thus the presence of macropores in compact soil will aid root development. By comparison root systems in soils without macropores are likely to be less developed. In crop rotation studies roots of the present crop have been shown to follow channels created by the roots of a previous crops. Such pores may also allow roots to penetrate through hardpans to less compact soils below (Dexter 1986b,c), but these pores do not always fully show up on penetrometer tests (Ehlers et al 1983). As stated earlier, water acts as a lubricant in regard to root growth but so also does clay. Madsen (1985) showed that clay contents in the range 10-20% can increase penetration, but at higher concentrations it tends to decrease pore-size range and aids soil cohesion, thus reducing penetration.

Root elongation is also affected by temperature, since metabolic activity increases with temperature. However, this effect is not linear, since associated factors (such as increased respiration, increased activity of pathogens and the vapourization of water in vacuoles) restrict water movements and offset the beneficial effect. Different plants have different optimum root growth temperatures - Moorby and Nye (1984) report 23°C for rape, whereas Pearson (1970) reported 32°C for cotton.

When considering these factors it must be remembered that roots in different parts of the network will be experiencing widely varying conditions (Barraclough and

Leigh 1984, Moorby and Nye 1984 and Huck et al 1986) and so responses in one part of the system may be affected by conditions elsewhere. Compensatory growth has been observed in several experiments where root growth is concentrated in favourable areas to the detriment of less favourable locations (Barraclough and Leigh 1984, Madsen 1985 and Russel 1977).

4.2.3 ABOVE GROUND DEVELOPMENT

Stems provide the structural support for the plant in the aerial environment and act as the conducting pathway for water and nutrients. Leaves provide the factory in which assimilates form. In times of no stress, above-ground development is paramount to the plant to ensure maximum reproduction. Increases in above-ground size allow the plant to compete better for light and space with its neighbours. Optimum leaf area will ensure that the plant has the leaf area to produce the maximum yield, however, as mentioned in Section 4.2.1, leaf area will not increase linearly with plant size due to the effects of shading (Huck and Hillel 1983).

4.2.4 PLANT GROWTH MODEL

The model developed below incorporates a number of the

factors discussed in the previous sections. Though simplistic in nature, it takes into account different development stages within the plant's growth cycle. Although the original aim was to produce a general growth model, the model developed here is only suitable for monocotyledons as it does not take into account secondary growth and the formation of tubers.

Several models presented in the literature calculate the amount of carbohydrate produced using the CO_2 concentration of the atmosphere coupled with the photosynthetically active radiation (PAR). The carbohydrate is then divided between respiration, growth, maintenance and storage components using a number of relationships which are generally plant dependent (Protopas and Bras 1988, Huck and Hillel 1983, Kvifte 1987, Johnson et al 1983 and Johnson and Thornley 1987). However, within the context of the present model, this approach requires too many variables and the availability of a wide range of meteorological data (e.g amount and type of incoming radiation). Taking this into account a simplified model was devised which related growth to actual transpiration - data for which are a function of radiation and the amount of time stomata are closed. Data for potential transpiration are widely available, and from this actual transpiration can be calculated using the water uptake model developed in Section 4.3.2. The following relationship between growth and potential transpiration was devised on the assumption that as potential transpiration

increases so does the PAR but not linearly, instead the increase is assumed to be exponential (Figure 4.2a):-

$$G_r = a(1-e^{-b \cdot AT}) \qquad -4.1$$

where G_r =dimensionless growth units

AT =actual transpiration (cm)

a =maximum possible number of growth units

b =dimensionless parameter

The growth parameter G_r represents total daily growth in terms of dimensionless units which may be partitioned between Leaf Area Index (LAI) and root density by equation 4.5a and 4.5b.

The curve representing equation 4.1 becomes limiting at high values of potential transpiration due to the inability of the plant to supply water, the effects of temperature and stomatal closure. The parameter 'a', the limiting factor for the exponential curve, decreases in value during the development stage of an annual plant as more assimilates are needed for maintenance, respiration and structural support (Caloin and Yu 1982). The following equation was thus developed to represent the decrease in parameter 'a' (equation 4.2.):

$$a = maxval-((dayno/(harv-emerg))^{ba}.maxval) \quad -4.2$$

where maxval = highest possible growth to be attained during the growth cycle;

dayno = number of days since the plant emerged;

emerg = number of days after start of simulation that the plant emerged;

harv = number of days from the start of the simulation to the harvest of the plant;

ba = curve shaping parameter;

The calculated growth units are then divided between the roots and shoots depending on the amount of stress the plant is under. Stress is defined by an index given by equation 4.3. as with Jong and Zentner (1985):

$$S = 1-(AT/PT) \quad -4.3$$

where S = dimensionless stress index;

AT = actual transpiration (cm);

PT = potential transpiration (cm);

Having defined the level of stress, a partitioning coefficient is required to assign the appropriate proportions of growth units to the roots and the leaves. The equation

developed (equation 4.4) was designed to produce a continuous function representing the graphical form given by Huck and Hillel (1983). The resulting function is a smooth S-shaped curve (Figure 4.2b).

$$Cp = minrat + \frac{(maxrat - minrat)}{(1+(a_1 S)^{np})^{mp}} \qquad -4.4a$$

$$mp = 1-(1/np) \qquad -4.4b$$

$$Cr = 1-Cp \qquad -4.4c$$

where Cp = proportion of growth units partitioned to leaves;

Cr = proportion of growth units partitioned to roots;

S = stress index;

minrat, maxrat = minimum and maximum possible partitioning of growth to leaves respectively;

a_1, np, mp = dimensionless curve-shaping parameters.

Once the partitioning coefficients have been calculated, the amount of leaf and root growth are calculated by equations 4.5a and 4.5b respectively. The dimensionless growth units being converted into the increase in LAI and root density by the use of the co-efficients Lc and Rc respectively. Leaf growth is the only aspect of above ground development considered within the model for several

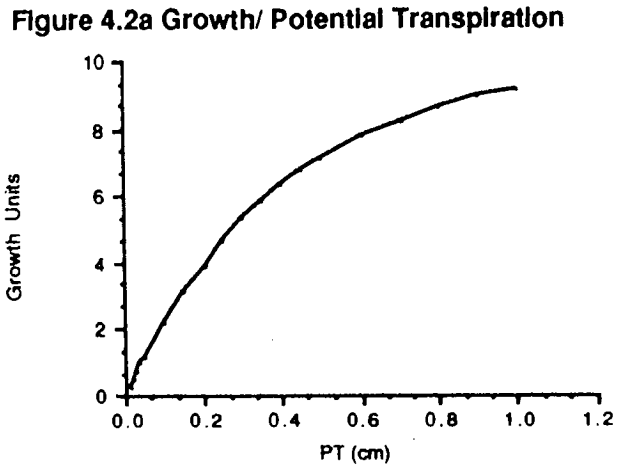

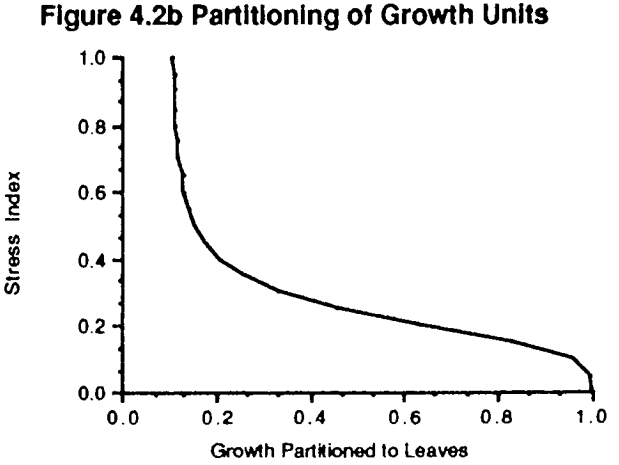

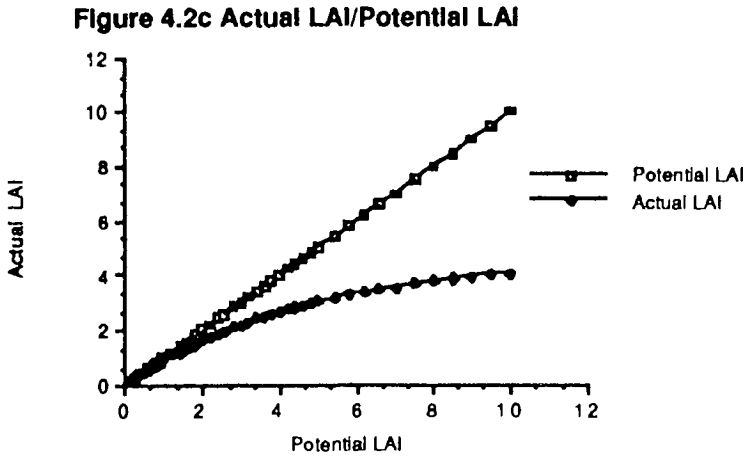

FIGURE 4.2 The Plant Model Parameter Determination Curves

reasons:-

a) although water stress may slow shoot growth it does not alter its basic phenological development (Huck et al 1986);

b) leaf area can be related to shoot size (Johnson et al 1983);

c) and finally, in the context of the model, it is only leaf area with its role of partitioning the evaporative demand (Section 5.3) which is of importance.

$$potlai_j = potlai_{j-1} + ((Cp.Gr).Lc) \quad -4.5a$$

$$rgrow = (Cr.Gr).Rc \quad -4.5b$$

where potlai = potential leaf area index;

L_c = constant that converts G_r into additional leaf area index;

rgrow = increase in cm cm^{-3} of roots for a representative volume of $1m^3$;

R_c = constant that converts G_r into cm cm^{-3} of root density.

subscript j refers to the timestep

Potential as opposed to actual LAI is calculated to allow for the phenomena of mutual shading discussed in Section 4.2.1. Actual LAI is calculated from equation 4.6

(Figure 4.2c). In formulating this relationship it is assumed the higher the potential LAI the greater the difference between potential and actual LAI as the greater the chance of mutual shading.

$$LAI = maxlai(1-e^{-c.potlai}) \qquad -4.6$$

where maxlai =maximum attainable LAI for plant

c =dimensionless curve-shaping parameter

For root growth the value of rgrow calculated for a representative volume of soil is partitioned between the layers by equation 4.7, which takes account of the direction of the hydraulic gradient. Starting with the surface layer each layer is tested to see if it is wetter than the layer above. If it is, the parameters $Cgo_{(j-1)}$ and $Cgi_{(j)}$ (indicating root growth out of or into a layer) in equation 4.7 are each assigned an empirical value, otherwise they are equated to zero. The parameter $Cg_{(j)}$ which indicates growth within the jth layer is the sum of $Cgo_{(j)}$ and $Cgi_{(j)}$. This is due to the fact that roots will grow from the layer above into the layer being tested so there will be growth in both layers. This procedure is continued until the routine reaches the bottom layer containing roots. At this point as long as the layer below does not contain the water table growth can proceed into the layer below provided three conditions are met within the program. Firstly, as before

the layer below must be wetter, secondly the roots in the basal layer must have been present long enough in this layer for them to have reached the bottom. With regard to the last point a value of root extension rate is input, the shortest possible time taken then for roots to reach the bottom of the layer is thus the depth of the layer divided by the extension rate. Finally, the depth must not exceed the maximum possible rooting depth. As Weier et al (1982) point out, though roots dont grow in search of water they grow only in moist soil, and according to Hufford (1978) they will grow only along moisture gradients towards wetter soil. The above assumptions take this into account.

$$Lp_j = \frac{Cg_j . Rd_j . D_j . rgrow}{\Sigma Cg_j . Rd_j . D_j} \qquad -4.7$$

where Cg = dimensionless multiplier indicating prescence of growth into (Cg_i) and out of the jth layer (Cg_o);

Rd = root density of jth layer (cm/cm^3);

d = depth of jth layer (cm);

Lp = increase in root density for a representative volume of $1m^3$ for layer j.

As well as growth, the model simulates senescence. It splits monocotyledons into two groups: pasture grasses and cereals. For pasture grasses it is assumed that there is no loss in LAI over time. In the case of cereals, LAI is

assumed to decrease linearly from anthesis until harvest. Maillette (1986) noted that in cereals leaf mortality increased after ear emergence and very few live leaves were left after the grain had ripened.

In the case of established permanent pastures, root weight has been observed to be constant over time (Anderson-Taylor and Marshall 1983 and Andrew 1987a), so the model assumes that root death is equivalent to root growth in value. As growth is partitioned to the wettest layer it seems reasonable to assume for the opposite reason that root death occurs in the driest layer.

For cereals it has been observed that there is a loss in root mass after anthesis (Gregory et al 1978), but it is worth noting that this refers to weight rather than density. Gregory et al (1978) and Soon (1988) have indicated that there are still continued root growth and increases in root density after anthesis, especially in the deeper layers, even though overall weight is reduced. For this reason it is assumed that root death is unimportant for cereals within the confines of this model. The reduction in root growth after anthesis will be accounted for by equation 4.2.

A relative yield function for cereals has been derived based on the relationship between yield and water use (Gajri and Prihar 1985) given by equation 4.8.

$$Y = \Sigma AT / \Sigma PT \qquad -4.8$$

where Y =relative yield index

AT =actual transpiration (cm)

PT =potential transpiration (cm)

The model requires the following inputs:

1. initial root density and layer into which they extend (ie at emergence for cereals);
2. initial leaf area index (assumed to be non-zero i.e early leaves have opened);
3. the number of days after start of simulation of crop emergence, anthesis and harvest (for cereals only).

At the present time insufficient data exist to permit the validation of the plant growth model. In Section 7 the parameters are varied in order to test the sensitivity of the model to the effects of differing hypothetical plants.

4.3 PLANT WATER UPTAKE

4.3.1 GENERAL

The uptake of water from the soil and its eventual transpiration from the leaves has been the subject of much research, mainly due to the fact that water movement is much

greater than that needed by the plant for such tasks as ion transport and the maintenance of turgor. The favoured postulate is that it is the inescapable consequence of the environment and the physiological needs of the organism. Water is lost through perforations in the leaves known collectively as stomata, these also act as a passageway for carbon dioxide uptake which is needed for growth. Closure of the stomata to reduce water loss stops carbon dioxide uptake thereby inhibiting growth. As there is no known membrane, natural or man-made, which allows the passage of carbon dioxide but not water (Russel 1977) it can be seen that in order to grow the plant must lose water.

Water moves through the plant in response to hydraulic gradients. Vapour pressure deficits within the atmosphere draw water from tight meniscuses which are maintained in the leaves and the resulting suction gradient pulls water from the soil via roots, stems and leaves. Resistances to water flow help the plant to minimize these losses. It was originally thought that this process could only lift water up to 10.13m (or 1 atmosphere) and that for plants taller than this an additional unknown mechanism must operate. It is now theorized that adhesion forces within the column of water are sufficient to maintain the height of the column up to 300 atmospheres or 3000 metres (Weier et al 1982). However, due to the increasing likelihood of gas formation (as suction forces increase) causing the column to collapse, plants do not reach this height. To counteract this process,

known as cavitation, plants have devised various mechanisms for protecting themselves. Isolating short lengths of conducting vessels or xylem, so that if failure occurs these may be isolated from the rest of the system, is one such mechanism. Plants also contain a large number of xylem routes in excess of those needed. The following paragraphs describe the movement of water from the soil via the plant to the atmosphere, and the importance of resistances to water flow at various stages.

The resistance to movement of water in soils has been considered to be very important in many plant-water uptake models (Feddes et al 1976, Gardner 1960 and Hussein 1979). Evidence from other authors has suggested otherwise, except at tensions approaching 15 bars (Gardner 1960 and Taylor and Klepper 1975). Trouse (1971b) notes that in dry soil, roots can grow faster along moisture gradients than water can migrate. Herkelrath et al (1977b) suggested that the effects attributed to the resistance to the flow of water in the soil were due to root shrinkage leaving a gap between the roots and the soils. Tardieu (1988a,b) suggested that soil resistance may be more important where roots are widely spaced, although as noted by Tinker (1976) these would have to be large to be effective. Cornish et al (1984) noted that for perennial grasses uptake rates were low indicating in this case that it is plant resistance which is most important. Reid and Hutchison (1986) conclude that plant resistance is far more important than soil resistance,

although as Russel (1977) pointed out root contact with the soil is also important.

Resistance to water flow within the roots is second only to that within the leaves. Water tends to flow primarily between the cell walls into the xylem. In older roots a casparian strip forms a "damp course" across adjacent cell walls thus further restricting water flow. Younger roots do not have this "damp course" and therefore are more efficient at water uptake (Feddes 1978, Gregory et al 1978, Hamblin and Tennant 1987 and Soon 1988). However, it has been observed that at high uptake rates, older parts of the root system can become many times more permeable, thereby suggesting a biological influence on root resistance as opposed to a purely mechanical one (Russel 1977). Root hairs tend to form in relatively dry soil and may be important in maintaining contact with the soil (Neuman 1976) especially if the roots shrink upon drying (Cole and Alston 1974). However, they do not offer any less resistance to flow than the root itself. Resistances within the stem are negligible compared to those in the leaves and roots. Friction forms the greatest component of resistance in the stem but this is still relatively insignificant (Hall 1976).

The leaves, and the stomata in particular, provide the greatest resistance to flow within the plant. Vapour deficits in the atmosphere can reach -1,000 bars, yet leaf

tension rarely exceeds -50 bars (Russel 1977). The resistance is the result of the conversion of water into vapour in the confined moist environment of the leaf cavity, and the ability of the stomata to close by the action of surrounding guard cells (Davies and Kozlowski 1974 and Szeicz et al 1973). Stomata have also been reported to close in reaction to a number of environmental factors including light intensity, time of day - usually noon (Fetcher 1976), concentration of CO_2 (Hall and Kaufmann 1975, Idso et al 1985,1986), vapour pressure deficit (Lange and Losch 1971, Schulze and Kuppers 1979, Rawson et al 1977 and Schulze et al 1972) and transpirational demand (Sheriff 1977). The potential formed in the leaves is the result of water demand. The leaf potential needed to fulfill this demand depends on root distribution, soil suction and resistance to flow. Leaf potential is commonly observed to be negative even when water flow is zero (Kaufmann 1976). Ritchie (1973) suggested that due to branching and the vertical non-homogeneity of the stem and leaf distribution the calculated values of leaf potential may not be reflected in individual leaves. Considering this Hillel et al (1976) suggested the use of "Crown Potential" to define the average leaf potential needed for water uptake.

4.3.2 PLANT WATER UPTAKE MODEL

The model presented here is based upon Lascano and

Bavel's (1984) and Herkelrath et al's (1977a,b) papers. The model was chosen as it has plant resistance as the main resistance to flow but also includes an empirically derived function for describing the effect of root contact. It also takes into account root density. All of these factors have been shown to be important in root water uptake in the preceeding discussion. The relationship adopted is that shown in equation 4.9 below.

$$U_j = (t_j/ts_j).Rd_j.((Sc-Ss_j)/PR) \quad -4.9$$

where U_j = uptake from jth layer (cm day^{-1});

t_j/ts_j = root contact component of Herkelrath et al (1977b);

t_j = moisture content of jth layer;

ts_j = saturated moisture content of jth layer;

Rd_j = root density of jth layer (cm cm^{-3});

Sc = crown suction (cm);

Ss_j = soil suction in the jth layer

PR = plant resistance (day^{-1})

The only unknown on the right hand side of the equation is the value of crown suction. This is found by firstly assuming that the transpiration is at the potential rate (PT) and substituting this into equation 4.9. Equations 4.10a and b show the solution of 4.9 used, and are employed to determine the potential crown suction (Sc_p)

$$Sc_p = \frac{PT + \sum \frac{Rd_j . Ss_j}{A_j}}{\sum \frac{Rd_j}{A_j}} \qquad -4.10a$$

$$PT = U_j \qquad -4.10b$$

where $A_j = PR.(ts_j / t_j)$

PT = potential transpiration rate cm d^{-1}

To find the actual crown suction (Sc_a) the relationship Hussein (1979) formulated from data presented by Ritjema (1965) is used (equation 4.11).

$$Sc_a = (a - a^3/3).70000 \qquad -4.11$$

where $a = Sc_p / 70000$

Using equation 4.9, the actual transpiration (AT) is calculated from the sum of the uptake from each layer.

The root contact component in equation 4.9 is seen as a vital addition to the model. Herkelrath et al (1977b) found that without such a component the closest fit of data was achieved by assuming a root density of 1.0 cm cm^{-3} for winter wheat, which they described as unrealistic. Hussein (1979) also found that in the case of grasses a root distribution factor of 1.0 for the top layer, but decreasing rapidly with depth, produced the best fit of results. This is also unrealistic for grasses as a review of

relevant data for various grass species showed: e.g subterranean clover (Pearson and Jacobs 1985), and ryegrass (Cornish et al 1984, Robinson and Rorison 1985).

4.4 SUMMARY

This chapter has described a method for calculating plant growth based on transpirational demand and supply. Though relatively simplistic in nature, it takes into account several processes such as the dynamic partitioning of growth between leaves and roots which is fundamental to plant development. Two outputs from the model are used in the water budget calculations: LAI distributes evaporative demand between plants and soil, and root density distributes water abstraction between the soil layers. These data are then used for determining plant growth.

The inadequacy of published field data and the fact that such practical work was outside the scope of this project has unfortunately meant that neither of these units have been tested directly. They have, however, been tested indirectly via their contributions to the performance of the overall model, see Chapter 7.

CHAPTER 5 ATMOSPHERIC PROCESSES

5.1 INTRODUCTION

The soil-moisture-plant model developed earlier needs two inputs: daily rainfall and daily evaporative demand.

In order to provide appropriate input to the infiltration routines, the daily rainfall totals must be distributed throughout the day into hourly values. It is one of the aims of this chapter to provide a simple algorithm to facilitate this.

The daily evaporative demand will have to be partitioned between soil evaporation and transpiration. Once this has been achieved the aim is to calculate actual soil evaporation, the calculation of actual transpiration has been described in Section 4.3.2.

5.2 RAINFALL

Rather than just dividing the daily rainfall into the twenty-four hours equally, two alternative methods are employed to calculate hourly amounts and then distribute them randomly throughout the day. This may result in some

hours of the day having large amounts of rain whilst others have none. There may also be two or more blocks of several hours of rainfall separated by gaps with none at all. This type of distribution is more realistic than just distributing the rain evenly. Random numbers are generated according to the method given by Meisner and Organik (1980).

The two methods used to distribute the rainfall are described below. Method 1 is used when the rainfall total is low, Method 2 when it is high. The dividing line between the two is subjective, being set where it is felt that the assumptions in Method 2 become justified. In the present project the dividing line is set at 5mm as it is felt that below this, the amount of rainfall is too low to give any pattern. The parameter containing the amount of rainfall at which the two methods are divided is known as R_{crit}.

The two methods are described below:-

a) Method 1 (used when daily rainfall is less than 5mm). In this method the daily total is split into 0.5mm blocks and one extra block, if required, containing the remainder. These blocks are then distributed randomly into the hours of the day. More than one block may be assigned to a specific hour.

b) Method 2. This makes use of an intensity/duration curve of the form described by Walley (1981). The curve is parabolic in nature and is described below by equation 5.1.

$$(R+b)(t+a) = c \qquad -5.1$$

where R =rainfall (mm/hr)

t =duration (hrs)

a,b,c are constants

This expression can be adapted to distribute the daily rainfall total (Rt). The resultant curve ranks the hourly rainfall values from the highest to the lowest, and indicates how many hours of the day it rained. In order to obtain these data for a known Rt the values of the parameters 'a', 'b' and 'c' must be known. The following study utilizes observed data to obtain relationships between the parameters and Rt.

Rainfall data collected from tipping-bucket gauges was supplied by Severn-Trent Water Authority in the form shown in Table 5.1. The data was combined to reproduce one single data set. The data are in 0.5mm units, describing each recorded tip of the bucket. In all, data from six tipping bucket gauges were used covering records ranging from as little as four months to as much as three years. However, there are some breaks in the data records covering the longer periods. Table 5.2 gives details of site (including height above ordinance datum and national grid reference), mean annual rainfall, length of records examined and details of missing data. Table 5.3 describes for each site how many

TABLE 5.1 Example of Rainfall Data Obtained from the Tipping Bucket Raingauges.

Content has been removed for copyright reas

TABLE 5.2 SUMMARY OF SITE DATA ACQUIRED FROM STWA PDL5 TIPPING BUCKET (0.5mm) RAINGAUGES

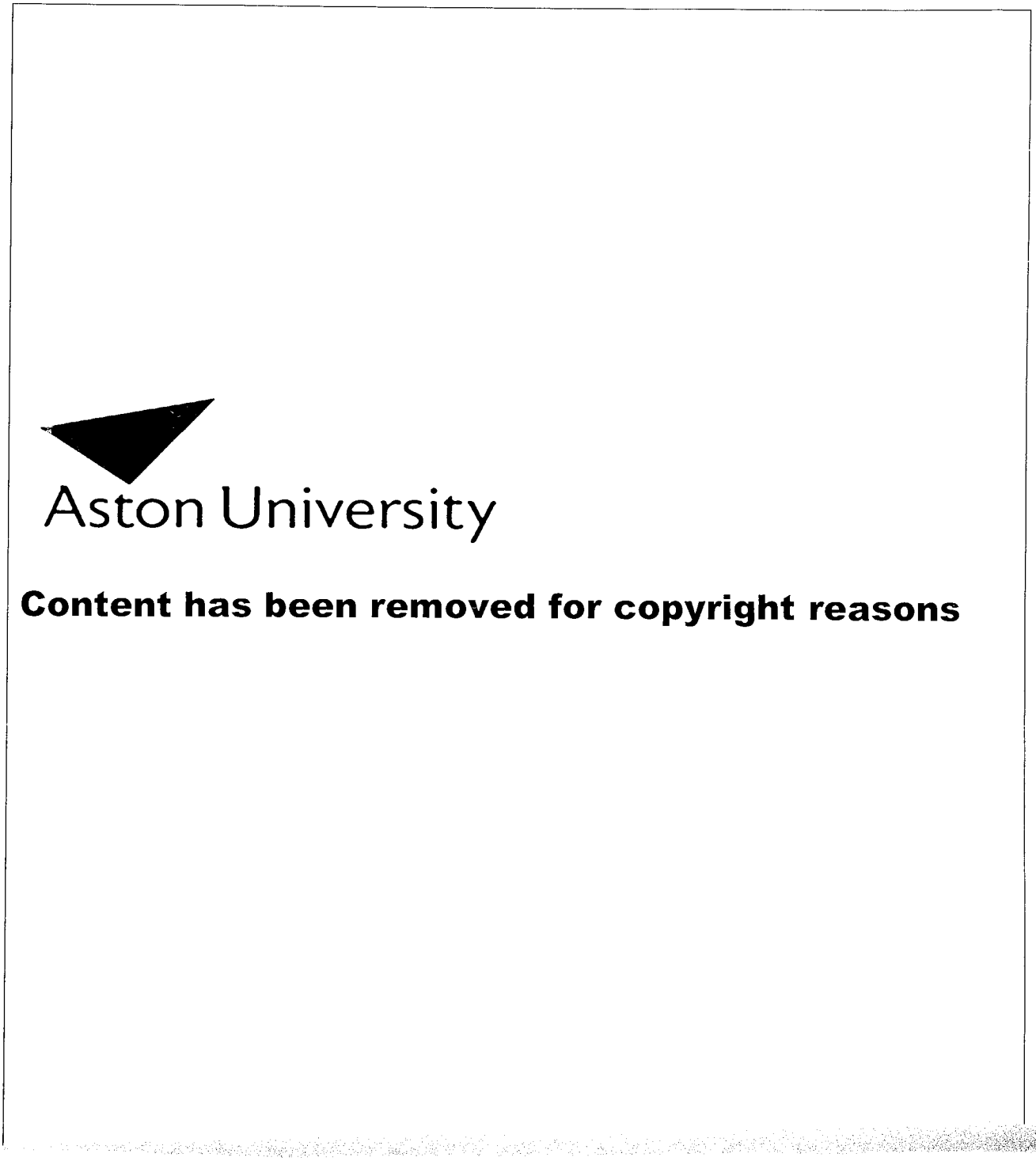

TABLE 5.3 SUMMARY OF SIZE OF RAINFALL EVENTS FOR 6 SITES (TABLE 5.2) ACQUIRED FROM STWA PDL5 TIPPING BUCKET (0.5mm) RAINGAUGES

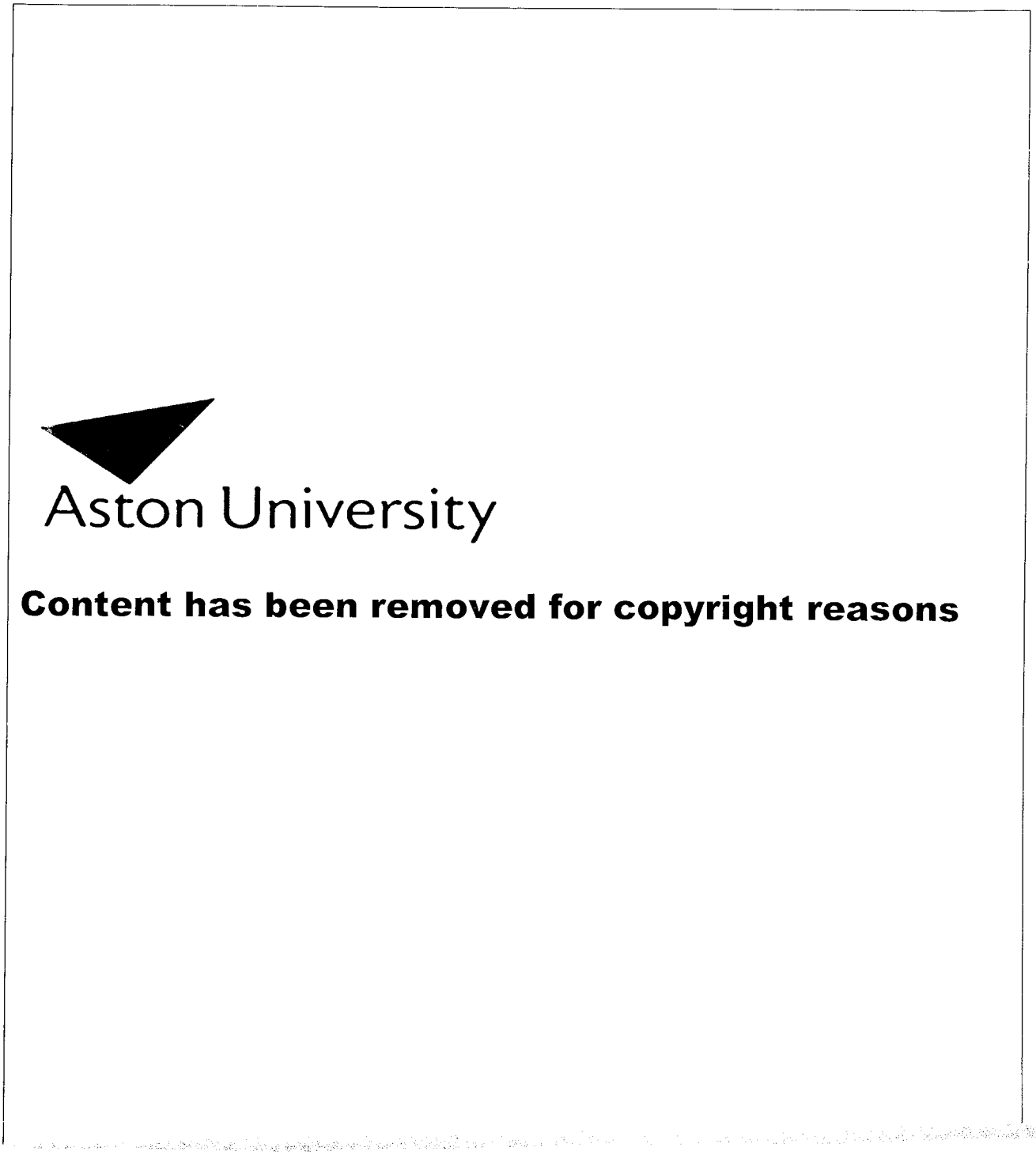

times a particular daily total was recorded. By examining Table 5.1 it can be seen that the daily data are collected from 9 a.m. to the same time the following day, as opposed to midnight to midnight. The fact that each daily record does not correspond to a calender day is a minor technicality and does not affect the calculation.

Using the daily total rainfall figures, a number of classes were defined for analysis, these being 6.0-6.5, 9.0-9.5, 12.0-14.5, 15.0-19.5 and >20.0mm. Although the choice of classes was somewhat arbitary the range of each class increased with magnitude in order to maintain a reasonable sample size. The number of classes chosen was deemed sufficient to form a simple relationship between the parameters 'a', 'b' and 'c' and the daily rainfall. More classes were not chosen at the lower rainfall range, where the number of events were high, so as not to bias the regression against the relatively few events at the higher rainfall end of the distribution.

Table 5.4 shows how, for each event within a class, the hours were ranked in terms of percentage rainfall from that containing the largest amount to the one containing the least. These percentages were then summed for each ranked hour and the average calculated. Table 5.4 illustrates the method for the class >20.0mm. These percentages were then plotted against ranked hours on a separate sheet for each class and a parabolic curve fitted to them. The values of

				Percentage of Total Daily Rainfall in Each Ranked Hour																					
Event No.																									Sum of
	1	2	3	4	5	6	7	8	9	10	11	12	13	14	15	16	17	18	19	20	21	22	23	24	%
1	58.2	14.6	10.9	7.3	3.6	1.8	1.8	1.8	0	0	0	0	0	0	0	0	0	0	0	0	0	0	0	0	100
2	10.3	10.3	6.9	6.9	5.2	5.2	5.2	5.2	5.2	3.4	3.4	3.4	3.4	3.4	3.4	3.4	3.4	3.4	1.7	1.7	1.7	1.7	1.7	0	99.5
3	34.1	22	19.5	17.1	4.9	2.4	0	0	0	0	0	0	0	0	0	0	0	0	0	0	0	0	0	0	100
4	23.9	17.9	16.4	10.4	6	4.5	4.5	3	3	3	3	1.5	1.5	1.5	0	0	0	0	0	0	0	0	0	0	100.1
5	21.4	21.4	9.5	9.5	9.5	7.1	7.1	7.1	4.8	2.4	0	0	0	0	0	0	0	0	0	0	0	0	0	0	99.8
6	18.5	14.1	7.6	7.6	6.5	6.5	5.4	5.4	4.3	3.3	3.3	3.3	3.3	2.2	2.2	2.2	2.2	1.1	0	0	0	0	0	0	100.1
7	15.6	11.1	11.1	11.1	8.9	8.9	8.9	6.7	6.7	4.4	2.2	2.2	2.2	0	0	0	0	0	0	0	0	0	0	0	100
8	33.3	19	19	14.3	7.1	4.8	2.4	0	0	0	0	0	0	0	0	0	0	0	0	0	0	0	0	0	99.9
9	33.3	13	9.3	7.4	7.4	7.4	5.6	5.6	5.6	3.7	1.8	1.8	0	0	0	0	0	0	0	0	0	0	0	0	101.9
10	13.3	8.9	8.9	6.7	6.7	6.7	4.4	4.4	4.4	4.4	4.4	4.4	4.4	4.4	2.2	2.2	2.2	2.2	2.2	2.2	2.2	2.2	0	0	98.6
11	34.8	19.6	10.9	6.5	4.3	4.3	4.3	4.3	2.2	2.2	2.2	2.2	2.2	0	0	0	0	0	0	0	0	0	0	0	100
12	17	15.1	9.4	9.4	7.5	7.5	7.5	5.7	5.7	5.7	3.8	1.9	1.9	1.9	0	0	0	0	0	0	0	0	0	0	100
13	25.3	18.7	9.3	8	8	6.7	6.7	4	4	4	2.7	1.3	1.3	0	0	0	0	0	0	0	0	0	0	0	100
14	13.3	13.3	11.1	11.1	8.9	8.9	8.9	6.7	4.4	4.4	2.2	2.2	2.2	2.2	0	0	0	0	0	0	0	0	0	0	99.8
15	20.8	16.7	16.7	10.4	6.2	6.2	6.2	6.2	4.2	4.2	2.1	0	0	0	0	0	0	0	0	0	0	0	0	0	99.9
16	25.5	17	10.6	10.6	8.5	6.4	4.3	2.1	2.1	2.1	2.1	2.1	2.1	2.1	2.1	0	0	0	0	0	0	0	0	0	99.7
17	11.9	9	7.5	7.5	7.5	7.5	6	4.5	4.5	4.5	4.5	4.5	3	3	3	3	1.5	1.5	1.5	1.5	1.5	1.5	0	0	100.4
18	19.1	11.7	10.6	10.6	9.6	6.4	6.4	5.3	4.3	3.2	2.1	2.1	2.1	2.1	2.1	1.1	1.1	0	0	0	0	0	0	0	99.9
19	55.1	39.8	4.1	2	0	0	0	0	0	0	0	0	0	0	0	0	0	0	0	0	0	0	0	0	100
20	22.6	17	15.1	15.1	7.5	5.7	3.8	3.8	1.9	1.9	1.9	1.9	1.9	0	0	0	0	0	0	0	0	0	0	0	100.1
21	13.9	11.6	11.6	11.6	9.3	9.3	9.3	9.3	7	2.3	2.3	2.3	0	0	0	0	0	0	0	0	0	0	0	0	99.8
22	11.7	10	6.7	6.7	6.7	5	5	5	3.3	3.3	3.3	3.3	3.3	3.3	3.3	3.3	3.3	3.3	3.3	1.7	1.7	1.7	1.7	0	99.9
23	18.4	16.3	12.2	8.2	8.2	6.1	4.1	4.1	4.1	4.1	4.1	2	2	2	2	2	0	0	0	0	0	0	0	0	99.9
24	20	18.5	16.9	9.2	6.1	6.1	4.6	3.1	3.1	3.1	3.1	1.5	1.5	1.5	1.5	0	0	0	0	0	0	0	0	0	99.8
25	17.5	15	10	10	7.5	7.5	5	5	5	5	2.5	2.5	2.5	2.5	2.5	0	0	0	0	0	0	0	0	0	100
Total	588.8	400.6	282.9	235.2	171.6	148.9	127.4	108.3	89.8	74.6	57	46.4	40.8	29.9	24.3	17.2	13.7	11.5	8.7	7.1	7.1	4.9	3.4	0	
% Total	23.55	16.02	11.32	9.41	6.86	5.96	5.1	4.33	3.59	2.98	2.28	1.86	1.63	1.2	0.97	0.69	0.55	0.46	0.35	0.28	0.28	0.2	0.14	0	100

Table 5.4 Rainfall Event Data for Days of 20mm or More

the parameters 'a', 'b' and 'c' could then be calculated. Figures 5.1a-c show the values of the parameters obtained plotted against the average rainfall for each class.

Regression analysis were performed between the parameters and the average daily rainfall for each class. Using correlation analysis the significance of the regression equations produced were determined. Results of the correlations are shown in Table 5.5. For this study, correlation coefficient values which were significant at greater than the 10% level or less (i.e $p<=0.1$) were considered adequate. Both 'a' and 'b' fell within this criterion. However, the parameter 'c' did not. Equations 5.2a and 5.2b give the regression equations for the parameters 'a' and 'b'. The value of 'c', due to its low correlation was taken as a constant equal to 67.6 (this being the average value of 'c' derived from the five groups).

$$a = 0.041482Rt + 1.040872 \qquad -5.2a$$

$$b = -0.08647Rt + 4.889794 \qquad -5.2b$$

The effect of the regression equations 5.2a and 5.2b is that as rainfall increases the intensity/duration curve becomes flatter (Figure 5.2) and the duration of the storm increases (Figure 5.1d). That is, 'a' increases whilst 'b'

TABLE 5.5 CORRELATION VALUES OBTAINED BETWEEN RAIN MAGNITUDE AND THE INTENSITY/DURATION EQUATION PARAMETERS a, b & c.

Variable	r	Degrees of Freedom
a	0.820	3
b	0.933	3
c	0.017	3

* parameter a is significant to the 10% level
** parameter b is significant to the 5% level

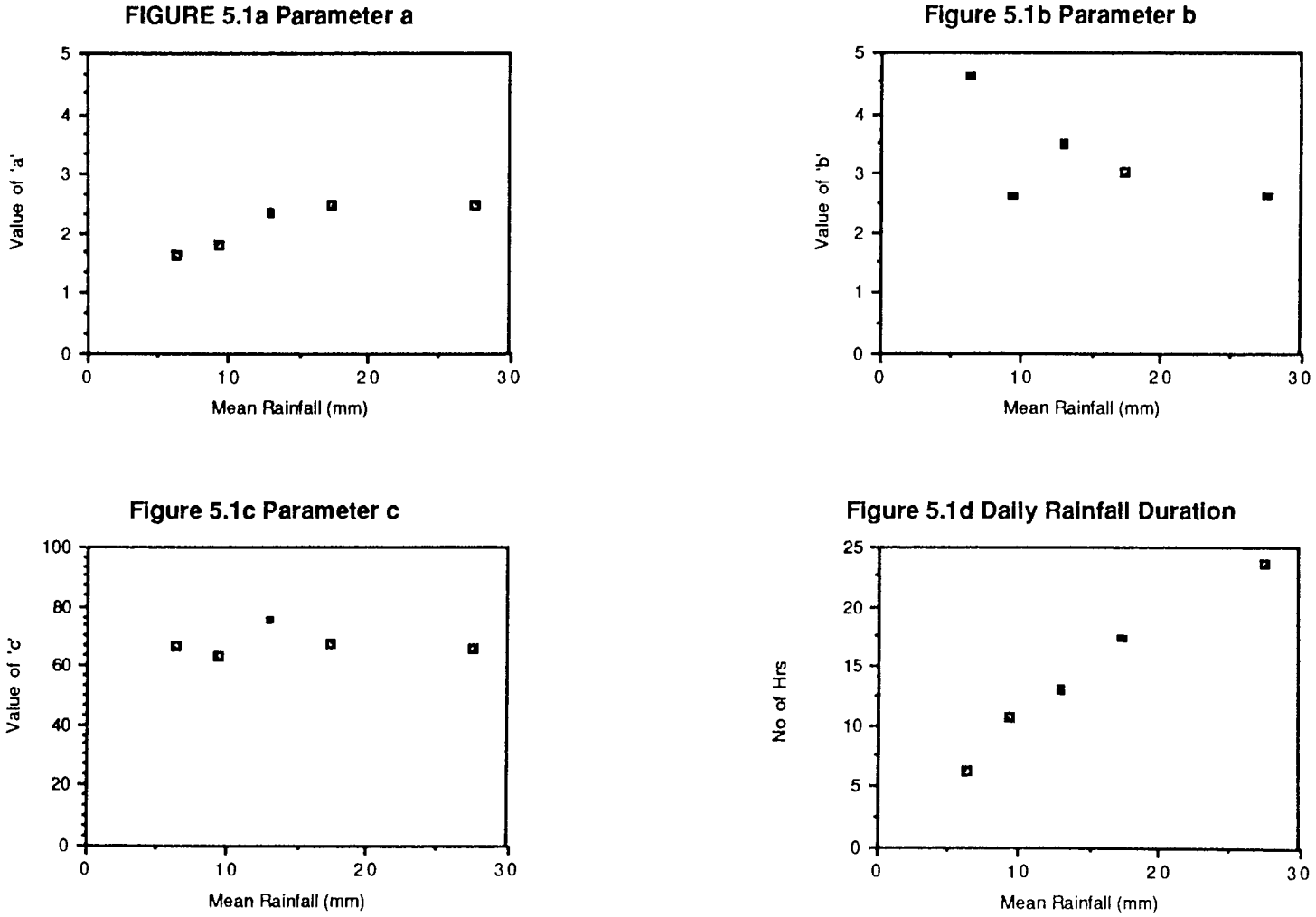

Figure 5.1 Values of Curve Parameters Obtained Against Daily Rainfall Amount

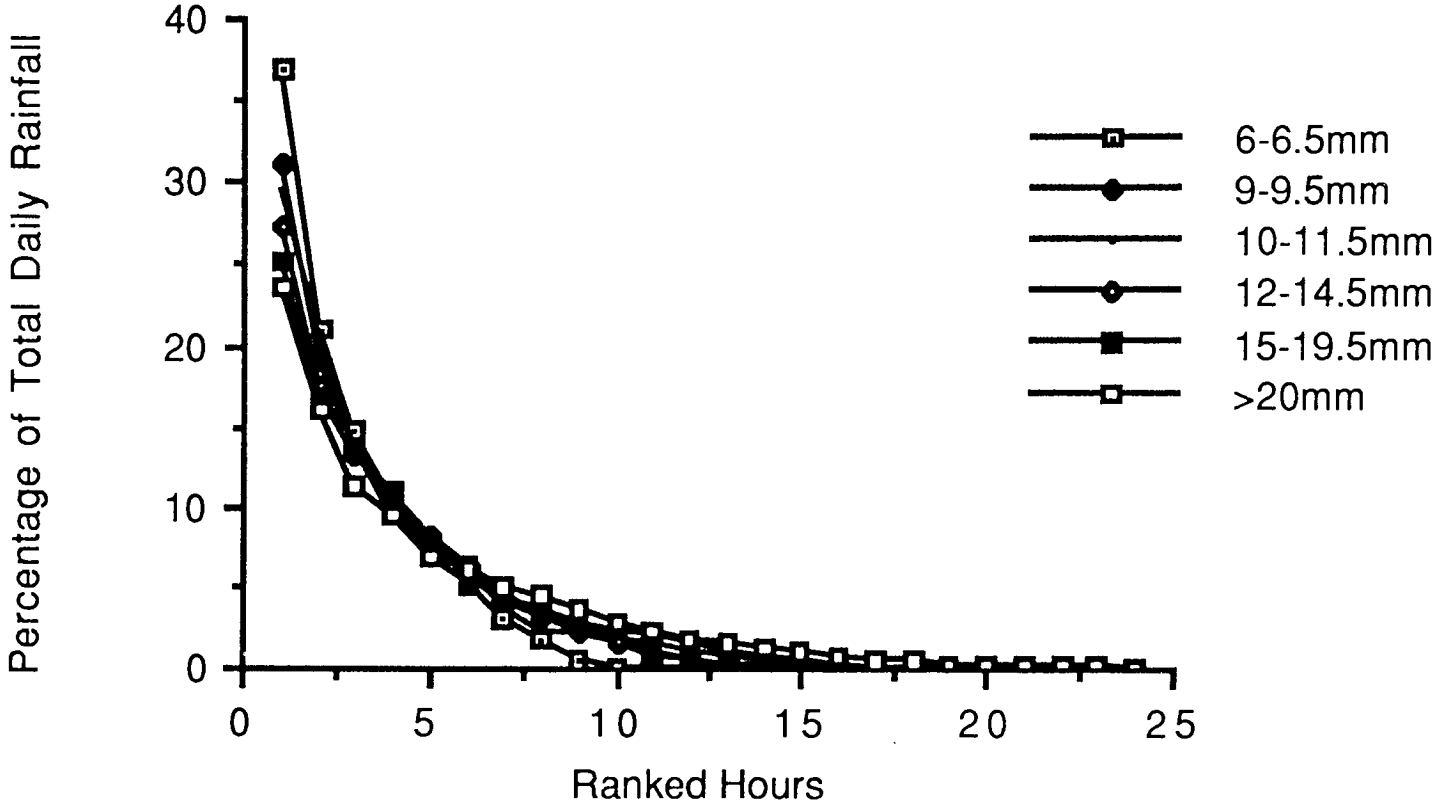

Figure 5.2 Intensity Duration Curves Formulated for Each Daily Rainfall Class

decreases. If the calculated duration exceeds 24 hours the percentage of rainfall contained in the extra time is divided equally between the hourly amounts.

From the above, an intensity/duration curve can be formed for any given value of Rt. The percentage of the total rainfall falling in each ranked hour is then derived by integrating equation 5.1 w.r.t time and solving to give equation 5.3, and from this the hourly amount of rain ($R_{(t)}$) is calculated. These ranked hourly amounts are then distributed randomly into the actual hours of the day, each actual hour containing only one ranked amount.

$$R_{(t)} = c.\log_e(t+a)-(b.t) \qquad -5.3$$

where t is the duration in ranked hours

When the timestep is smaller than 1 hour the hourly rainfall amount is divided evenly between the steps.

5.3 EVAPORATION

The evaporative demand, like rainfall, is input as a daily total. The following section describes how this is split between evaporation from the soil surface and transpiration from plants. It goes on to describe how bare soil evaporation is calculated, transpiration having been

described in Section 4.3.2.

Evaporative demand is distributed between the soil and plant by equation 5.4 (Hussein 1979)

$$EDS = ED(1-LAI) \quad \text{FOR } LAI<1 \qquad -5.4$$
$$EDS = 0 \quad \text{FOR } LAI>=1$$

where EDS =potential evaporative demand from the soil ($cm\ d^{-1}$)

ED =evaporative demand ($cm\ d^{-1}$)

LAI =leaf area index (definition is that of Hussein 1979 where it refers to the percentage of crop cover)

For bare soil evaporation, Hussein's (1979) method was used. Where daily rainfall was greater than daily evapotranspiration, actual evaporation from the soil (ES) was assumed equal to the potential. Otherwise it was calculated as a function of moisture content and the difference between evaporative demand and rainfall shown by equation 5.5.

$$ES = (Rt + Se^{n}(ED - Rt))(1 - LAI) \qquad -5.5$$

where $Se = (t - tr)/(ts - tr)$

t =moisture content of surface layer

ts =saturated moisture content of surface layer

tr =residual moisture content of surface layer

n =a constant (given by Hussein 1979 as 2.0)

Equation 5.5 reduces to 5.6 in the absence of rainfall.

$$ES = Se^{n}.EDS \qquad -5.6$$

5.4 SUMMARY

The chapter has described how the model handles the daily input of rainfall and evaporative demand. The daily rainfall is divided into hourly totals by one of two methods and these are then distributed randomly into the hours of the day. Evaporative demand is distributed between the soil and the plant depending on the value of the percentage crop cover. Actual evaporation from the soil is then calculated from an expression formulated by Hussein (1979), the calculation of actual transpiration is described in Section 4.3.2.

CHAPTER 6 THE SOIL-MOISTURE-PLANT MODEL

6.1 INTRODUCTION

The aim of this chapter is to describe how the model is structured, how it operates and how the various processes within it interact. The first two sections describe respectively the model structure and how the timestep is determined. The following sections describe suites of subroutines which represent various processes within the model and also explain how the simulation treats them. Flowcharts are used to help elucidate certain points.

6.2 MODEL STRUCTURE

The model works as a one-dimensional representation of the soil-moisture-plant system with properties being homogeneous in the horizontal direction and heterogeneous in the vertical. Vertical variability is approximated by the use of discrete layers, up to 50 if required, whose properties in terms of soil type and characteristics, moisture content and root density may vary from layer to layer. With the exception of conditions during infiltration, as described later, properties are constant within the layers. The model is bounded at the bottom by the basal

layer which contains the water table, output from this layer being the product of the height of the water table above the base and an empirically derived drainage constant. If there is no vegetation the upper boundary is at the soil surface otherwise it is at the top of the vegetation. Outputs are in the form of evapotranspiration losses and drainage to the water table inputs are in terms of rainfall. Water flow is in the vertical direction with the exception of infiltration (which is both vertical and lateral). The ground is assumed to have zero slope. Figure 6.1a illustrates these points.

Exceptions to the one-dimension discete layered model can occur during infiltration. Under ponded conditions a zone wetted by infiltration moves down the profile in a continuous way. The interface between this wetted zone and the unaffected soil is known as the infiltration wetting front (IWF) and is homogeneous in the vertical direction. When rainfall exceeds the amount that can be infiltrated directly into the soil matrix the water builds up at the surface and flows into the macropores and from these into the soil layers, the flow rate being determined by vertical wetting fronts (MWF). This causes layers to be heterogeneous in both vertical and horizontal directions in terms of water content and for flow to be two-dimensional. However, the presence of MWF's is only used to calculate water flow bypassing surface layers and percolation is still considered only in the vertical direction. The distribution of macropores is considered to be homogeneous. The presence of

FIGURE 6.1 MODEL STRUCTURE

A) WITHOUT WETTING FRONTS

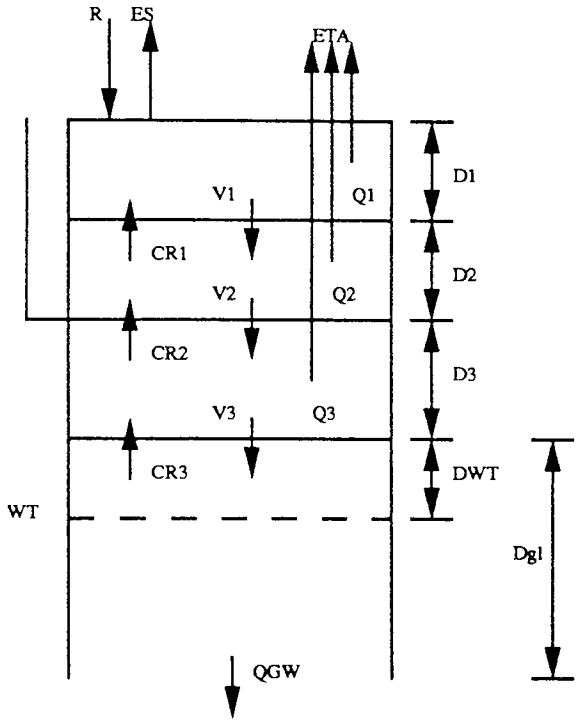

B) WITH WETTING FRONTS

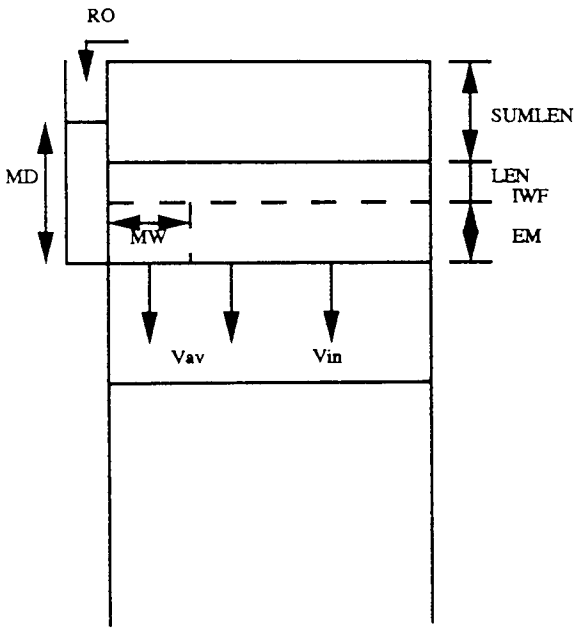

SUBSCRIPTS 1,2,3 REFER TO LAYER` NUMBER
GL REFERS TO GROUNDWATER LAYER

ES = ACTUAL TRANSPIRATION FROM SOIL (cm)
ETA = ACTUAL TRANSPIRATION (cm)
Qj = PLANT WATER UPTAKE FROM jTH LAYER (cm)
RO = RUNOFF (cm)
P = PONDED (cm)
Dj = DEPTH OF jTH LAYER (cm)
Hj = SUCTION HEAD OF jTH LAYER (cm)
KSj = SATURATED CONDUCTIVITY OF THE jTH LAYER (cm/s)
Kj = CONDUCTIVITY OF jTH LAYER (cm/s)
KBj = CONDUCTIVITY OF jTH BOUNDARY (cm/s)
Tj = MOISTURE VOLUME FRACTION (MWF) OF jTH LAYER
TSj = SATURATED MWF OF jTH LAYER
TRj = RESIDUAL MWF OF jTH LAYER
Vj = PERCOLATION ACROSS jTH BOUNDARY (cm/s)
Vavj = PERCOLATION ACROSS jTH BOUNDARY WHEN A MWF AND MATRIX ARE AVERAGED (cm/s)
Vinj = PERCOLATION ACROSS jTH BOUNDARY FOR MATRIX UNAFFECTED BY MWF (cm/s)
CRj = CAPILLARY-RISE ACROSS jTH BOUNDARY (cm/s)
DWT = DEPTH TO WATER TABLE (cm)
WT = WATER TABLE
RDj = ROOT DENSITY OF jTH LAYER (cm/cm3)
MD = HEIGHT OF WATER COLUMN IN MACROPORE (cm)
ND = LAYER INTO WHICH THE TOP OF MACROPORE`S WATER COLUMN EXTENDS UP INTO
DM = LAYER CONTAINING THE BASE OF THE MACROPORE
MR = RADIUS OF MACROPORE (cm)
MW = RADIUS OF WETTING FRONT - MR (cm)
MWF = MACROPORE WETTING FRONT
IWF = SURFACE INFILTRATION WETTING FRONT
LEN = DEPTH TO IWF FROM TOP OF LAYER (cm)
SUMLEN = DEPTH TO IWF FROM SURFACE - LEN (cm)
EM = Dj - LEN (cm)

wetting fronts is illustrated by Figure 6.1b.

6.3 MODEL OPERATION AND PROGRAM

The soil-moisture-plant model is written in VAX/VMS FORTRAN and has been run on Aston University's Vax Cluster. Fortran was chosen due to its widespread use and comprehension within the earth sciences. The following discussion describes the order in which the program algorithms are used and what timesteps they run under. The model is summarized in flowchart form in Figure 6.2.

The program opens by asking if the operator requires program parameters to be altered from previous runs. If they do soil and plant properties can be changed (Section 6.4) and new relationships such as suction-moisture characteristics are calculated. Returning to the main program, or continuing from the start if parameters are not altered, the program asks if some other key parameters (i.e. saturated conductivity) are to be altered. The length of the simulation in days is read from an external file, the same file that contains the daily rainfall and evaporative demand data.

At the start of each day daily rainfall and potential evaporative demand are input from an external file. If there is any rainfall it is distributed into hourly blocks by the

FIGURE 6.2 FLOWCHART OF SOIL-PLANT MODEL

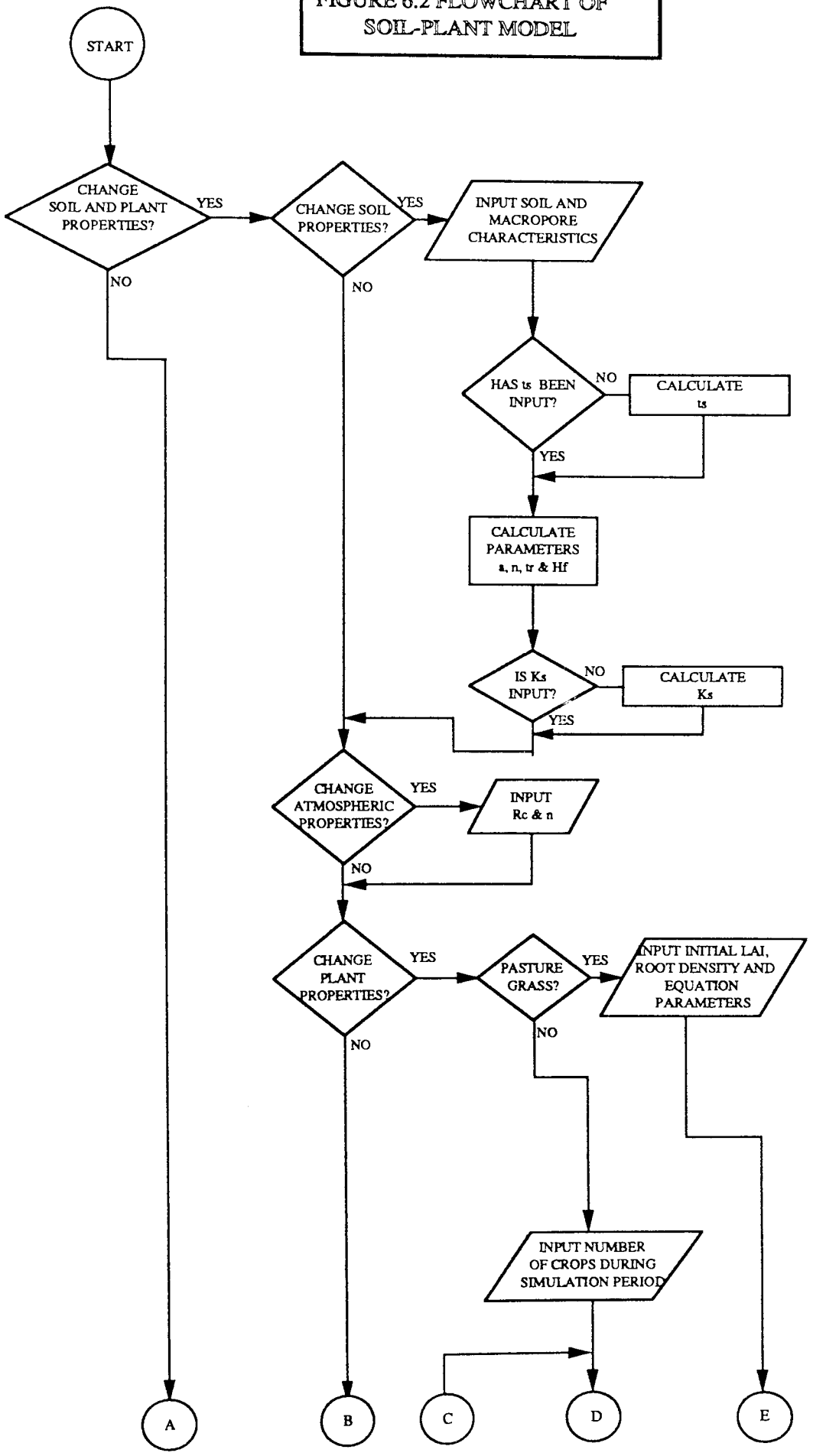

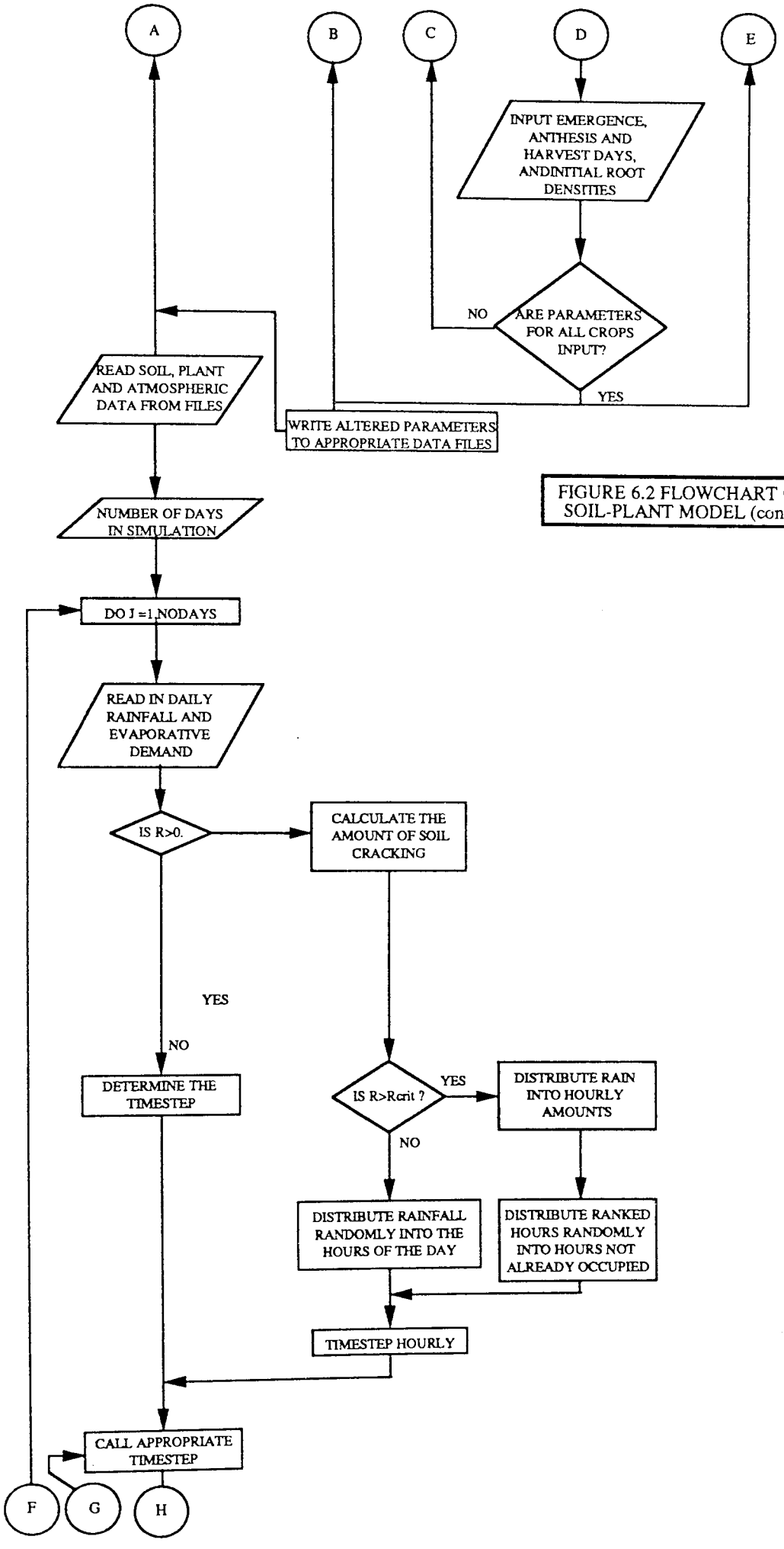

FIGURE 6.2 FLOWCHART OF SOIL-PLANT MODEL (contd)

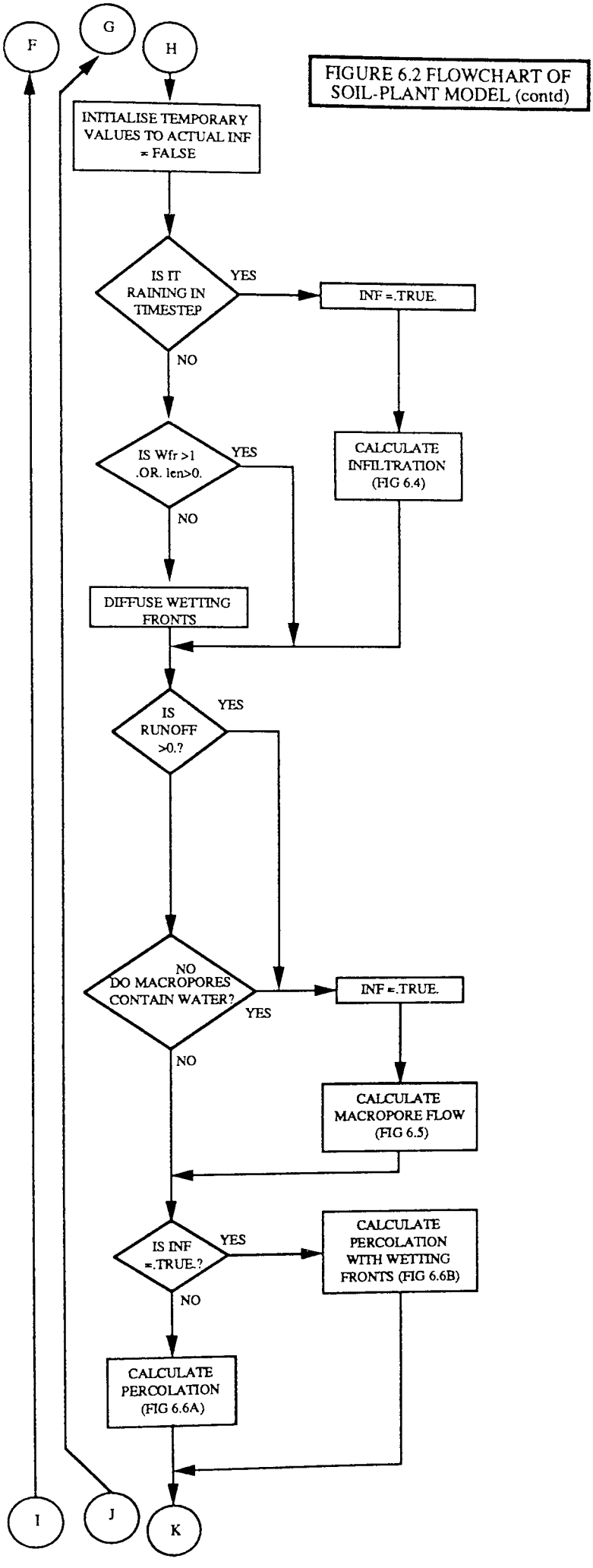

FIGURE 6.2 FLOWCHART OF SOIL-PLANT MODEL (contd)

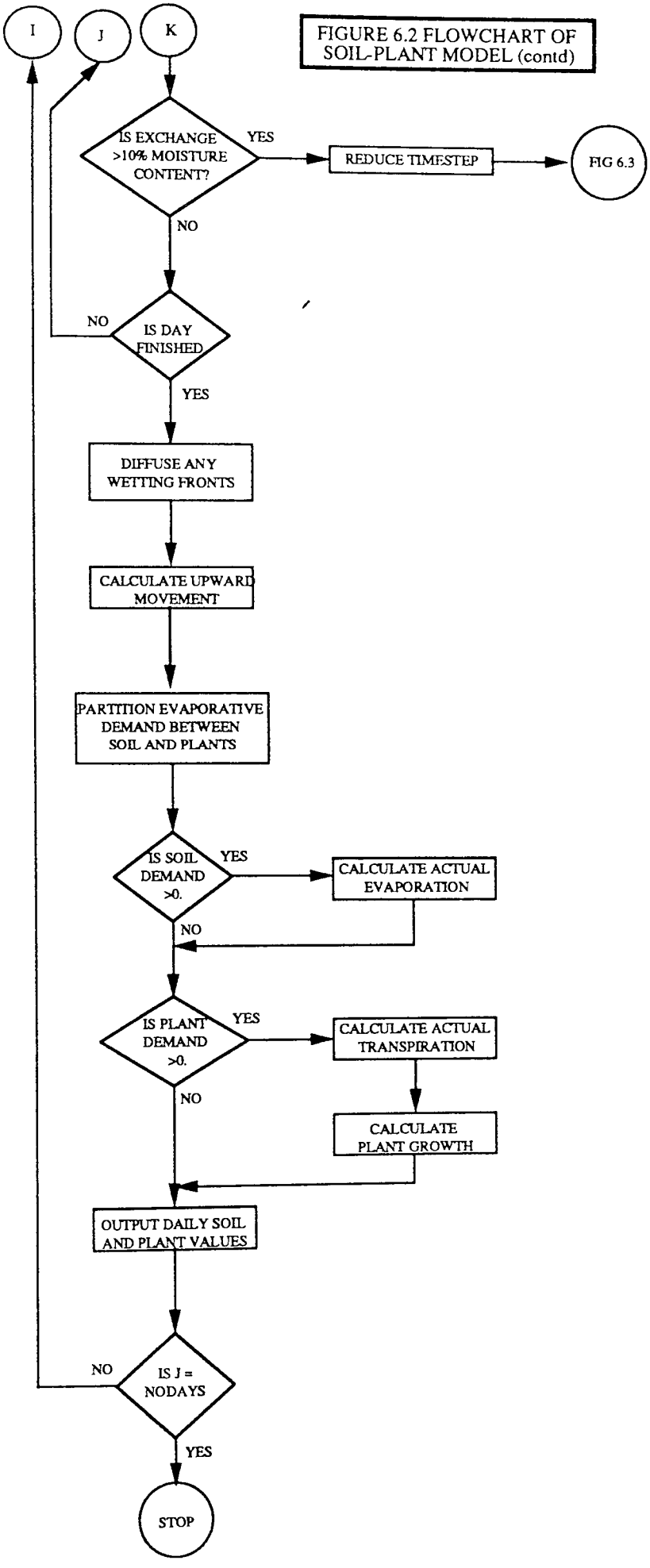

FIGURE 6.2 FLOWCHART OF SOIL-PLANT MODEL (contd)

rainfall algorithms. The program then enters a large block of algorithms which run on a variable timestep. The timestep is initially set at 1 hour but may be reduced if water exchanged between layers by percolation is too high (i.e greater than 10% of a layer's water content). The algorithms included in this section calculate infiltration, macropore flow and percolation. The infiltration routines are only called if there is rainfall within the timestep, whilst the macropore units are called if there is excess water left after infiltration or if there is water still left in the macropores from the previous timestep or day. All exchanges are kept as temporary values until the above condition (i.e no more than 10% of a layer's water content is exchanged by percolation in a timestep) is satisfied whence the program variables are then updated. If this condition is not met the calculations are restarted at a reduced timestep which only operate until the higher order timestep has expired, once this happens the timesteps reverts back to the higher value (Figure 6.3). This process continues until a total of 24 hours is complete. The program then starts on the second phase of algorithms which run on a daily timestep.

First of all any wetting fronts are diffused, with water content being averaged across the layer concerned. This simplifies later calculations as the water uptake and capillary-rise algorithms would not only be complicated by wetted and unwetted zones but would also have to be included within the variable timestep routines. Within the daily

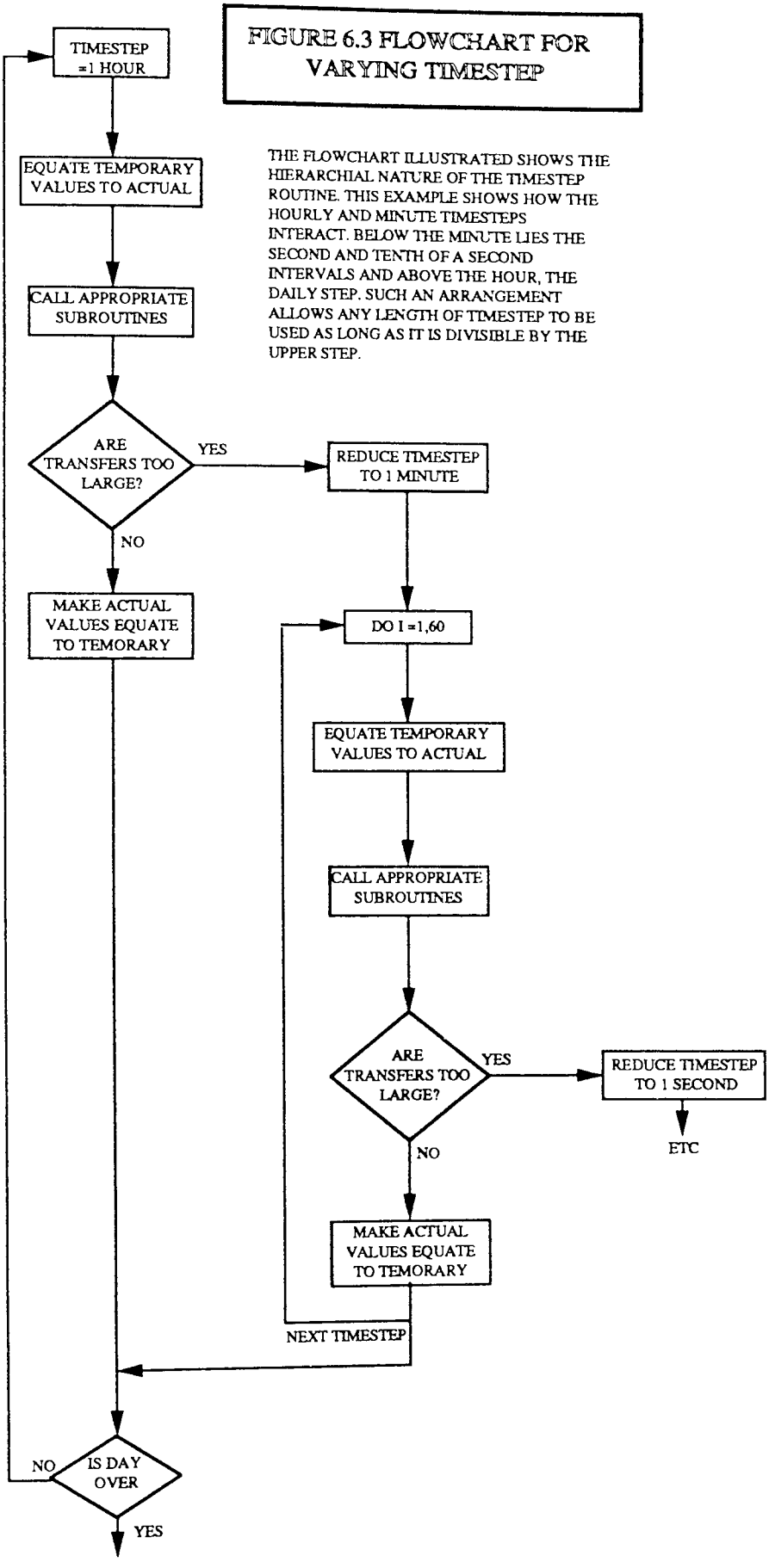

FIGURE 6.3 FLOWCHART FOR VARYING TIMESTEP

THE FLOWCHART ILLUSTRATED SHOWS THE HIERARCHIAL NATURE OF THE TIMESTEP ROUTINE. THIS EXAMPLE SHOWS HOW THE HOURLY AND MINUTE TIMESTEPS INTERACT. BELOW THE MINUTE LIES THE SECOND AND TENTH OF A SECOND INTERVALS AND ABOVE THE HOUR, THE DAILY STEP. SUCH AN ARRANGEMENT ALLOWS ANY LENGTH OF TIMESTEP TO BE USED AS LONG AS IT IS DIVISIBLE BY THE UPPER STEP.

timestep routines potential evaporative demand is partitioned between soil evaporation and transpiration. These are then calculated, the value of actual and potential transpiration then being used to determine plant development. Finally the capillary-rise algorithm is called to determine the amount of upward water movement between the layers.

The daily information is then output to external files before the program loops to start the next days calculations if the simulation period has not expired.

6.4 INPUT ALGORITHMS

The input algorithms may be selected from the screen before any simulations are run. Their purpose is to define variables or parameters within the equations which remain constant throughout the simulation. They refer to soil, plant and atmospheric components as described below. The length of the simulation in terms of days, and daily data for rainfall totals and evaporative demand are entered into data files using programs independent of the simulation algorithm. Their position within the program can be seen in Figure 6.2.

The following soil parameters are required to be input: particle-size distribution and bulk density. The following

properties: saturated moisture content (ts) and saturated conductivity (Ks) are optional. The former can be calculated using Equation 6.1.

$$e = 1-(p_b/p_s) \qquad -6.1a$$

$$ts = 0.9e \qquad -6.1b$$

where e = porosity (%)

p_b = bulk density (g/cc)

p_s = particle density (usually taken as 2.65 g/cc that of SiO_2) (g/cc)

The relationship in equation 6.1b was given by Rogowoski (1971). Examination of data collected from the SCS-USDA (1974) showed that on average ts is 0.93e. In several other references ts is equated to porosity (e.g Brutsaert 1966, Laliberte et al 1966 and Green and Corey 1971). The relationship by Rogowoski (1971) was used in the model.

In the case of Ks, it can be calculated from the retention curve using equation 6.2 as determined by Brutsaert (1966):

$$Ks = a1(te/h_b)^2.(q/[(q+1).(q+2)]) \qquad -6.2$$

where $te = ts-tr$

h_b, q = Brooks and Corey Parameters (Section 3.2.1.2)

a1 =calibration parameter (a1 =21, Rawls et al 1982)

Though the equation uses Brooks and Corey (1965) retention parameters, Section 3.2.1.2 shows how these can be converted to Genuchten's (1978) variables giving equation 6.3 below:

$$Ks = a1(a.te)^2([n-1]/[n^2+n]) \qquad -6.3$$

Though Rawls et al (1982) found this relationship to be useful when no data on Ks were available, when they tested it against experimental soils it was found to produce errors in excess of an order of magnitude for several soils. This equation is therefore only included within the model where Ks cannot be determined by measurement or calibration.

As discussed in Section 3.2.2 measured Ks may be unrepresentative of the matrix conductivity at saturation and may be primarily determined by the macropores. The model separates mico- and macropore flow, with infiltration into the macropores only occurring when the rainfall rate exceeds the infiltration capacity of the matrix. As has been noted earlier (Section 3.3) the matrix capacity is dependent on the Ks of the matrix. Measured Ks values tend to include both macropore and micropore conductivities, and if this is the case then they cannot be used. Instead, it may be better to determine the matrix Ks by calibration if suitable data are available, or even by interpolating Ks from

conductivity measurements at small suctions when the macropores are empty as suggested by Genuchten and Nielsen (1985).

The particle-size data are input as percentage values by weight of the fraction less than or equal to 2mm. The range of the classes used is that described below:

1. very coarse sand (2-1mm);
2. coarse sand (1-0.5mm);
3. medium sand (0.5-0.25mm);
4. fine sand (0.25-0.1mm);
5. very fine sand (0.1-0.05mm);
6. coarse silt (0.05-0.02mm);
7. fine silt (0.02-0.002mm);
8. clay (<0.002mm);

The total sand content is the sum of 1-5 and total silt content the sum of points 6 and 7. The sieve sizes being those used by the Soil Conservation Service of the United States Department of Agriculture (SCS-USDA). This approach was chosen as it is compatible with the data used to form the regression equations in Section 3.2.1.2.

Using the soil data input the parameters of Genuchten's (1978) equation are calculated by employing the regression equations given in Section 3.2.1.2. From these the infiltration parameter Hf is determined using equation 3.11. Characteristics for each macropore class are input separately, with the exception of dessication cracks which

are calculated daily and are dependent on clay content. The following macropore data are input: number per square metre, radius and layer into which they extend.

The parameters used for the plant algorithms are directly input into the model. The form of the input depends upon which one of the two plant groups simulated by the model is to be used: permanent pasture grasses or annual cereals. Grass leys can be treated as annual cereals. For the permanent grasses, the initial values required are:

1. the layer into which the roots initially extend;
2. their density in the layers they occupy;
3. the leaf area index;
4. the leaf area index at which they are cut if appropriate.

For cereals the following inputs are required:

1. number of crops grown in the simulation time;
2. at what day after simulation commencement they emerge, reach anthesis and are harvested;
3. the layer into which the roots initially extend;
4. the root density in the layers they occupy at emergence;
5. the leaf area index of the emerged plant.

The initial values of the input variables are continuously updated throughout the simulation. The parameters needed for the growth equations (equations 4.1-4.5) have been described in Section 4. For cereals the values of these parameters can be changed to represent individual crop types.

Only two atmospheric variables may be altered by the input algorithms. The first of these is n, as used in equation 5.4 in relation to soil evaporation and the second R_{crit} (section 5.2), which determines which method of rainfall distribution and is used when converting daily rainfall total into hourly amounts.

All of the variables described above are input into data files which are then read by the main program before the commencement of the simulation.

6.5 DETERMINATION OF THE TIMESTEP

The need for a variable timestep arises from the fact that calculations within the model assume that conditions at the start of the timestep remain constant throughout it. If the timestep is long this could lead to substantial errors in the simulation of fast acting processes like infiltration. For instance, if a layer is draining from saturation at the start of a timestep, the drainage rate will quickly drop as conductivity drops and suction forces come into play. However, within the model this does not happen since suction and conductivity remain constant until they are recalculated at the commencement of the next timestep. Hence, it is possible for the calculated loss to greatly exceed the actual loss and even exceed the volume in storage. To counter this a condition is built into the

program that if the exchange is more than a specified amount the timestep is reduced and exchanges recalulated (Figure 6.3). The variation in timestep is controlled by the drainage equations and affects all the soil processes (Section 3) with the exception of capillary rise. The timestep may also be reduced from one day to one hour by the occurrence of rain or if the layers are very wet.

The variation in timesteps ranges from a day down to one hour, one minute, one second and a tenth of a second. All steps work within one cycle of the timestep above it. For example, if an hourly timestep is considered appropriate for a given day but in the first hour water exchanges are too rapid, the timestep is reduced to one minute and the exchanges recalculated. The minute timestep is not then used for the whole day but only for the first hour, after which the timestep reverts back to an hour until exchanges indicate otherwise or until the end of the day. Before the timestep is reduced by the percolation subroutine, the exchange between two layers must be greater than 10% of the moisture content of the upper layer. The capillary rise algorithm also uses a variable timestep if exchange between layers exceeds 10% of the moisture content. However, this algorithm is not part of the same block as the percolation, infiltration and macropore routines.

Several processes within the model only work on a daily timestep these being evapotranspiration, plant growth and

soil cracking.

6.6 RAINFALL ALGORITHMS

If the rainfall input is greater than zero the program initiates the rainfall algorithms where one of two paths is followed depending on the total rainfall magnitude. If it is less than or equal to a specified amount, termed R_{crit}, it is divided up into blocks of 0.5mm with one containing any remainder. If the rainfall is greater than R_{crit} then the intensity duration curve as described in Section 5.1 is calculated. For timesteps less than an hour, the hourly rainfall is divided up equally between them.

6.7 INFILTRATION ALGORITHMS

The infiltration subroutines determine which method, ponded or non-ponded is to be used to calculate the influx and redistribution of water. Section 3.3.2 describes fully the methods used. One important simplification within the model involves the calculation of Fs (equation 3.7)- the amount of water needed, after rainfall intensity has exceeded Ks, before ponded infiltration can commence. If Fs is not satisfied within one timestep the water is simply added to the top layer and ponding is assumed not to have occured. Another feature of the algorithm, is that when the

wetting front passes over a layer boundary the parameter values Hf and Kf change (equation 3.8). This means that the time taken to reach the boundary and the amount of water required to attain this are calculated. The remaining time and water volume are then used to calculate infiltration into the underlying layer. This happens every time a boundary is crossed until the time within the timestep is exhausted.

The ponded method of calculating infiltration ceases if rainfall intensity is less than the infiltration capacity, as the wetting front cannot maintain continuity. When this happens the rain is added to the layer previously containing the front, and for all layers the water content is averaged out. If intensity is greater than Ks this may indicate the formation of a new wetting front in the next timestep. When rainfall exceeds infiltration capacity, the excess is added to the ponded store from where it may reach the macropores. If at the end of the day there is still water in the ponded store this is assumed to have been lost from the system.

At the end of the day the infiltration wetting front is diffused if it is still present. This is purely to simplify the process as the presence of wetting fronts would greatly complicate the calculation of evapotranspiration.

Figure 6.4 describes in flowchart form the operation of the infiltration subroutines.

FIGURE 6.4 FLOWCHART FOR INFILTRATION SUBROUTINE

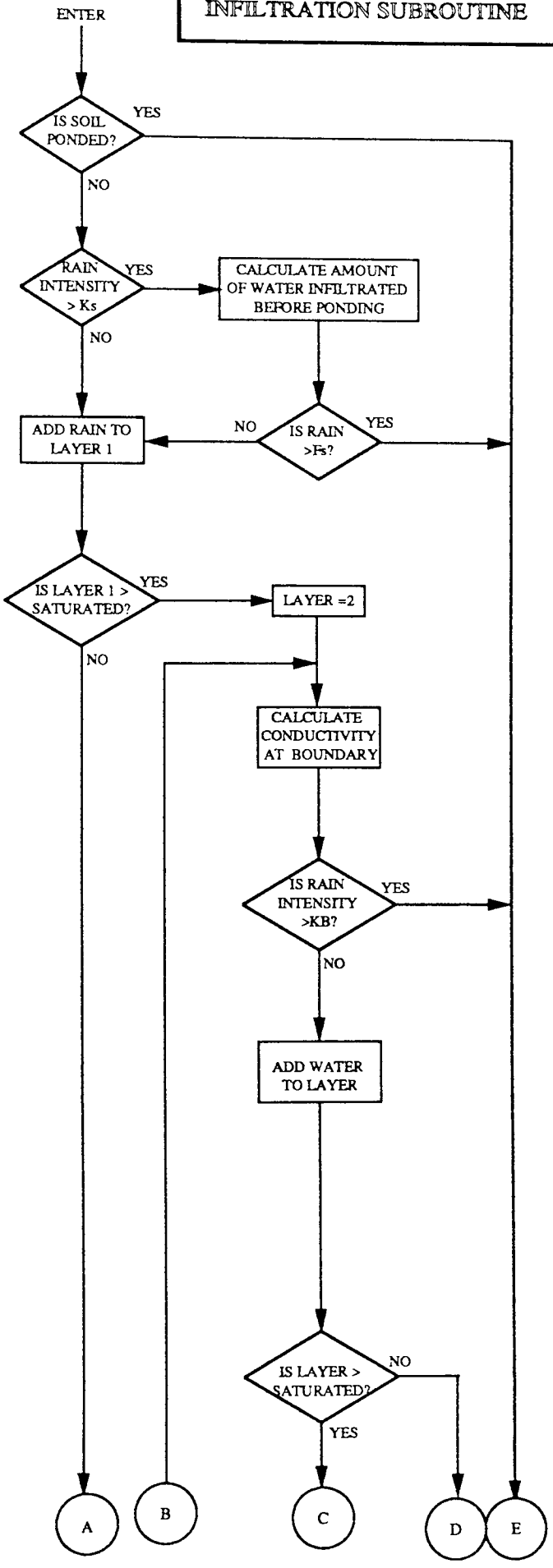

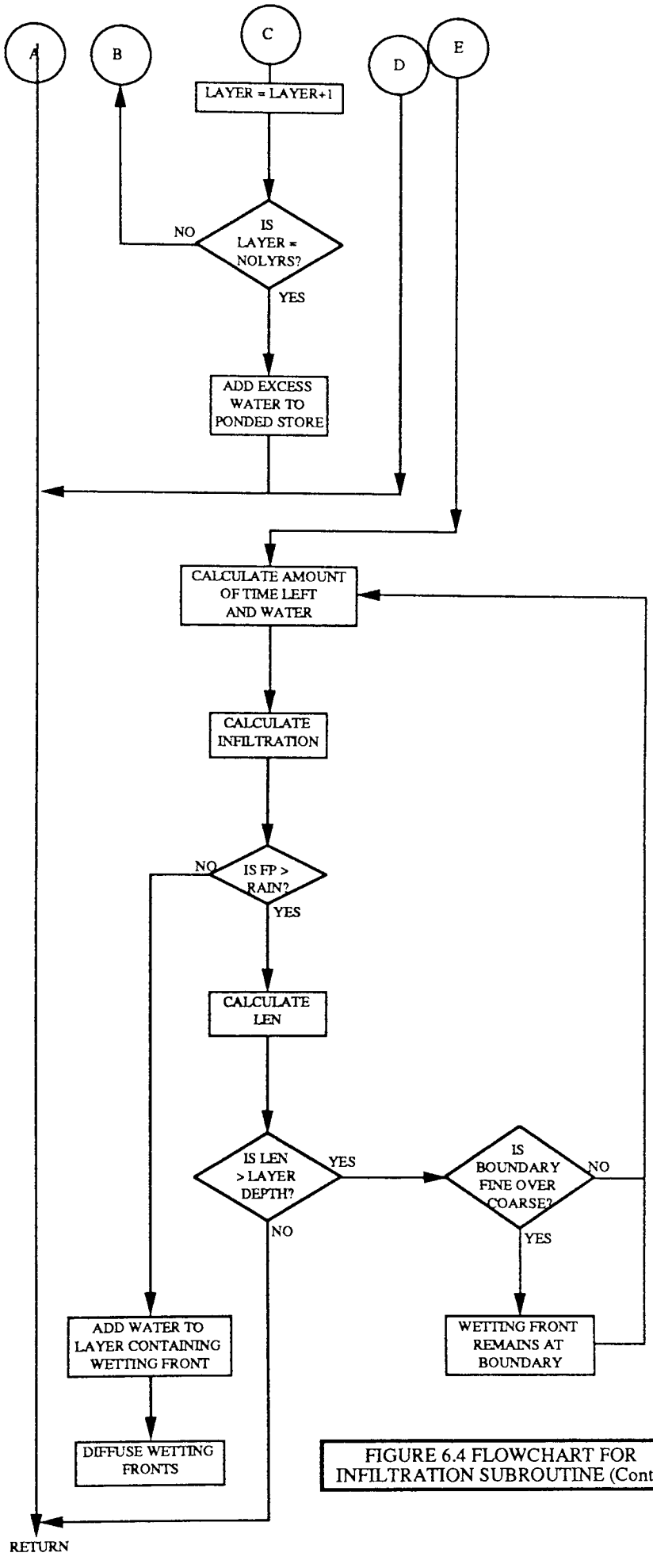

FIGURE 6.4 FLOWCHART FOR INFILTRATION SUBROUTINE (Contd)

6.8 MACROPORES

The macropore subroutines are only called if there is surface ponding or water within the macropores. The filling of the macropores with water from the ponded store occurs instantaneously - as assumed by Beven and Clarke (1986). Once the level of water within each macropore class is established, lateral infiltration is calculated according to the method given in Section 3.4.3.

The presence of an infiltration wetting front (IWF) complicates the calculations. If the layer is above an IWF no infiltration can take place from the macropore. If the IWF is within the layer concerned the macropore can only transfer water to the part of the layer below the IWF.

Macropore wetting fronts are, like infiltration fronts, diffused at the end of the day as leaving them intact would greatly complicate the calculation of evapotranspiration. However, if there is water remaining in the channels this is carried over to the next day, except in the case of cracks where as their size may change from day to day the water is added back to the ponded store. As mentioned in the previous section, water within the ponded store is lost from the system at the end of the day.

Figure 6.5 describes in flowchart form the operation of the macropore subroutines.

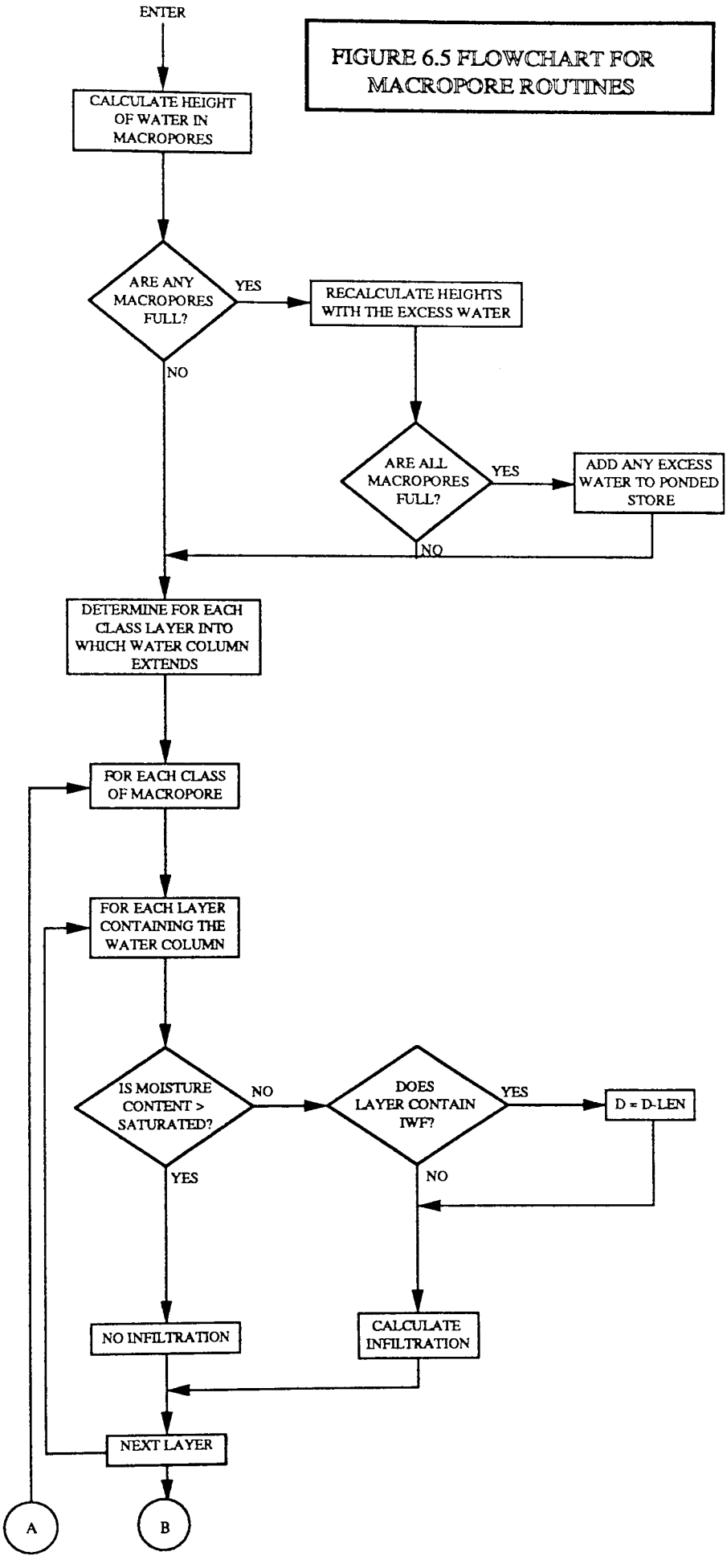

FIGURE 6.5 FLOWCHART FOR MACROPORE ROUTINES

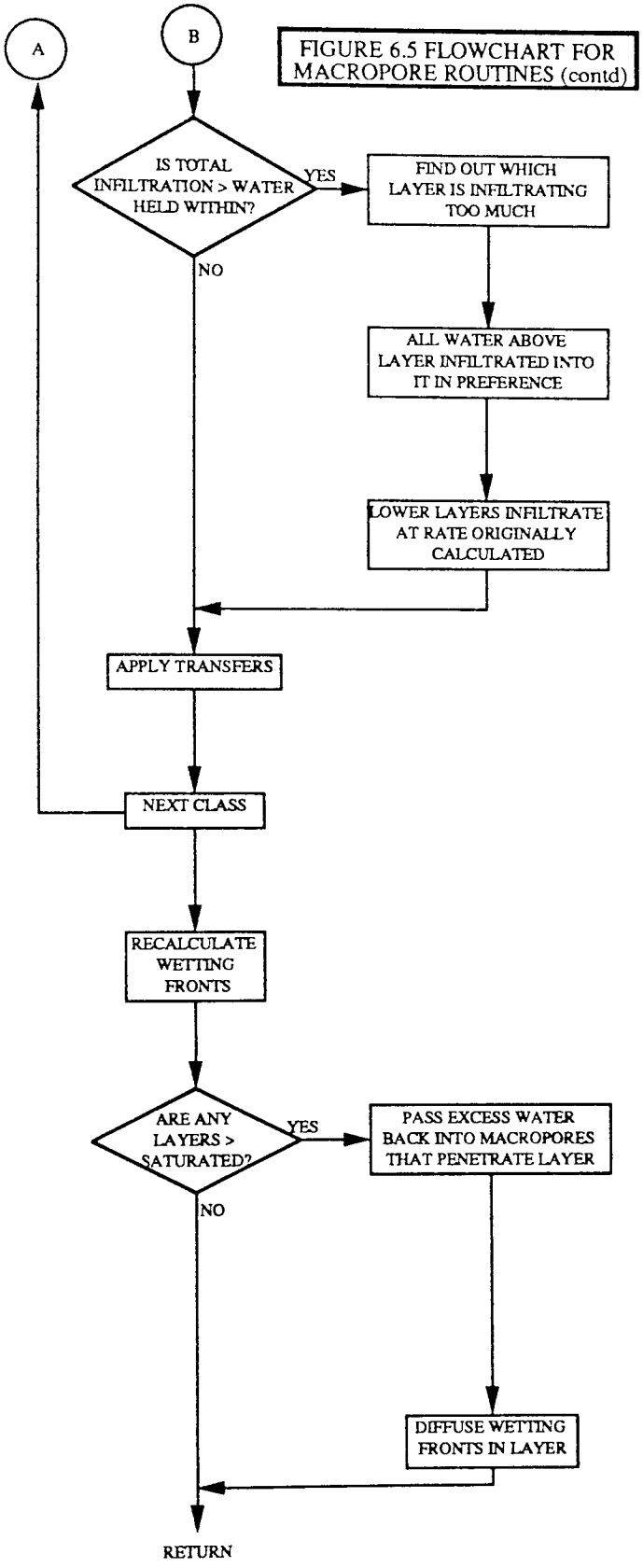

FIGURE 6.5 FLOWCHART FOR MACROPORE ROUTINES (contd)

6.9 PERCOLATION

There are two percolation routines, one for use in the presence of wetting fronts (Redist_Percolation Figure 6.6a) and one for use in their absence (Percolation Figure 6.6b). The latter simply uses equation 3.6 for calculating exchanges between layers except for exchanges between the two basal layers, the mechanisms for which are described later. For the other routine, percolation is assumed to only take place from the layer containing the infiltration wetting front (IWF) and the layers below. In the layer containing the IWF the percolation calculation only considers the area below the IWF. Flow across the boundary layers above the IWF having already being accounted for by the infiltration routines. The presence of MWF's leads to a new set of assumptions. Exchange is calculated for the average moisture content of the layer (Vav), or if an IWF is present for the average moisture content below this. It is also calculated for the zone of the layer unaffected by wetting fronts (Vin). If Vin is greater than Vav then this is considered as the amount exchanged and the MWF's are unaffected. If it is not (i.e. Vin < Vav), then as long as Vav is greater than zero the front's radii must be recalculated based on the percentage contribution of each macropore class.

In both percolation routines if the moisture content of the underlying layers is greater than saturation then the

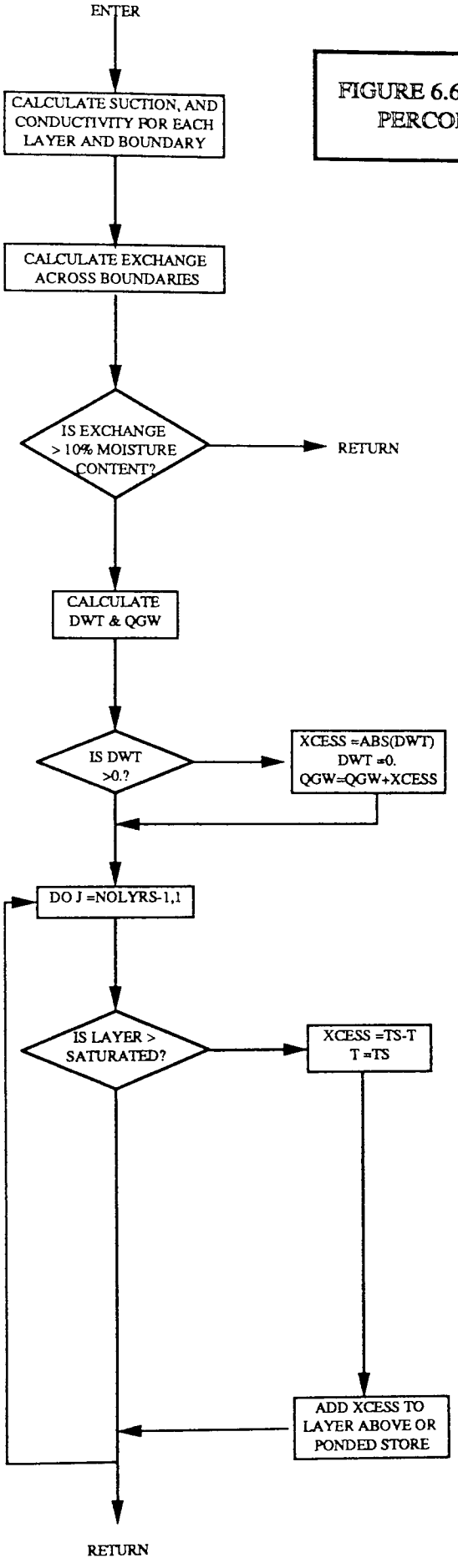

FIGURE 6.6A FLOWCHART FOR PERCOLATION ROUTINE

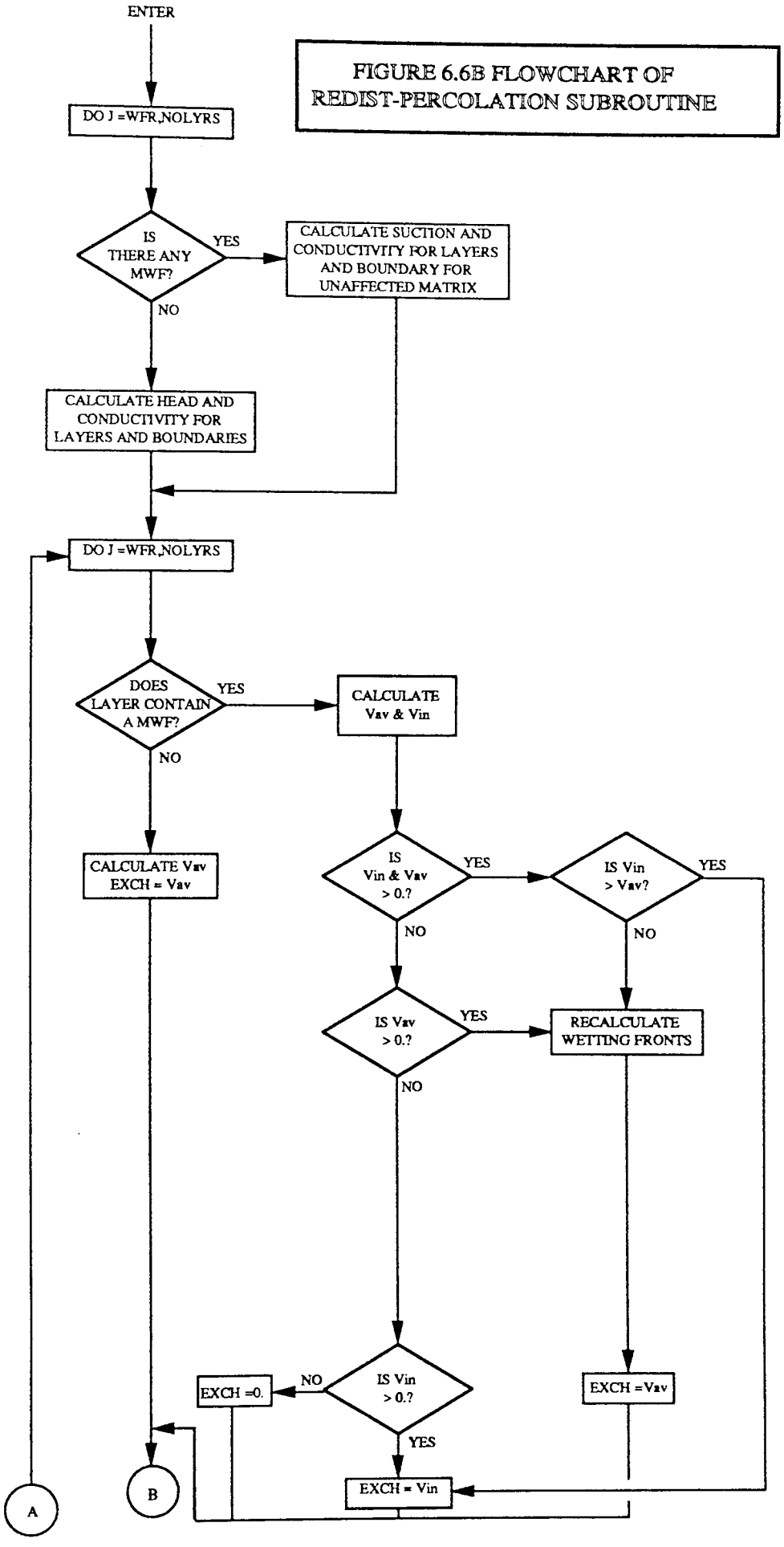

FIGURE 6.6B FLOWCHART OF REDIST-PERCOLATION SUBROUTINE

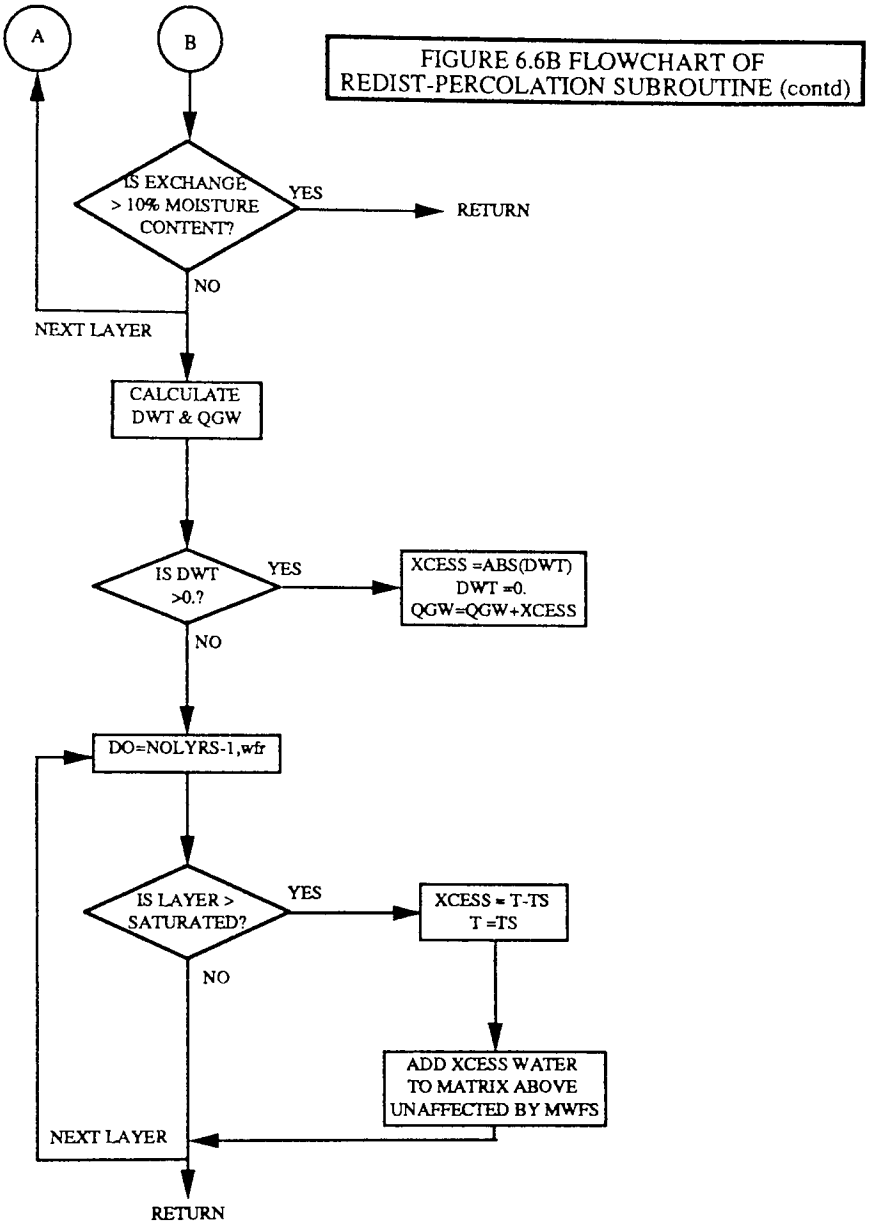

FIGURE 6.6B FLOWCHART OF REDIST-PERCOLATION SUBROUTINE (contd)

excess is passed back to the overlying layer. In the case of the wetting front percolation routine the water is passed back up into the area unaffected by macropore fronts, no water is passed back up into the macropore wetting fronts even if they originally contributed. This assumption greatly simplifies the routine and is consistent with the original objective in redistributing water by bypass flow as stated in Section 3.4.

In the case of the calculation of the exchange between the two basal layers this is achieved using a modification of equation 3.6 necessitated by the presence of a water table within the basal layer. The modified equation is given by equation 6.4 below:

$$V_j = K_{j-1} \cdot \left[\frac{1 - h_{j-1}}{(d_{j-1}/2)+dwt} + 1 \right] \qquad -6.4$$

where V_j = flow across the boundary (cm/s);

K_{j-1} = conductivity of the layer above the basal boundary (cm/s);

h_{j-1} = suction of the overlying layer (cm);

d_{j-1} = thickness of overlying layer (cm);

dwt = depth from the top of the basal layer to the water table (cm);

The model of water movement across the basal boundary follows the procedure adopted by Hussein (1979), where the water table is assumed to occur within the basal layer. The

parameter dwt is determined from the inflow into the layer and the outflow from the base (qgw). Outflow is based on the assumption that the groundwater store behaves as a linear reservoir and is calculated from equation 6.5 (Hussein 1979) below:

$$qgw = a(d_{gl} - dwt) \qquad -6.5$$

where a =empirical constant

d_{gl} =thickness of basal layer (cm)

If dwt becomes negative (i.e the water table rises into the overlying layer) then for simplicity it is assumed that the excess water is lost to groundwater flow and dwt is set equal to zero.

Capillary rise is treated as negative percolation, thus the percolation routine is used but the flows appear as negative values and thus move upwards. For calculation of head the wetting curve equation is used (Section 3.2.1.2). Capillary rise is only called daily after the wetting fronts have been dissolved (Section 3.2.3). It is not calculated at the same time as percolation as when one layer is near saturation, the water exchanged in the previous timestep may have been sufficient to give a negative answer to exchange within the present one. So the inferred rise may only be a function of timestep not reality. The presence of wetting fronts would also complicate the process immensely.

6.10 PLANT ROUTINES

These algorithms run on a daily basis. Evaporative demand is split between soil evaporation and potential transpiration. Actual transpiration is calculated using the soil conditions arrived at at the end of the day and from the plant characteristics determined in the previous day's timestep. The actual transpiration is then used to calculate the amount of growth, and the ratio of actual to potential transpiration to partition this between the leaves and the roots.

6.11 SUMMARY

With the aid of a number of flow charts (Figures 6.1, 6.3-6.6) this chapter has described the way the model operates, the order in which the routines are accessed, and when, why and how they interact with each other.

CHAPTER 7 SOIL-MOISTURE-PLANT MODEL SIMULATIONS

There are two primary objectives of this chapter: firstly, to compare and calibrate the model to field data collected by Hussein (1979); and secondly to use the soil-moisture-plant model to simulate certain processes within the environment and to see how model predictions compare to results obtained in the field or by controlled experiments.

The first section of the chapter uses the fully developed model to simulate the results collected from Preston Vale Farm during the period Jan. 1977 to Oct. 1978 by Hussein (1979). Using the model developed by Hussein (1979) and soil samples collected from the field the model is calibrated. From resulting analysis further calibration is performed with special regard to the plant, macropore, groundwater discharge and saturated conductivity parameters.

The processes simulated are water uptake, plant growth and infiltration. The model is used to see how these processes react to varying soil types, environmental conditions and vegetation characteristics. Results are compared in a qualitative manner to results obtained from the literature. Comments and observations are also put forward for situations not yet covered by experimental or field results as well as stating the limitations of the work.

7.1 TESTING THE SOIL-MOISTURE-PLANT MODEL

The aim of this section is to assess the ability of the soil-moisture-plant model, developed in Chapters 3-6, to simulate field conditions. The model was calibrated against and tested against field soil moisture data collected by Hussein in 1979 using a neutron probe. The calibration period was from March-October 1977, and the model was then tested against data from October 1977-August 1978. The performance of the model was then assessed in relation to the results of these tests and by comparison with Walley and Husseins' (1982) model. The latter was considered important because one of the objectives of this project was to improve on the performance of the original model.

7.1.1 MODEL INPUT DATA

7.1.1.1 HUSSEINS' DATA

The data used in assessing the soil-moisture-plant model was collected from an area of permanent pasture at Preston Vale Farm near Penkridge, Staffordshire (Figure 7.1). Detailed field measurements were collected from January 1977 to October 1978. These included rainfall, soil moisture and soil type. In addition, the full range of data required for the estimation of potential evapotranspiration were available for a Meteorological Station situated 2 miles

FIGURE 7.1 Location Maps (Adapted from Hussein 1979)

FIGURE 7.1a Preston Vale Farm

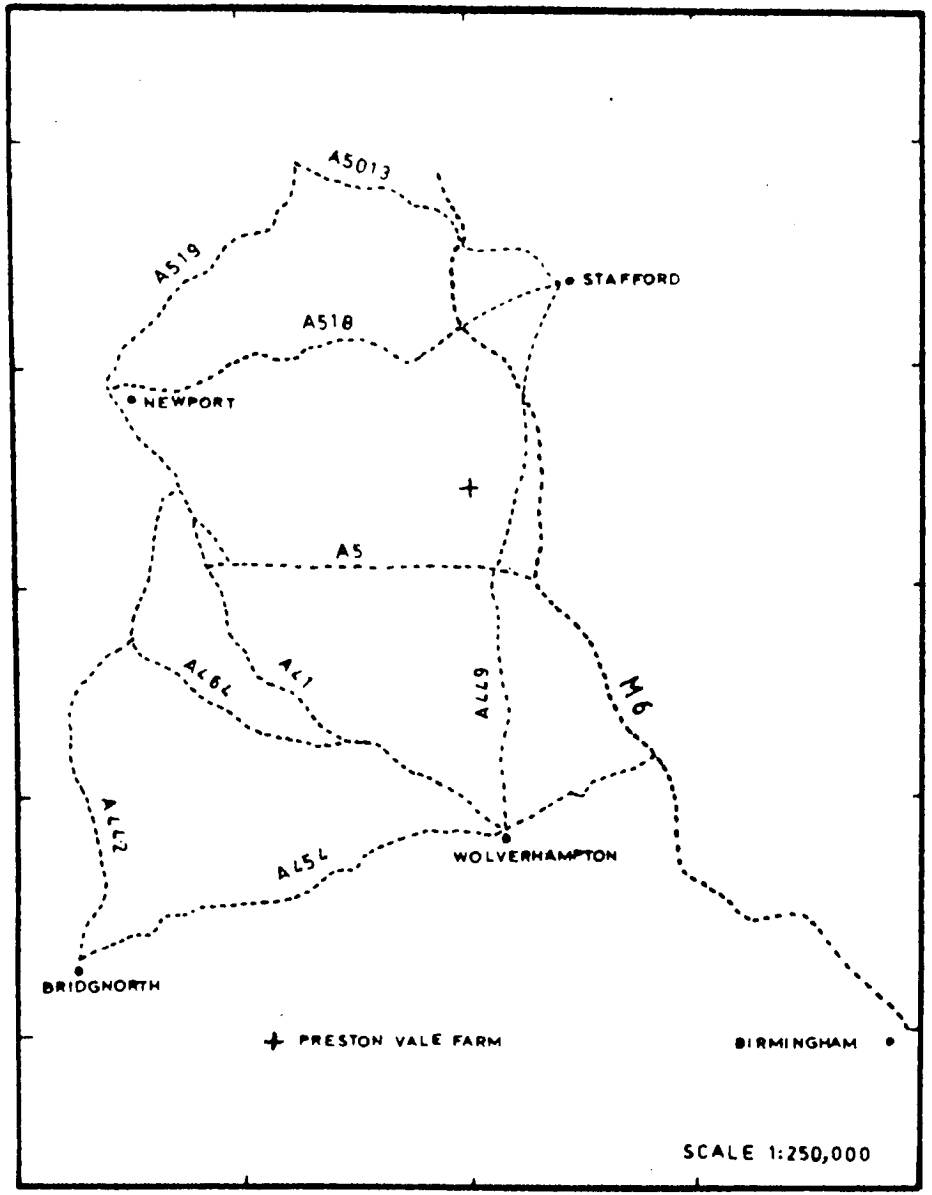

FIGURE 7.1b Location of Probe Tubes

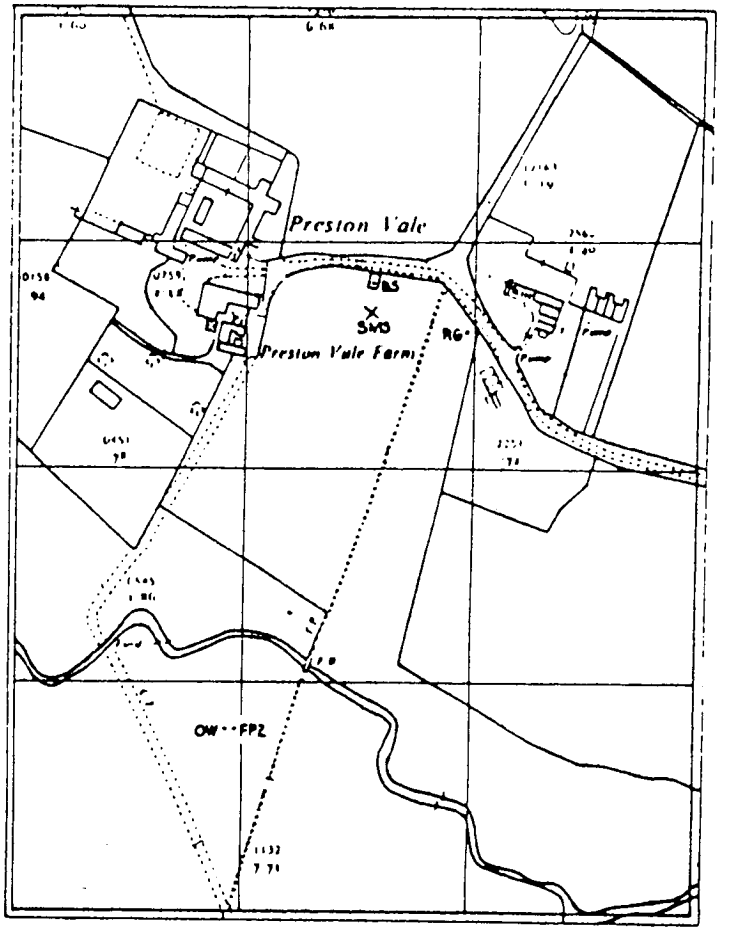

SMS Location of Neutron Probe Station

RG rain gauge

away. Rainfall data were also available from this site and an autographic raingauge situated 3.5 miles away.

The soil moisture profiles were recorded using a neutron probe (Wallingford No. 225). Data were collected in the form of the count rate per second of neutrons recorded by the detector. This count rate is proportional to the moisture content of the soil, thus with the use of a calibration curve the count rate can be converted to moisture content. In order to overcome the problems of spatial variation within the site, profiles were recorded in five access tubes within a 4m x 4m level plot. Soil moisture was recorded at 0.1m depth increments within each tube at approximately weekly intervals during the summer months and monthly intervals during the winter.

During the initial installation of the tubes Hussein (1979) collected samples from each of the five tubes to their full depth. For each of these samples the particle-size distribution was determined using the sieving procedure described in BS 1377 (1975). This gave the percentage of sand and the combined silt/clay fraction. Due to the large number of samples, Hussein then used hand methods to determine whether the combined silt/clay fraction was predominantly silt or clay. Using the USDA soil triangle classification soil type was then determined. For the Preston Vale Farm site four soil layers were defined:-

1. 0. - 0.15m (layer 1) Humus Sandy Loam

2. 0.15 - 0.35m (layer 2) Loamy Sand

3. 0.35 - 0.95m (layer 3) Sand

4. >0.95m (layer 4) Sand

Though layer 4 is the same soil type as layer 3 it is described separately, because it is the layer within the model which contains the fluctuating groundwater table.

The total rainfall occurring between site visits was recorded using a standard Meteorological Office raingauge. This was then distributed into daily amounts by reference to the rainfall data from the Meteorological Station and the Autographic gauge at the project supervisor's home (Figure 7.1a). Daily potential evapotranspiration was estimated by the Penman Equation using the data from the local Meteorological Station.

7.1.1.2 ADDITIONAL DATA REQUIRED

Hussein (1979) used the soil data he collected to assign a soil type to each layer. Then using data from the literature he produced suction-conductivity-moisture content relationships for each of the three described soils (see Section 2.3). The present work however relates suction-conductivity-moisture content curves directly to particle-size distribution, saturated moisture content and saturated conductivity (Section 3.2.1.2). In view of the need for a more complete description of the particle-size distribution

and measurements not originally done (i.e saturated moisture content and saturated conductivity), it was necessary to revisit the site in the summer of 1989 in order to take further samples.

Using a corer based on a design by Hall et al (1977) in situ samples were taken from the top three of the previously identified soil layers in 150mm long pvc plastic liners (Hussein 1979). Since the top layer was only 150mm deep, the sample taken from it was restricted to 100mm using a split liner (i.e. 100mm and 50mm lengths). Samples were not taken from layer 4 because the model does not require the suction-conductivity-moisture content relationship for this layer. Samples were taken at the original site which was located from Husseins' original map (Figure 7.1b the Soil Moisture Main Star SMS) and confirmed by the presence of the original tubes.

The samples were then tested for four properties: particle-size distribution, organic content, bulk density and saturated conductivity (Ks). In the particle-size analysis sand fractions were determined by dry-sieving, the pipette method being used for the finer fraction as described in BS 1377 (1975). The results obtained in this analysis conform to the British classification of grain sizes. However, the USDA classification was required in order to produce the suction-conductivity-moisture content curves. This was achieved by plotting the data on a

particle-size distribution chart, and drawing the best fit curve by eye. From this curve the particle-size distribution data, in terms of the USDA classification, was read off. The results are presented in Table 7.1.

Organic matter content was determined by the chemical method (Test No. 8) given in BS 1377 (1975). Bulk density was determined from the dry weight of the sample divided by the volume of the pvc liners. Saturated conductivity was determined using undisturbed samples and a constant head permeameter designed to hold the samples within their 150mm long pvc tubes (Hedges (1989) and Figure 7.2). Data collected from these tests are given in Table 7.1.

From Table 7.1 it can be seen that data on Ks were only determined for the surface layer. Tests determining the Ks of the lower layers were not performed due to the conclusions drawn from the analysis of layer 1, which are described below. The value obtained for the surface layer i.e a Ks of 10.5m day^{-1}, seems unrealistic when compared with the values given in the literature for soils of similar composition (e.g Mualem 1976b, SCS-USDA 1974, Long et al 1969) The conductivity of the surface layer being several orders of magnitude higher. The large values obtained for the surface layer are probably related to the high number of root channels and other macropores (such as wormholes) within the soil and are not therefore representative of the soils matrix. Since the object of the model is to

TABLE 7.1 RESULTS OF ANALYSIS OF SOILS FROM PRESTON VALE FARM

Soil Property	Layer 1	Layer 2	Layer 3
Sand (%)	72	83	91
Silt (%)	13	14	9
Clay (%)	15	3	0
V. Co. Sand (%)	2	2	3
Co. Sand (%)	9	7	7
Med. Sand (%)	27	33	35
Fine Sand (%)	23	26	35
V. Fine Sand (%)	11	15	11
Co. Silt (%)	12	13	9
Fine Silt (%)	1	1	0
Bulk Density (g/cc)	1.175	1.555	1.444
Saturated Conductivity (m d^{-1})	10.86	-	-
Organic Matter (%)	7.74	3.59	0.10

particle-size classes as defined by USDA (appendix 1)

TABLE 7.2 CALIBRATION EQUATIONS DERIVED FOR ASTON'S NEUTRON PROBE

Bell (1976)	
Silts, sands and Gravels	R/Rw = 1.266t + 0.030
Loams	R/Rw = 1.153t + 0.018
Clay (and peat)	R/Rw = 1.044t + 0.013
Binding (1975)	
Field Calibration	R/Rw = 1.333t - 0.007
Lab Calibration (sand)	R/Rw = 1.212t + 0.003
Rw = 1178	
Hussein (1979)	
Field Calibration	R/Rw = 0.940t + 0.075
Rw = 1177	
Wood (1982)	
Lab Calibration (sand)	R/Rw = 1.266t + 0.030

* R = observed count rate in counts per second (c.p.s)
Rw = count rate in standard water
R/Rw = relative count rate
t = volumetric moisture content

** Bell's (1976) curves refer to the general Wallingford Neutron Probe Model, the rest refer specifically to the one at Aston

FIGURE 7.2 Apparatus for Determining Saturated Conductivity (from Hedges 1989)

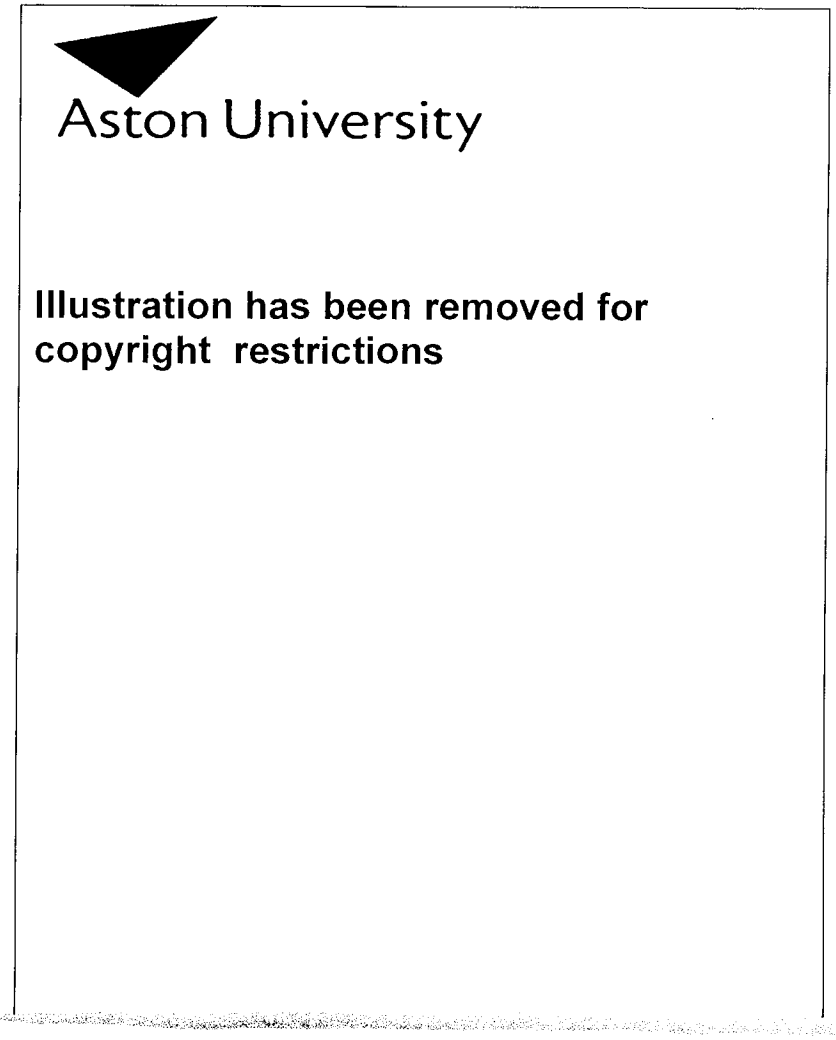

distinguish between the matrix conductivity and the macropore conductivity within the model and these are difficult to separate in the field, it appears that the Ks values obtained are of little value here. It was thus decided that the matrix saturated conductivity value for each of the layers should be determined by calibration.

7.1.2 DETERMINATION OF THE PARAMETER VALUES

Using the data described in Section 7.1.1, several of the model's parameter values could be determined. These included parameters within the suction-conductivity-moisture content, infiltration and macropore routines. The derived curves for suction-moisture content and relative conductivity-moisture content for each of the layers are shown in Figures 7.3 and 7.4 respectively. Saturated moisture content (ts) was determined from bulk density using the relationship described by equation 6.1. However, initial model testing showed that the ts value for the surface layer was presenting problems, seemingly far too high. It was decided that ts for the surface layer would be determined by calibration. The high value obtained from field data may be the result of the large number of macropores within the layer.

The soil moisture data, collected as neutron count rates, was converted to moisture values by the use of a

Figure 7.3

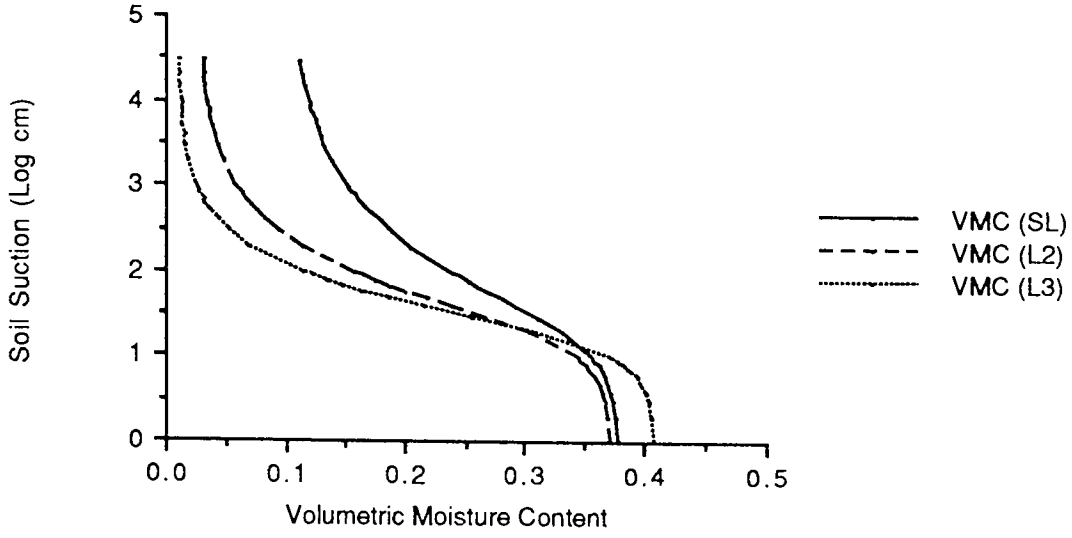

Figure 7.4

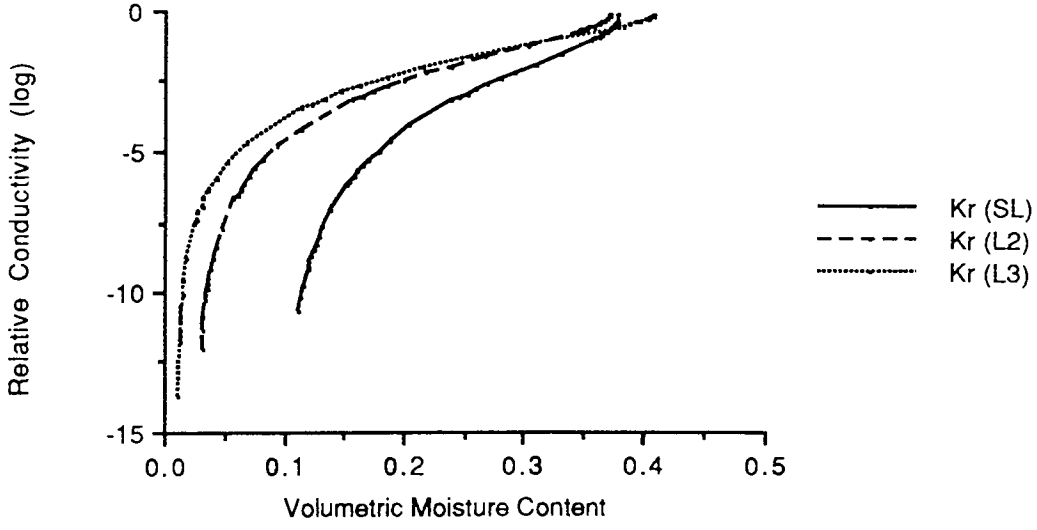

Figure 7.3 Calculated Soil Suction Curves for Preston Vale Farm

Figure 7.4 Calculated Relative Conductivity Curves (Kr) for Preston Vale Farm

* SL Surface Layer or Layer 1

L2 Layer 2

L3 Layer 3

VMC Volumetric Moisture Content (t)

calibration curve. Several such curves have been produced for the probe used at Aston, and the same model of probe used elsewhere. Table 7.2 lists the equations obtained. Hussein (1979) based his curve on a small data set obtained from several sites used within his field monitoring programme. The limitations of his data set was admitted by Hussein (1979) as too small to give a precise calibration curve, but he justifies its use on the grounds that precise curves are "only essential when absolute values of moisture fraction are required. When it is intended to determine the change of soil moisture between dates ..... only the slope of the calibration curve is of importance". However, examination of the slopes of the other curves show them to be significantly different to Husseins' but similar to each other. It was thus decided to use one of the other calibration equations and the relationship derived by Wood (1982) was chosen due to its use by Hedges (1989).

The remaining soil parameters were derived by calibration sometimes in the light of published results.

Within the soil factors the following parameters needed to be defined:

a) saturated conductivity (Ks);

b) the groundwater discharge parameters;

c) the initial moisture content of each layer;

d) the field-capacity values of each layer.

The field-capacity parameters are not used within the

simulation itself, but are used to present the soil moisture status in terms of the moisture deficit (i.e. for the sake of those agriculturalists who are used to using this measure of moisture status). The parameter values not found by calibration are listed in Table 7.3. These were the same as given by Walley and Hussein (1982).

Within the macropore routines information was required for the permanent and temporary macropore divisions. For the permanent (of fauna and floral origin) macropores data are needed on the number of classes and, within each of these classes, information on the the number of macropores, their radius and the layer to which they penetrate is also needed. For the temporary (mechanically formed) macropores Section 3.4.3 describes how the radius and number of channels are calculated for each timestep, the layer into which they penetrate being input. For faunal and floral formed channels the parameter values were derived by a combination of general knowledge gained from the literature for other sites (e.g Ehlers, 1975, Edwards et al, 1988) and calibration.

Several parameter values were required for use in the plant equations described in Section 4. In the case of water uptake, the value for plant resistance was obtained by calibration, though account was taken of values given in the literature (Lascano and Bavel, 1984). The initial root density in each layer was also required, and these values were determined by calibration. All later values of root

density were derived by the plant growth algorithm. This algorithm itself requires parameter values for:

a) the growth unit-transpiration relationship;

b) the partitioning of growth units between leaf area index and root density;

c) the actual to potential leaf area index relationship;

d) the weighting factors in root growth distribution between layers.

Since these functions were formulated by the author, it was not possible to draw on published results to assist in their calibration. However, since the crop in this field test was permanent pasture it could be assumed that leaf area index was always greater than one. In this simulation leaf area index is only required to partition evaporative demand between the soil evaporation and transpiration. If leaf area index is greater than or equal to one all evaporative demand is partitioned to transpiration. So as long as the index is greater than one the actual value is unimportant. The parameter values chosen to produce the assimilate partitioning curve were designed to produce a curve where the increase in the partitioning of assimilates to the roots for the crop does not start as soon as the plant is stressed (i.e. sensitive to stress) or require large values of stress (i.e. tolerant to stress). Furthermore, the partitioning curve is assumed to increase gradually with increasing stress. The parameter values chosen bear these points in mind. The growth unit used took into account the limited

TABLE 7.3 MODEL PARAMETER VALUES NOT DETERMINED BY CALIBRATION

parameter	layer 1	2	3	4
ts	-	0.3729	0.4096	0.4096
a	0.0470	0.0433	0.0463	0.0463
n	1.4242	1.6376	1.8642	1.8642
tr	0.0990	0.0273	0.0109	0.0109
tfc	0.3200	0.2410	0.1390	0.1390
Hf (cm)	15.3317	15.5029	13.8036	13.8036
D (cm)	15.0000	20.0000	60.0000	250.0000
a	0.0002			
R_{crit}	0.5	(cm)		
n	2.0			

* The parameters ts, a, n and tr which are given values for each layer are from Genuchten's Suction Equation and are not related to the other a (equation 6.5) and n (equation 5.5).

TABLE 7.4 MODEL PARAMETER VALUES DETERMINED BY CALIBRATION

parameter	layer 1	2	3	4
Ks	0.000001	0.0003	0.005	0.005
ts	0.38	-	-	-
t	0.30	0.24	0.22	0.22
Rd	1.80	0.20	0.20	-
PR	10000			
LAI	1			

Permanent Macropore Classes =2
Class 1
120 holes 0.15cm radius 105.0 cm depth
Class 2
5000 holes 0.05cm radius 45.0 cm depth

range of potential evaporative demands experienced in the U.K, and the parameters Lc and Rc (equation 4.5) used in converting growth units into increased leaf area index and root density respectively, were determined by calibration. The parameter values not found by calibration are listed in Table 7.3.

Calibration was performed using field data for the period March-October 1977. Once calibrated, the model was tested on data from October 1977-August 1978. A large number of simulations were performed to see the effect each parameter had on the overall model.

In summary, this section has shown that the following parameters: Ks, Lc, Rc, ts of surface layer, initial root densities, macropore numbers, radii and layer of penetration, and plant resistance were all variables which had to be found by calibration.

7.1.3 RESULTS AND DISCUSSION

The final results of the simulations are shown in Figure 7.5 and 7.6. Table 7.4 lists the values of the parameters determined by calibration. The results indicate clearly that the model can represent conditions within the field to a high degree of accuracy. A number of points about the working of the model, its accuracy and how it was

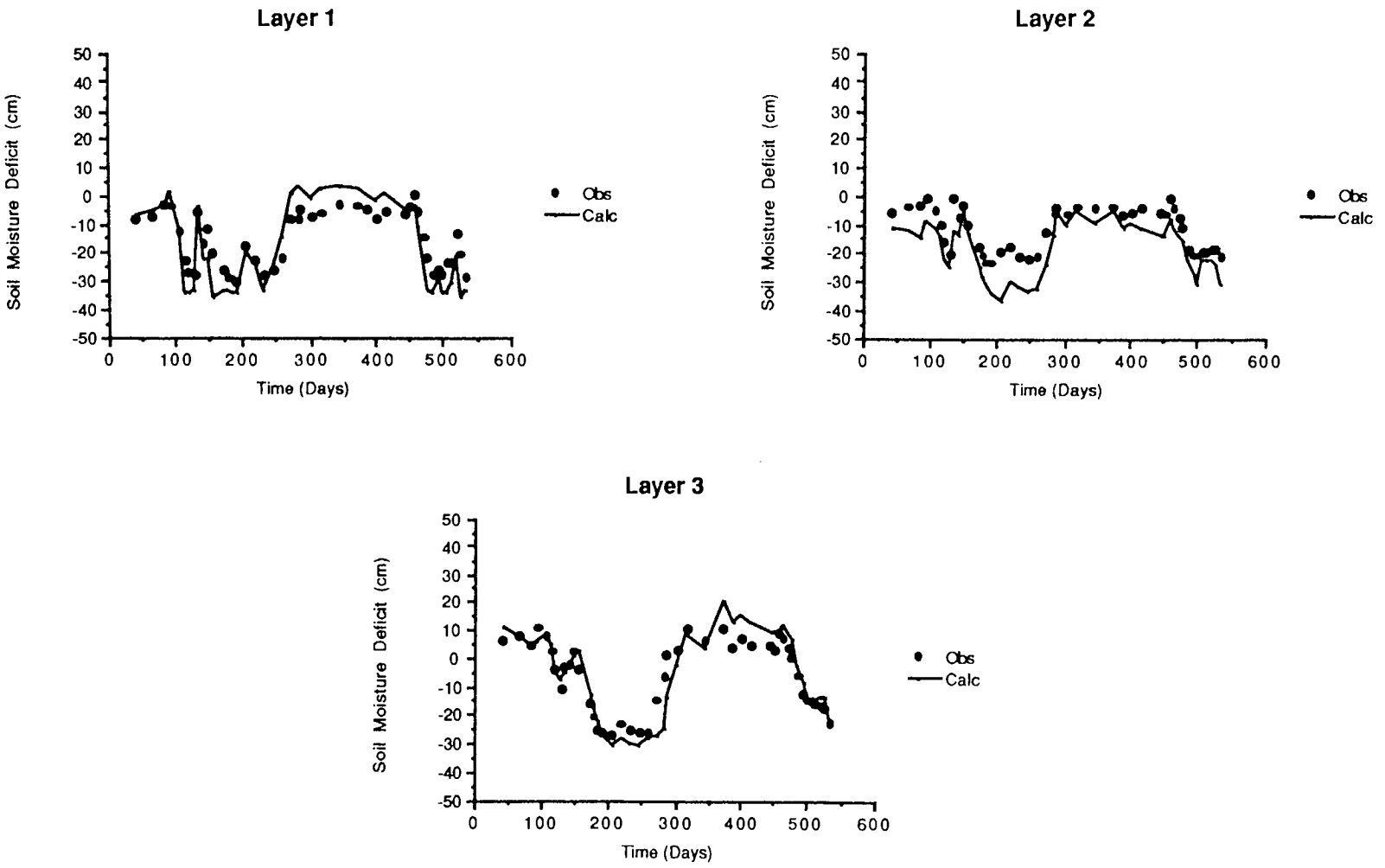

Figure 7.5 Calculated and Observed Soil Moisture Deficits for Each Soil Layer - Final Results

(probe calibrated using the relationship derived by Wood (1982))

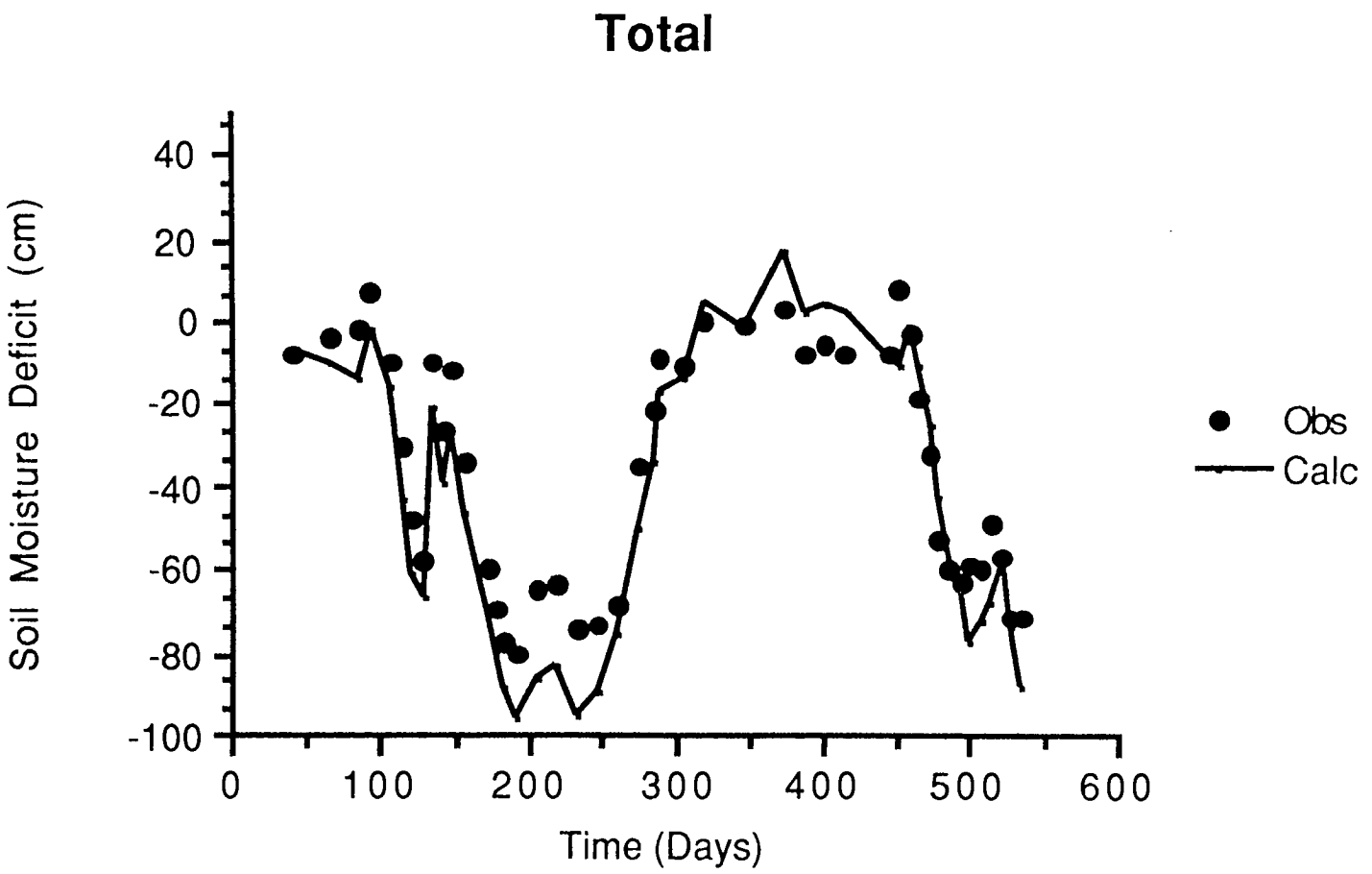

Figure 7.6 Calculated and Observed Soil Moisture Deficits for the Three Layers - Final Results

(probe calibrated using the relationship derived by Wood (1982))

modified during the calibration process are discussed below. The discussion is split into four areas describing the plant algorithms, macropore and micropore flow interactions, rainfall distribution and overall model performance.

1. Plant Algorithms

The two plant components of the soil-moisture-plant model are inter-dependant due to the root density and leaf area index parameters. Leaf area index partitions evaporative demand between the soil and the plant, the transpirational demand determining the amount of new growth for the plant: i.e the increase in the leaf area index and the root density. The root density in each layer affects the amount of water uptake from that layer as do soil suction, moisture content and transpirational demand. The actual transpiration being the sum of the water uptake from each layer. Using a stress index (equation 4.3) based on the relationship between actual and potential transpiration, growth is partitioned between the leaf and the roots.

In the case of Preston Vale Farm the crop is permanent pasture. For permanent pasture it is assumed that the leaf area index is greater than 1 and as such all evaporative demand is considered as potential transpiration. For the whole root profile root density is assumed to remain constant (see Section 4.2.4) though for individual layers it is allowed to vary according to moisture status. Partitioning of root growth to each layer is determined by

moisture gradients (Section 4.2.4) and root death is assumed to take place in the layer within the root profile with the highest suction.

Early testing of the model showed the model to give good results in terms of soil moisture deficits, with particulary good results during the summer of 1978 (450 days - end of simulation). Analysis of the calculated evapotranspiration showed that the plant was able to maintain transpiration close to the potential value for most of the year including the summer months. Examination of which layers were calculated to contribute towards transpiration showed that for the winter months the main contribution was from the surface layer with the lower layers becoming more significant in the summer, as the upper layer dries, especially layer 3. Though layer 2 contributed water to transpiration during the summer of 1977 it did not contribute at all during the following summer. The reason for this is that during the simulation there has been a significant loss in calculated root density in layer 2 with layers 1 and 3 showing an increase. As the root density for the whole profile remains constant it can be seen that layers 1 and 3 have benefited from the demise of root density in layer 2. Further simulations starting with different initial values of root density show a similar trend. These results are in marked contrast to what one would expect to see from an established crop in the field. With such a crop root densities would be expected to vary

within the layers between seasons but to remain fairly stable from year to year (Andrew 1987a,b).

The problem with the calculated root density within a layer not remaining fairly stable from year to year arises mainly from the following two assumptions within the model: firstly that there is no net growth in the overall root density so any gain in root density in one or more layers must be balanced by root death in another layer; secondly all root death within a timestep occurs within the least favourable horizon within the root zone: i.e the layer with the greatest suction.

The first assumption is that root mass remains constant (Andrew 1987a,b). Deinum (1985) showed that for *Lolium perenne*, a perennial grass, root mass increased in the spring and autumn but decreased during the summer as conditions for soil organisms that damage roots became more favourable. Deinum (1985) clearly illustrates the fact that root density varies between the seasons even for an established crop.

The second assumption is that all root death within a timestep occurs within the layer containing the highest suction. The formulation of this premise was based on the principle that the plant would maximise its uptake capability by shedding unprofitable areas to concentrate resources into more favourable ones (Barraclough and Leigh

1984, Madsen 1985 and Russel 1977). Such a process is, however, likely to take place over a longer period than a day especially with Deinum (1985) reporting average root lifespans of 191 days for *Lolium perenne*.

Bearing in mind the above points on root death a more flexible approach is needed. This should be one in which root density would be allowed to vary between seasons, but the average would still have to remain fairly stable over longer periods. In determining where root death is occurring a longer term approach needs to be taken. Though early results had shown within the context of the overall model that the plant growth model predicted water deficits well, it was felt that more work was required on it. Unfortunately time for this was not available.

Simulations where root density remained constant throughout the simulation period (i.e when the plant growth algorithm was not included) had produced acceptable results compared to the simulations in which root density was allowed to vary. It was thus decided in testing the model further to use this approach. The results discussed in the rest of this section were produced without the plant growth model.

The calibration of initial root densites gave a better fit to the field data if the rooting density of layer 2 was not greater than that of layer 3. From general observations

of cores taken in the field, taken in the summer of 1989 for soil analysis, this would not seem to be the case, and indeed from patterns of root distribution mentioned in the literature one would expect root density to decrease with depth. However, as pointed out by a number of authors (e.g Hamblin and Tennant 1987, Tan and Fulton 1985 and Soon 1988) root density is not directly related to the amount of water uptake: some roots being more efficient at removing water than others (see Taylor and Klepper 1973, Feddes 1978 and Gregory et al 1978). The calibration procedure has perhaps highlighted a weakness in the water uptake model used (see Section 4.3.2), in that all roots are assumed to be equally efficient at removing water. However, appropriate calibration enables the model to cope with this, as illustrated here.

During calibration of the model it became clear that the root abstraction component was very important in determining flow between layers. If the calculated abstraction was too high from an overlying layer this could retard flow into the lower layer and consequently might cause significant over estimation of moisture deficits. Conversely if abstraction is too low the opposite may be true. These effects are especially noticeable during periods of recharge.

The results produced by the root abstraction model show that the lower layers contribute significant amounts of

water to the transpiration total during the summer months (Figure 7.7). During these periods the depth of abstraction is seen generally to increase with time. Abstraction from these lower layers enabled the plant to maintain transpiration near to the potential rate during the summers of 1977 and 1978.

2. Macropore and Micropore Domains

The micropore and macropore domains in the model are interlinked by the saturated conductivity of the matrix. It is this variable which determines how much water enters the macropore by its influence on the calculation of infiltration. It is assumed that any water not infiltrated at the surface is added to the macropores, when there is available capacity (Section 3.4). The saturated conductivity also affects how much water is lost from the macropores to the matrix. Furthermore this parameter is also important in determining water flow in the micropores between layers since it is used in calculating the unsaturated conductivity (Section 3.2.2). The saturated conductivity for each layer was determined by calibration. The problems encountered with the calibration are discussed below.

The relationship between the two domains was clearly demonstrated when trying to determine the saturated conductivity of layer 2. Early simulations showed that layer 2 was discharging water into layer 3 too rapidly, causing it to dry-out and thus giving an over-estimate of the moisture

FIGURE 7.7 Water Uptake From Each Layer

Final Results

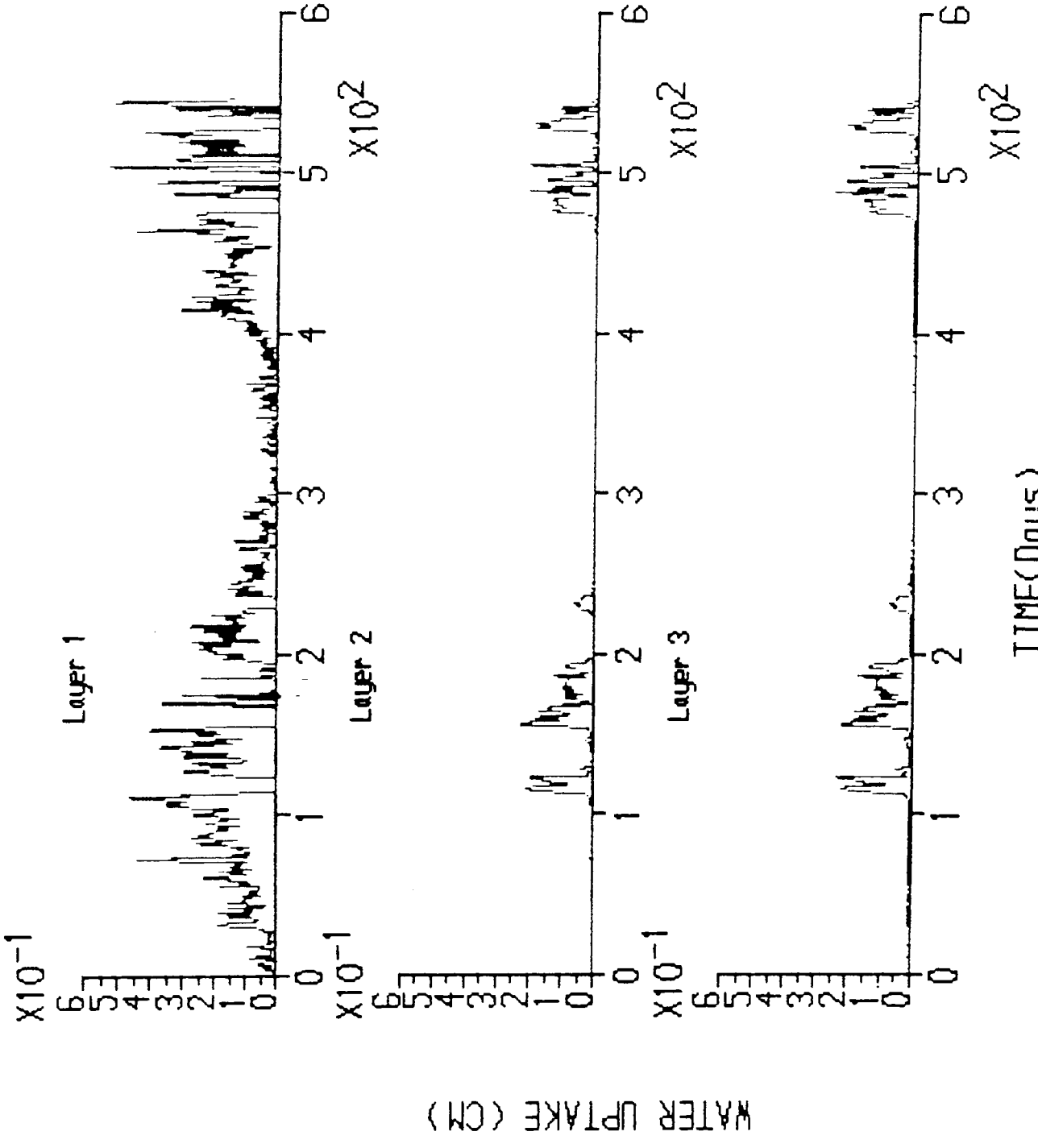

deficit. To counteract this the saturated conductivity of layer 2 was reduced. This was found to partially solve the problem but after a period deficits started to be over-estimated again. This was attributed to the fact that, although the outflow of water from layer 2 to 3 had been reduced, the reduction in saturated conductivity also decreased the input of water from the macropores into the layer. These two factors have to be balanced out when determining the saturated conductivity.

In determining the saturated conductivity of the surface layer it was found that not only was the accuracy of the calculation of this layer's moisture deficit affected by the value used but it also influenced the layers below. This is best demonstrated for two time periods during the simulation: the autumn of 1977 (180-250 days) and early 1978 (280-390 days). Examination of Figure 7.8, where Ks of the surface layer was 0.5E-05cm s^{-1}, shows that for the autumn of 1977 there is little variation in the calculated soil moisture deficit for layer 2 though field data show there is. In Figure 7.9 the Ks value of layer 2 has been reduced to 0.5E-06 cm s^{-1}, here the variation in layer 2 during the autumn is better accounted for. However, too much water has been retained in layer 1 in early 1978, a problem not seen in Figure 7.8. The cause of these errors is that with the higher Ks value not enough water has been distributed to the macropores during the autumn of 1977 instead it has been infiltrated via the matrix. If the value of Ks is reduced to

account for this the water flow between layers 1 and 2 is affected. So why does the higher value of Ks, which simulates water flow between layers 1 and 2 well, not produce the macropore flow in the autumn of 1977 which observed data suggest occurs? The problem here is not the determination of surface layer saturated conductivity but rather with the distribution of the daily rainfall total.

3. Rainfall Distribution Algorithm

The rainfall algorithm distributes daily rainfall totals firstly into a series of hourly intensities, these then being distributed randomly into the hours of the day. Hourly intensities are calculated from an intensity/duration curve formulated from rainfall data as described in Section 5.1. No attempt was made to differentiate between different types of rainfall.

The lack of calculated macropore flow seen in the autumn of 1977, when the surface layer saturated conductivity was taken as 0.5E-05 cm s^{-1}, can be attributed to the incorrect distribution of daily rainfall totals into sufficient intensities to produce excess water at the surface for macropore flow. Rain falling in the autumn period is likely to have been in the form of convectional storms, which are of shorter duration and of greater intensity than other rainfall types, and would have produced more macropore flow. This seems to be the case at Preston Vale Farm where, from measured data, layer 2 is seen to

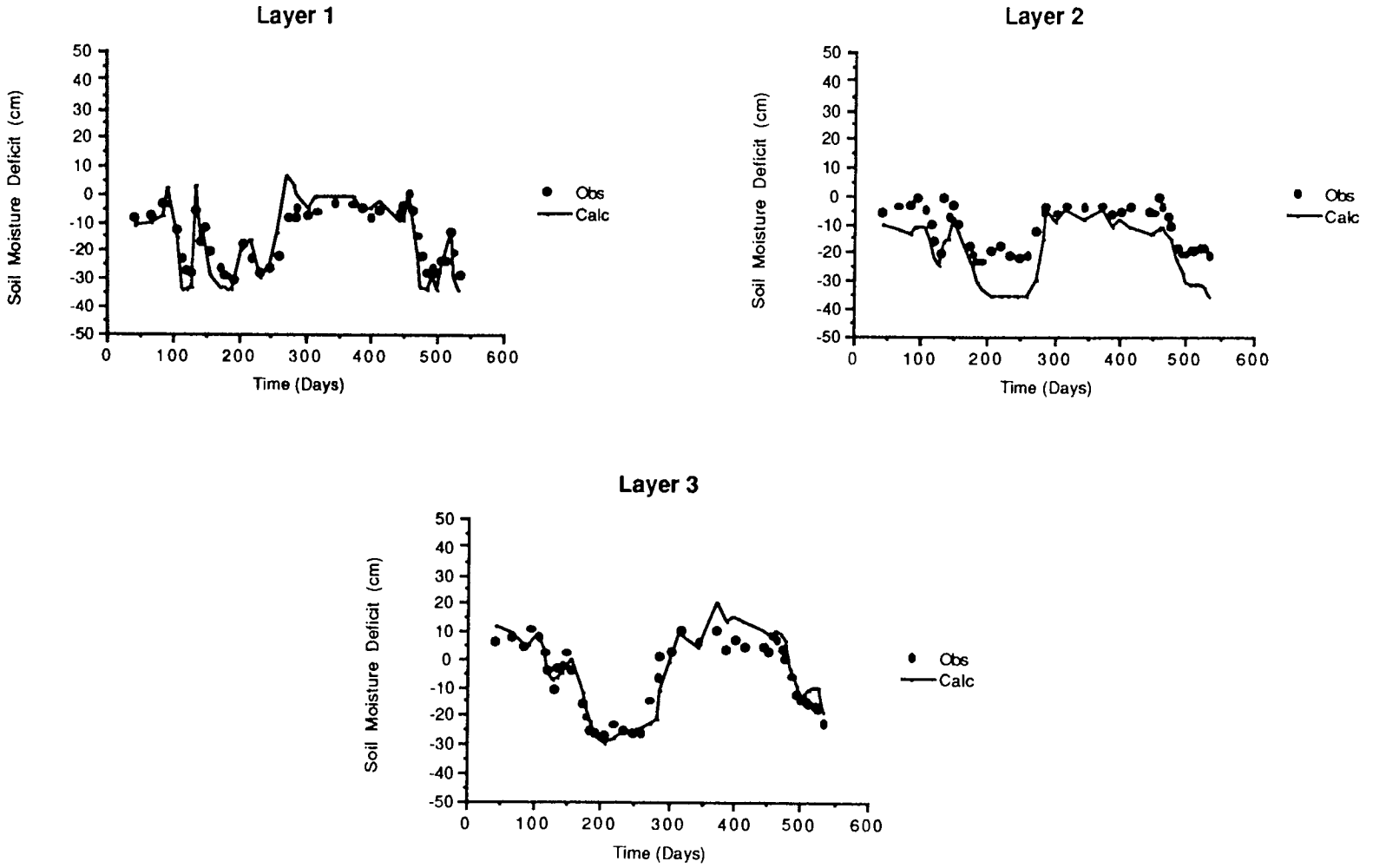

Figure 7.8 Calculated and Observed Soil Moisture Deficits for Each Soil Layer when Surface Layer Ks =0.5E-05

(probe calibrated using the relationship derived by Wood (1982))

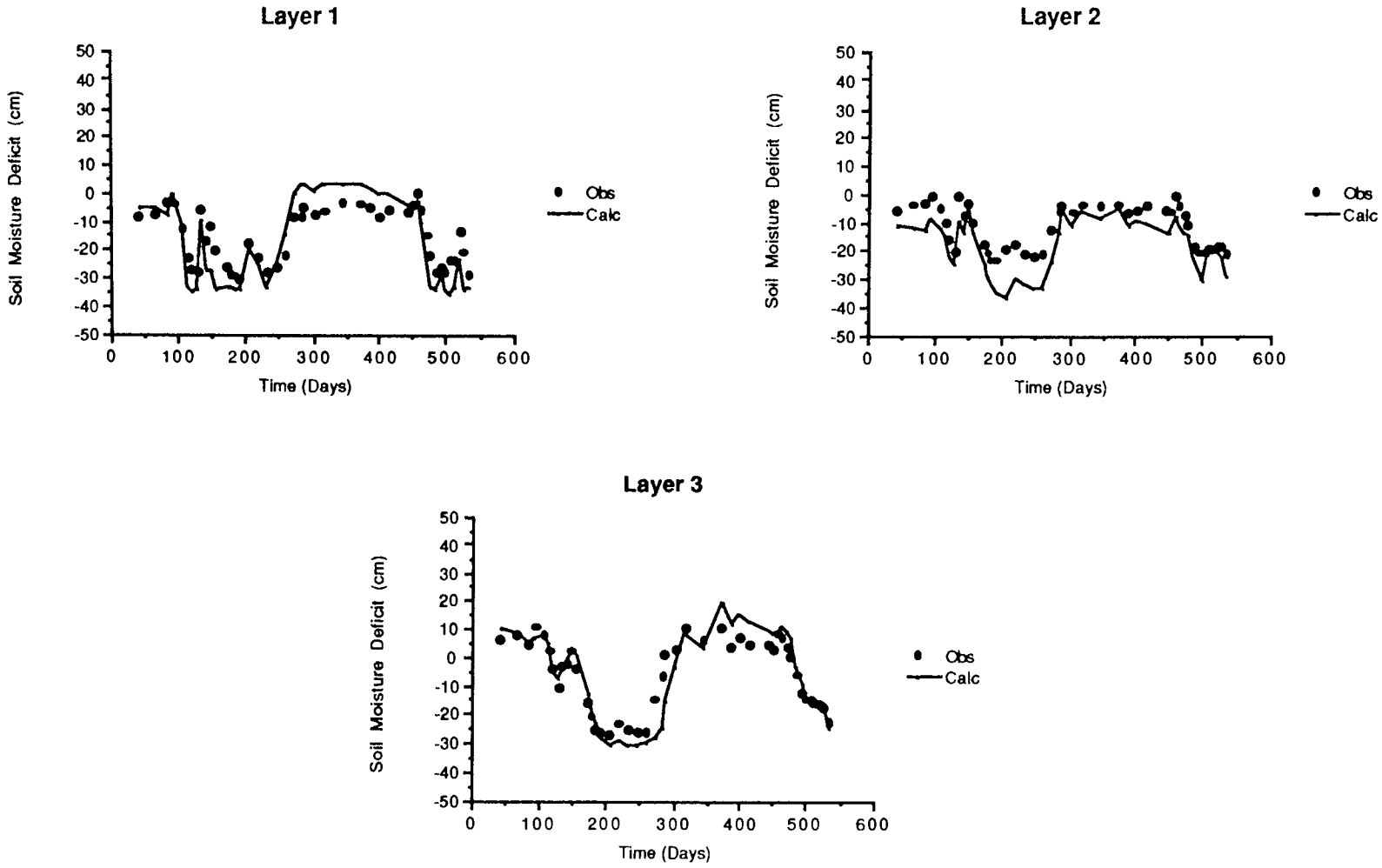

Figure 7.9 Calculated and Observed Soil Moisture Deficits for Each Layer when Surface Layer Ks =0.5E-06

(probe calibrated using the relationship derived by Wood (1982))

recharge rapidly. Lowering the Ks value of the surface layer can to some extent correct for the model producing rainfall intensities too low to result in macropore flow. However, not only does this affect the calculation of water flow in the micropores but it does not solve the problem. To overcome this two approaches could be employed: firstly, intensity/duration curves for different rainfall types or time of year could be produced; secondly, hourly rainfall could be recorded in the field. In the case of the first approach if it is to be used more work is required to produce such intensity/duration curves. With the latter alternative the time spent obtaining field data may be greatly increased. Clearly if the macropore routines within the model are to be fully utilised one of these approaches is needed. Unfortunately time has not permitted either of these alternatives to be implemented within the present model.

4. The Overall Model

Overall the final model, with all the parameters having been determined, represents the relative changes in soil moisture deficit between dates as well as the actual values (Figure 7.5). The total moisture deficit for all three layers is also well simulated (Figure 7.6) though there is a tendency to slightly over-estimate deficits in the autumn of 1977 and under-estimate them slightly at the start of 1978. These two periods correspond to the problems mentioned earlier in the section with regard to determining the Ks

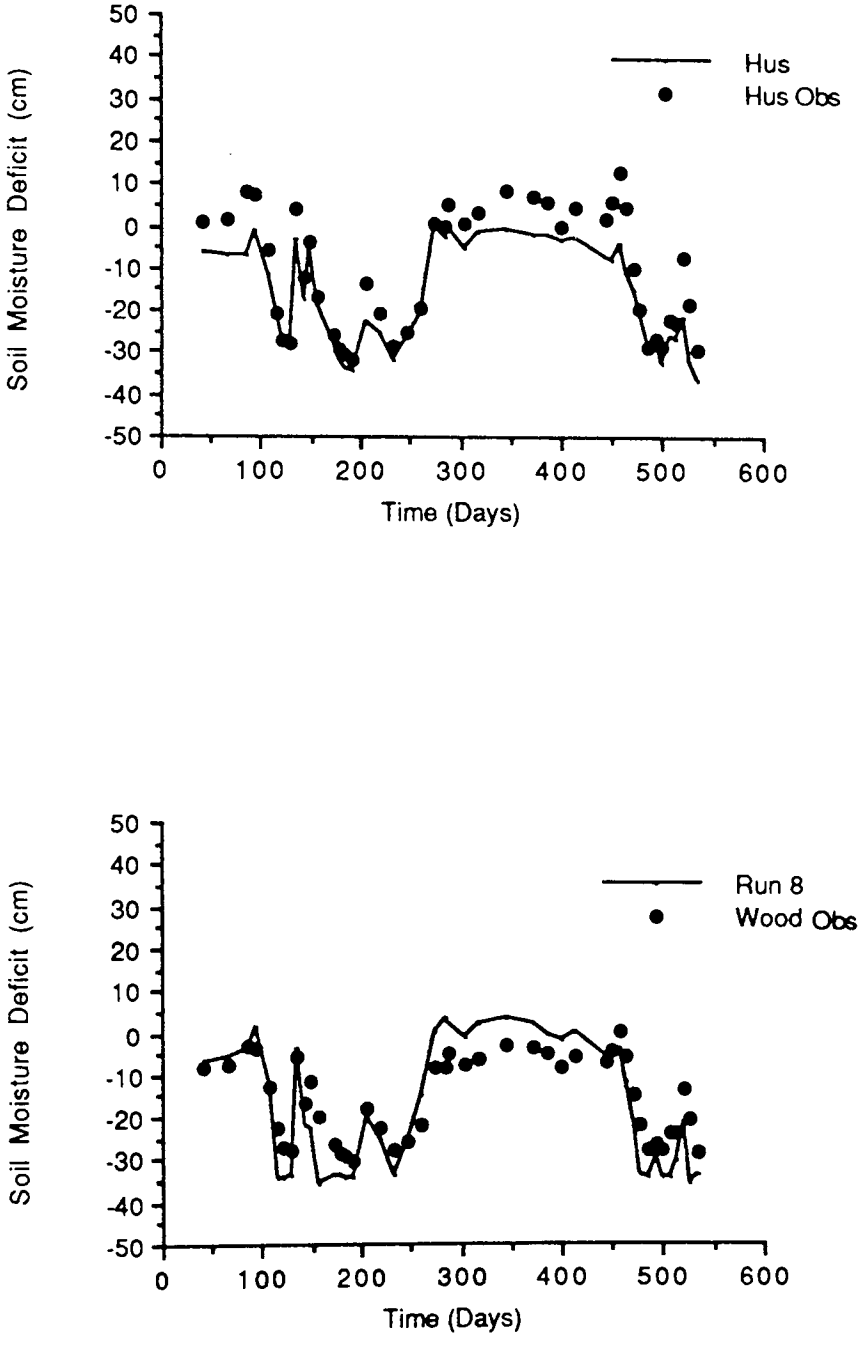

FIGURE 7.10a Comparison of Calculated Soil Moisture Deficits by Hussein's Model and the Developed Model for Layer 1

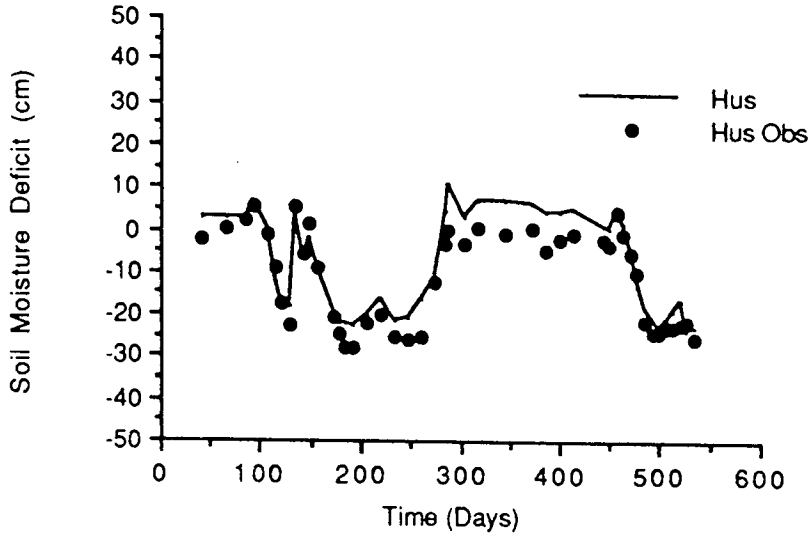

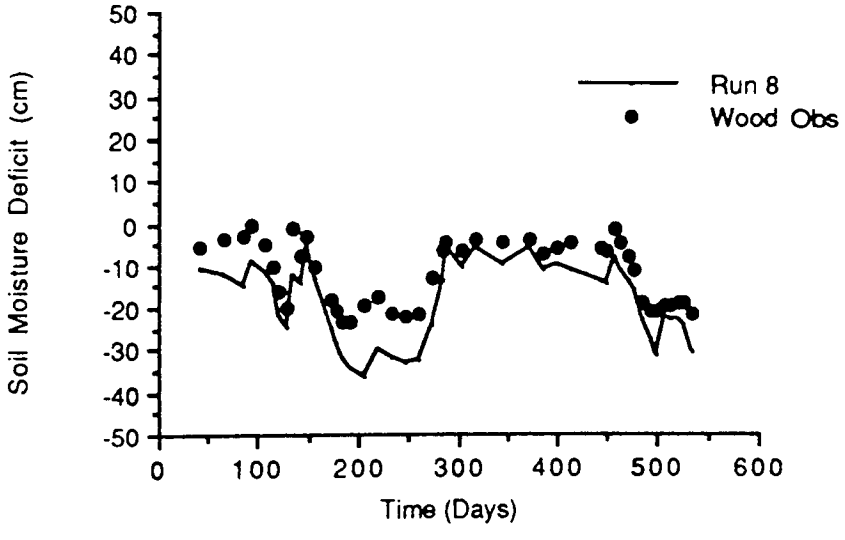

FIGURE 7.10b Comparison of Calculated Soil Moisture Deficits by Hussein's Model and the Developed Model for Layer 2

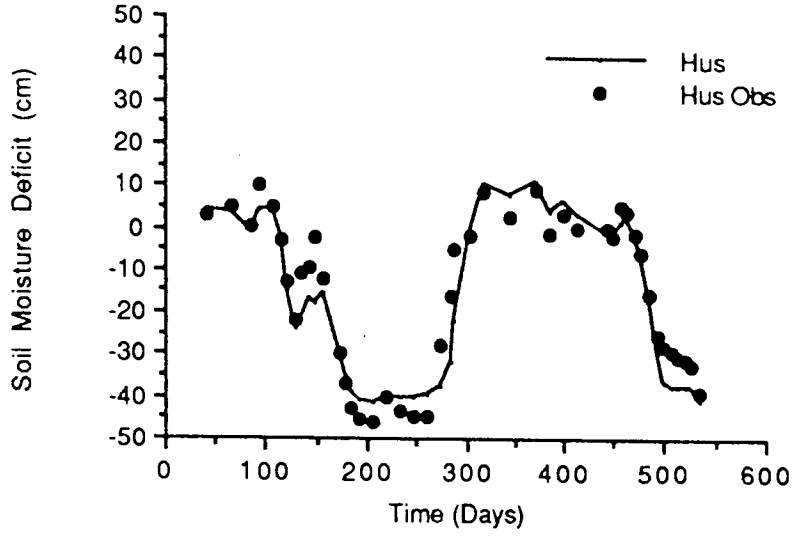

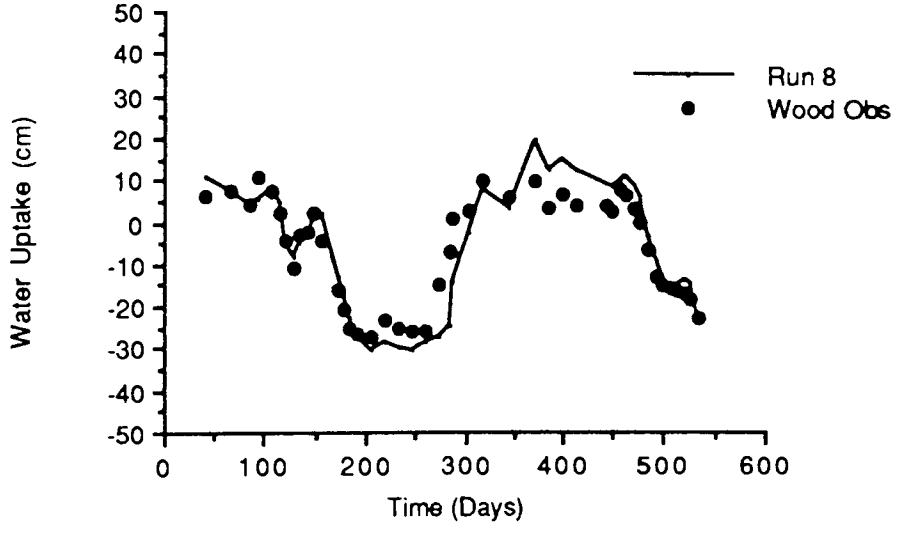

FIGURE 7.10c Comparison of Calculated Soil Moisture Deficits by Hussein's Model and the Developed Model for Layer 3

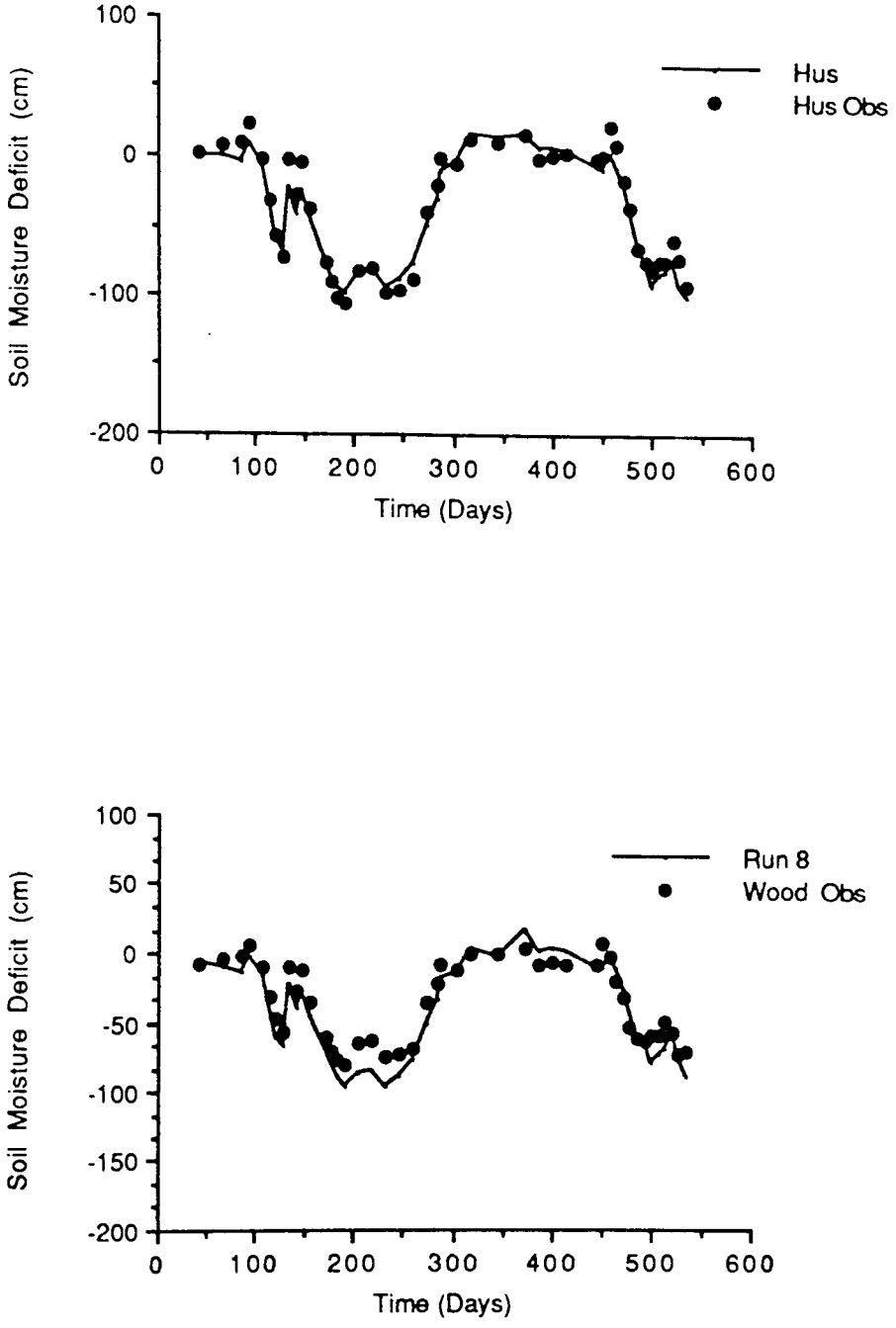

FIGURE 7.11 Comparison of the Calculated Total Soil Moisture Deficit from the New Model to Hussein's Model

value of layer 1 and the rainfall distribution algorithm.

Direct comparison of actual values cannot be made as Hussein fitted the parameters within his model to moisture data determined from neutron probe data obtained in the field using a different calibration curve (see Section 7.1.2). However, comparison of the output from the updated model with Hussein's original model (Hussein 1979) shows that the new model simulates the relative change in soil moisture deficit between dates more accurately (Figure 7.10 and 7.11).

It is clear from the preceeding discussion that the new model can be used to successfully simulate processes within the field.

7.2 PLANT WATER UPTAKE

Using equation 4.9 described in Section 4.3.2, the following section examines this relationship to see how it is affected by various factors, such as the magnitude of the evaporative demand, root density, and soil type. Two studies were initiated to achieve these objectives.

1. Individual parameter values were altered independently, with the aid of a spreadsheet, to see their effects on the resultant expressions.
2. Computer simulations were performed to see how

actual transpiration was affected by root density, soil type and evaporative demand rates.

Once the results of both studies were obtained they were compared qualitatively with the available data found in the literature. This was to see, were possible, if the present model allowed factors such as soil type, root density, plant resistance, soil suction and evaporative demand rates to have the same general effects on actual transpiration as those seen in the field or from experimental work.

7.2.1 SPREADSHEET ANALYSIS

The purpose of this study was to see how changing individual parameters within equation 4.9 affect the overall performance of the equation. At first this was done for the 20 soils described in Table 7.5, the shape of the soil characteristic being determined from the statistical relationships described in Section 3.2.1. The initial values used for root density and plant resistance were 1.0 cm^3/cm^3 and 5000 respectively.

Results from this early analysis show that for fine soils it is the lower evaporative demands which first cause actual transpiration to decline from the potential rate, as soil suction increases. However, this only occurs at high suctions (see Figure 7.12) and very little real difference exists between high and low demand rates. With the coarser

Soil	Particle-Size Classes <2mm					Sand Fractions			Silt Fractions		Particles >2mm	Bulk Density	Saturated Moisture Content
	Sand	Silt	Clay	V. Coarse	Coarse	Medium	Fine	V. Fine	Coarse	Fine			
1	94.5	2.9	2.6	0	0.5	1.3	35.1	57.6	2.6	0.3	0	1.39	0.44
2	91.9	2.9	5.2	0.1	0.4	1	35.3	55.1	2.6	0.3	0	1.37	0.435
3	80.2	15.1	4.7	0.8	3.4	3.2	29.3	43.5	8.5	6.6	0	1.59	0.356
4	81.7	11.9	6.4	0.9	3.3	4	35.6	37.9	7.6	4.3	4	1.46	0.418
5	76.7	12.5	10.8	0.7	2.7	2.5	32.8	38	6.9	5.6	0	1.48	0.386
6	66.6	17.4	16	0.2	0.8	0.9	10.6	54.1	8	9.4	0	1.46	0.409
7	58.8	20.8	20.4	0.2	6.4	21.9	22.5	7.8	9.5	11.3	0	1.62	0.376
8	94.3	2.7	3	1.8	15.5	35.4	32.8	8.8	1.7	1	0	1.54	0.362
9	89.3	3.1	7.6	0.6	9.9	30.6	39.4	8.8	2.1	1	0	1.53	0.415
10	71.5	7.7	10.8	4.8	27.6	36.4	10.4	2.3	2	5.7	0	1.59	0.368
11	48.6	41.5	9.9	2.6	14.7	13	11.5	6.8	22.8	18.7	3	1.58	0.378
12	47	37.9	15.1	2.8	16.2	13.3	9.4	5.3	16	21.9	2	1.69	0.35
13	95.2	3.6	1.2	1.2	36.3	37.7	19.3	0.7	1.6	2	0	1.4	0.454
14	94.1	3.9	2	0.8	32.4	36	23.8	1.1	1.3	2.6	0	1.38	0.451
15	62.2	9.2	28.6	7.5	19.9	25.1	6.9	2.8	2.8	6.4	0	1.33	0.485
16	76.8	10.4	12.8	8.1	26.3	32.7	7.9	1.8	2.5	7.9	0	1.26	0.491
17	18.9	69.3	11.8	0.6	2.7	3.2	4.9	7.5	31.9	37.7	14	1.2	0.508
18	41	27	32	0.1	6.1	18.6	12	4.2			0	1.03	0.56
19	13.5	56.4	30.1	0.1	0.7	1	2.1	9.6	28.9	27.5	0	1.49	0.435
20	26	29	45	0	0.4	1.6	11.2	12.8			0	1.59	0.41

* Particle-Size data refers to SCS_USDA Classification (Appendix 1)

** Soils 1-17 & 19 are from SCS_USDA (1974)

*** Soils 18 & 20 are from Cassel (1974) silt fractions and saturated values were not provided. The silt percentages for coarse and fine silt though are not required for the model calibrations so this was not important. For saturated moisture content this was assumed to be 0.9 of the porosity (eq 3.4).

Table 7.5 Particle-Size (%), Bulk Density (g/cc) and Saturated Moisture Content (cc/cc) for the Twenty Soils Used in the Evapotranspiration Simulations

(i.e sandier) soils the potential rate is only maintained to high suctions by the lower evaporative demands, and it is the higher demands that decline first as suction increases. The highest demand curves also show two phases of reduction from the potential rate; a rapid decline from the potential is followed by a lesser one before another phase of rapid fall, as shown by Figure 7.13.

Following on from this preliminary testing, one soil was chosen for more detailed study. Various parameters were then altered in order to examine their effects on the resultant relative transpiration/soil suction (RTSS) curve.

As was noted above, the finer soils produce different relationships than the coarser soils. Since the soil moisture characteristic is determined from soil properties, it seemed appropriate to investigate the parameters 'a', 'n' and 'tr'(which define the curve) in order to examine what effect altering these would have on the RTSS curve. In Section 3.2.1.2 it was shown that the value of 'n' tends to increase the sandier the soil, the opposite being true of 'a' and 'tr'. With this in mind it would be expected that the RTSS curves would look less and less like the finer soil relationships as 'n' increases and 'a' and 'tr' decrease. Figures 7.14-7.16 show that this is indeed the case. However, the transition is not as smooth if the parameters are changed together, as opposed to independently.

Figure 7.12

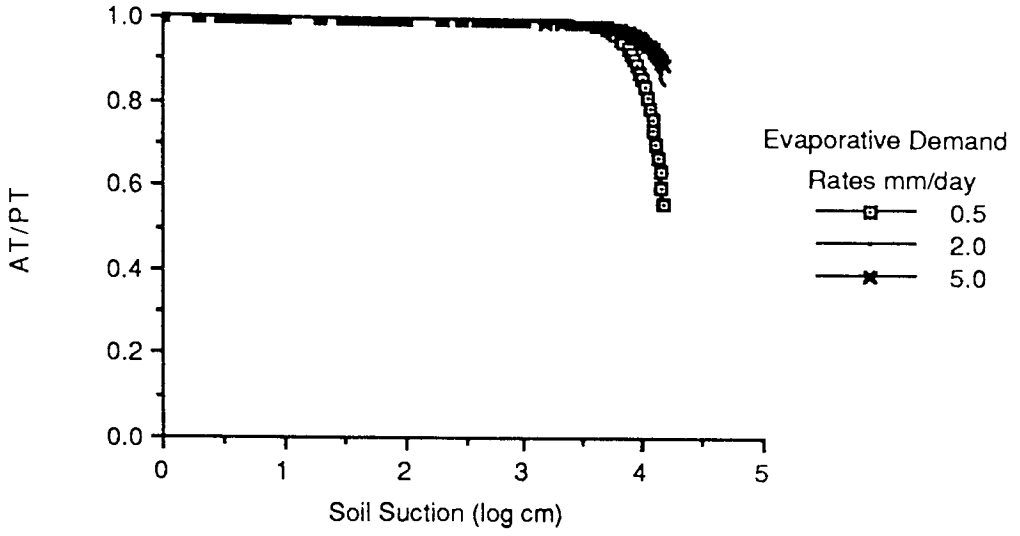

Figure 7.13

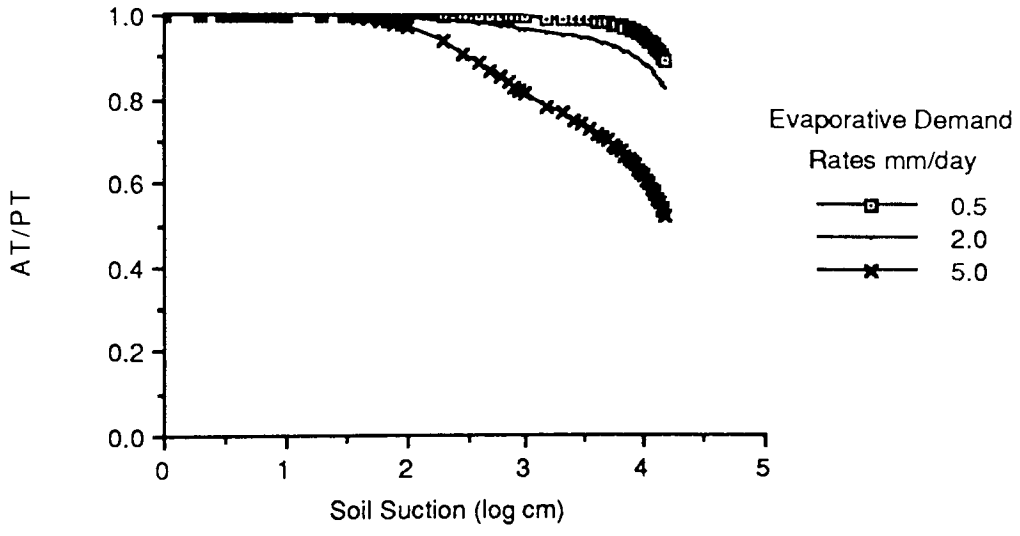

Figure 7.12 Relative Transpiration/ Soil Suction for a Fine Soil

Figure 7.13 Relative Transpiration/ Soil Suction for a Coarse Soil

The higher the evaporative demand rate the higher the leaf suction required in order to enable the plant to abstract the water. The higher the potential leaf suction calculated the greater the deviation between actual and potential leaf suction. From Figures 7.12 and 7.13 it can be seen that with fine soils it is the lower evaporative demand rates that deviate from the potential rate first whereas with the coarse soils it is the higher evaporative demand rates. With the fine soils the higher evaporative demand rates allow greater leaf suctions to be generated, however they are not so great that the difference between actual leaf suction and potential leaf suction is large. With the coarse soils very high potential leaf suctions are required to extract the water at the potential rate for high evaporative demands. This means that the calculated actual leaf suction varies greatly from the potential causing the rate to deviate from the potential rate much earlier.

Sensitivity tests were then applied to the root density and plant resistance parameters. Increasing the root density had the same effect as increasing 'n' and decreasing 'a' and 'tr'. That is evaporation was maintained at the potential rate for longer (Figures 7.14-7.16). Increasing the plant resistance had the opposite effect, as might be expected. The stepped effect seen in Figure 7.13 is a result of the rapid decline in moisture content over a narrow suction range which is common in coarse soils.

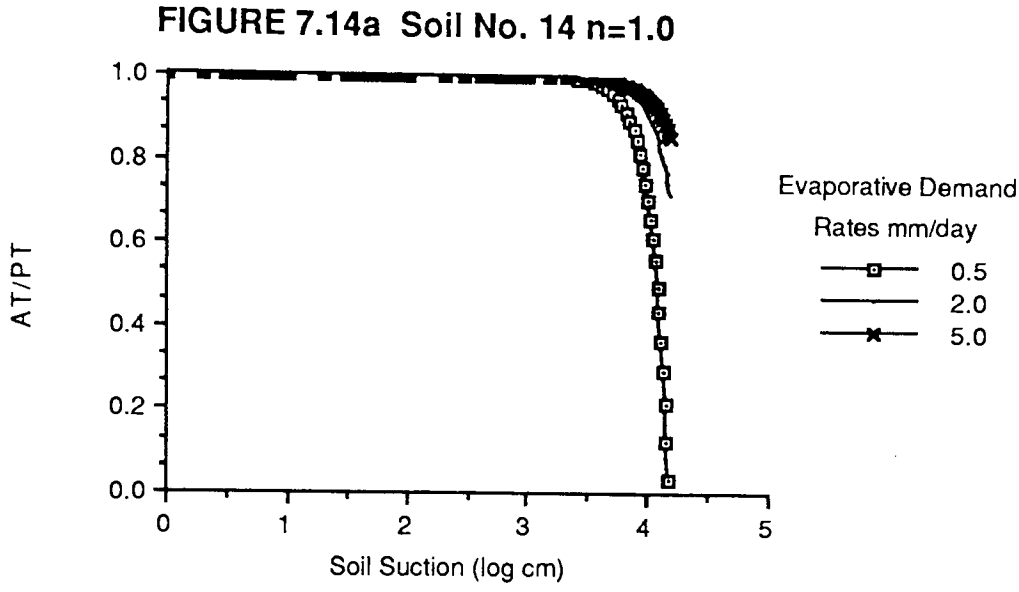

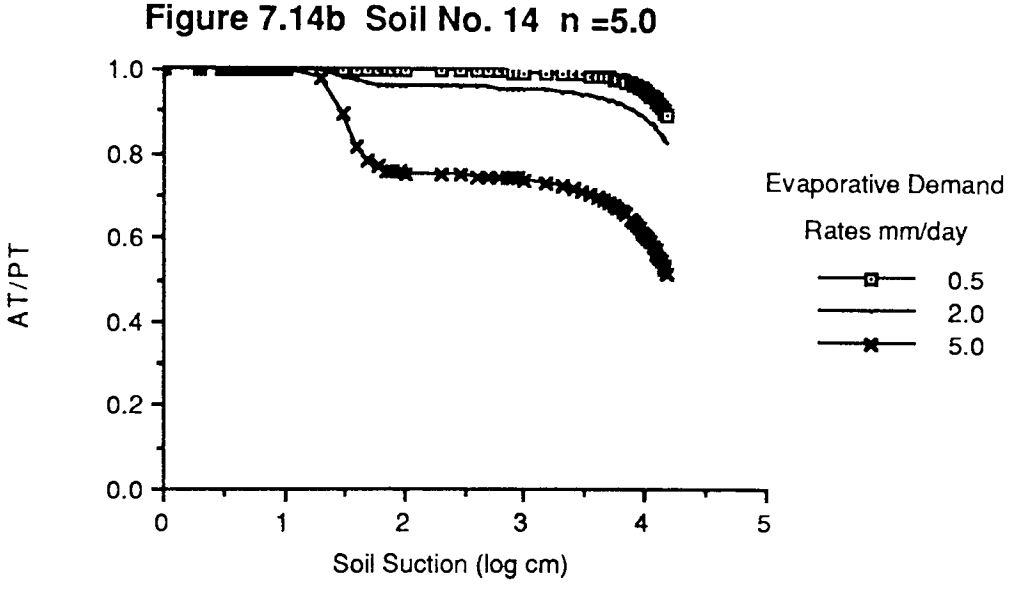

Figure 7.14 The Effect of Increasing Parameter 'n' on Relative Transpiration/ Soil Suction for Soil Number 14

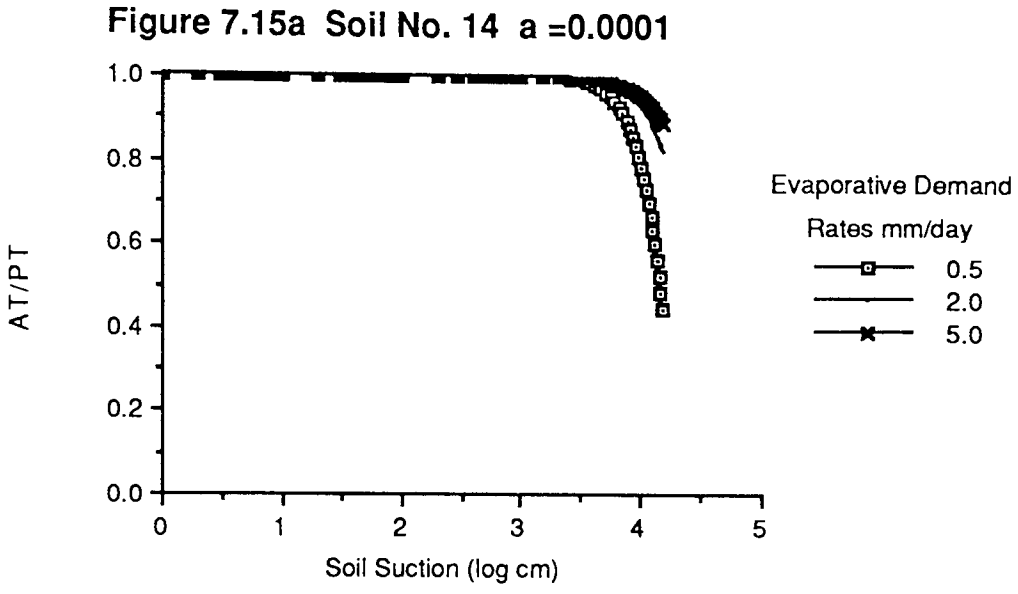

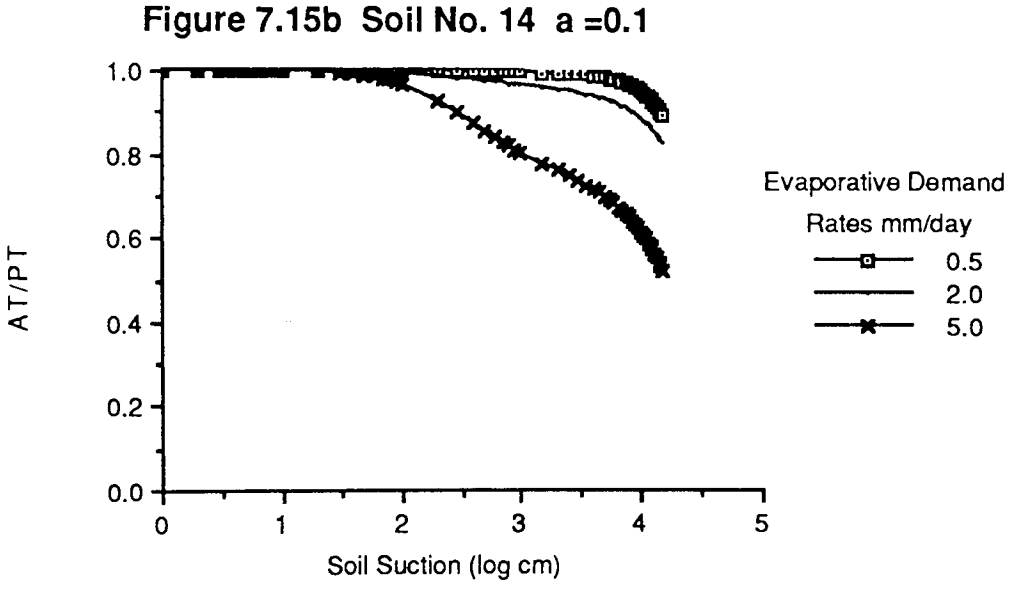

Figure 7.15 The Effect of Increasing Parameter 'a' on Relative Transpiration/ Soil Suction for Soil Number 14

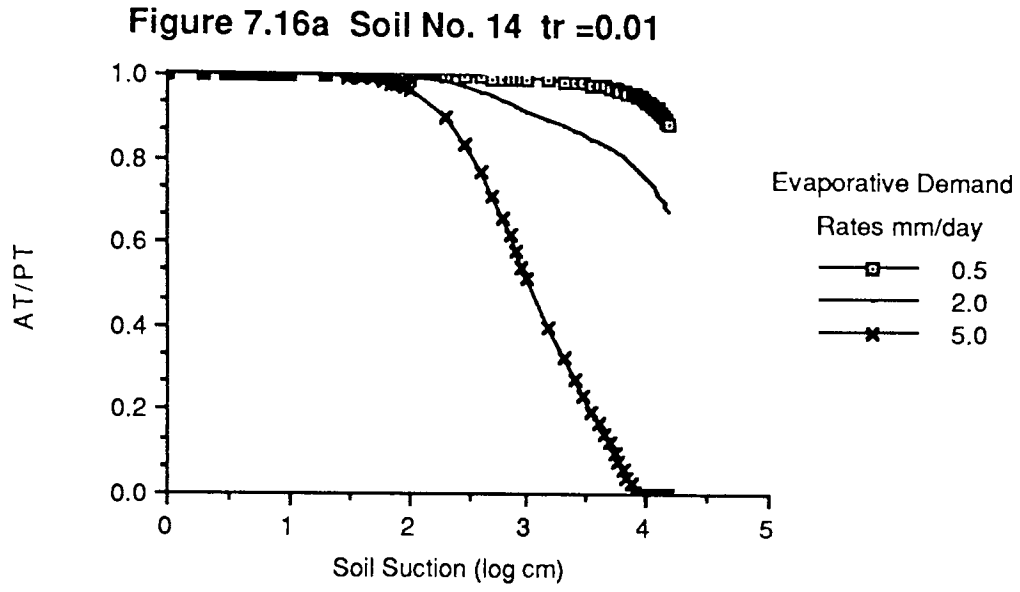

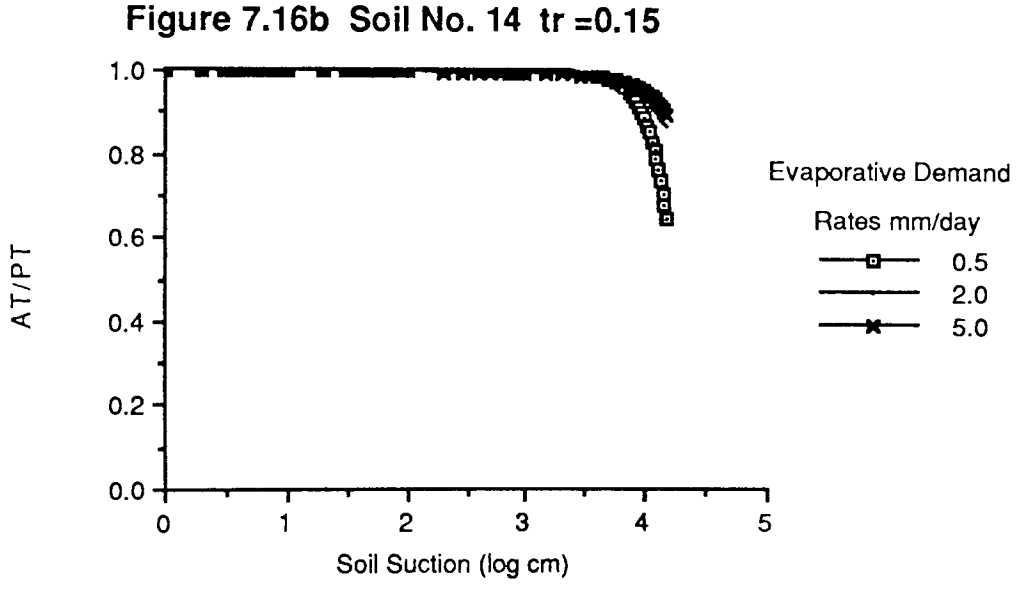

Figure 7.16 The Effect of Increasing Parameter 'tr' on Relative Transpiration/ Soil Suction for Soil Number 14

7.2.2 SIMULATION ANALYSIS

The following section aims to see the effects of soil type, evaporative demand and root density on the calculation of actual transpiration in a drying soil profile. As there was no inputs of rainfall during the simulation and the hypothetical plant had a LAI > 1.0 the rainfall distribution, infiltration, macropore and bare soil evaporation subroutines were not required. Using the same 20 soils as in the previous section a series of simulations were performed. Each soil was split into 4 layers of varying thickness from the surface layer of 15cm down through layers of 30cm, 60cm and 250cm. The bottom layer contained the groundwater table. Water flow between layers, by percolation or upward moisture movement was calculated in addition to transpiration.

For each soil type six simulations were performed, each for a different potential evaporative demand. The six potential demands being 0.05, 0.1, 0.15, 0.2, 0.3 and 0.4 cm d^{-1}. Each run was started with the groundwater table at the top of layer 4. The moisture contents of the overlying layers were then estimated by equating the suction of each layer to the height of its midpoint above the groundwater surface, and then substituting these values into the appropriate layers moisture characteristic curve (equation 3.3). The parameter values of equation 3.3 were determined from soil properties. As well as the fact that no water was

added to the soil during the simulation, no water was also allowed to flow from the base of layer 4. The length of the simulation was determined by the evaporative demand (ED) so that each simulation run had approximately the same total potential evapotranspiration. The number of days for each run was determined by dividing 100 by ED, the resultant value being rounded down. The results of this analysis are discussed below.

The curves produced are similar in form to those given by Jackson (1977). In Jackson's case the curves were plotted against suction whereas here they are plotted against cumulative demand (ED*time), however since no water was added to the system, suction increased with time. Figures 7.17 and 7.18 illustrate the form of the curves and also show, as did Jackson (1977), that the higher the value of ED the quicker the curve drops from its potential rate. This was also noted by Yang and Jong (1972), Makkink and Heemst (1956) and Cowan (1965).

Closer examination of the results shows that the lower the evaporative demand the greater the amount of total evaporation over the simulation period. The reason for this is that the lower demands are able to draw up more water from the basal layer. Table 7.6 illustrates for several of the soils, the greater amount of upward moisture movement and hence the lower water table produced by the simulations with the lower evaporative demands. The amount of upward

FIGURE 7.17 Fall in Actual Evaporation Rate with Time for Several Potential Rates

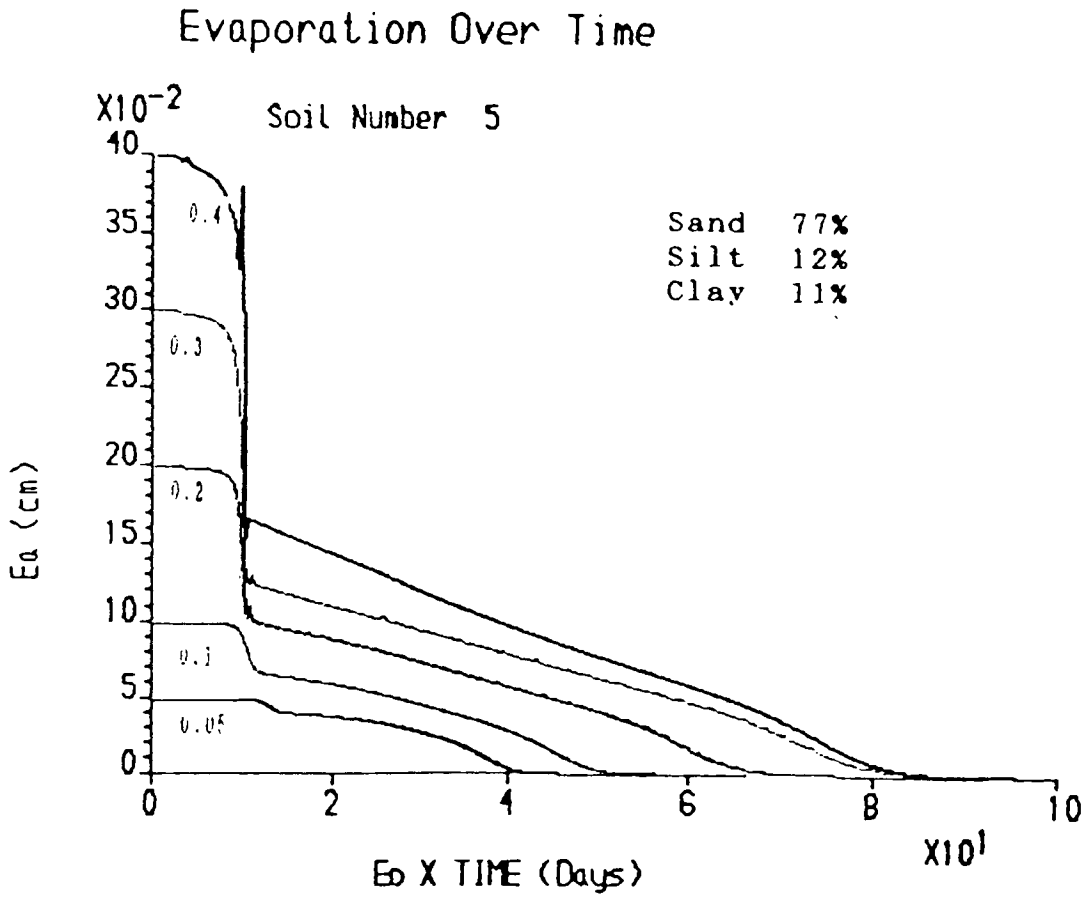

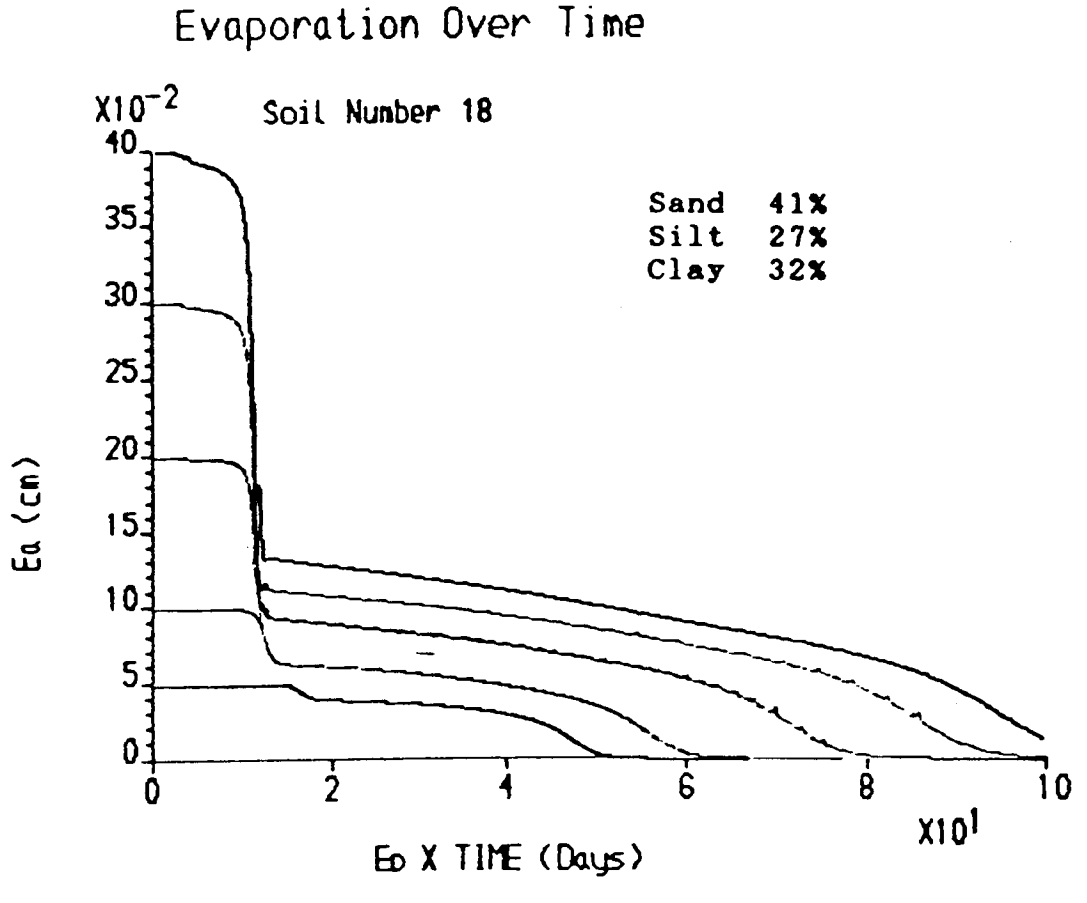

FIGURE 7.18 Decline from the Relative Transpiration Rate with Time for Several Potential Rates

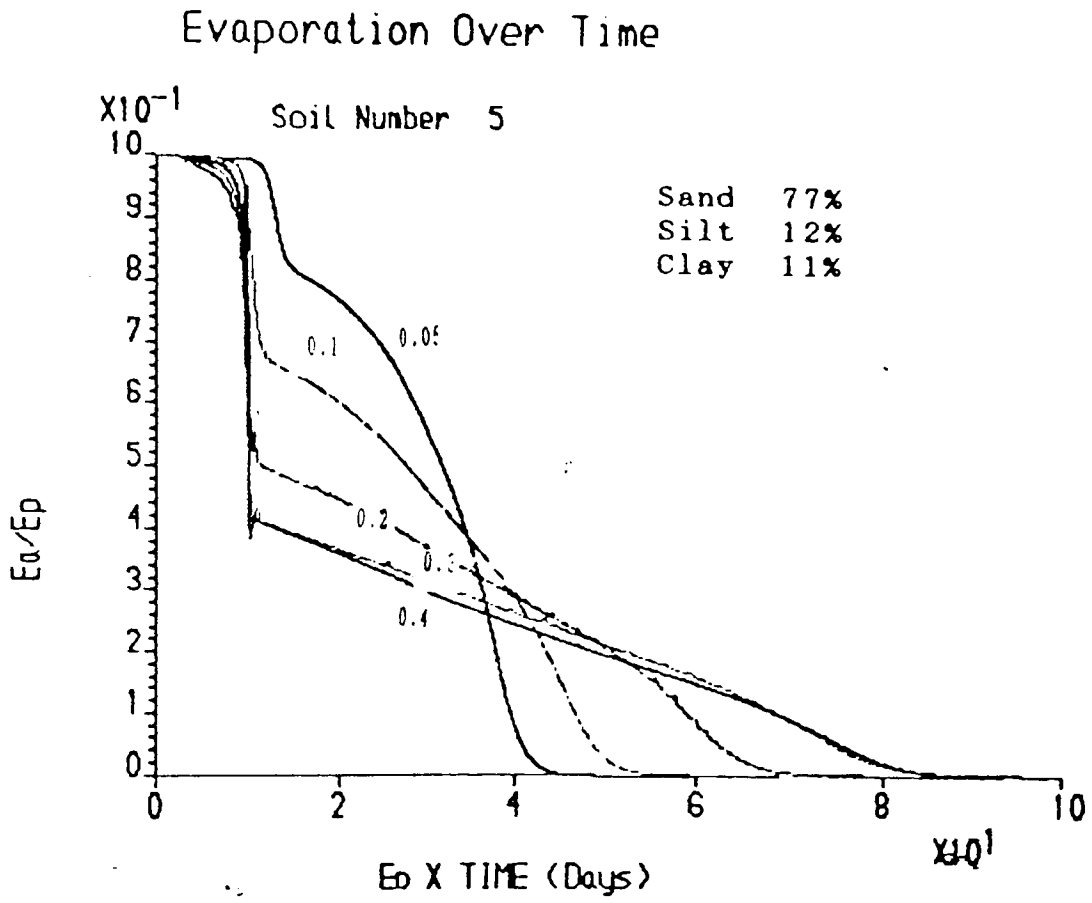

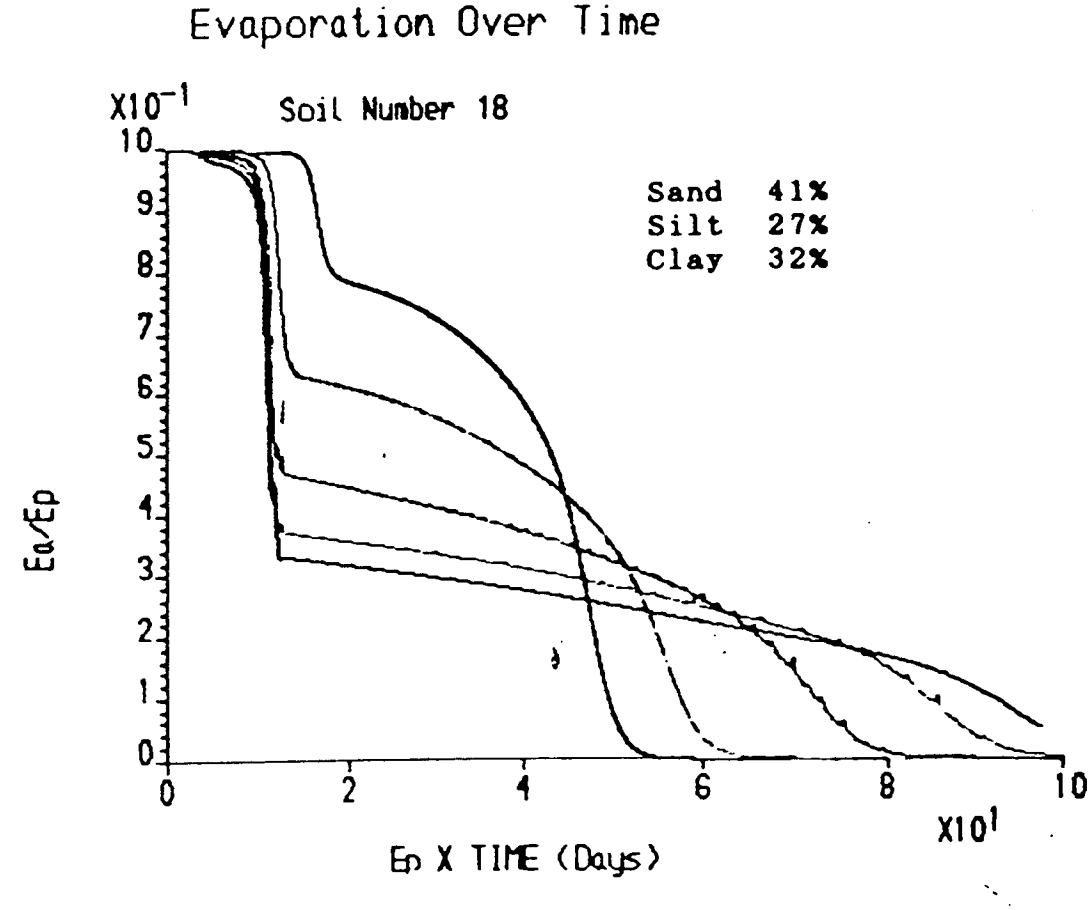

moisture movement is soil dependent. Figure 7.19 shows that all evaporation rates drop below the potential rate at roughly the same cumulative demand. This can be traced back to the fact that soil No. 15 had very limited upward moisture movement. To maintain the actual transpiration at the potential rate it is important that upward moisture movement from the basal layer continues up to the surface layers where plant resistance is much lower and so more able to maintain the potential rate.

However, there are some exceptions to the above statement that for lower evaporative demands the total amount of evaporation is greater. An examination of moisture contents at the end of each simulation gives a clue to the occurrence of these anomalies. The higher the demand the drier the soil layers, but only up to a point as layers cannot become drier than the residual moisture content. The greater drying out effect of the higher evaporative demands is due to the fact that they can produce greater leaf suctions and hence can extract water at lower potentials (Gardner 1960, Feddes et al 1978). So where the contribution of water from upward moisture movement is negligible it is the higher demands which will transpire the most water over the cumulative time.

With respect to the different soil types, it can be seen that the sandier the soil the greater the upward moisture movement and hence amount evaporated, but also the

TABLE 7.6 UPWARD MOISTURE MOVEMENT FOR SEVERAL SOILS AND EVAPORATIVE DEMANDS PRODUCED BY EVAPOTRANSPIRATION SIMULATIONS.

Soil No.	Evaporative Demand (cm)	Upward Moisture Movement Into Layer (cm) 1	2	3	Depth of Water Table
1	.05	12.18	18.81	17.89	59.64
	.10	3.09	10.52	15.57	51.90
	.15	1.27	6.24	12.17	40.55
	.20	0.79	4.01	11.44	38.12
	.30	0.45	2.20	11.22	37.41
	.40	0.30	1.50	11.22	37.40
8	.05	0.11	0.58	5.29	23.81
	.10	0.05	0.24	4.22	19.00
	.15	0.03	0.15	3.45	15.53
	.20	0.02	0.11	3.32	14.97
	.30	0.01	0.07	3.31	14.91
	.40	0.01	0.05	3.31	14.91
12	.05	0.22	0.37	1.80	8.57
	.10	0.08	0.17	1.11	5.29
	.15	0.05	0.11	0.86	4.07
	.20	0.03	0.08	0.72	3.45
	.30	0.02	0.05	0.55	2.60
	.40	0.01	0.04	0.28	1.36
17	.05	20.45	24.74	24.78	67.35
	.10	7.34	12.72	17.68	48.05
	.15	3.14	7.19	14.83	40.31
	.20	1.93	4.76	13.36	36.30
	.30	1.08	2.74	11.64	31.63
	.40	0.74	1.90	10.55	28.68

* 'Depth of Water Table' refers to the depth of the water table in layer 4 at the end of the simulation.

TABLE 7.7 UPWARD MOISTURE MOVEMENT FOR SOIL 15 Illustrates the fact that when conductivity is small total evaporation may be greater when demand is high due to the greater suction forces operating.

Evaporative Demand	Upward Moisture Movement Into Layer (cm) 1	2	3	Total Evap	Moisture Content of Layer 1	2	3
0.05	0.10	0.14	0.65	14.99	0.279	0.279	0.279
0.10	0.04	0.07	0.37	15.10	0.275	0.275	0.275
0.15	0.02	0.04	0.28	15.22	0.273	0.273	0.273
0.20	0.02	0.03	0.23	15.32	0.272	0.272	0.272
0.30	0.01	0.02	0.18	15.47	0.270	0.270	0.270
0.40	0.01	0.02	0.16	15.58	0.269	0.269	0.269

FIGURE 7.19 Decline from Potential Rate Over Time for Several Potential Rates in a Soil with Limited Capillary-Rise.

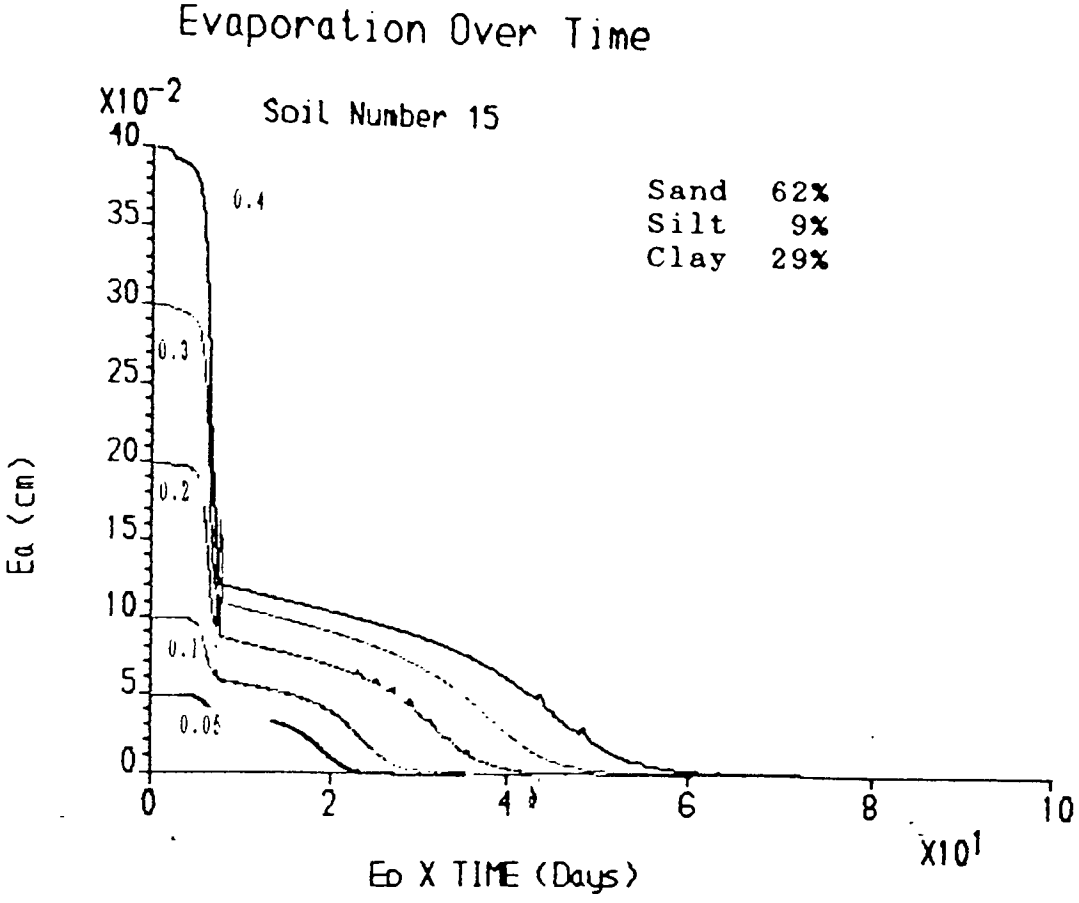

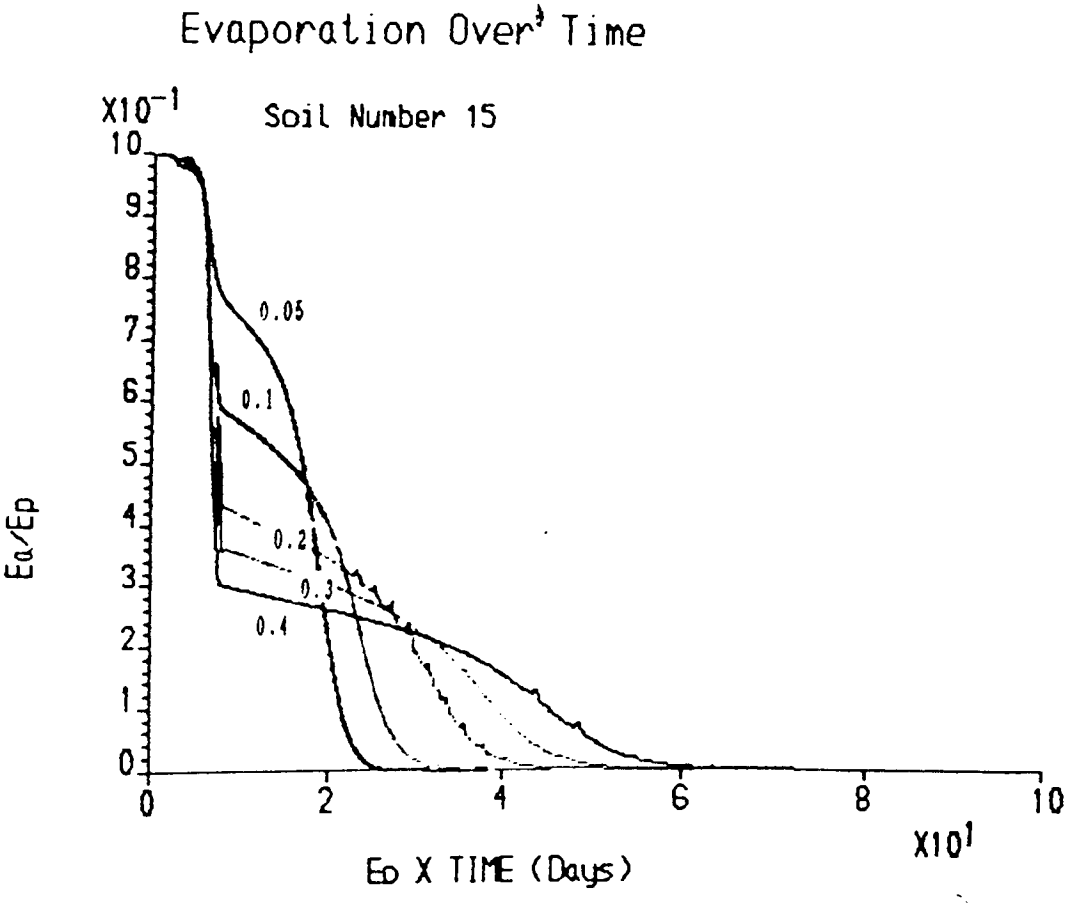

greater the contrast between the low and high rates. The high rates decrease moisture content so rapidly that the soil's conductivity falls sharply, this quickly reduces the initial high rate of upward water flow. The silty soils also exhibit large upward moisture movements. It is the clays and the clay loams which show least moisture movement and the smallest uptakes. These soils decline from the potential rate quicker than the others but have flatter gradients at the lower end of the curve. The effect on transpiration of changing root density can be seen in Figures 7.20 and 7.21 where the potential rate is maintained for a longer period but the drop from this rate is much more steep. From 7.2.1 it is noted that finer soils can maintain the potential rate at higher suctions than coarser soils, yet in these simulations it is the finer scils that deviate from potential first. This apparent contradiction is caused by the shape of the soil moisture characteristic of fine soils where the soil holds a greater amount of water at very high suctions. An increase in root density allows the plant to abstract water more easily so that it maintains the potential rate for longer. However, it does not increase upward moisture movement so once the actual rate of transpiration starts to fall below the potential rate its decline is sharper. By contrast a change in plant resistance has the opposite effect.

Inspection of the curves (e.g Figure 7.20) illustrates a number of irregularities which upset the smooth shape of

FIGURE 7.20 The Effect of Increasing Root Density (the Lower Graph) on the Transpiration Rate for Soil No. 17

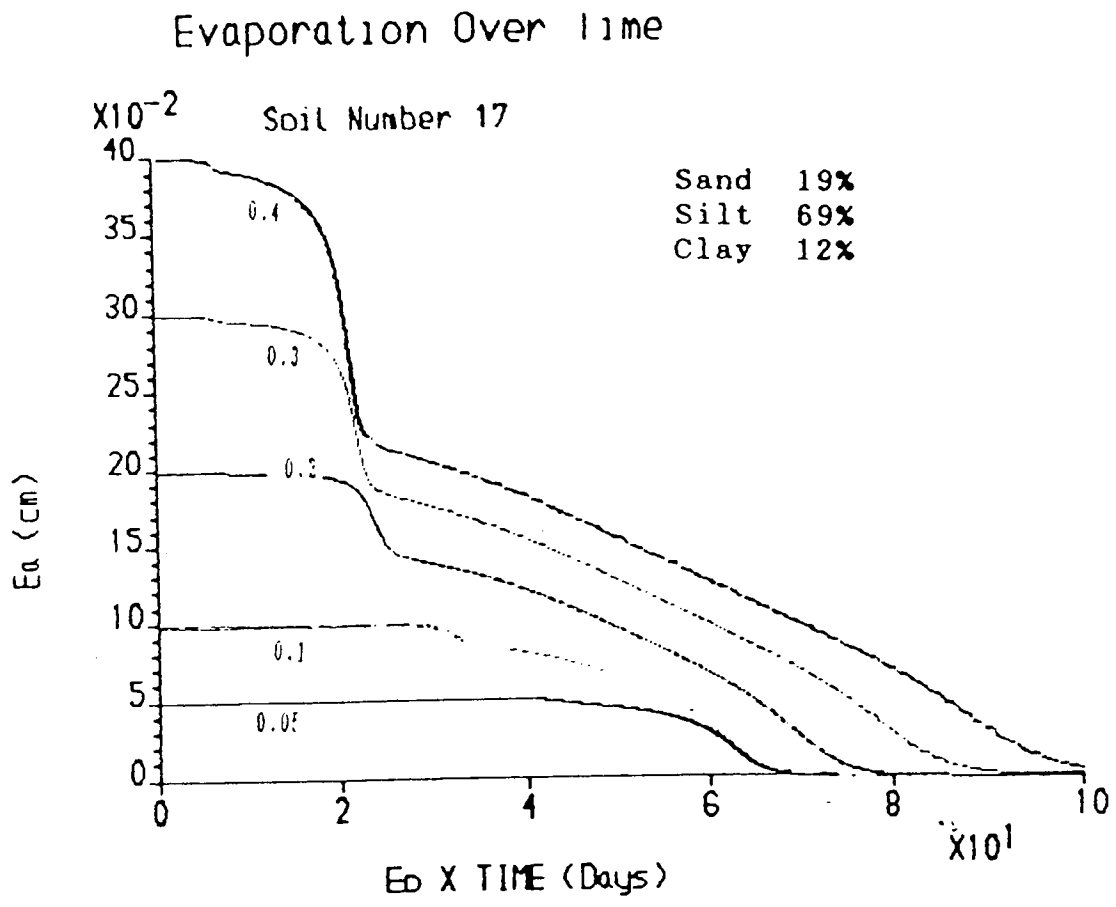

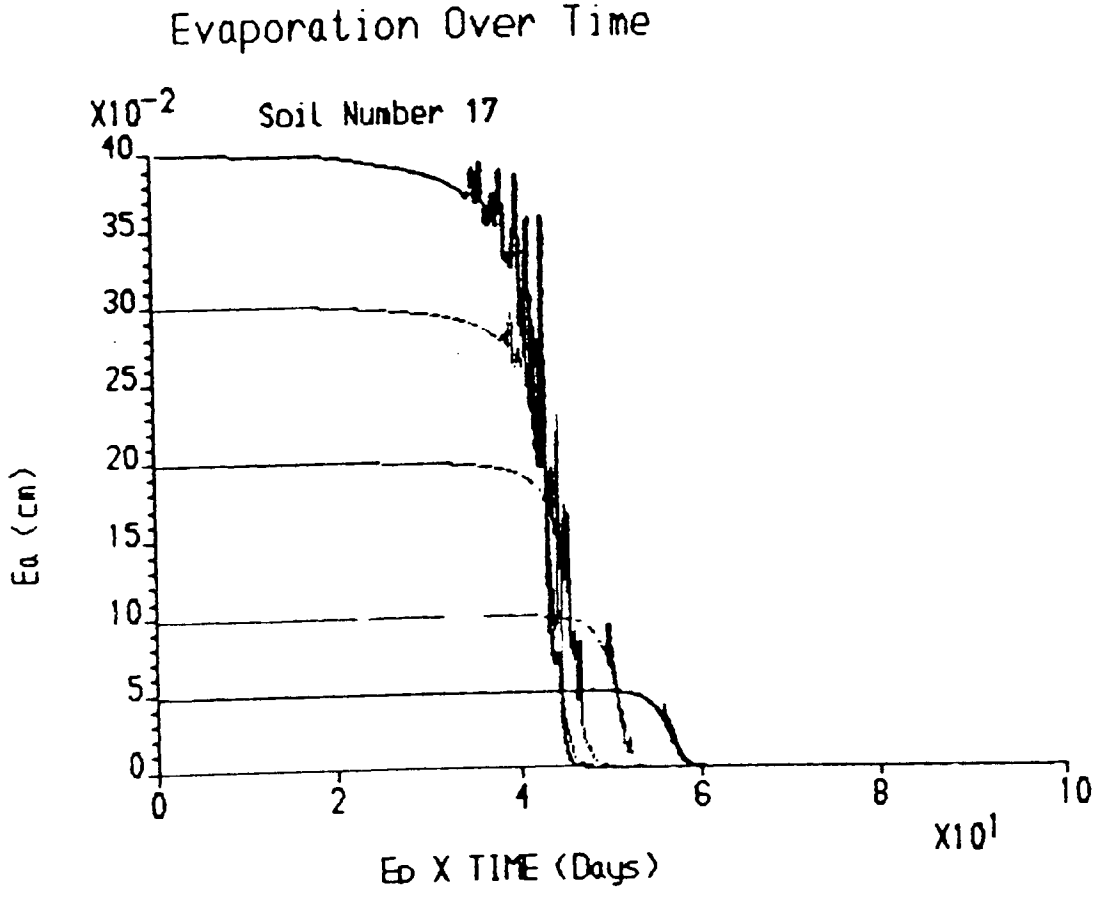

FIGURE 7.21 The Effect of Decreasing Root Density (the lower graph) on the Transpiration Rate for Soil No. 17

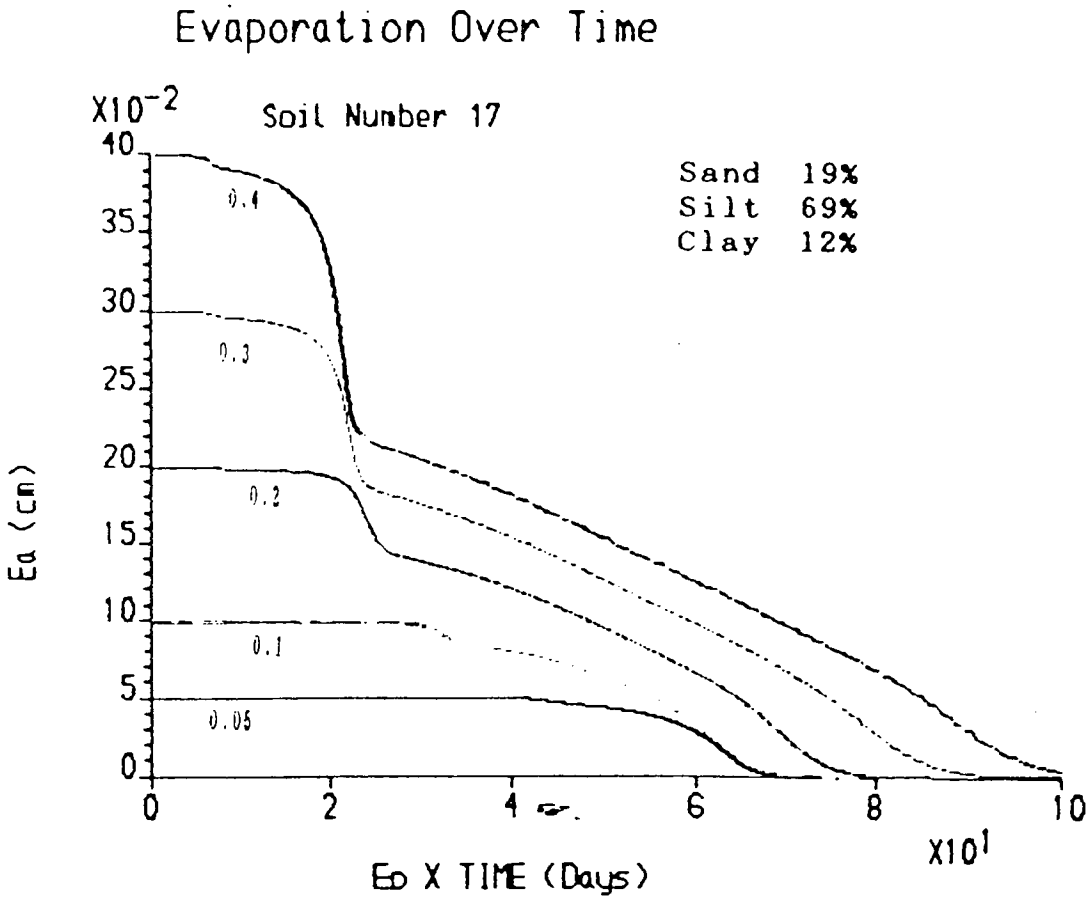

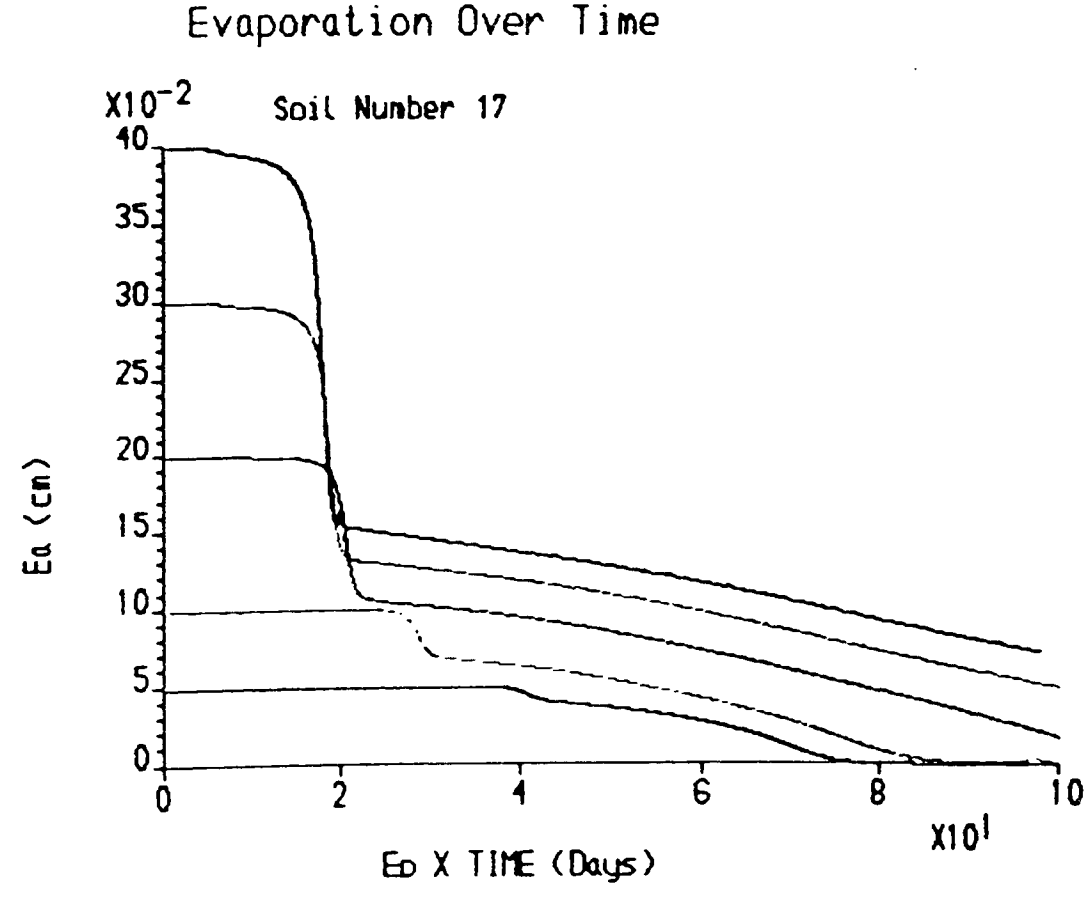

the curve. There are two reasons for this. Firstly, a problem arises with the calculation of potential leaf suction which is determined by substituting the potential evaporative demand into equation 4.8. If the potential value obtained causes negative flow in one or more of the layers these layers are discounted and the value recalculated. The problem occurs when one layer is very dry, sometimes the layer will be included in the determination of the potential leaf suction and in some it will not, depending on the state of the other layers. Such borderline interpretations cause lower values of actual transpiration if the layer is included as the potential leaf suction calculated is lower as the resistances in the top layers are lower. Secondly, at high evaporative demands the calculated abstraction from a layer in a given timestep may exceed that which is available within the layer. In such cases only that available is allowed to be evaporated.

7.2.3 CONCLUSIONS

The previous discussion has shown how the interrelated factors of soil type, root density and plant resistance can affect the plant water uptake. Soil type affects uptake in a number of ways, through the shape of the soil moisture characteristic with its effect on the root contact component of the model and the soil suction and indirectly its effects on soil moisture movement. Root density affects uptake by

the effect it has on gathering water. Increasing root density is analogous to increasing the conductivity of the soil (Cowan 1965 and Gajri and Prihar 1985) allowing a higher rate of water uptake at higher suctions. Conversely an increase in plant resistance reduces the rate of water uptake.

The rate of evaporative demand is also seen to be important. Low rates encourage greater upward moisture movement and can evaporate greater overall amounts. However, when conductivity is low the greater drawing power generated by the higher demands can reverse this situation, but the differences in fact are fairly small, Table 7.7.

The present work has produced results which are comparable to the limited amount of results found in the literature. It has also shown from theory, the importance and effect of various factors on actual transpiration and water uptake from individual layers which need to be verified in the field. As regards the less than smooth shape of the curves an independant method of calculating leaf suction and a smaller timestep may alleviate this problem.

7.3 INFILTRATION

The aim of the present analysis is to compare results obtained in the literature with computer simulations

performed by the soil-moisture-plant model. The object is to see if certain factors such as soil type, macropore distribution, soil layering and initial moisture content produce the same general effects within the model as in the field. There are two main parts to this work:

1. Infiltration of water into the matrix is only assumed to take place at the soil surface i.e there is no bypass flow.
2. Infiltration into the matrix can either occur at the surface or from macropores.

Early work on infiltration emphasized the importance of initial soil conditions and rainfall intensity on the flux of water entering the soil. The first part of this section concentrates on this. More recent studies have shown that macropores also play an important role (e.g Beven and Germann 1981), and the second part of the section concentrates on this and examines the way in which water introduced by the macropores affects the infiltration at the surface. The discussion also deals with the limitations of the model and how certain simplifications affect the model results.

7.3.1 METHOD

The simulations use the infiltration, macropore and percolation subroutines of the soil-moisture-plant model. A

number of simulations are performed; all taking place over a period of a day, the timestep is initially set at one hour but may be decreased depending on the rapidity of the processes (see Section 6.5). Several hypothetical soils are simulated the properties of which are described in Table 7.8. As well as varying the soil type, other properties were altered such as initial moisture content, rainfall intensity, saturated hydraulic conductivity and the number and distribution of macropores. Table 7.9 gives the starting conditions of each of the 21 simulations. Rainfall was assumed to remain steady throughout the 24 hours of the simulation.

7.3.2 RESULTS AND DISCUSSION

The first part of this section deals exclusively with situations where water is infiltrated at the surface. This is followed by considering the effects of macropores on infiltration. Results are discussed in terms of the initiation and depth of ponding, the depth of the wetting front, infiltration rate and cumulative infiltration.

The characteristic infiltration curve presented within numerous texts (eg Marshall and Holmes 1979, Tarchitzky et al 1984) shows a steeper than exponential decline in the early stages, flattening out later as it reaches the value of hydraulic conductivity at residual air saturation, which

Soil	Particle-Sizes <2mm			Sand Fractions					Silt Fractions		Particles >2mm	Bulk Density	Saturated Moisture Content
	Sand	Silt	Clay	V. Coarse	Coarse	Medium	Fine	V. fine	Coarse	Fine			
1(1)	94	3	3	2	4	16	40	32	1	2		1.45	0.35
1(2)	89	6	5	5	10	24	28	22	3	3		1.56	0.34
1(3)	91	6	3	1	5	36	38	11	3	3		1.62	0.345
2(1)	62	28	10	2	9	15	20	16	14	14		1.4	0.4
2(2)	58	24	18		3	18	27	10	10	14		1.39	0.42
2(3)	66	20	14	1	10	12	15	28	8	12		1.41	0.41
3(1)	58	12	30		9	14	17	18	6	6		1.35	0.45
3(2)	62	6	32	1	15	18	12	16	2	4		1.56	0.48
3(3)	54	14	32	2	12	16	16	8	5	9		1.45	0.46
4(1)	60.9	25.3	13.8	0.2	3.9	12.3	31.3	13.2	11	14.3		1.6	0.379
4(2)	65.1	25.2	9.7	0.2	4	12.5	34.1	14.3	11.8	13.4		1.65	0.37
4(3)	60.9	20.2	18.9	0.3	3.2	11	32.6	13.8	9.6	10.6		1.59	0.418
4(4)	69.7	13.8	16.5	0.4	4.4	13.8	38.3	12.8	7.3	6.5		1.67	0.404
4(5)	69.7	10.4	14.6	0.4	5.6	15.4	41.9	11.7	5.7	4.7		1.62	0.375
4(6)	89	4.7	6.3	0.7	5.1	15.2	54.5	13.5	2.6	2.1		1.55	0.41
4(7)	80.4	8.2	11.4	0.2	5.6	17.6	44.5	12.5	4.8	3.4		1.63	0.42
5(1)	78	16	6	2	10	30	24	12	10	6		1.48	0.36
5(2)	78	16	6	2	10	30	24	12	10	6		1.48	0.36

* Particle-Sizes are based on SCS_USDA Classification (Appendix 1)

** The first number refers to the soil, the number in brackets to the layer

*** Soils 1-3 & 5 are invented soils. Each has 4 layers, except soil 5. The basal layer is indentical to the one above in all but depth. The depths for each layer starting from layer 1 is 20., 30., 40., and 250. cm. Soil 5 has only 3 layers all of the same composition. They are, from layer 1 down, 30., 70., and 250. cm thick.

**** Soil 4 is from SCS_USDA (1974) pp 2. A basal layer is added 120. cm thick and of the same composition as layer 7. The other depths starting from layer 1 are 28., 7.6, 20.3, 12.7, 15.2, and 15.2cm.

Table 7.8 Particle-Size (%), Bulk Density (g/cc) and Saturated Moisture Content (cc/cc) for the Five Soils Used in the Infiltration Simulations.

Run No.	Initial Properties For Each Layer			Permanent Macropore Properties			
	Soil No.	Head (cm)	Kl (cm/s)	Class No.	No. of Pores	Pore Radius (cm)	Pore Depth (cm)
1	1	10000	1.39E-04				
		8000	1.00E-04				
		4000	5.00E-05				
2	1	200	1.39E-04				
		100	1.00E-04				
		50	5.00E-05				
3	1	100	1.39E-04				
		50	1.00E-04				
		20	5.00E-05				
4	1	100	7.00E-05				
		50	1.39E-04				
		20	7.00E-05				
5	1	200	1.39E-04	1	120	0.15	90
		100	1.00E-04				
		50	5.00E-05				
6	2	10000	1.00E-05				
		8000	5.00E-06				
		4000	5.00E-06				
7	1	50	7.00E-05				
		30	1.39E-04				
		20	7.00E-05				
8	2	200	1.00E-05				
		100	5.00E-06				
		50	5.00E-06				
9	2	200	1.00E-05	1	120	0.15	90
		100	5.00E-06				
		50	5.00E-06				
10	2	200	7.50E-05	1	120	0.15	90
		100	5.00E-06				
		50	5.00E-06				
11	2	200	7.50E-05	1	120	0.15	90
		100	6.50E-05				
		50	9.00E-06				
12	2	200	7.50E-05				
		100	6.50E-05				
		50	9.00E-06				
13	3	200	5.00E-06				
		100	2.00E-06				
		50	1.50E-06				
14	3	200	5.00E-06	1	120	0.15	90
		100	2.00E-06				
		50	1.50E-06				
15	3	200	5.00E-06	1	120	0.15	90
		100	2.00E-06	2	20	0.5	90
		50	1.50E-06	3	500	0.2	50
16	4	20	4.94E-04	1	120	0.15	76.2
		30	4.23E-05				
		50	1.41E-04				
		90	7.06E-05				
		120	2.08E-04				
		70	2.38E-03				
		50	5.64E-04				
17	4	20	4.94E-04	1	120	0.15	88.9
		30	4.23E-05				
		50	1.41E-04				
		90	7.06E-05				
		120	2.08E-04				
		70	2.38E-03				
		50	5.64E-04				
18	4	20	4.94E-04	1	120	0.15	88.9
		30	4.23E-05				
		50	1.41E-04				
		90	7.06E-05				
		120	2.08E-04				
		70	2.38E-03				
		50	5.64E-04				
19	5	20	2.08E-04				
		100	2.08E-05				
20	5	100	5.60E-05				
		100	5.60E-05				
21	5	1000	5.60E-05				
		1000	5.60E-05				

* Rain intensity is specified at 0.75cm/hr for all runs with the exception of runs 16 & 17 where the rain intensity is 0.5cm/hr

Table 7.9 Initial Conditions for the 21 Simulation Runs Done for the Infiltration Model.

is comparable to Kf. The shape of the curve depends on a number of factors one of which is the rainfall intensity. If rainfall intensity is less than kf the curve will be flat as all the water will be infiltrated, though it may start to decline if the water reaches a layer with a lower Kf below. Even if it is higher than kf the steepness of the curve will depend on the intensity. Duration of the storm is also an important factor as the complete infiltration curve for the soil may not have adequate time to fully form. Temporal variations in rainfall are also important since the rain intensity may fluctuate above and below the surface value of Kf. However, the present study assumes that rainfall application maintains a steady rate and has a duration of 24 hours.

Other factors which affect the infiltration curve include the vegetation and soil conditions. Vegetation can intercept rainfall, thus acting as a temporary store, and can also alter the spatial distribution of rainfall by directing water down the stems towards the roots (Specht 1957). However, the effects of interception are insignificant for crops and pasture grasses (section 4.1) and time was not sufficient to allow for the development of an algorithm to account for the effects seen with other plants and mixed plant communities. Horton (1933, 1939, 1940) considered the reduction in infiltration rate was controlled by processes operating at the soil surface, however more recently Gardner (1967) and others have shown

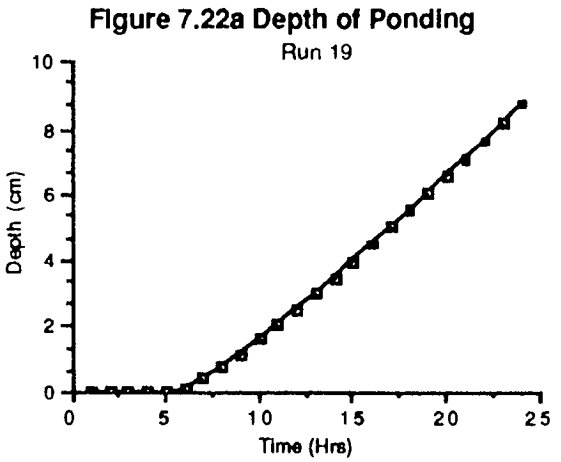

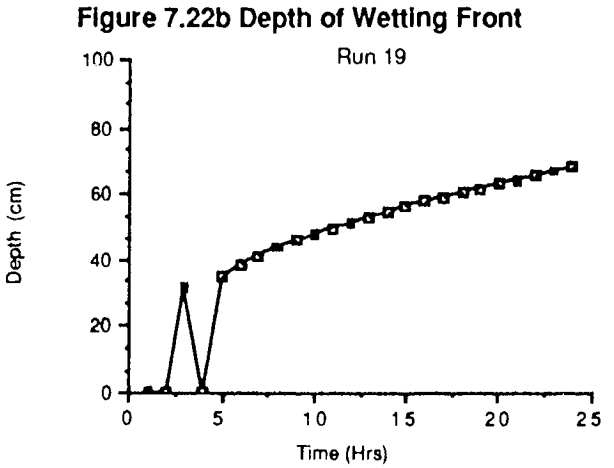

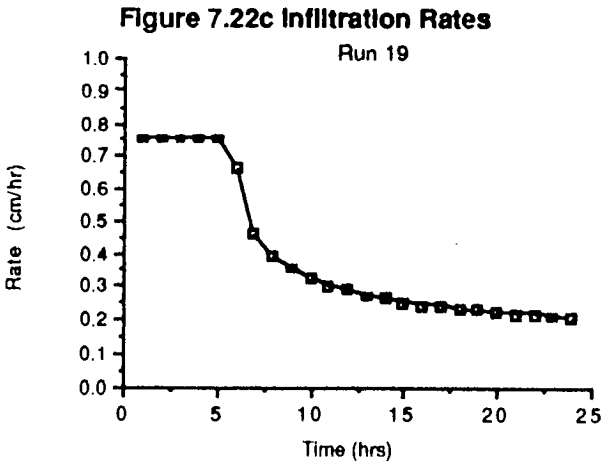

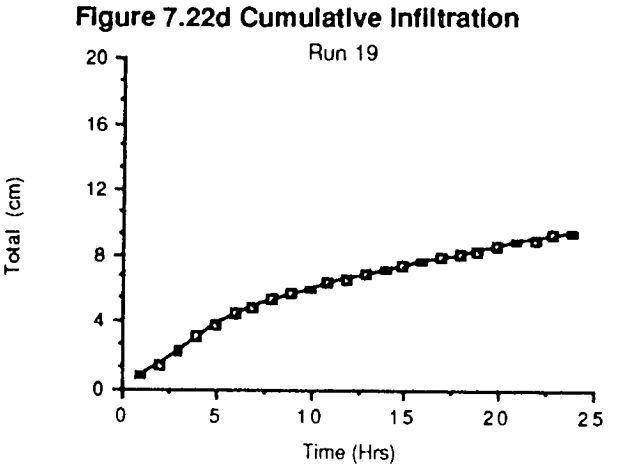

Figure 7.22 Infiltration Characteristics of Run Number 19

Shows how a layer of lower Kf at depth can reduce the infiltration rate though the rainfall intensity is less than the Kf of the surface layer

that it is flow regimes within the soil which are most important. Though surface factors, such as localised crusting may be occasionally important. Figure 7.22 (run 19) shows an extreme example of how flow within the soil can affect infiltration. Here the rain intensity (I) is less than the Kf of the surface layer but the presence of a layer of lower Kf than 'I' at depth causes ponding and the establishment of a wetting front once the surface layer has become saturated.

Layering affects the flow regimes within the soil and hence the infiltration curves. Turner (1963) noted a rapid reduction in infiltration as a front crossed a boundary into a more restrictive layer before tending slowly towards a rate near the Kf of the new layer. This is seen in Figure 7.23 with runs 2 & 3 which cross the boundaries separating layers 1 & 2 and layers 2 & 3. Examination of the point when the two fronts crossed the first boundary shows that infiltration actually increased. This was due to layer 2 having a higher value of Hf (i.e less air resistance to the advancement of the wetting front). In run 3 there was no infiltration in the final hours as the soil profile had become saturated.

In runs 1-3, coarser layers were overlying finer layers. In the converse situation, the model assumes that the wetting front is halted at the boundary until the coarser layer is saturated and the front moves to its base. The

infiltration rate being calculated using the parameters of the layer overlying the coarse layer with the exception of Hf. Run 7 though it uses the same soil as runs 1-3, which becomes finer as it descends, simulates the effect of fine over coarse by greatly reducing the conductivites of layer 1 and layer 3 below that of layer 2. Figure 7.24 shows the results gained from such a situation. Recent work has shown that fingers of rapidly infiltrating water form at such a boundary following a small delay in the wetting front at the juncture (Hillel 1987, Glass et al 1989a,b). Such complex processes still need further work before a full understanding is gained, since the occurrence and positioning of these fingers is not fully understood, and as such the present model which assumes that it is the conductivity of the overlying layer which determines infiltration (Colman and Bodman 1945) is adequate for the present model.

The effect of the initial moisture content on infiltration is seen in Figure 7.23. An increase in the initial moisture content, from run 1 to run 3, increases the depth of ponding and the initiation time, it increases the rate of the advance of the wetting front, decreases the rate of growth of cumulative infiltration and causes the infiltration rate to decrease from its maximum value sooner and more rapidly. These observations have been noted by numerous authors (eg Linsley et al 1949, Philip 1957e, Raudkivi 1979). Though as Figure 7.25 (runs 20 & 21)

Figure 7.23a Depth of Ponding

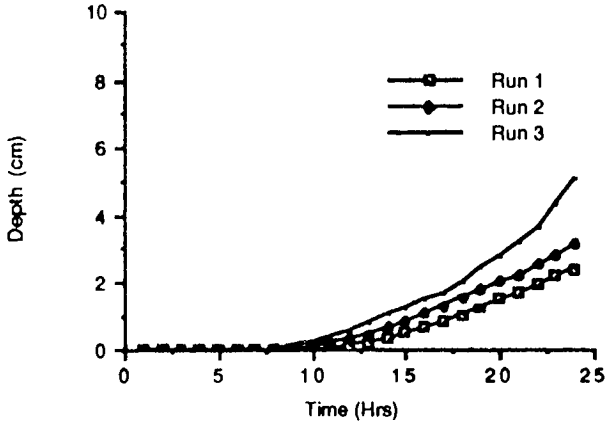

Figure 7.23b Depth of Wetting Front

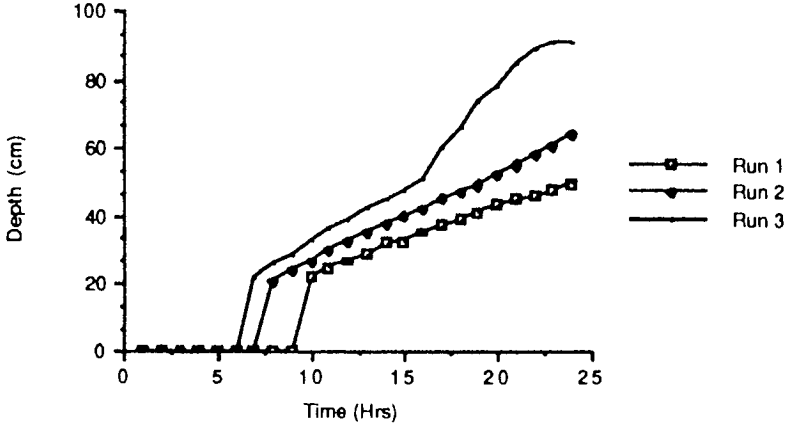

Figure 7.23c Infiltration Rates

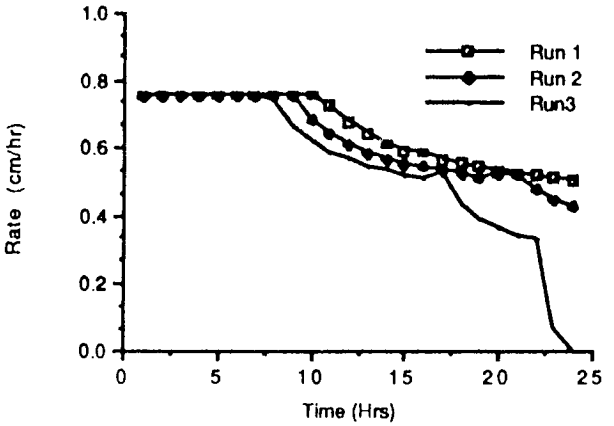

Figure 7.23d Cumulative Infiltration

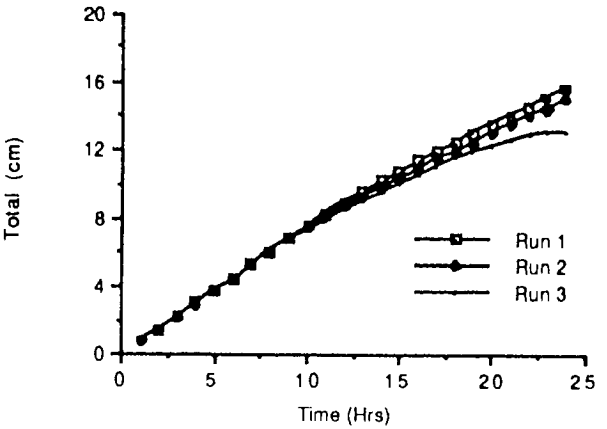

Figure 7.23 Infiltration Characteristics of Runs 1-3

Illustrates the effect of the initial moisture content and soil layering on infiltration. The initial moisture content increases from run 1 to run 3.

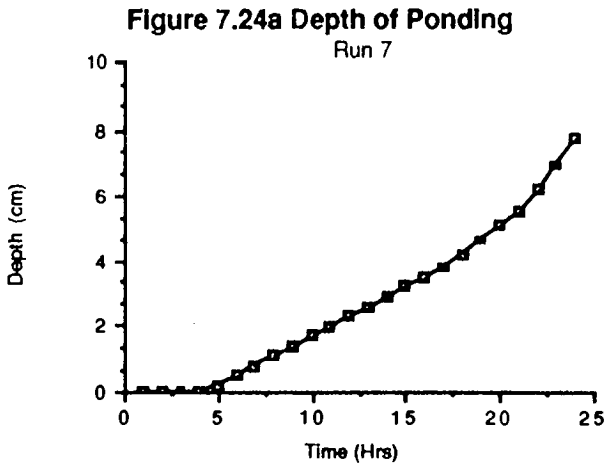

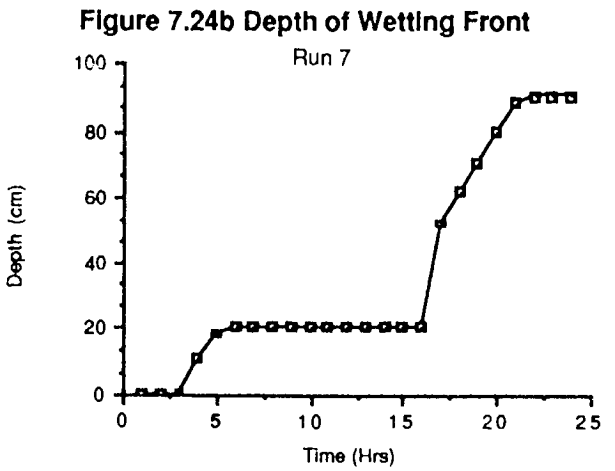

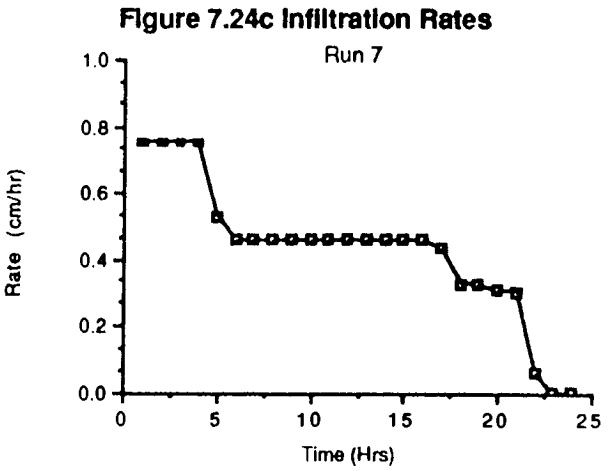

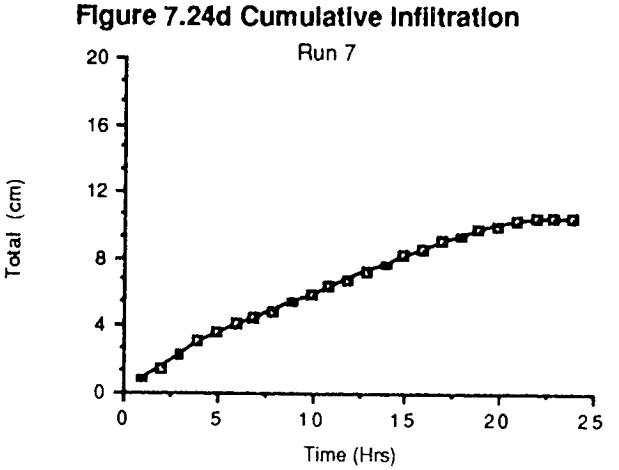

Figure 7.24 Infiltration Characteristics of Run Number 7

Illustrates how the model deals with fine over coarse textured boundaries.

demonstrates the dependance of infiltration on the initial moisture content decreases with time, the two curves becoming closer as they near Kf (Haan et al 1984). This is also seen in Figure 7.23, before the wetting fronts cross the layer boundaries, but is not as clear due to the presence of soil layers of differing textures.

The addition of macropores has several effects:-

1. To delay the onset of ponding as seen between runs 8 & 9 (Figure 7.26), this was also noted by Edwards et al (1979).
2. Figure 7.27 shows that it increases the total amount of infiltration when comparing runs 11 & 12 (Beven and Germann 1981)
3. It also increases the depth of infiltration (Figure 7.27a).
4. The infiltration rate decreases at a slower rate and may be kept at the rain intensity rate for longer (Figure 7.28 runs 8 & 9).

The greater the number of macropores the greater are these effects (Figure 7.29 runs 13-15) assuming there is no limit to the infiltration influx caused by layers becoming saturated.

The effect of bypass flow into deeper layers can affect the rate of infiltration into the matrix at the surface by affecting the flow regimes deeper within the soil. This may be achieved by increasing the initial

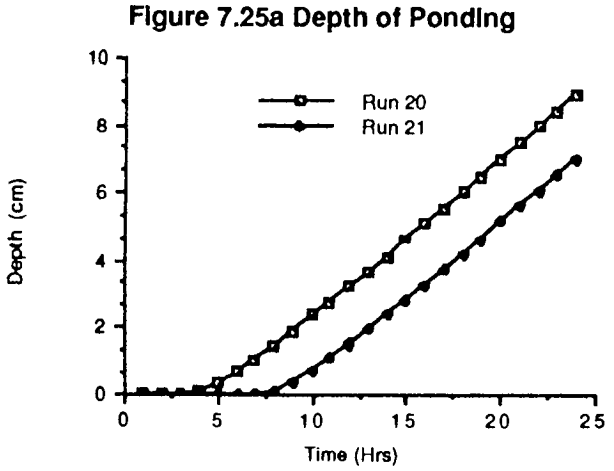

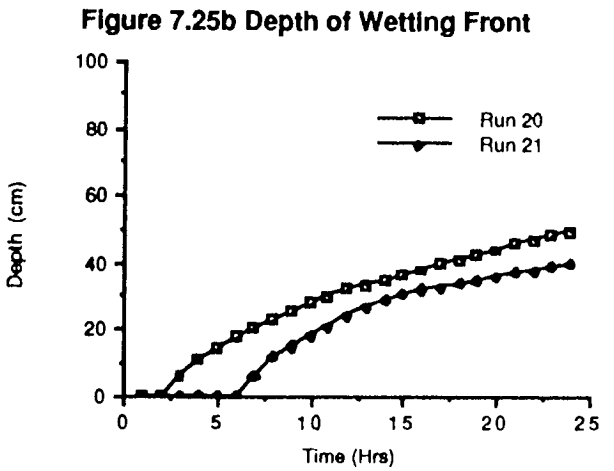

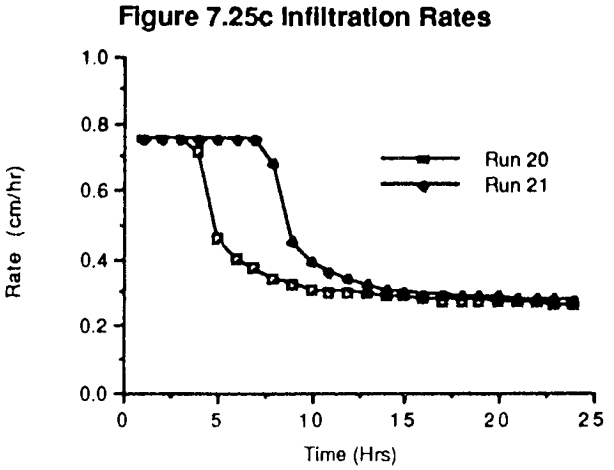

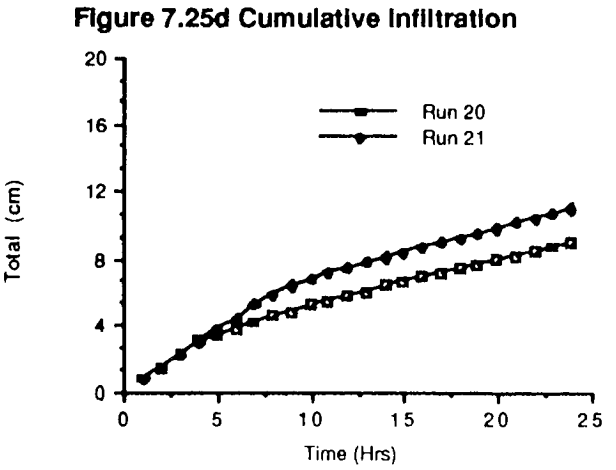

Figure 7.25 Infiltration Characteristics of Run Numbers 20 & 21

Illustrates the decreasing effect of the initial moisture content on the infiltration rate with time. Run 20 has a higher initial moisture content than run 21.

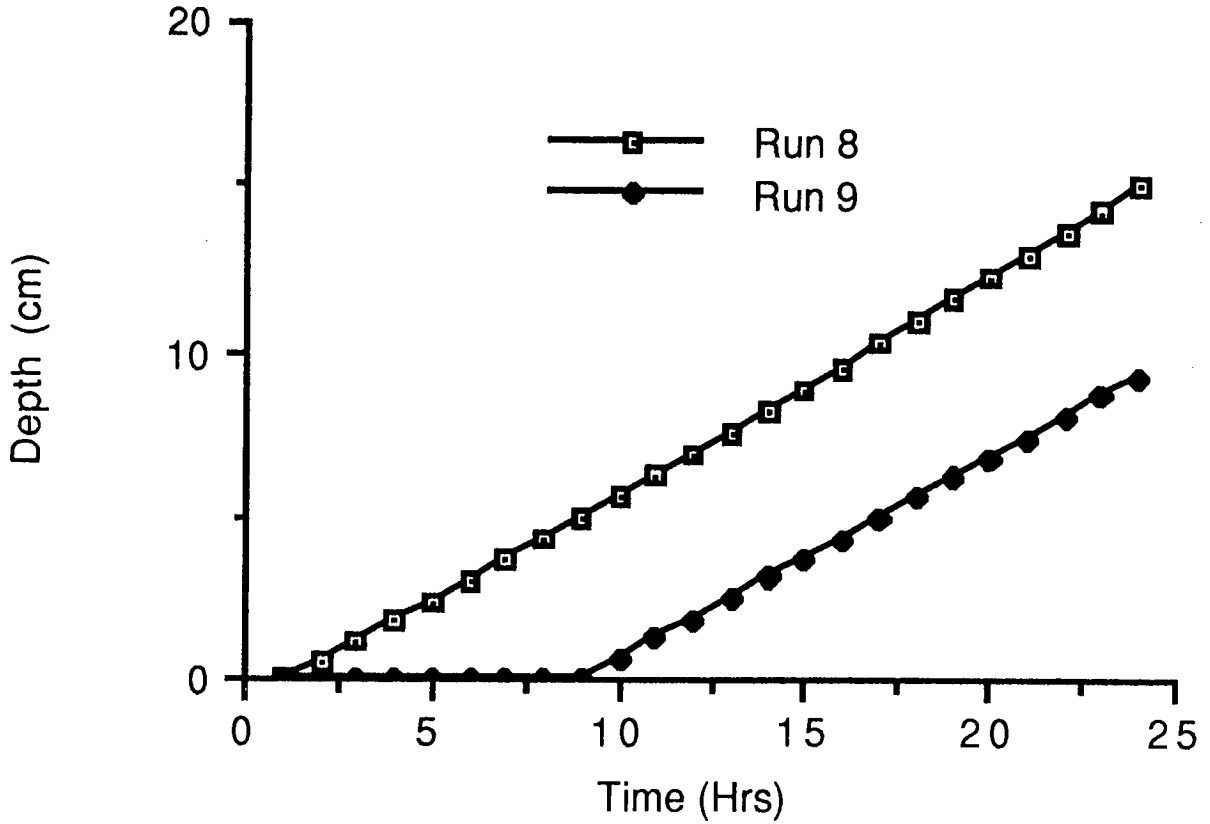

Figure 7.26 The Effects of Macropores on the Depth of Ponding in runs 8 & 9

In run 8 the soil contains no macropores whereas in run 9 it contains 1 permanent macropore class

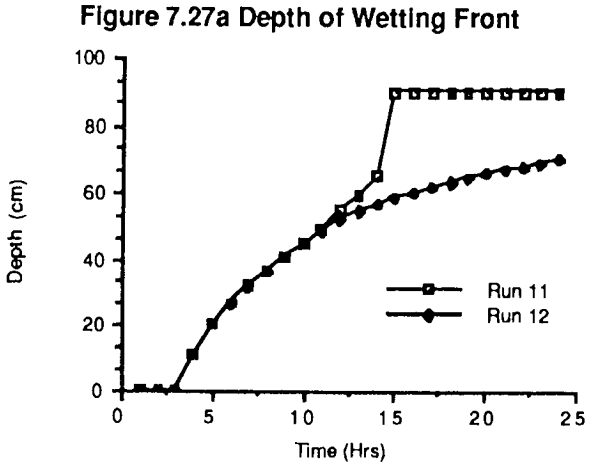

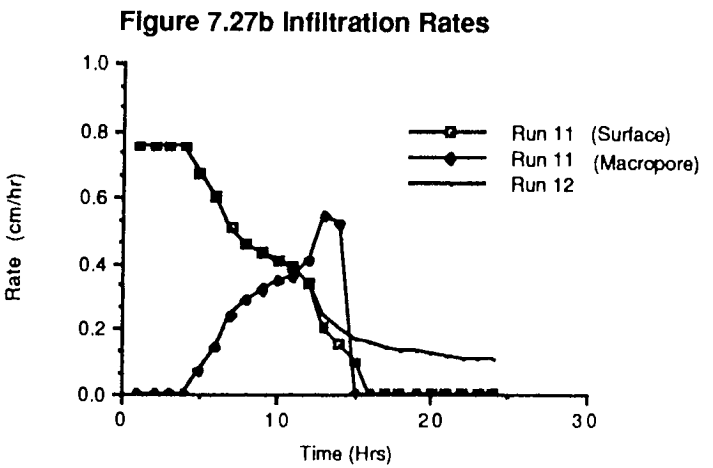

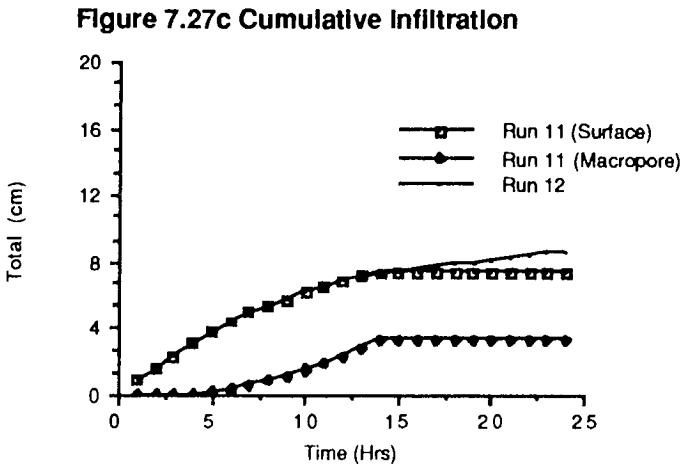

Figure 7.27 The Effect of Macropores on Infiltration Characteristics For Run Numbers 11 &12

Illustrates the effects of macropores on infiltration characteristics. The difference between run 11 and 12 is that run 11 has macropores.

moisture content ahead of the surface infiltrating wetting front so effectively decreasing the intake at the surface but increasing the rate of advancement of the wetting front (Figure 7.27 runs 11 & 12).

Runs 13-18 illustrate several problems within the model caused by simplifying assumptions. With runs 13-15 (Figure 7.29) a complex pattern of macropore infiltration can be seen. The rate increases then decreases before repeating this pattern again. The cause of this is twofold: firstly if there is no macropore wetting fronts present within the layer at commencement of macropore infiltration, equation 3.17 calculates that infiltration is infinite (as the radius of the wetting front is zero and to divide by zero gives infinity) so all water available is passed into the layer, the lower layers receiving preferential treatment. Secondly no infiltration occurs from water running down the sides of the macropore but only from below the level of standing water in the column. This produces the curves shown in run 15 (Figure 7.19). The high initial rates of infiltration occur as wetting fronts in the lowest layer are small, and with time the radii of these fronts increase so decreasing infiltration. If the water entering the macropores from the surface exceeds that infiltrated, the water level in the macropores will increase. If the level of the water increases until it reaches the layer above, there will be another rapid phase of infiltration until the wetting fronts become established in this layer.

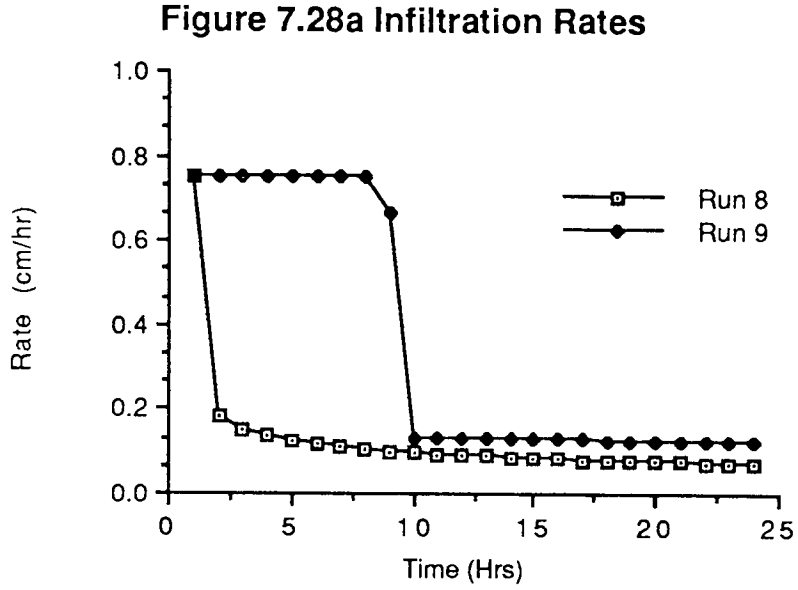

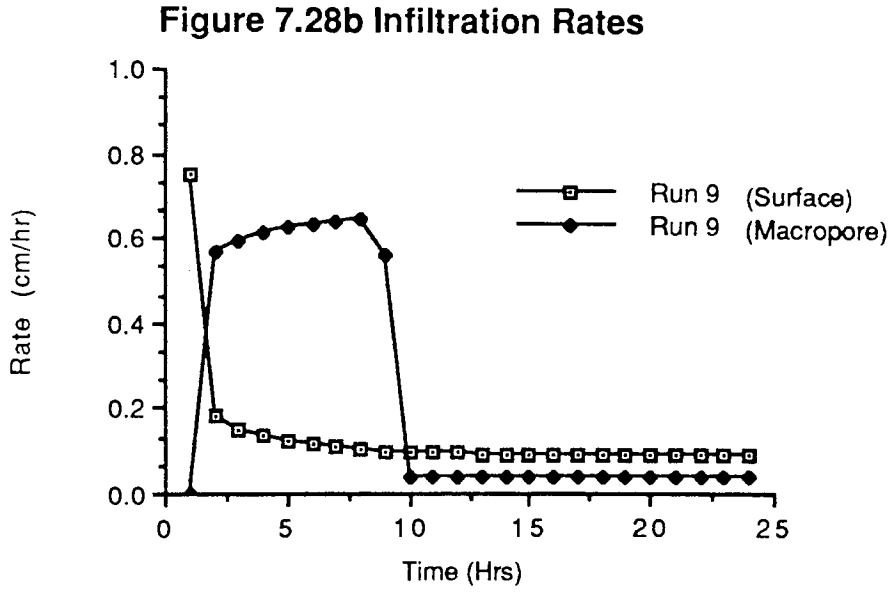

Figure 7.28 Infiltration Rates for Run Numbers 8 & 9

Illustrates the increase in the infiltration rate with the presence of macropores (Run 9). Run 8 does not include any permanent or temporary macropores.

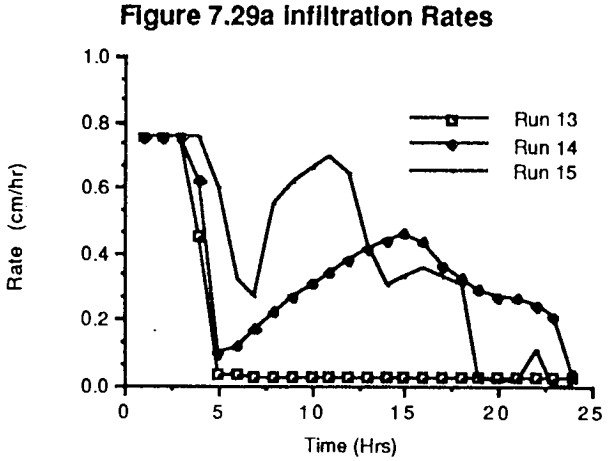

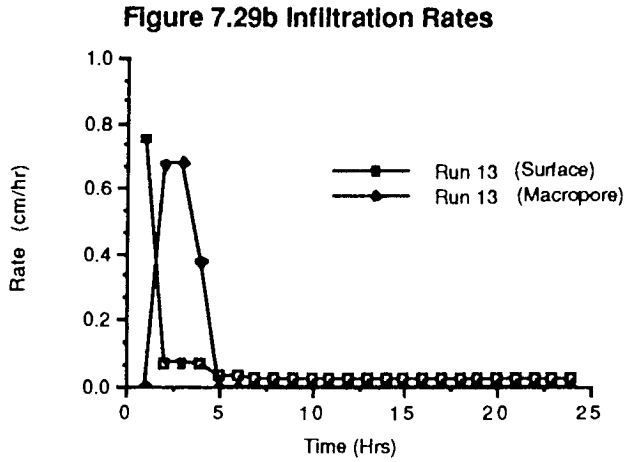

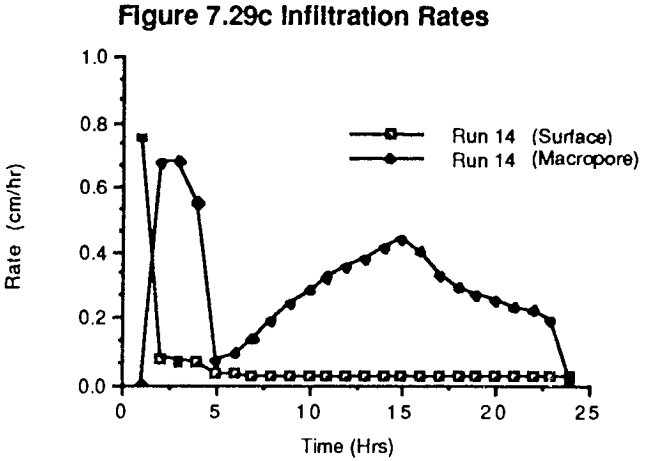

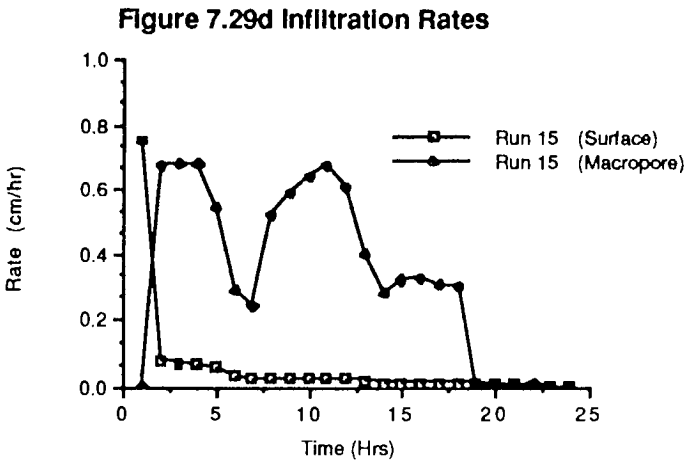

Figure 7.29a-d The Effect of Macropores on Infiltration Characteristics For Runs 13-15

Illustrates the effect of increasing the number of macropores on infiltration. Runs 13-15 use the same temporary macropore class in addition Run 14 includes 1 additional permanent class and Run 15 3 additional permanent classes.

Figure 7.29e Depth of Ponding

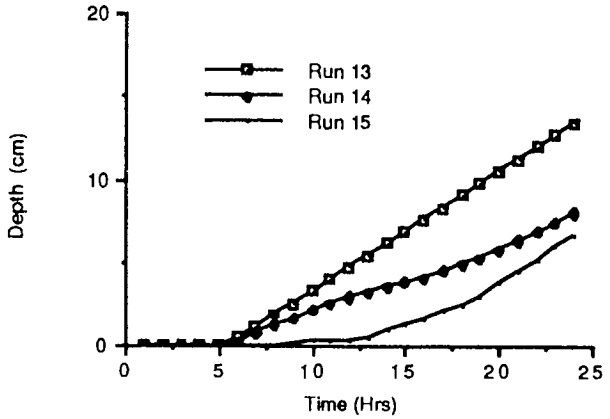

Figure 7.29f Depth of Wetting Front

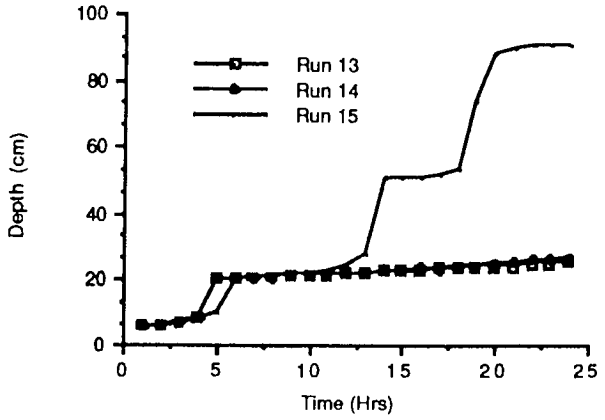

Figure 7.29g Cumulative Infiltration

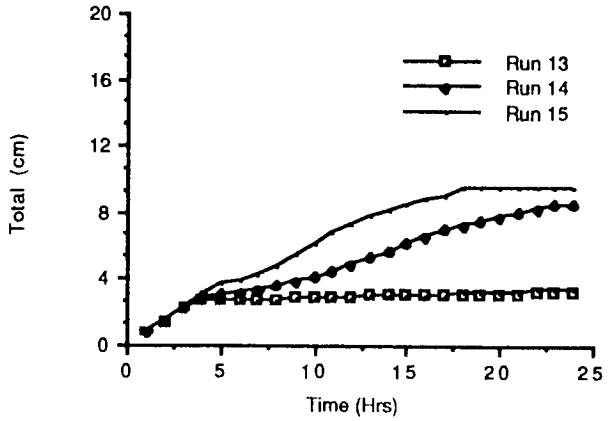

Figure 7.29e-g The Effect of Macropores on Infiltration Characteristics For Runs 13-15

Illustrates the effect of increasing the number of macropores on infiltration. Runs 13-15 use the same temporary macropore class in addition Run 14 includes 1 additional permanent class and Run 15 3 additional permanent classes.

Runs 16-18 illustrate another error resulting from the assumptions. Looking at Figure 7.30 it can be seen that for runs 16-18 the macropore infiltration rate increases with time, though for 16 this is shortlived as the layers into which the macropores are contributing and those above have become saturated. The reason for this can be found in the assumption that the percentage of the ponded store received by each macropore class depends on the number of pores it has in relation to the total number. If the class does not use up its water allocation, the excess is passed back to the ponded store for the next timestep. In runs 16-18 there are a large number of cracks at the surface due to the clay content of the surface layer. The surface layer rapidly becomes saturated, however water is still allocated to these pores from the ponded store. Water allocated to the permanent macropore class is rapidly used up. At the end of each timestep the water not infiltrated and in excess of the storage capacity of the macropore class is allocated back to the ponded store. With the cracks it means that once the surface layer is saturated and the pores filled all water allocated to the pores at the start of the timestep is passed back to the ponded store at the end. This added to the water not infiltrated at the surface exceeds the amount infiltrated by the deeper macropores in the previous timestep, so the depth of ponding increases. Which means more water is available to be allocated to the deeper pores so increasing the infiltration rate.

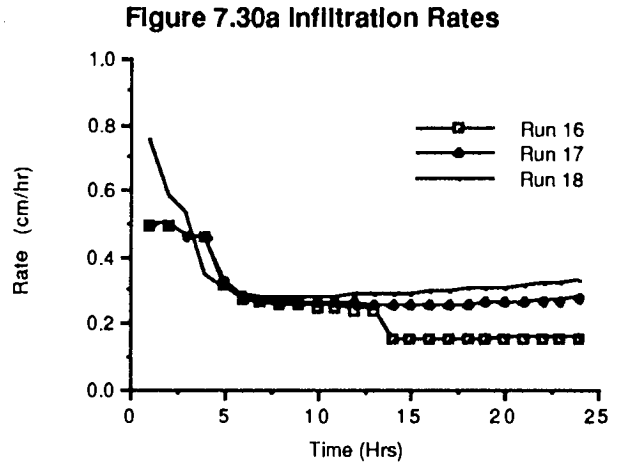

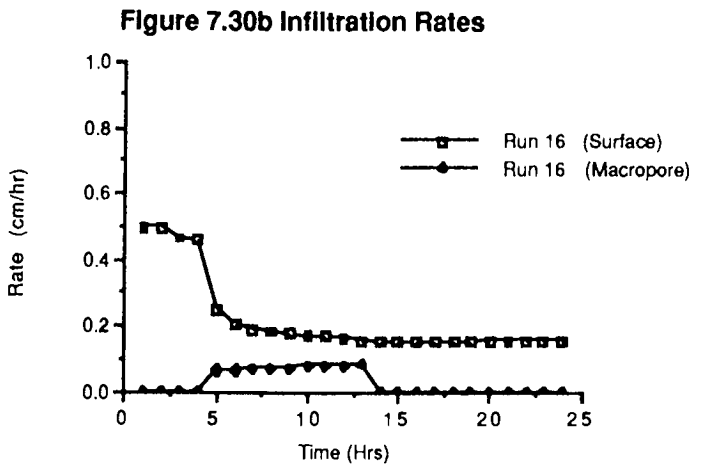

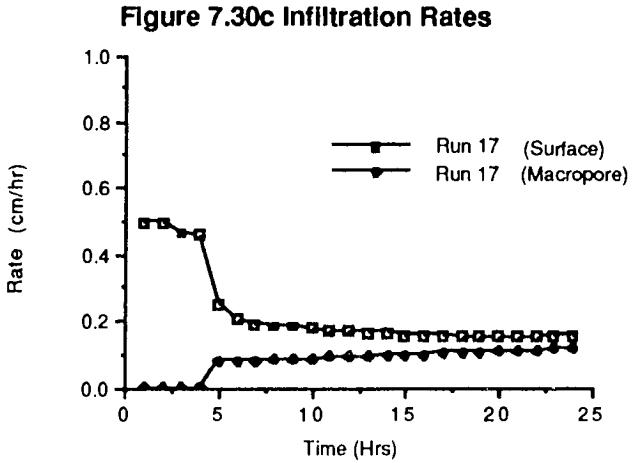

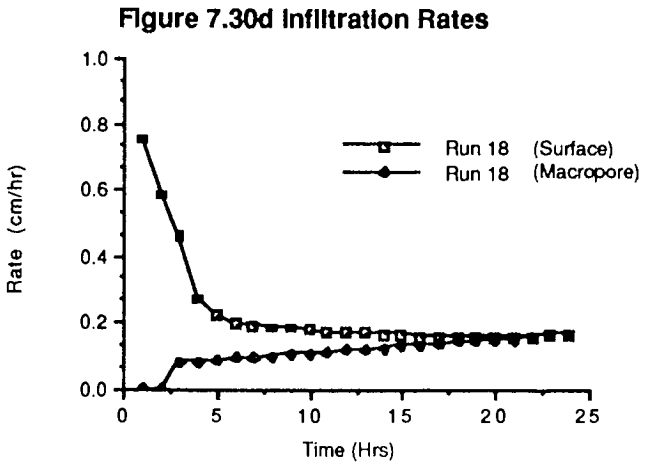

Figure 7.30a-d The Effect of Macropores on the Infiltration Characteristics of Runs 16-18

The same temporary and permanent macropore classes are used for runs 16-18 with the exception of the permanent class extends deeper in runs 17 & 18. In runs 16 & 17 the rain intensity is 0.5cm/hr while in run 18 it is 0.75cm/hr.

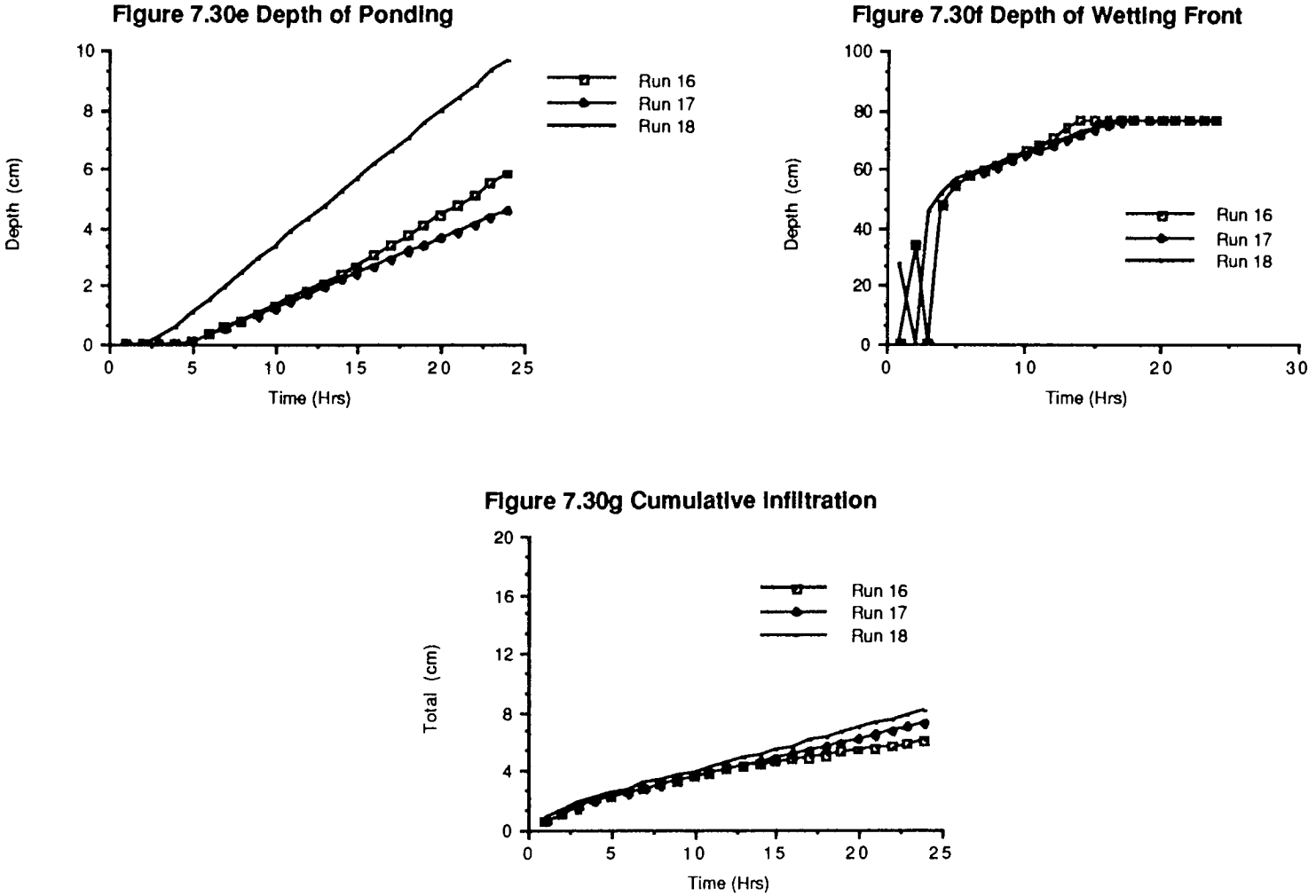

Figure 7.30e-g The Effects of Macropores on the Infiltration Characteristics of Runs 16-18

The same temporary and permanent macropore classes are used for runs 16-18 with the exception of the permanent class extends deeper in runs 17 & 18. In runs 16 & 17 the rain intensity is 0.5cm/hr while in run 18 it is 0.75cm/hr.

In summary the model has been shown to produce patterns of infiltration comparable to those obtained in the field. However, certain assumptions within the macropore model have been shown to need reassessment.

7.4 PLANT GROWTH

Plant growth and yield are limited by environmental conditions. Studies of plants grown under irrigation have shown the availabilty of water to be an important factor. They have also shown that there is a feedback mechanism between plant development and water use. The study described below was undertaken to test whether the effects seen in the field could be reproduced by the soil-moisture-plant model, and whether the model had the potential for predicting crop yields.

Within the context of this study, the plant is described as being 'stressed' if the actual rate of transpiration is below the potential rate. The amount of stress is then indicated by the stress index (equation 4.3).

7.4.1 METHOD

The soil-moisture-plant model used in this study differs from the full version in two respects:-

1. Water was input by irrigation, not rainfall, and its rate of application was assumed to be constant throughout the
2. Evaporative demand was assumed to be constant over the length of the simulation.

These modifications allowed the results to be more easily interpretated as they reduce the number of variables.

A large number of simulation runs were performed in order to identify the effects of different irrigation frequencies, evaporative demand rates and plant growth strategies.

The irrigation treatments were designed to be consistent with data given by Shalhevet et al (1976) for the irrigation of corn in Israel. Shalhevet et al (1976) recommend that the first water application should be made 30-35 days after seeding and then every 10-14 days. They also described pre-planting irrigation and stated that the growing period of corn was 125-130 days. Although the plants 'grown' in this present study were hypothetical, they were intended to be representative of grain crops. Bearing these points in mind the simulations used the following conditions:

a) a 140 day simulation period;

b) first irrigation 28 days after emergence;

c) emergence occurred on day 1 of the simulation;

d) no initial irrigation;

e) initial moisture state equal to field capacity.

Following the first irrigation, four different irrigation frequencies were investigated within each simulation:-

1. an irrigation application every 7 days (T7);
2. every 14 days (T14);
3. every 28 days (T28);
4. no irrigation (T0).

These were chosen in order to identify the effect of different irrigation treatments on plant development and water uptake.

In addition the effects of evaporative demand, amount of irrigation and plant strategies were studied. Two different evaporative demands were used:

a) 0.2 cm d^{-1} (a relatively low stress environment);

b) 0.5 cm d^{-1} (a high stress environment).

Two different plant growth strategies were used, these were referred to as 'Plant A' and 'Plant B'. With Plant A, an increased proportion of assimilates was distributed to the roots almost immediately after the actual transpiration had fallen below the potential rate. Whereas for Plant B, a much higher stress was required before the proportion of assimilates distributed to the roots was increased. Figure 7.31 shows the partitioning curves for both Plant A and Plant B. The amount of water applied at each irrigation was equal to either 25%, 50% or 100% of the accumulated potential demand between irrigations, the irrigation demand. The accumulated potential demand was used as it indicates

the amount of total potential soil moisture loss which the irrigation application is intended to replace. Ten simulations were performed in total. Details of these are set out in Table 7.10 along with the soil and plant parameters used in the study.

The effects of irrigation (i.e frequency and quantity) plant strategy and evaporative demand on plant performance and actual evapotranspiration are described in the following sections.

7.4.2 RESULTS

In some of the simulations, especially with regard to the higher evaporative demands, the plants show sustained periods when they are highly stressed. In some cases the plants would almost certainly wilt and die. However, survival not only depends on the size of the actual deficit and amount of stress but also on the stage of development. For the purposes of this study it was assumed that all plants survived the irrigation periods.

The results of the ten simulation runs are described in terms of: potential and actual plant water use; the temporal distribution of actual transpiration, root density, leaf area index; the amount of growth; and the pattern of water uptake from each layer.

Layer	Particle-Sizes <2mm (%)					Sand Fractions (%)			Silt Fractions (%)		Particles >2mm (%)	Bulk Density (g/cc)	Saturated Moisture Content (cc/cc)	Thickness (cm)
	Sand	Silt	Clay	V. Coarse	Coarse	Medium	Fine	V. fine	Coarse	Fine				
1	68	22	10	2	6	24	22	14	12	10	0	1.42	0.42	20
2	92	4	4	12	16	34	18	12	2	2	0	1.54	0.36	12
3	90	4	6	0	2	26	36	26	2	2	0	1.58	0.38	16
4	64	24	12	4	12	20	16	12	14	10	0	1.46	0.44	20
5	48	20	32	4	8	12	16	8	8	12	0	1.4	0.48	30
6	92	4	4	12	16	34	18	12	2	2	0	1.54	0.36	250

Plant Parameters	a	b	c	minrat	maxrat	ap	np	lc	rc	maxial	maxval	f4
Runs 1,2,3,7 & 8	10	2.5	0.22474	0.1	0.9	8	6	0.008	0.0008	4.5	1.1	4
Runs 4,5,6,9 & 10	10	2.5	0.22474	0.1	0.9	1.2	12	0.008	0.0008	4.5	1.1	4

Initial Plant Conditions	
Layer Roots Extend Into	1
Initial Root Density	0.8
Initial LAI	0.2

Length of Simulation	108 days	Day Crop Emerges in Simulation	Day 1
Number of Crops	1 Crop	Day Crop is Harvested in Simulation	Day 108

Simulation Run No.	Evaporative Demand (cm/day)	Plant Type	Percent Irrigation Application	Irrigation Frequencies
1	0.2	A	25	T7,T14,T28,T0
2	0.2	A	50	T7,T14,T28,T0
3	0.2	A	100	T7,T14,T28,T0
4	0.2	B	25	T7,T14,T28,T0
5	0.2	B	50	T7,T14,T28,T0
6	0.2	B	100	T7,T14,T28,T0
7	0.5	A	50	T7,T14,T28,T0
8	0.5	A	100	T7,T14,T28,T0
9	0.5	B	50	T7,T14,T28,T0
10	0.5	B	100	T7,T14,T28,T0

* The Water Table is present in layer 6. Initially it is placed at the top of this layer.

Table 7.10 Summary of the Ten Irrigation Simulations.

Table 7.11 shows the potential and actual plant water use, and highlights several points which are worth noting.

1. Both potential and actual water use were much greater for the runs with the higher evaporative demands (runs 7-10).
2. Potential water use varied little for treatments T7, T14 and T28, but treatment T0 showed much lower values.
3. As regards actual plant water use, treatment T7 uses the most, followed in order by T14, T28 and T0, with the exception of run number 9. The greater the percentage of the irrigation demand that was satisfied, the smaller was the difference between T7, T14 and T28 in terms of actual plant water use, and the greater was its difference between these three treatments and T0.
4. Actual plant water use was greater, the greater the percentage of irrigation demand that was satisfied.
5. Actual plant water use was greater for plant A than plant B in all cases except when the irrigation demand was fully satisfied. The difference then was minimal.
6. The difference between actual and potential water use decreased with: a lower evaporative demand; the greater the percentage of irrigation demand that was satisfied; the more frequent the irrigation application; and, from plant B to plant A.

TABLE 7.11 ACTUAL AND POTENTIAL WATER USE RESULTS FOR EACH IRRIGATION TREATMENT SIMULATION.

Run Number	Treatment			
	T7	T14	T28	T0
1	15.04	14.96	14.07	10.78
	22.30	22.33	22.34	19.78
2	18.59	18.51	18.40	10.78
	22.38	22.38	22.38	19.78
3	22.18	22.18	22.18	10.78
	22.39	22.39	22.39	19.78
4	13.16	13.14	13.04	7.87
	22.37	22.37	22.37	21.78
5	17.92	17.92	17.63	7.87
	22.38	22.38	22.38	21.78
6	22.18	22.18	22.18	7.87
	22.39	22.39	22.39	21.78
7	40.12	39.55	39.28	12.55
	61.64	61.77	61.80	47.91
8	59.56	59.48	44.97	12.55
	61.80	61.80	61.80	47.91
9	37.70	39.09	37.82	11.72
	62.42	62.46	62.46	61.38
10	59.72	59.37	41.40	11.72
	62.46	62.46	62.46	61.38

* its Actual layout for each run and treatment
Potential

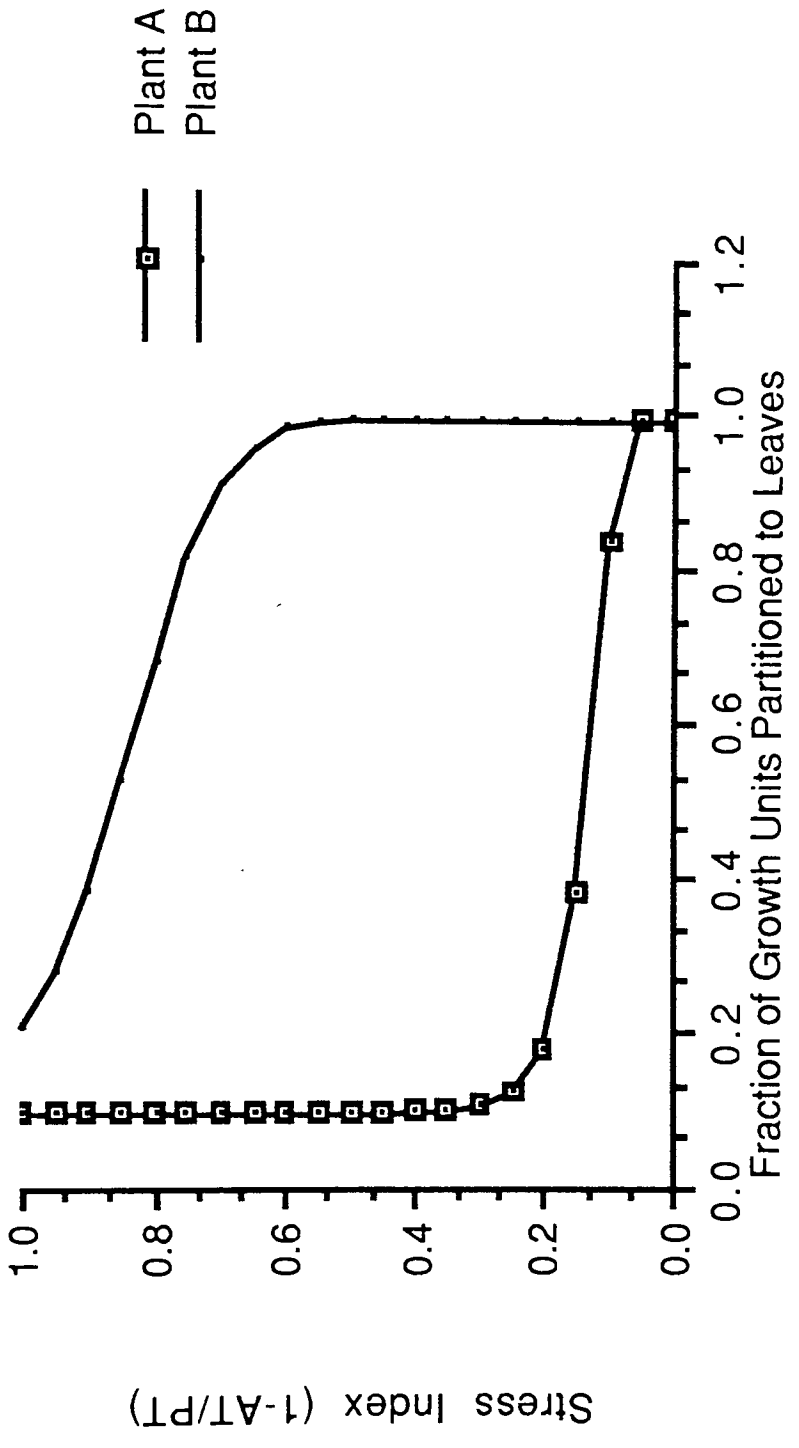

Figure 7.31 Growth Unit Partitioning Curves for Plant A and B.

Examination of the pattern of water use and evaporation during periods of stress within treatments T7, T14 and T28 revealed a number of observations which are worthy of note.

1. With plant A, the amount of water uptake between irrigation applications, increased markedly with time before dropping off again towards the end of the simulation (Figure 7.32).
2. After a brief initial increase, plant B showed a slight increase in water uptake between irrigations throughout the simulation. However, by the end of the simulation it was as high, if not higher, than that of Plant A (Figure 7.33).
3. The amount of soil evaporation slowly decreased with time until all evaporative demand was partitioned to transpiration (i.e leaf area index was 1 or greater). Soil evaporation also peaked where there was an irrigation application, and the greater the application the higher the peak.

The pattern of water use by plants is best demonstrated by the relative transpiration data. From these, two further points may be made. Firstly, with treatment T0 the relative transpiration curve (Figure 7.34) showed that actual transpiration fell rapidly from the potential value and then started to increase before decreasing again and repeating the cycle. This pattern was much sharper and more condensed in time for the higher evaporative demands and for plant A (Figure 7.34) than it was for other cases. Secondly, for the

Figure 7.32a Run No. 2 T7

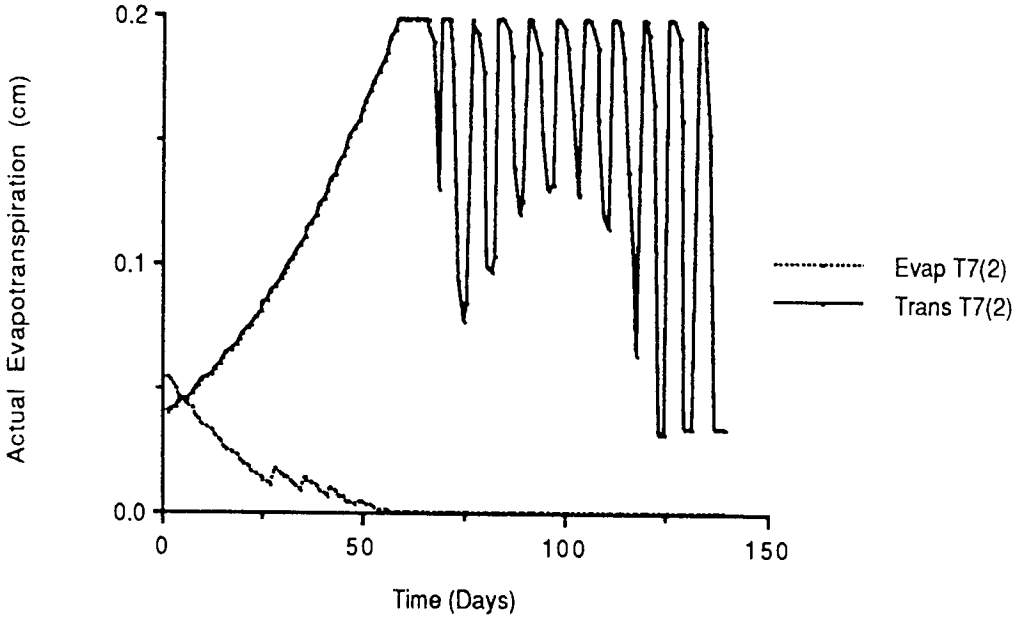

FIGURE 7.32b Run No. 7 T7

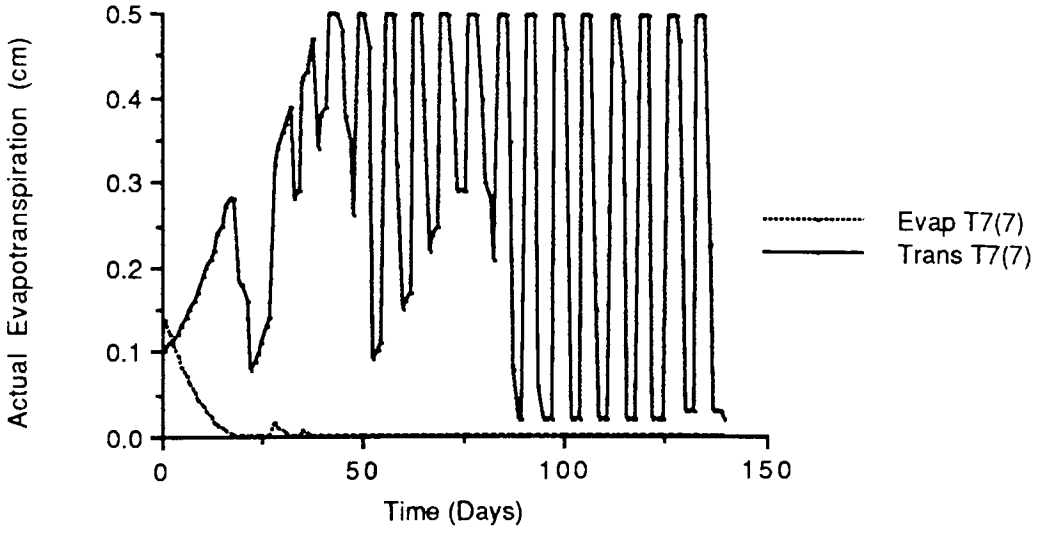

Figure 7.32 Actual Evapotranspiration Over Time for Plant A

a) Evaporative Demand 0.2cm/day

b) Evaporative Demand 0.5cm/day

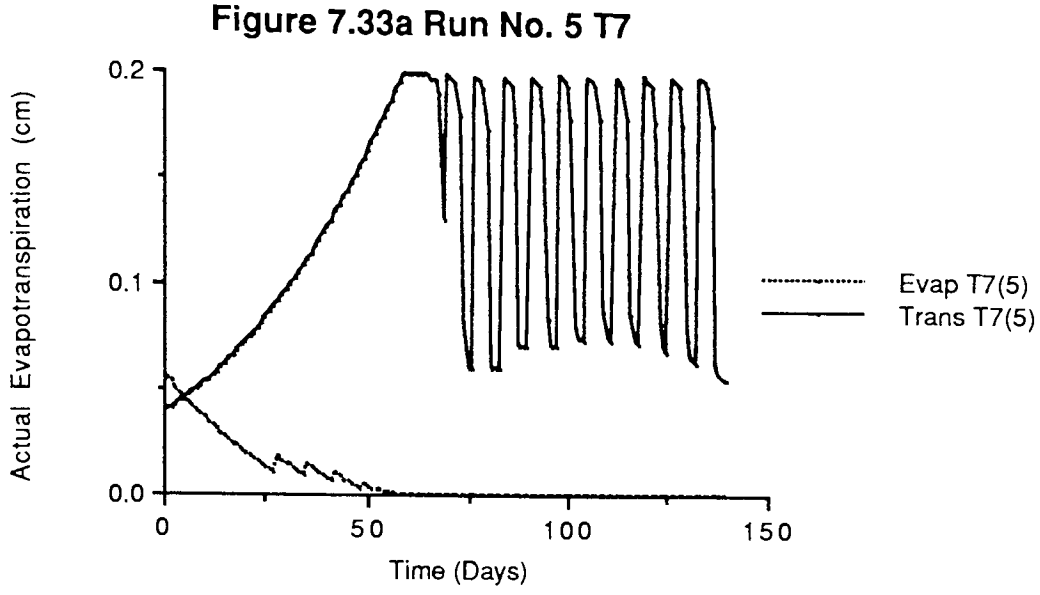

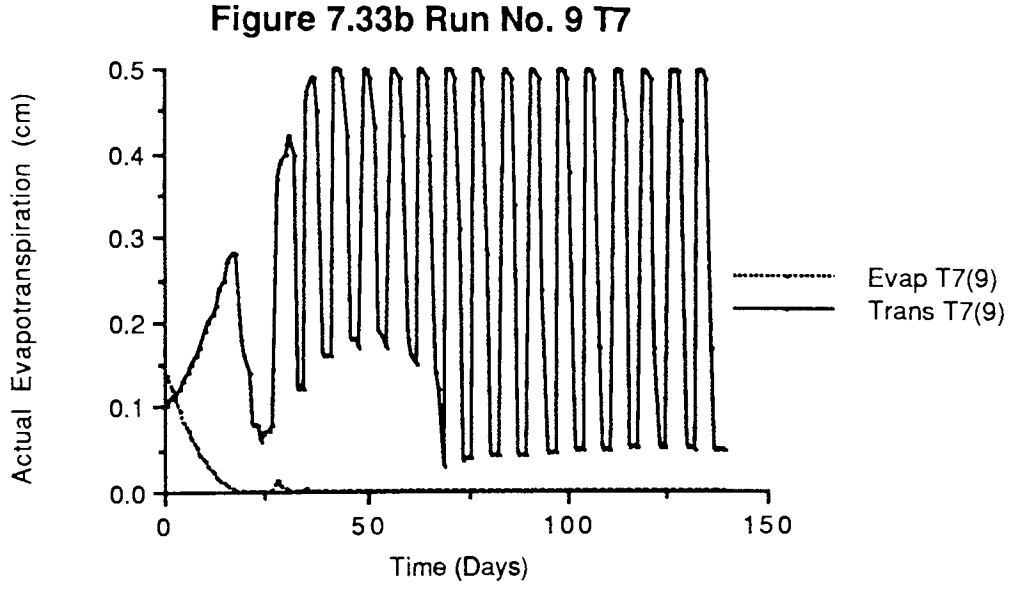

Figure 7.33 Actual Evapotranspiration Over Time for Plant B

a) Evaporative Demand 0.2cm/day

b) Evaporative Demand 0.5cm/day

higher evaporative demand rate the plants were far more stressed between irrigations than at the lower rates. In the case of plant B, this was also true even when the irrigation demand was satisfied (e.g in runs 8 (T28) and 10 (T14 and T28) the plants shows stress in between applications).

The pattern of water uptake from individual layers shows that over time more water was taken from the lower layers. The influence of the deeper layers became more important for: the lower the percentage of the irrigation demand satisfied (Figure 7.35a); the greater the gap between irrigation applications (Figure 7.35b); the greater the plant is stressed; and, the higher the evaporative demand. Plant A also tends to utilse the lower layers more especially when stressed (Figure 7.35c).

In cases where the irrigation demand was not fully satisfied, the depth of the water table was the same for all irrigation treatments. Where the demand was fully satisfied, the water table was shallowest for treatment T28 and deepest for treatment T7. The difference between these was greatest for the lower evaporative demand rates (run 3 and 6). Figure 7.36 illustrates these points.

Leaf area index was found to increase with: potential evaporative demand: the greater the percentage of irrigation demand satisfied; the greater the gap between irrigation applications; and, the less the plant is stressed. Leaf area

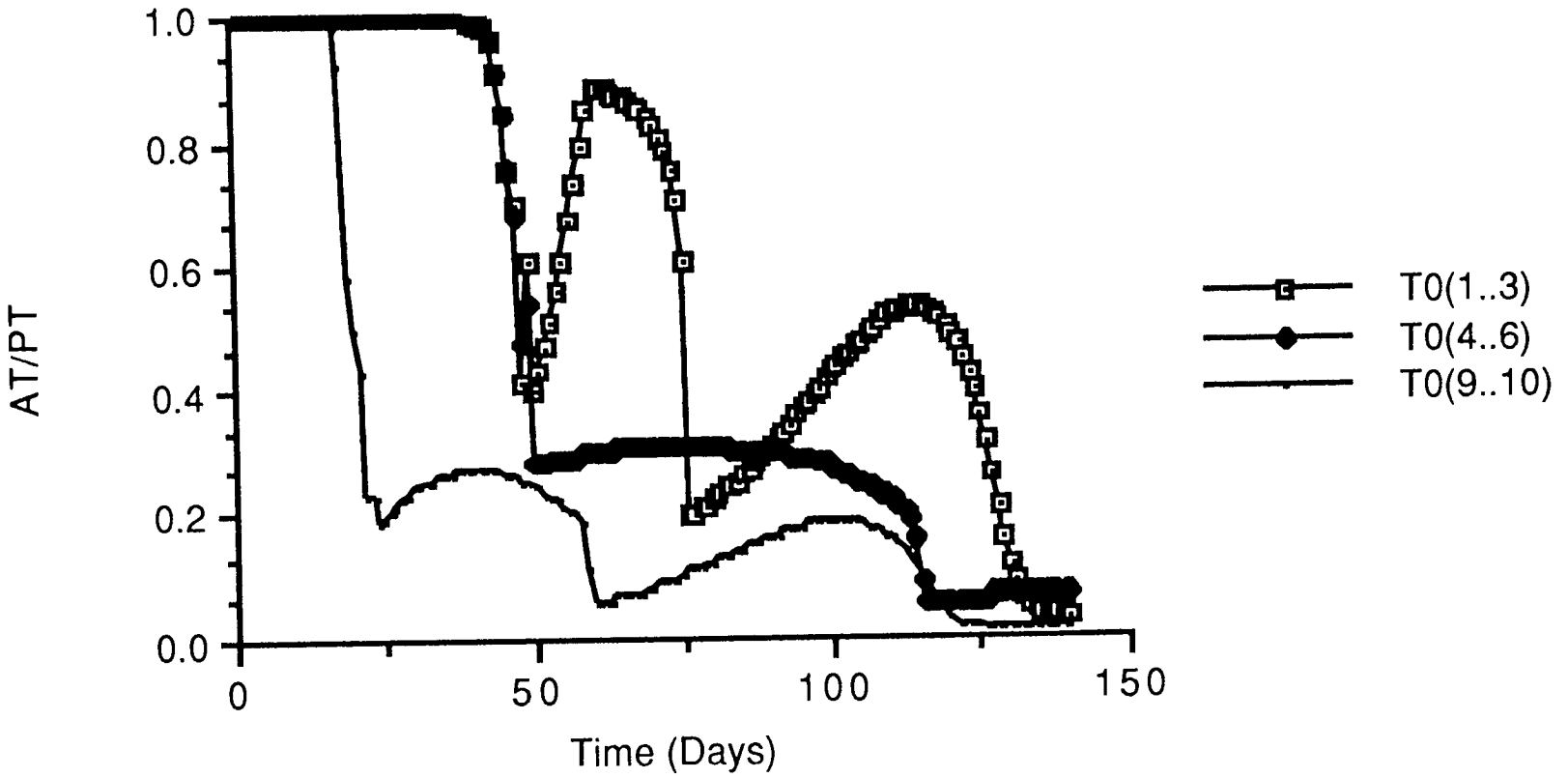

Figure 7.34 The Effect of Plant Strategy and Evaporative Demand Rate on Relative Transpiration Curves

i) T0(1..3): ED 0.2cm/day and Plant A ii) T0(4..6): ED 0.2cm/day and Plant B iii) T0(9..10): ED 0.5cm/day and Plant B

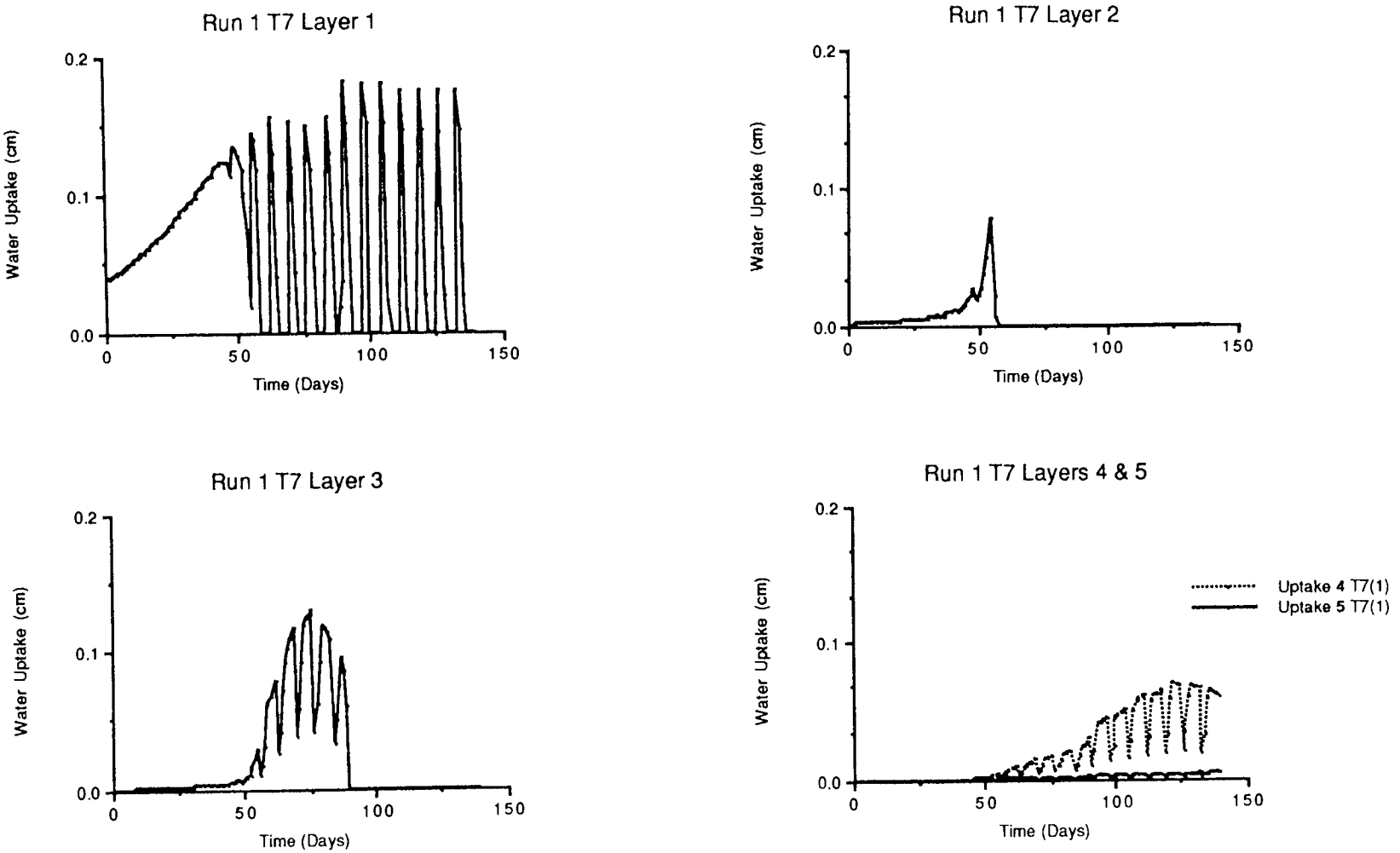

Figure 7.35a The Effect of the Amount of Irrigation on Water Uptake From Different Layers

T7, Plant A, Evaporative Demand 0.2cm/day and an Irrigation Application of 25%

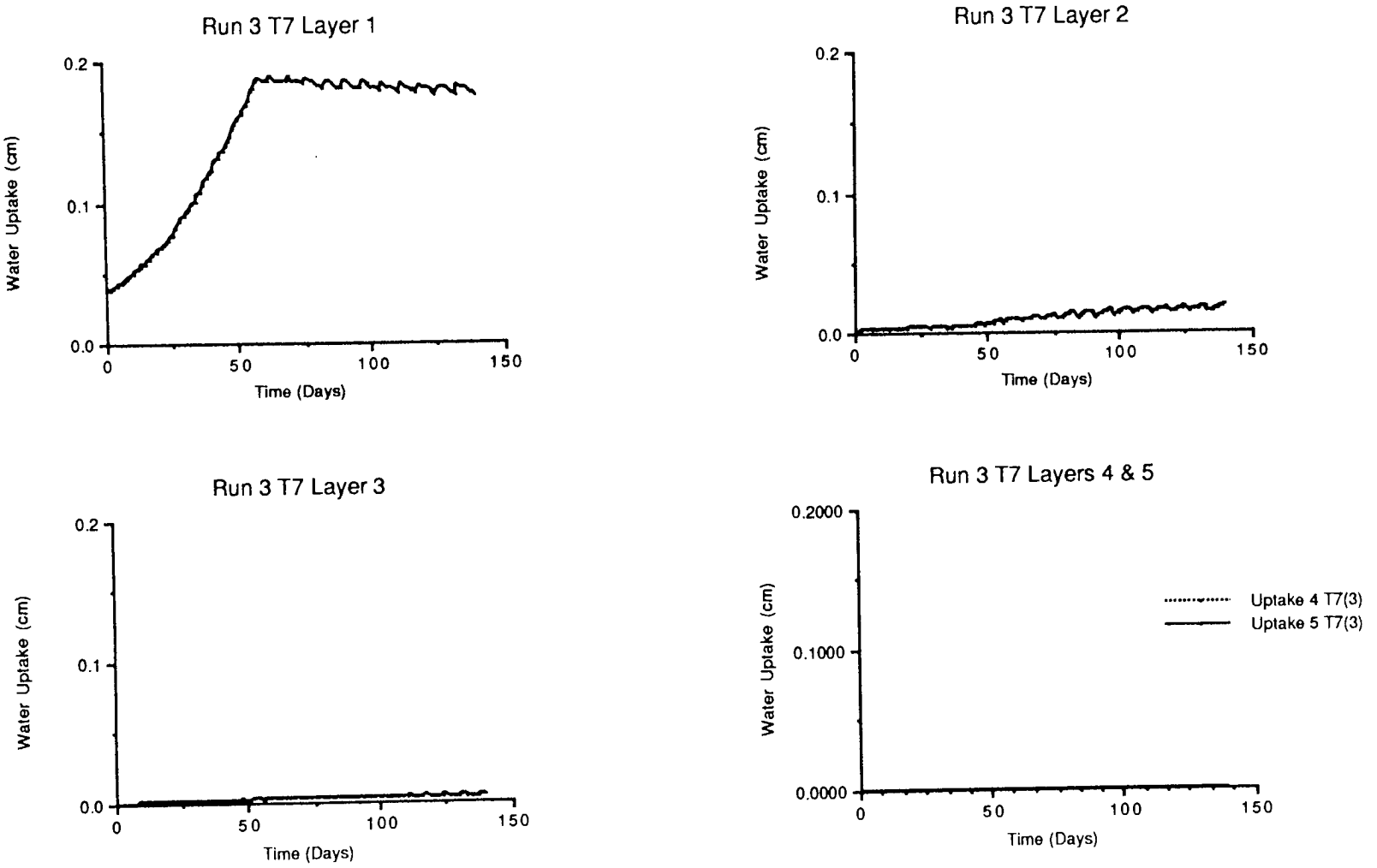

Figure 7.35a The Effect of the Irrigation Amount on Water Uptake from Different Layers

T7, Plant A, Evaporative Demand 0.2cm/day and an Irrigation Application of 100%

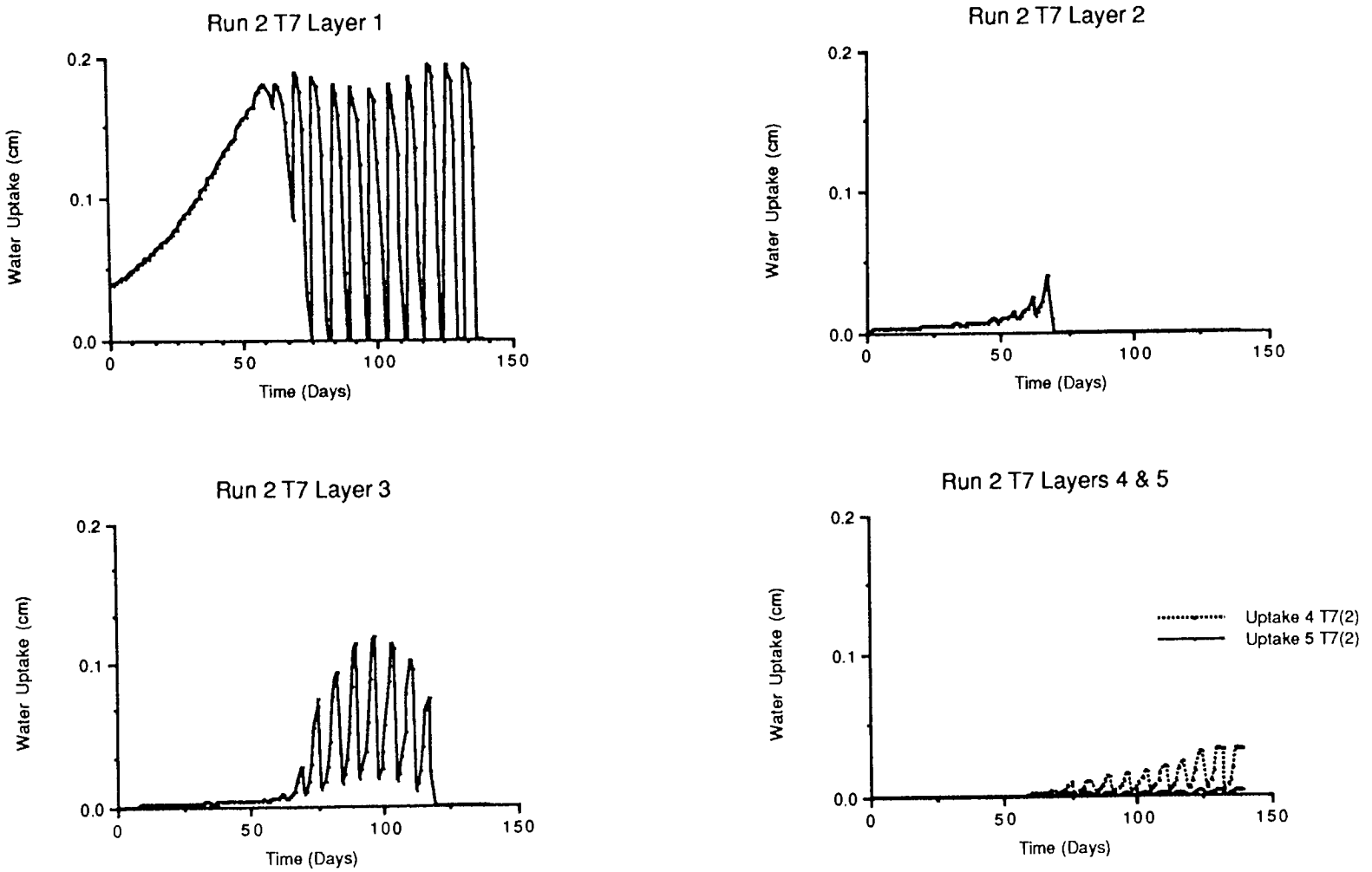

Figure 7.35b The Effect of Irrigation Frequency on Water Uptake from Different Layers

T7, Plant A, Evaporative Demand 0.2cm/day and an Irrigation Application of 50%

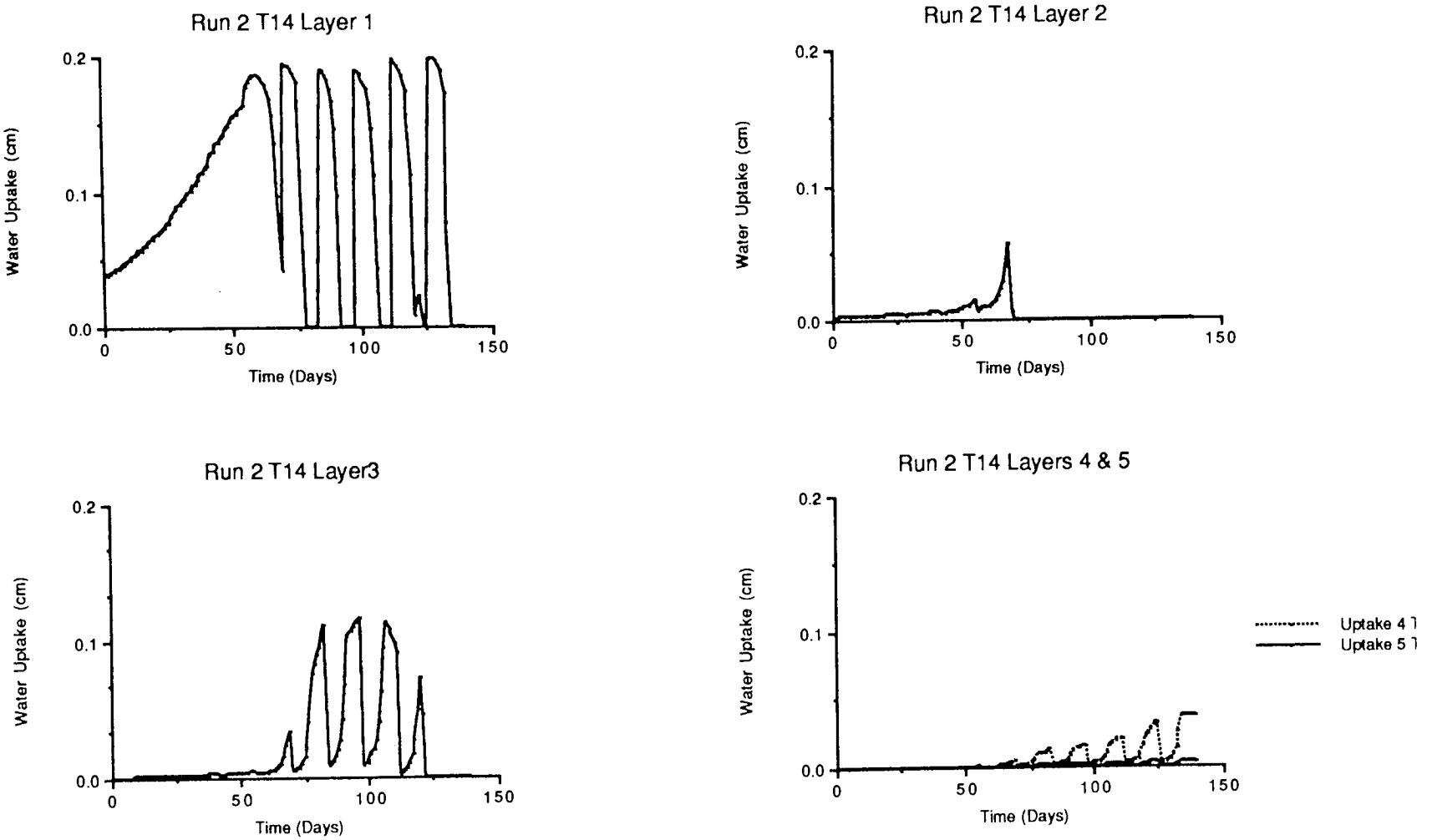

Figure 7.35b The Effect of Irrigation Frequency on Water Uptake from Different Layers

T14, Plant A, Evaporative Demand 0.2cm/day and an Irrigation Application of 50%

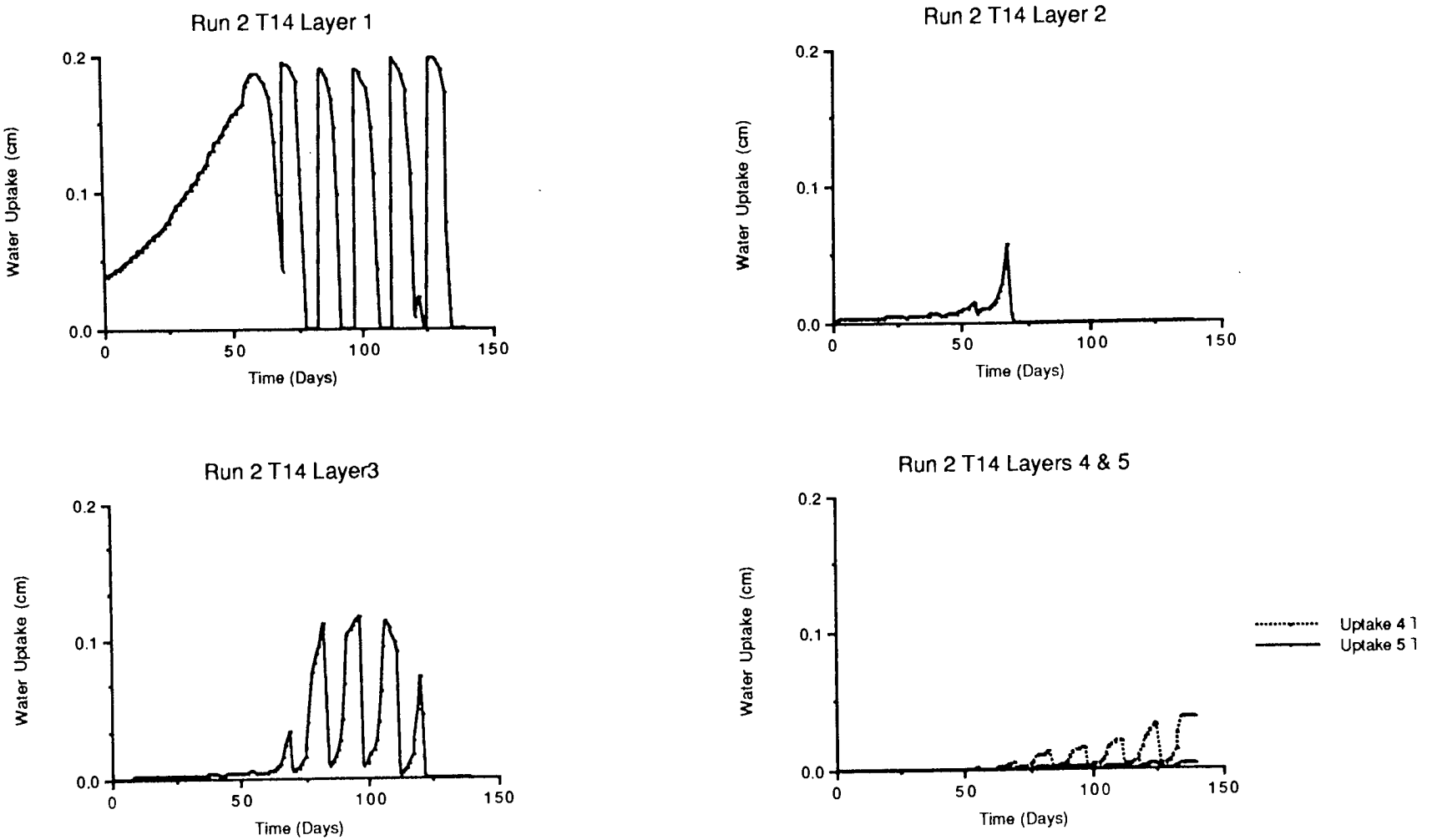

Figure 7.35c The Effect of Plant Strategy on Water Uptake from Different Layers

T14, Plant A, Evaporative Demand 0.2cm/day and an Irrigation Application of 50%

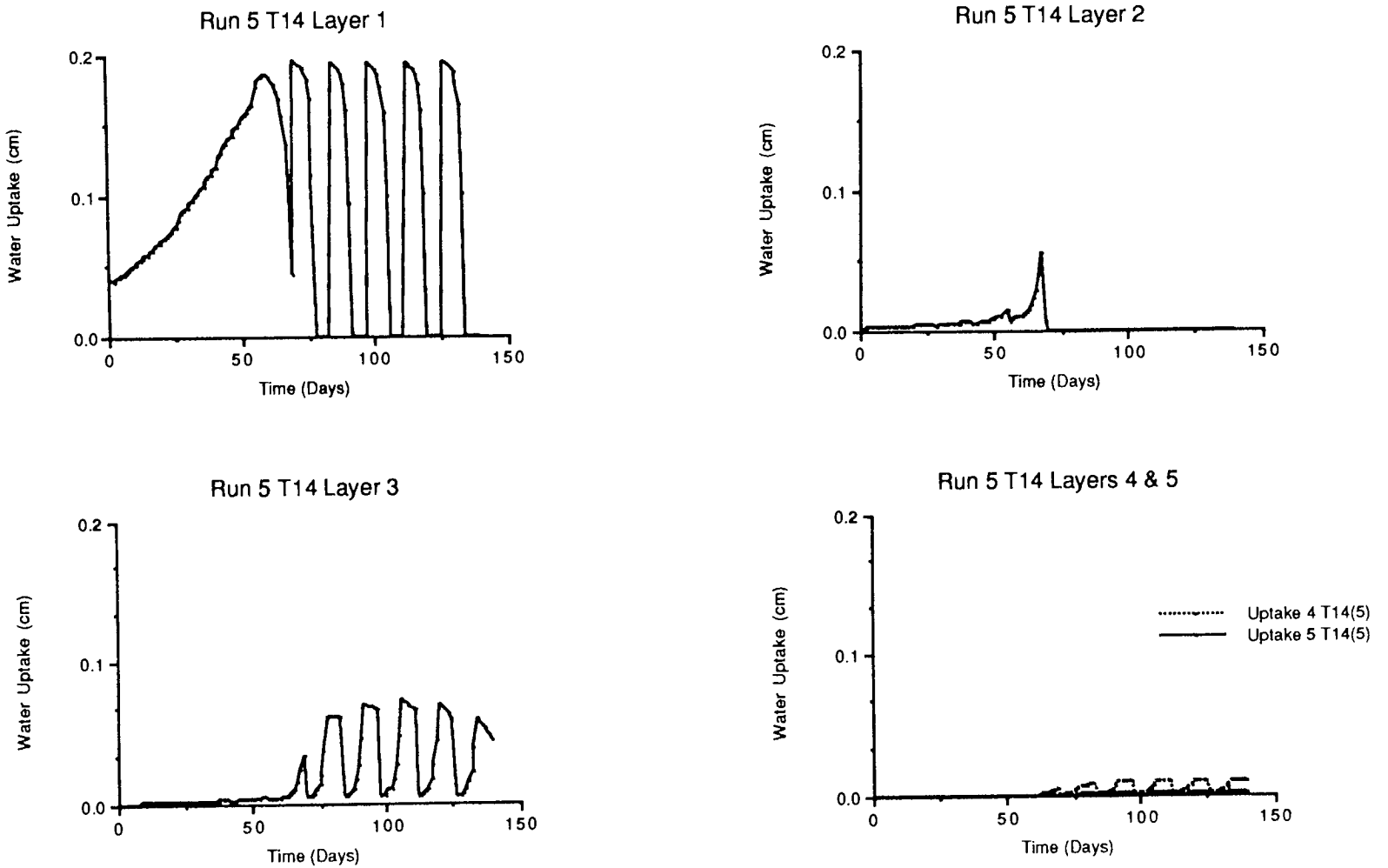

Figure 7.35c The Effect of Plant Strategy on Water Uptake from Different Layers

T14, Plant B, Evaporative Demand 0.2cm/day and an Irrigation Application of 50%

index was greater for plant B than A. For the lower evaporative demand rates (i.e runs 1-6) differences between plant A and B were minimal (Figure 7.37a), but for the higher rates (i.e runs 7-10) the differences were quite noticeable (Figure 7.37b). With treatment T0, leaf area index only reached a value of 1 (or slightly more) in runs 9 and 10 and fell below the other treatments at day 28 (i.e after the first irrigation application).

Root density increased with increased potential evaporative demand, both in terms of overall amount and in terms of increased density in the deeper layers. It was also higher for Plant A than Plant B. In general, root density was also higher for treatments which only partially satisfied the irrigation demand.

7.4.3 DISCUSSION

Plant growth, and consequently yield, is influenced by the availability of water to a large extent. Numerous authors have related crop yield to actual evapotranspiration (e.g Stewart et al 1975, Hillel and Guron 1973 and Bielorai et al 1964) and to actual transpiration (e.g Downey 1972, Wit 1958 and Shalhevet et al 1976). Hanks and Hill (1980) note that the relation of yield to transpiration is more appropriate than to evapotranspiration, since the former consists only of water travelling through the plant.

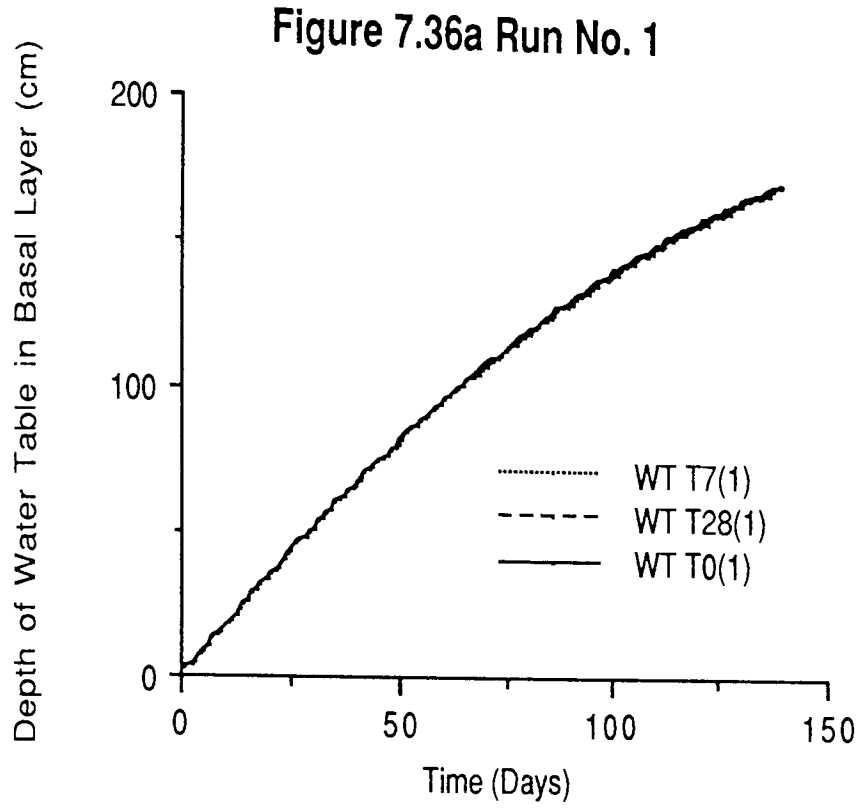

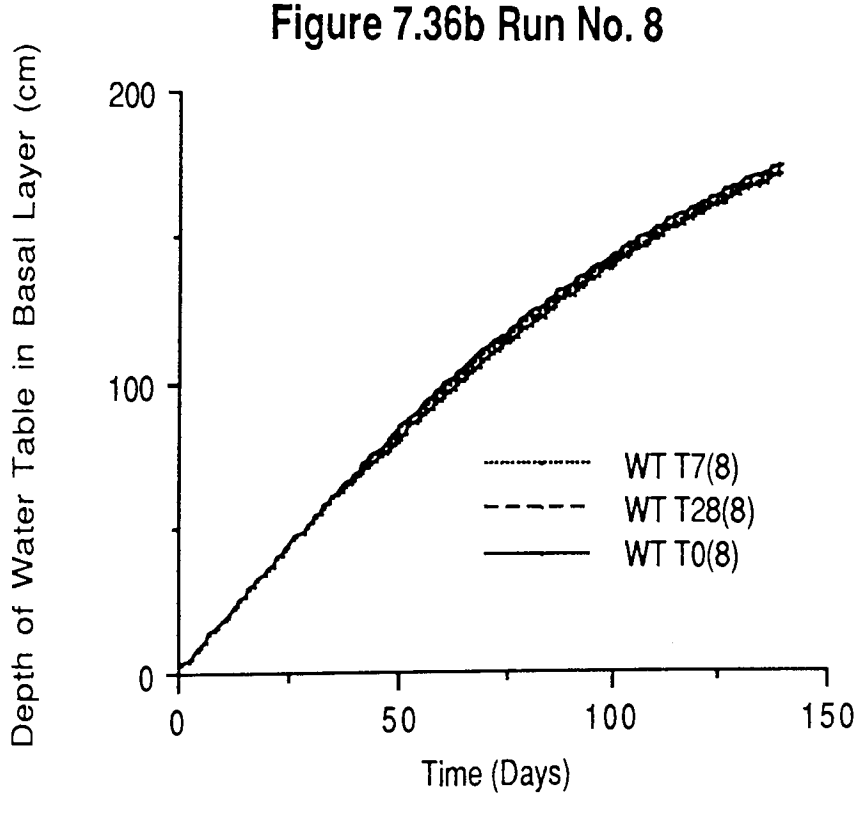

Figure 7.36 The Effect of the Amount of the Evaporative Demand on the Depth of the Water Table.

a) Plant A, ED 0.2cm/day and Irrigation Application 25%

b) Plant A, ED 0.5cm/day and Irrigation Application 100%

Figure 7.37a Run No. 1

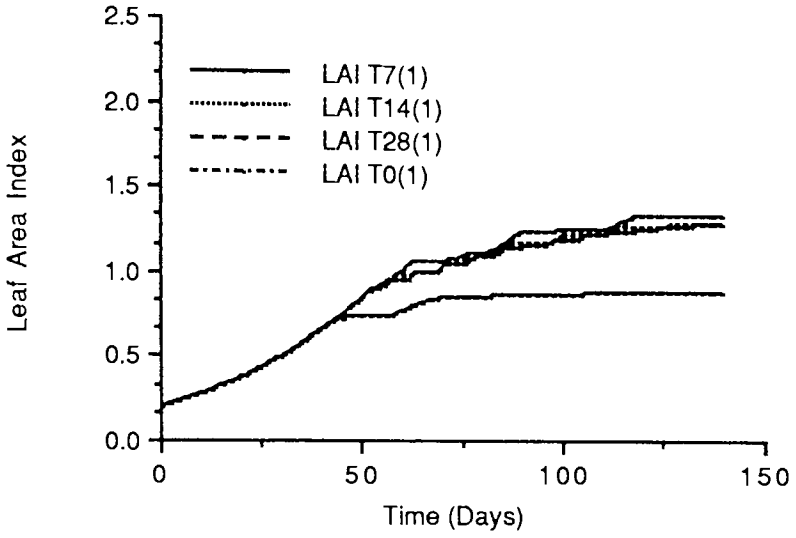

Figure 7.37b Run No. 7

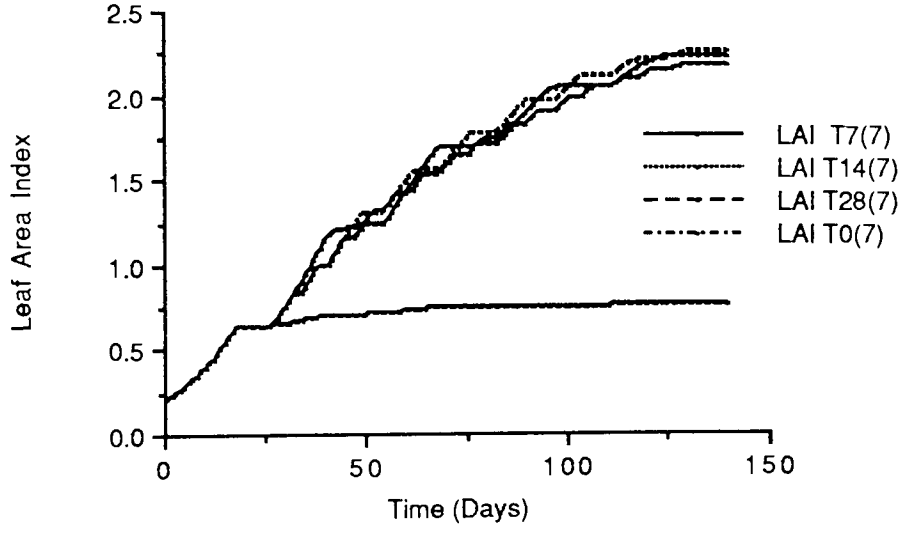

Figure 7.37 The Effect of the Amount of the Evaporative Demand on the Leaf Area Index

a) Plant A, ED 0.2cm/day and Irrigation Application of 75%

b) Plant A, ED 0.5cm/day and Irrigation Application of 50%

However, they also point out that it is hard to separate actual transpiration from actual evaporation in the field. Several other authors have related crop yield to the maximum possible yield by the ratio of actual to potential transpiration (e.g Downey 1972 and Wit 1958).

The above models all assume that a shortage of water at any stage of crop development has an equal effect. Downey (1972) suggested that this is true for alfalfa and other forage crops, but that for non-forage crops water stress at varying stages of growth has different effects. For example, the same amount of water can produce yields between 40% and 95% of the maximum (Downey 1972). Hanks and Hill (1980) further noted that the effect of a water deficit at a growth stage is also dependent upon whether or not deficits have occurred before. Models have been developed which take these points into account by splitting the plant's growth into 4 or 5 stages (see review Hanks and Hill 1980). What is really needed is a dynamic model which follows the growth of the plant through its cycle with the factors of growth and water uptake being interrelated. Section 4.2.4 describes the formation of the model and 7.1-7.3 describe its implementation and initial simulations. The remainder of this section discusses the results and how the plant growth algorithm would fit into a crop yield model.

Table 7.11 shows the sum of the actual and potential water use for 10 simulations. These results show several

points already noted in the literature. Plant A is seen generally to have had a greater plant water use than plant B due to a more extensive rooting system (Hanks and Hill 1980, Aina and Fapohunda 1986). Plant A also responded better to periods of stress, Profitt et al 1985 attributing this to the more extensive area of rooting available. A longer interval between irrigations reduces water uptake when the plant is stressed, this was also noted by Guitjens (1982), it also increases the depth of extraction, as Myers et al (1984) point out. In general rooting depth and density was seen to increase with increased stress. However, this effect was limited as too much stress reduced overall growth despite a higher proportion of synthates being distributed to the roots, as was also noted by Day (1981). The greater the application of irrigation water, the greater the leaf area index and the shallower the rooting system, agreeing with the observations of Myers et al (1984). The results also show that for high demands the greater the amount of water applied, the greater the amount that is utilised by the plant if it is stressed, as would be expected if yield is a function of transpiration. The pattern of water use shown by the plants for treatment T0 illustrates the roots ability to exploit new layers for water. Increased usage was reflected by increased root growth in unexploited layers and decreased usage by the exhaustion of available water supplies and/or the failure of plants to produce suctions to utilise the available water. The sharper increases and declines in actual transpiration from the potential rate

seen with Plant A and higher evaporative demands reflect their more rapid water usage. The greater stresses which occurred between irrigations with the higher evaporative demand rates compared to the lower rates reflect the higher rate of use of the available water. The plant growth model thus behaved like a real plant in these respects.

In developing a crop yield model for forage crops it would appear that total water use would provide a sufficient indicator of yield (Downey 1942). However, it should be noted that the increased water use observed in runs 7-10 would not necessarily produce higher yields than in runs 1-6. This is due to the fact that water use - crop yield relationships are climate, plant and soil type related and the two runs obviously represent different climates. For non-forage crops the dynamic nature of the above model could be used. Figures 7.32 and 7.33 show that although plant A used the most water this was mainly at the start and middle of the simulation. At the end of the simulation the difference in water uptake between plant A and plant B was minimal. In cases where only a small proportion of the irrigation demand was satisfied it was plant B which had the highest water uptake. The reason for this was that plant A had utilised the soil water reserves earlier in the simulation, whereas plant B had used a smaller fraction. In terms of yield, as Wit (1958) points out, it is better to save water for use later, as 90% of grain-size is determined by photosynthesis after flowering. Stress early in

development only affects leaf area and plant size, but these are normally sufficient for later photosynthesis even if the plant is stressed (Downey 1972).

The next step in the development of the model would have been to produce a crop yield algorithm which could utilise the dynamic nature of the model, and then to test and calibrate this in the field. Unfortunately, sufficient time was not available within this project to do this. A point worthy of mention is that the flexibility of the model could be further increased by using factor Cg (equation 4.7) to divide root growth between layers. The value of Cg could be varied to take into account the effect of soil properties such as strength and temperature on root growth.

7.5 SUMMARY

The previous section involved the application of the soil-moisture-plant model (as developed in Sections 3-6) to field data acquired by Hussein (1979), and the simulation of infiltration, evapotranspiration and plant growth processes.

The model was seen to accurately represent the soil moisture deficit data, but analysis of the simulations indicate that there are still problems remaining with respect to the distribution of rainfall throughout the day. It is concluded that the new model performs better than

Hussein's (1979) model and that it is more applicable to other sites. However, further work is required to test the model's performance against data from other locations.

The model was also used to produce data on infiltration and evapotranspiration over time for different soils. Although the results generated were hypothetical the model did allow ideas to be tested that would have been impracticable, or too time consuming, to do in the field. The results produced in these simulations were shown to exhibit similar patterns to those reported in the literature. Finally, the plant growth model developed in Section 4 was tested with a view to including it in a crop yield algorithm. However, this aspect of the model is still only at a very early stage of development.

CHAPTER 8 CONCLUSIONS

The aim of the project,

> "Improve and extend an existing computer-based model of the soil-moisture-plant sub-system, and to increase its flexibility in terms of allowing variation in soil type and the number of layers",

has been achieved. The model includes new algorithms describing macropore flow (Section 3.4), the temporal distribution of daily rainfall (Section 5.2) and plant growth (Section 4.2). The infiltration process has been more realistically represented (Section 3.3) and the suction-conductivity-moisture content relationships have been extended to include a wide range of soils based on particle-size distribution (Section 3.2). Results described in Section 7 shows the model to perform better than Hussein's original model when compared to field data and also shows it to be able to simulate a wider range of processes when used to model hypothetical situations.

The following discussion describes how this aim was achieved with respect to the objectives listed in Section 1.2 using the theories and results presented in Chapters 3 through to 7.

The chapter concludes with recommendations for further work and last of all a brief summary of the project.

8.1 OBJECTIVES

The first objective was

> "the development of new algorithms to simulate the effects of macropore flow, plant growth, hysteresis and lateral flow".

A macropore flow model was developed in Section 3.4. In the model a number of two macropore divisions are defined: 1) permanent; and, 2) temporary. Within each of these divisions a number of classes may be designated based on depth and radius. Water from the ponded store is distributed between the macropores based on the percentage of area they cover. Water then passes from the macropores to the soil based on the occurrence and radius of existing wetting fronts, the saturated conductivity and the suction head across the wetting front. The importance of including such a process is clearly demonstrated in Section 7.3 where it is seen that macropores increase the total amount of infiltration, hence reducing runoff and ponding. They also allow the infiltration rate to remain higher for longer and allow the infiltrating water to penetrate deeper into the profile. The inclusion of the algorithm in the model

simulating the soil moisture deficits at Preston Vale Farm has enabled the model to successfully represent the movement of water in the soil in the autumn of 1977 (Section 7.2).

Walley (1983) stressed the need for future models to include algorithms to simulate crop development especially in terms of leaf and root growth. A model was formulated in Section 4.2.4 which related overall plant growth to actual transpiration this was then distributed between the roots and the leaves based upon the stress the plant was under. The amount of root growth partitioned to each soil layer is then determined by the moisture status of the strata. The model derived, however, is in an early stage of development, having only been initially developed for cereals and grasses. Furthermore the model requires validation from field results, which was beyond the scope of this project. Early work with the model, as presented in Section 7.4, is promising as the plants appear to behave in the same complex manner as would be expected in the field. However, Section 7.1.3 shows that, although the algorithm worked well as a component of the overall soil-moisture-plant model, closer examination showed problems with distributing root density between layers in a realistic manner.

A restricted model as used by Kool and Parker (1987) demonstrated that only the parameter 'a' in Genuchten's equation for the soil moisture characteristic (Section 3.2.1.2) needs to be altered to give both the main drying

and wetting curves of the hysteretic relationship. A study presented in Section 3.2.1.2, where Genuchten's equation is fitted to drying and wetting curves for several soils taken from the literature, shows that the wetting curve value of parameter 'a' is on average twice that of the drying curve for the same soil. This fact enables the wetting relationship to be calculated and used both in the capillary-rise algorithm and also within the infiltration routine. This is justified since the reciprocal of the wetting value of parameter 'a' is used to calculate the head at the wetting front (Section 3.3 and 3.4).

No algorithms were developed to describe lateral flow due to the lack of time.

It can be seen that with the exception of lateral flow, the first objective has been fulfilled. Work within Section 7 on infiltration and plant growth studies has shown that the inclusion of such algorithms produces an improvement on the model developed by Hussein, which was the overall aim of the research.

The second objective was

> "to relate the soil-moisture characteristic curve and conductivity relationships to the soils physical properties".

To achieve this objective several sources of data quoting suction-moisture content relationships for a wide range of soil textures (see Table 3.1 for summary) were consulted. The data thus acquired related moisture contents to specific suctions for a wide variety of soils. Section 3.2.1.2 describes how these data were then utilized to produce regression equations which enabled the soil-moisture characteristic curves to be estimated from easily measured physical properties of the soil (e.g particle-size distribution). These equations were then tested against independant data reported by Hedges (1989) for soils with sand and loamy sand textures. These tests yielded high correlations, thus indicating a good match between the predicted and actual characteristic curves.

To obtain the conductivity relationship it was decided to use Genuchten's (Genuchten 1978) expression which relates conductivity to moisture content (as described in Section 3.2.2). By applying the same parameters as used in the suction equation and matching the curves at saturation, high correlations were obtained between the predicted and the independently observed data provided by Mualem (1976b).

To check the validity of the suction-moisture content and the conductivity-moisture content relationships, they were incorporated into the water flow model (described in Section 3.2.3) and tested against data derived from draining soil columns (Hedges 1989). Again very high correlations

were obtained (Table 3.9) between observed and predicted rates.

In summary it can be seen that the second objective has also been attained. The result being a significant improvement on the original model, which only incorporated three soil types and allowed no variation within these types.

The third objective was

> "to derive an algorithm which treats the process of infiltration in a more realistic manner, this incorporates the need to develop an algorithm for distributing daily rainfall totals into hourly amounts".

Section 3.3.2 describes the new infiltration model which was based on the Mein and Larson (1973) model, but with modifications to allow for layered soils. Section 7.3 shows that qualitatively the infiltration algorithm represents the process well, except in the case when a fine layer overlies a coarse one. The algorithm deals simply with the fine over coarse layer scenario by assuming that infiltration through the coarse layer proceeds at the same rate as the overlying finer layer. This assumption proved adequate within the context of this project (Section 7.3). A beneficial feature of the parameters used in the

infiltration equations is that they can be calculated from the parameters of Genuchten's suction equation.

To produce a more accurate simulation of the infiltration process Walley (1983) suggested the need for timesteps smaller than a day. Since rainfall input to the overall model is as a daily value, it was decided that a means for distributing this throughout the day was required. Section 5.2 describes how this was achieved. Section 7.2 shows in most situations it could be summised that the model worked adequately in terms of the overall soil-moisture-plant model in its simulation of the soil-moisture deficits at Preston Vale Farm. However, problems were encountered in the autumn months when short duration convectional storms were poorly distributed.

In summary, the third objective has been realised and a substantial improvement has been made on Hussein's model which represented infiltration on a daily timestep using a purely empirical formula which took no account of the effects of soil properties.

The fourth objective was

> "to incorporate into the evapotranspiration algorithm the effects of interception and the surface roughness of plants on the potential evaporative demand calculations".

This objective, for the reasons given below, was abandoned at a fairly early stage and has not therefore been realised. However, the original evapotranspiration algorithm developed by Hussein has been updated.

It was concluded, after an extensive literature review, that for the plants being simulated (i.e cereals and grasses) the effects of interception were negligible, both in terms of extra evaporation loss (Gash and Stewart 1977 and Calder 1979) and in terms of redistribution (Reynolds 1967).

The surface roughness of plants has been shown by a number of authors to affect the calculation of the potential evaporative demand (e.g Monteith 1965, Penman 1967 and Thom 1975). It was originally intended to add a correcting factor which would depend on the height of the crop and the plant type. This was not however carried out for the reasons given below:-

a) lack of time;

b) lack of appropriate data;

c) the relatively insignificant magnitude of this effect for the plants being simulated (i.e cereals and grasses) indicated that such a procedure was not required (e.g Rutter 1975 and McNaughton and Jarvis 1983).

The work on these two aspects did, however, draw attention to the fact that the plant water uptake algorithm

developed by Hussein needed updating. This was necessary in order to take account of prevailing theories. Section 4.3.2 describes the new plant water uptake algorithm. The simulation as described in Section 7.2 suggests that the algorithm represents the processes well. It differs from Hussein's algorithm in the following repects:-

a) The exclusion from the equation of the parameter representing soil resistance to water flow. Several authors have shown that soil resistance is not important except at very high suctions: i.e >10 bars (Tinker 1976 and Reid and Hutchison 1986);

b) Instead of soil resistance, a root contact function has been added to describe the soil/root interface at high suctions when the root dries and shrinks away from the peds. Herkelrath (1977a,b) found this to represent the uptake phenomena better than soil resistance;

c) The exclusion of a root search function. Roots do not grow in search of water. They do however grow along increasing water gradients and this has been taken into account in calculating the increase in root density for each layer (Section 4.2.4).

d) Hussein's transmissivity coefficient divided by depth has been replaced by a plant water resistance factor;

e) The radius of the root is no longer input, because its sphere of influence is not required since the concept of soil water resistance is no longer

employed.

The changes described above have generally simplified the model whilst bringing the simulation methodology more in line with the latest theoretical thinking.

Although the original objectives have not been achieved, the work carried out did show the need for the plant water uptake model to be updated, and this has successfully been achieved.

The final stated objective was

> "to allow the model to work on different time intervals depending on the rapidity of the process under consideration".

Section 6.4 and Figure 6.3 show how the timesteps employed within the model can be varied according to the rapidity with which the current soil processes are taking place. For the plant routines a timestep of one day is considered adequate. Therefore it can be seen that the final objective has been realised.

8.2 FURTHER WORK

From the previous discussion and earlier sections it is apparent that there are several areas in which further work

is still required:-

1) The soil-moisture-plant model developed here requires further testing against field data.
2) The plant growth algorithm requires further development, especially with regards to the calculation of root death and the distribution of root growth to each layer. In the latter case, the effects of soil properties on root growth, and hence the root distribution Cg (equation 4.7) could be taken into account. Future work could also extend the plant growth model to other crops and plant types - for instance trees. This would require new routines to be developed to take into account the process of interception and the effect of surface roughness in calculating evapotranspiration.
3) For the plant growth model to be a valid agricultural predictive tool, a relationship between water use and yield needs to be developed. Use could then be made of the model in evaluating the effects of water shortage on yield at different stages of growth.
4) The distribution of measured daily rainfall totals into hourly blocks needs to take into account the different seasonal rainfall patterns (i.e convectional storms in late summer and autumn).
5) More data are required on the nature of macropores together with their distribution and formation,

for input into the simulation of the infiltration process. The soil cracking component of the model also requires further work in order to relate crack size to moisture content and clay content.

8.3 SUMMATION

The overall aim of the project has been achieved and a substantially improved soil-moisture-plant model has been developed and validated against available field data. However, as detailed in Section 8.2, further research and development is still needed in a number of areas. If this is carried out and incorporated into the soil-moisture-plant model developed here, the result will be a comprehensive general purpose model suitable for application to many hydrological and agricultural problems. Such a model could be used on a local farm basis, thus enabling on site monitoring of crops and soil moisture deficits.

REFERENCES

Adrian, D. D., and Franzini, J. B., 1966
Impedance to Infiltration by Pressure Build Up Ahead of the Wetting Front.
Geophys Res v71 pp5857-5862

Ahuja, L. R., Naney, J. W., and Williams, R. D., 1985
Estimating Soil Water Characteristics from Simpler Properties or Limited Data.
Soil Sci Soc Am J v49 pp1100-1105

Aina, P. O., and Fapohunda, H. O., 1986
Root Distribution and Water Uptake Patterns of Maize Cultivars Field Grown Under Differential Irrigation.
Plant Soil v94 pp257-265

Anderson, E. L., 1987
Corn Root Growth and Distribution as Influenced by Tillage and Nitrogen Fertilization.
Agron J v79 pp544-549

Anderson-Taylor, G., and Marshall, C., 1983
Root Tiller Relationships in Spring Barley (Hordeum distichum (L.) Lam.).
Ann Bot v51 pp47-58

Andrew, S. P. S., 1987a
A Mathematical Model of Plant Growth with Particular Reference to Winter Wheat.
Fert Res v11 pp245-266

Andrew, S. P. S., 1987b
A Mathematical Model of Root Exploration and of Grain Fill with Particular Reference to Winter Wheat.
Fert Res v11 pp267-281

Asseed, M., and Swartzendruber, D., 1974
Water Infiltration into Uniform and Stratified Soils 1. Review and Use of Approximate Theory.
Libyan J Agric v3 pp19-26

Asseed, M., and Swartzendruber, D., 1975
Water Infiltration into Uniform and Stratified Soils 2. Experimental Evaluation of an Approximate Theory.
Libyan J Agric v4 pp129-140

Avery, B. W., 1973
Soil Classification in the Soil Survey of England and Wales.
Jnl Soil Sci v24 pp324-338

Aylor, D. E., and Parlange, J. -Y., 1973
Vertical Infiltration into a Layered Soil.
Soil Sci Soc Am Proc v37 pp673-676

Ayra, L. M., and Paris, J. F., 1981
A Physicoempirical Model to Predict the Soil Moisture Characteristic from Particle-Size Distribution and Bulk

Density Data.
Soil Sci Soc Am J v45 pp1023-1030

Ayra, L. M., and Paris, J. F., 1982
Reply to "Comment on a Physicoempirical Model to Predict the Soil Moisture Characteristic from Particle-Size Distribution and Bulk Density Data".
Soil Sci Soc Am J v46 pp1348-1349

Barraclough, P. B., and Leigh, R. A., 1984
The Growth and Activity of Winter Wheat Roots in the Field: The Effect of Sowing Date and Soil Type on Root Growth on High Yielding Crops.
J Agric Sci Camb v103 pp59-74

Bavel, C. H. M. van., 1969
The Three Phase Domain in Hydrology.
Proc Wageningen Sympos pp23-32

Belford, R. K., Klepper, B., and Rickman, R. W., 1987
Studies of Intact Shoot-Root Systems of Field-Grown Winter Wheat 2. Root and Shoot Developmental Patterns as Related to Nitrogen Fertilizer.
Agron J v79 pp310-319

Bell, J. P., 1976
Neutron Probe Practice.
Inst. Hydrol. Rep. No. 19 2nd Ed.

Bell, J. P., 1981
Problems Arising from the Field Capacity Concept in Comparing Measured Soil Moisture Deficits with Morecs Predictions: in The Morecs Discussion Meeting.
Inst Hydrol Rep. No. 78

Beven, K. J., and Clarke, R. T., 1986
On the Variation of Infiltration into a Homogeneous Soil Matrix Containing a Population of Macropores.
Water Res Res v22 pp383-388

Beven, K. J., and Germann, P., 1981
Water Flow in Macropores: 2. A Combined Flow Model.
Jnl Soil Sci v32 pp15-29

Beven, K. J., and Germann, P., 1982
Macropores and Water Flow in Soils.
Water Res Res v18 pp1311-1325

Bielorai, H., Arnon, I., Blum, A., Elkana, Y., and Reiss, A., (1964)
The Effects of Irrigation and Inter-Row Spacing on Grain Sorghum Production.
Israel J. Agric. Res. v14 pp227-236

Binding, D., (1975)
The Neutron Probe
Unpubl. Final Yr Undergrad. Project Univ. Aston UK

Blake, G., Schlichting, E., and Zimmermann, U., 1973
Water Recharge in a Soil with Shrinkage Cracks.

Soil Sci Soc Am Proc v37 pp669-672

Bonnel, M., and Williams, J., 1986
The Two Parameters of the Philip Infiltration Equation: Their Properties and Spatial and Temporal Heterogeneity in a Red Earth of Tropical Semi-Arid Queensland.
Jnl Hydrol v87 pp9-31

Bouma, J., and Anderson, J. L., 1977
Water and Chloride Movement Through Soil Columns Simulating Pedal Soils.
Soil Sci Soc Am J v41 pp766-770

Bouma, J., Belmans, C. F. M., and Dekker, L. W., 1982
Water Infiltration in a Silt Loam Subsoil with Vertical Worm Channels.
Soil Sci Soc Am J v46 pp917-921

Bouma, J., and Dekker, L. W., 1978
A Case Study on Infiltration into Dry Clay Soil 1. Morphological Observations.
Geoderma v20 pp27-40

Boushi, I. M. El., and Davis, S. N., 1969
Water Retention Characteristic of Coarse Rock Particles.
Jnl Hydrol v8 pp431-441

Bouwer, H., 1964
Unsaturated Flow in Groundwater Hydraulics.
Proc ASCE J Hyd Div v90 HY5 pp121-144

Bouwer, H., 1969a
Planning and Interpretating Soil Permeability Measurements.
Proc ASCE J Irrig Drain Div v95 pp391-402

Bouwer, H., 1969b
Infiltration of Water into Non-Uniform Soil.
Proc ASCE J Irrig Drain Div v95 IR4 pp451-462

Brakensiek, D. L., and Rawls, W. J., 1983
Agricultural Management Effects on Soil Water Processes 2. Green and Ampt Parameters for Crusting Soils.
Trans ASAE v26 pp1753-1757

Brooks, R. H., and Corey, A. T., 1964
Hydraulic Properties of Porous Media.
Colombia State Uni Hydrol Pap. No. 2 27pp

Brooks, R. H., and Corey, A. T., 1966
Properties of Porous Media Affecting Fluid Flow.
Proc ASCE J Irrig Drain Div v92 pp61-88

Brownwijk, J. J. B., 1988
Modelling of Water Balance, Cracking and Subsidence of Clay Soils.
Jnl Hydrol v97 pp199-212

Brutsaert, W., 1966

Probability Laws for Pore-Size Distributions.
Soil Sci v101 pp85-92

Bryson, H. R., 1939
The Identification of Soil Animals by Their Burrow Characteristics.
Trans Kansas Acad Sci v42 pp245-254

BS 1377 (1975)
Methods of Test for Soils for Civil Engineering Purposes.
British Standards Institute

Burdine, N. T., 1953
Relative Permeability Calculations from Pore-Size Distribution Data.
Petrol Trans Am Inst Met Engs v198 pp71-78

Calder, I. R., 1979
Do Trees Use More Water Than Grass.
Wat Serv v83 pp11-14

Caloin, M., and Yu, O., 1982
An Extension of the Logistic Model of Plant Growth.
Ann Bot v49 pp599-607

Campbell, S. Y., Molen, W. H. van. der., Rose, C. W., and Parlange, J. -Y., 1985
A New Method for Obtaining a Spatially Averaged Infiltration Rate from Rainfall and Runoff Rates.
Jnl Hydrol v82 pp57-68

Carman, P. C., 1953
Properties of Capillary-Held Liquids.
J Phys Chem v57 pp56-64

Carvallo, H. O., Cassel, D. K., Hammond, J., and Bauer, A., 1976
Spatial Variability of in Situ Unsaturated Hydraulic Conductivity of Maddock Sandy Loam.
Soil Sci v121 pp1-8

Cary, J. W., 1967
Experimental Measurements of Soil Moisture Hysteresis and Entrapped Air.
Soil Sci v104 pp174-180

Cassel, D. K., 1974
In Situ Unsaturated Soil Hydraulic Conductivity for Selected North Dakota Soils.
N Dak Agric Exp Stn Bull No. 494 20pp

Childs, E. C., 1940
The Use of Soil Moisture Characteristic in Soil Studies.
Soil Sci v50 pp239-252

Childs, E. C., and Byobordi, M., 1969
The Vertical Movement of Water in Stratified Porous Material 1. Infiltration.

Water Res Res v5 pp446-459

Childs, E. C., and Collis-George, N., 1950
The Permeability of Porous Materials.
Proc Roy Soc Lond Ser A v201 pp392-404

Colman, E. A., and Bodman, G. B., 1945
Moisture and Energy Conditions During Downward Entry of Water into Moist and Layered Soils.
Soil Sci Soc Am Proc v9 pp3-11

Cornish, P. S., McWilliam, J. R., and So, H. B., 1984a
Root Morphology, Water Uptake, Growth and Survival of Seedlings of Ryegrass and Phalaris.
Aust J Agric Res v35 pp479-492

Cornish, P. S., So, H. B., and McWilliam, J. R., 1984b
Effects of Soil Bulk Density and Water Regimen on Root Growth and Uptake of Phosphorus by Ryegrass.
Aust J Agric Res v35 pp631-644

Cowan, I. R., 1965
Transport of Water in the Soil Plant Atmosphere System.
J Appl Ecol v2 pp221-239

Dane, J. H., and Wierenga, P. J., 1975
Effect of Hysteresis on the Prediction of Infiltration, Redistribution and Drainage of Water in a Layered Soil.
Jnl Hydrol v25 pp229-242

Davies, W. J., and Kozlowski, T. T., 1974
Stomatal Responses of Five Woody Angiosperms to Light Intensity and Humidity.
Can J Bot v52 pp1525-1534

Day, W., 1981
Water Stress and Crop Growth: in Physiological Processes Limiting Plant Productivity (Ed Johnson, C. B.)
Butterworths pp199-215

Deinum, B., 1985
Root Mass of Grass Swards in Different Grazing Systems.
Neth J Agric Sci v33 pp377-384

Dexter, A. R., 1986a
Model Experiments on the Behaviour of Roots at the Interface Between a Tilled Seed Bed and a Compacted Sub-Soil 1. Effects of Seed Bed Aggregate Size and Subsoil Strength.
Plant Soil v95 pp123-133

Dexter, A. R., 1986b
Model Experiments on the Behaviour of Roots at the Interface Between a Tilled Seed Bed and a Compacted Sub-Soil 2. Entry of Pea and Wheat Roots into Sub-Soil Cracks.
Plant Soil v95 pp135-147

Dexter, A. R., 1986c
Model Experiments on the Behaviour of Roots at the Interface Between a Tilled Seed Bed and a Compacted Sub-Soil 3. Entry of Pea and Wheat Roots into Cylindrical Biopores.

Plant Soil v95 pp149-161

Downey, L. A., 1972
Relations for Non-Forage Crops.
J. Irrig. Drain. Div. v98 pp107-115

Edwards, C. A., and Lofty, J. R., 1972
Biology of Earthworms.
Chapman and Hall 283pp

Edwards, C. A., and Lofty, J. R., 1980
Effects of Earthworm Innoculation upon the Root Growth of Direct Drilled Cereals.
J Appl Ecol v17 pp533-543

Edwards, W. M., and Larson, W. E., 1969
Infiltration of Water into Soils as Influenced by Surface Seal Development.
Trans ASAE v12 pp463-465,470

Edwards, W. M., Norton, L. D., and Redmond, C. E., 1988
Characterizing Macropores that Affect Infiltration into Nontilled Soil.
Soil Sci Soc Am J v52 pp483-487

Edwards, W. M., Ploeg, R. R. van der., and Ehlers, W., 1979
A Numerical Study of Non-Capillary-Sized Pores Upon Infiltration.
Soil Sci Soc Am J v43 pp851-856

Edwards, W. M., Ploeg, R. R. van der., and Ehlers, W., 1980
Effect of Hydraulic Properties of Crust and Plow Layer Horizons on Infiltration During Heavy Rainfall.
Zeit Pflan und Boden v143 pp84-92

Ehlers, W., 1975
Observations on Earthworm Channels and Infiltration on Tilled and Untilled Loess Soil.
Soil Sci v119 pp242-249

Ehlers, W., Kopke, U., Hesse, F., and Bohm, W., 1983
Penetration Resistance and Root Growth of Oats in Tilled and Untilled Loess Soil.
Soil Till Res v3 pp261-275

Ennik, G. C., and Hofman, T. B., 1983
Variation in the Root Mass of Ryegrass Types and its Ecological Consequences.
Neth J Agric Sci v31 pp325-334

Evans, D. A. (1986)
Development of a Comprehensive Conceptual Model of the Soil-Moisture-Plant Subsystem.
Unpubl. First Yr Postgrad Rep. Univ. Aston UK

Feddes, R. A., 1978
Water Uptake by Plants: in Soil Water and Plant Aspects of the Unsaturated Zone Controlling Groundwater Recharge
Am Geophys Un Smpos, Miami Beach, Florida. pp1-16

Feddes, R. A., Kowalik, P., Neuman, S. P., and Bresler, E., 1976
Finite Difference and Finite Element Simulation of Field Water Uptake by Plants.
Hydrol Sci Bull v21 pp81-98

Feddes, R. A., Kowalik, P. J., and Zaradny, H., 1978
Simulation of Field Water Use and Crop Yield.
Pudoc 189pp

Fetcher, N., 1976
Patterns of Leaf Resistance to Lodge Pole Pine Transpiration in Wyoming.
Ecology v57 pp339-345

Flerchinger, G. N., Watts, F. J., and Bloomsburg, G. L., 1988
Explicit Solution to Green-Ampt Equation for Nonuniform Soils.
Proc ASCE J Irrig Drain Div v114 pp561-565

Fok, Y. -S., 1970
One Dimensional Infiltration into layered Soils.
Proc ASCE J Irrig Drain Div v96 pp121-129

Foster, A. G., 1932
The Sorption of Condensible Vapours by Porous Solids Part 1. The Applicability of the Capillary Theory.
Trans Far Soc v28 pp645-657

Foster, A. G., 1951
Sorption Hysteresis 1. Some Factors Determining the Size of the Hysteresis Loop.
J Phys Chem v55 pp638-643

Freeze, R. A., 1969
The Mechanism of Natural Groundwater Recharge and Discharge 1. One Dimensional Vertical Unsteady, Unsaturated Flow Above a Recharging or Discharging Groundwater Flow System.
Water Res Res v5 pp153-171

Gajri, P. R., and Prihar, S. S., 1985
Rooting Water Use and Yield Relations in Wheat on Loamy Sand and Sandy Loam Soils.
Field Crops Res v12 pp115-132

Gardner, C. M. K., 1981
Preliminary Comparisons Between MORECS and Measured Soil Moisture Deficits:in The MORECS Discussion Meeting.
Inst Hydrol Rep. No. 78

Gardner, W. R., 1958
Some Steady State Solutions of the Unsaturated Moisture Flow Equation with Application to Evaporation from a Water Table.
Soil Sci v85 pp228-232

Gardner, W. R., 1959
Dynamic Aspects of Water Availability to Plants.

Soil Sci v89 pp63-73

Gardner, W. R., 1962
Relation of Root Distribution to Water Uptake and Availability.
Agron J v54 pp41-45

Gardner, W. R., 1967a
Development of Modern Infiltration Theory and Application in Hydrology.
Trans ASAE v10 pp379-381,390

Gardner, W. R., 1967b
Present Knowledge of the Interrelationships Between Soil Moisture, Irrigation, Drainage and Water Use Efficiency: in Symposium on "Atomic Energy in Food and Agriculture", Vienna.
IAEA pp77-82

Gash, J. H. C., and Stewart, J. B., 1977
The Evaporation from Thetford Forest During 1975.
Jnl Hydrol v35 pp385-396

Genuchten, R. van., 1978
Calculating the Unsaturated Hydraulic Conductivity with a New Closed Form Analytical Model.
Res Rep 78-WR-08, Dept Civ Eng, Princeton Univ New Jersey

Genuchten, M th van., 1980
A Closed Form Equation for Predicting the Hydraulic Conductivity of Unsaturated Soils.
Soil Sci Soc Am J v44 pp892-898

Genuchten, M. th van., and Nielsen, D. R., 1985
On Describing and Predicting the Hydraulic Properties of Unsaturated Soils.
Annales Geophysica v3 pp615-627

Gifford, G. F., 1976
Applicability of some Infiltration Formulae to Rangeland Infiltrometer Data.
Jnl Hydrol v28 pp1-11

Gilman, K., and Newson, M., 1980
Soil Pipes and Pipeflow- A Hydrological Study in Upland Wales.
Res Monogr No. 1 Br Geomorph Gr, Geobooks, Norwich. 111pp

Glass, R. J., Parlange, J. -Y., and Steenhuis, T. S., 1989a
Wetting Front Instability 1. Theoretical Discussion and Dimensional Analysis.
Wat Res Res v25 pp1187-1194

Glass, R. J., Steenhuis, T. S., and Parlange, J. -Y., 1989b
Wetting Front Instability 2. Experimental Determination of Relationships Between System Parameters and Two-Dimensional Unstable Flow Field Behaviour in Initially Dry Porous Media.
Wat Res Res v25 pp1195-1207

Gorny, A. G., and Patyna, H., 1983
The Development of the Root System in Seven Spring Barley Varieties Under High and Low Soil Irrigations.
Zeit Acker Und Pflanz v153 pp264-273

Gradwell, M. W., 1974
Measured and Predicted Hydraulic Conductivities for some New Zealand Subsoils at Water Contents near Field Capacity.
N Z J Sci v17 pp463-473

Gray, D. M., and Norum, D. I., 1968
Effect of Soil Moisture on Infiltration as Related to Runoff and Recharge.
Dept En Mines Res, Canada. Proc Hydrol Sympos No. 6 pp133-153

Green, R. D., and Askew, G. P., 1965
Observations on the Biological Development of Macropores in Soils of Romney Marsh.
J Soil Sci v16 pp342-349

Green, R. E., and Corey, J. C., 1971
Calculation of Hydraulic Conductivity: A Further Evaluation of some Predictive Methods.
Soil Sci Soc Am Proc v35 pp3-8

Green, W. H., and Ampt, G. A., 1911
Studies in Soil Physics 1. The Flow of Air and Water Through Soils.
J Agric Sci v4 pp1-24

Greene-Kelly, R., 1974
Shrinkage of Clay Soils: A Statistical Correlation with other Soil Properties.
Geoderma v11 pp243-257

Greenwood, D. J., (1969)
Effect of Oxygen Distribution in the Soil on Plant Growth: in Root Growth (Ed Whittington, W. J.)
Butterworths pp202-221

Gregory, P. J., McGowan, M., Biscoe, P. V., and Hunter, B., 1978
Water Relations of Winter Wheat 1. Growth of the Root System.
J Agric Sci Camb v91 pp91-102

Guitjens, J. C., 1982
Models of Alfalfa Yield and Evapotranspiration.
J. Irrig. Drain. Div. v95 pp91-104

Gupta, S. C., and Larson, W. E., 1979b
Estimating Soil Water Retention Characteristics from Particle-Size Distribution, Organic Matter and Bulk Density.
Water Res Res v15 pp1633-1635

Haan, C. T., Johnson, H. P., and Brakensiek, D. L., 1982
Hydrologic Modelling of Small Watersheds.
ASAE 533pp

Haines, W. B., 1930
Studies in the Physical Properties of Soils 5. The Hysteresis Effect in Capillary Properties, and the Modes of Moisture Distribution Associated Therewith.
J Agric Sci v20 pp97-116

Hall, W. A., 1969
The Computer and Hydrology: in The Progress of Hydrology.
Proc 1st Int Sem Hydrol Profs. July 13-25th v1 pp226-232

Hall, M. A., 1976
Plant Structure, Function and Adaptation
Macmillan

Hall, A. E., and Kaufmann, M. R., 1975
Stomatal Response to Environment with *Sesamum indicum* L.
Plant Physiol v55 pp455-459

Hall, D. G. M., Reeve, M. J., Thomasson, A. J., and Wright, V. F., 1977
Water Retention, Porosity and Density of Field Soils.
Tech. Mono. No. 9 Soil Survey, Harpenden, UK.

Hamblin, A, P., and Hamblin, J., 1985
Root Characteristics of Some Temperate Legume Species and Varieties on Deep Free Draining Entisols.
Aust J Agric Res v36 pp63-72

Hamblin, A. P, and Tennant, D., 1987
Root Length Density and Water Uptake in Cereals and Grain Legumes: How Well are They Correlated.
Aust J Agric Res v38 pp513-527

Hanks, R. J., and Hill, R. W., 1980
Modelling Crop Responses to Irrigation
Int. Irrig. Inf. Centre 66pp

Hansen, G. J., 1979
Simulation of Water State and Flow in the Soil-Plant-Atmosphere System by a Model Named HEJMDAL: in Comparison of Forest Water and Energy Exchange Models (Ed. Halldin, S.)
Int. Soc. Ecol. Mod. Copenhagen pp117-131

Haverkamp, R., and Parlange, J. Y., 1982
Comments on "A Physicoempirical Model to Predict the Soil Moisture Characteristic from Particle-Size Distribution and Bulk Density Data".
Soil Sci Soc Am J v46 pp1348

Haverkamp, R., and Parlange, J. Y., 1986
Predicting the Water Retention Curve from Particle-Size Distribution: 1. Sandy Soils Without Organic Matter.
Soil Sci v142 pp325-339

Hedges, P. D., 1989
The Impact on Agriculture of the Drawdown of Shallow Watertables.
PhD Thesis, Univ Aston UK

Herkelrath, W. N., Miller, E. E., and Gardner, W. R., 1977a
Water Uptake by Plants: 1. Divided Root Experiments.
Soil Sci Soc Am J v41 pp1033-1038

Herkelrath, W. N., Miller, E. E., and Gardner, W. R., 1977b
Water Uptake by Plants: 2. The Root Contact Model.
Soil Sci Soc Am J v41 pp1039-1043

Hettiaratchi, D. R. P., and Ferguson, C. A., 1973
Stress- Deformation Behaviour of Soil in Root Growth Mechanics
J Agric Eng Res v18 pp309-320

Hillel, D., 1971
Soil and Water.
Academic Press 288pp

Hillel, D., 1987
Unstable Flow in Layered Soils: A Review.
Hydrological Processes v1 pp143-147

Hillel, D., and Guron, Y., 1973
Relation Between Evapotranspiration Rate and Maize Yield.
Water Res Res v9 pp743-748

Hillel, D., Talpaz, H., and Keulen, H. van., 1976
A Macroscopic Scale Model of Water Uptake by a Non-Uniform Root System and of Water and Salt Movement in the Soil Profile.
Soil Sci v121 pp242-255

Hole, F. D., 1981
Effects of Animals on Soils
Geoderma v25 pp75-112

Holtan, H. N., 1961
A Concept for Infiltration Estimates in Watershed Engineering.
Agric Res Serv USDA ARS pp41-51

Holtan, H. N., England, C. B., and Shanholtz, V. O., 1967
Concepts in Hydrologic Soil Grouping.
Trans ASAE v10 pp407-410

Hoogenboom, G., Huck, M. G., and Peterson, C. M., 1986
Measured and Simulated Drought Stress Effects on Daily Shoot and Root Growth Rates of Soybean.
Neth J Agric Sci v34 pp497-500

Hoogenboom, G., Huck,M. G., and Peterson, C. M., 1987
Root Growth Rate of Soybean as Affected by Drought Stress.
Agron J v79 pp607-614

Hoogmoed, W. B., and Bouma, J., 1980
A Simulation Model for Predicting Infiltration into Cracked Clay Soil.
Soil Sci Soc Am J v44 pp458-461

Hopmans, J. W., and Dane, J. H., 1986
Combined Effects of Hysteresis and Temperature on Soil-Water Movement.
Jnl Hydrol v83 pp161-171

Horton, R. E., 1933
The Role of Infiltration in the Hydrologic Cycle.
Trans Am Geophys Un v14 pp446-460

Horton, R. E., 1939
Analysis of Runoff- Plot Experiments with Varying Infiltration Capacity.
Trans Am Geophys Un v20 pp693-694

Horton, R. E., 1940
An Approach Toward a Physical Interpretation of Infiltration Capacity.
Soil Sci Soc Am Proc v5 pp399-417

Huck, M. G., and Hillel, D., 1983
A Model of Root Growth and Water Uptake Accounting for Photosynthesis, Respiration, Transpiration and Soil Hydraulics.
Adv Irrig v2 pp273-327

Huck, M. G., Peterson, C. M., Hoogenboom, G., and Busch, C. D., 1986
Distribution of Dry Matter Between Shoots and Roots of Irrigated and Non-Irrigated Determinate Soybeans.
Agron J v78 pp807-813

Hufford, T. L., 1978
Botany: Basic Concepts in Plant Biology.
Harper and Row 535pp

Hussein, D. E. D. A., 1979
Soil Moisture Monitoring with Special Reference to Irrigation Management.
PhD Thesis Aston University, Birmingham. 430pp

Idso, S. B., Anderson, M. G., and Kimball, B. A., 1985
Atmospheric CO_2 Enrichment of Water Hyacinths: Effects on Transpiration and Water Use Efficiency.
Water Res Res v21 pp1787-1790

Idso, S. B., Clawson, K. L., and Anderson, M. G., 1986
Foliage Temperature: Effects of Environmental Factors with Implications for Plant Water Stress Assessment and their CO_2/Climate Connection.
Water Res Res v22 pp1702-1716

Institute of Hydrology 1981
Morecs Discussion Meeting.
Inst. Hydrol. Rep. No. 78 55pp

Jackson, I. J., 1977
Climate, Water and Agriculture in the Tropics.
Longman 248pp

Jackson, R. D., Reginato, R. J., and Bavel, C. H. M. van.,

1965
Comparison of Measured and Calculated Hydraulic Conductivities of Unsaturated Soils.
Water Res Res v1 pp375-380

Jamison, V. C., and Kroth, E. M., 1958
Available Moisture Storage Capacity in Relation to Textural Composition and Organic Matter Content of Several Missouri Soils.
Soil Sci Soc Am Proc v22 pp189-192

Jarvis, N. J., and Leeds-Harrison, P. B., 1987a
Modelling Water Movement in Drained Clay Soil 1. Description of the Model, Sample Output and Sensitivity Analysis.
J Soil Sci v38 pp487-498

Jarvis, N. J., and Leeds-Harrison, P. B., 1987b
Modelling Water Movement in Drained Clay Soil 2. Application of the Model in Evesham Series Clay Soil.
J Soil Sci v38 pp499-509

Jayawardena, A. W., and Kaluarachiki, J. J., 1986
Infiltration into Decomposed Granite Soils: Numerical Modelling, Application and some Laboratory Observations.
Jnl Hydrol v84 pp231-260

Jaynes, D. B., 1984
Comparison of Soil Water Hysteresis Models.
Jnl Hydrol v75 pp287-299

Jaynes, D. B., and Tyler, E. J., 1984
Using Soil Physical Properties to Estimate Hydraulic Conductivity.
Soil Sci v138 pp298-305

Jensen, K. H., 1981
Application of Soil Water Flow Theory in Field Simulation.
Nord Hydrol v12 pp167-184

Jensen, K. H., 1983
Simulation of Water Flow in the Unsaturated Zone, Including the Root Zone.
Inst Hydrodyn Hyd Eng. Eng Pap. No. 33 259pp

Johnson, I. R., Ameziane, T. E., and Thornley, J. H. M., 1983
A Model of Grass Growth.
Ann Bot v51 pp599-609

Johnson, I. R., and Thornley, J. H. M., 1987
A Model of Shoot:Root Partitioning with Optimal Growth.
Ann Bot v60 pp133-142

Jong, R. de., and Zentner, R. P., 1985
Assessment of the SPAW Model for Semi-Arid Growing Conditions with Minimal Local Calibration.
Agric Wat Man v10 pp31-46

Joost, R. E., and Hoveland, C. S., 1986
Root Development of *Sericea lespedeza* and Alfalfa in Acid Soils.
Agron J v78 pp711-714

Kaufmann, M. R., 1976
Stomatal Response of Englemann Spruce to Humidity, Light and Water Stress.
Plant Physiol v57 pp898-901

Kivisaari, S., 1971
Influence of Texture on Some Soil Moisture Constants.
Acta Agric Fenica v123 pp217-222

Klepper, B., Taylor, H. M., Huck, M. G., and Fiscus, E. L., 1973
Water Relations and Growth of Cotton in Drying Soils.
Agron J v65 pp307-310

Klute, A., 1969
The Movement of Water in Unsaturated Soils.
Prog Hydrol, Univ Illinois. v2 pp821-888

Kool, J. B., and Parker, J. C., 1987
Development and Evaluation of Closed-Form Expressions for Hysteretic Soil Hydraulic Properties.
Water Res Res v23 pp105-114

Kvifte, G., 1987
Crop Production and Growth Model for Cereals, Rape and Grass at Aaa Norway.
Acta Agric Scand v37 pp137-158

Laat, P. J. M. de., 1976
A Pseudo-Steady State Solution of Water Movement in the Unsaturated Zone of the Soil.
Jnl Hydrol v30 pp19-27

Laliberte, G. E., Corey, A. T., and Brooks, R. H., 1966
Properties of Unsaturated Porous Media.
Colarado State Univ Hydrol Pap. No. 17 40pp

Lange, O. L., and Losch, R., 1971
Responses of Stomata to Changes in Humidity.
Planta v100 pp76-86

Lascano, R. J., and Bavel, C. H. M. van., 1984
Root Water Uptake and Soil Water Distribution: Test of an Availability Concept.
Soil Sci Soc Am J v48 pp233-237

Linsley, R. K., Kohler, M. A., and Pulhus, J. L. H., 1949
Applied Hydrology.
Mc Graw-Hill

Logsdon, S. D., Parker, J. C., and Reneau, R. B., 1987
Root Growth as Influenced by Aggregate Size.
Plant Soil v99 pp267-275

Long, F. L., Perkins, H. F., Carreker, J. R., and Daniels,

J. M., 1969
Morphological Chemical and Physical Characteristics of Eighteen Representative Soils of the Atlantic Coast Flatwoods.
Univ Georgia Res Bull No. 59 74pp

Lund, Z. F., 1959
Available Water-Holding Capacity of Alluvial Soils in Lousiana.
Soil Sci Soc Am Proc v23 pp1-3

Madsen, H. B., 1985
Distribution of Spring Barley Roots in Danish Soils of Different Texture and Under Different Climatic Conditions.
Plant and Soil v88 pp31-43

Maillette, L., 1986
Canopy Development, Leaf Demography and Growth Dynamics of Wheat and Three Weed Species Growing in Pure and Mixed Stands.
J Appl Ecol v23 pp929-944

Makkink, G. F., and Heemst, H. D. J. van., 1956
The Actual Evapotranspiration as a Function of the Potential Evapotranspiration and the Soil Moisture Tension.
Neth J Agric Sci v4 pp67-72

Marshall, T. J., 1958
A Relation Between Permeability and Size Distribution of Pores.
J Soil Sci v9 pp1-8

Marshall, T. J., and Holmes, J. W., (1979)
Soil Physics
Cambridge University Press 345pp

McCormack, D. E., and Wilding, L. P., 1975
Soil Properties Influencing Swelling in Canfield and Geeburg Soils.
Soil Sci Soc Am Proc v39 pp496-502

McIntyre, D. S., 1958
Permeability Measurements of Soil Crusts Formed by Raindrop Impact.
Soil Sci v85 pp185-189

McNaughton, K. G., and Jarvis, P. G., 1983
Predicting Effects of Vegetation Changes on Transpiration and Evaporation: in Water Deficits and Plant Growth v7 Additional Woody Crop Plants (Ed Kozlowski, T. T.).
Academic Press pp1-47

McNeil, K. A., Kelly, F. J., and McNeil, J. T., 1975
Testing Research Hypothesis Using Multiple Linear Regression.
Southern Illinois University Press 587pp

Mein, R. G., and Larson, C. L., 1973
Modelling Infiltration During a Steady Rain.

Water Res Res v2 pp384-394

Meisner, L. P., and Organik, E. I., 1980
Fortran 77: Featuring Structured Programming
Addison-Wesely 500pp

Millington, R. J., and Quirk, J. P., 1959
Permeability of Porous Media.
Nature v183 pp387-388

Millington, R. J., and Quirk, J. P., 1960
Transport in Porous Media.
Trans Inter Cong Soil Sci 7th, Madison pp97-106

Miranda, R. A. C. de., and Butler, D. R., 1986
Interception Of Rainfall in a Hedgerow Apple Orchard.
Jnl Hydrol v87 pp245-253

Molen, W. H. van der., 1986
A Predictor- Corrector Solution of the Modified Horton Equation.
Jnl Hydrol v89 pp165-167

Molyneux, D. E., and Davies, W. J., 1983
Rooting Pattern and Water Relations of Three Pasture Grasses Growing in Drying Soil.
Oecologia v58 pp220-224

Monteith, J. L., 1965
Evaporation and Environment.
Proc Sympos Exp Biol v19 pp205-234

Monteith, J. L., 1981
MORECS: An Agricultural Perspective: in Morecs Discussion Meeting (Inst Hydrol)
Inst Hydrol Rep No. 78 pp36-38

Moorby, H., and Nye, P. H., 1984
The Effect of Temperature Variation Over the Root System on Root Extension and Phosphate Uptake by Rape.
Plant Soil v78 pp283-293

Moore, I. D., 1981a
Infiltration Equations Modified for Surface Effects.
Proc ASCE J Irrig Drain Div v107 pp71-86

Moore, I. D., 1981b
Effect of Surface Sealing on Infiltration.
Trans ASAE v24 pp1546-1553,1561

Morin, J., and Benyamini, Y., 1977
Rainfall Infiltration into Bare Soils.
Wat Res Res v13 pp813-817

Mualem, Y., 1976a
A New Model for Predicting the Hydraulic Conductivity of Unsaturated Porous Media.
Water Res Res v12 pp513-522

Mualem, Y., 1976b

A Catalogue of the Hydraulic Properties of Unsaturated Soils.
Technion Israel Inst Tech 118pp

Myers, R. J. K., Foale, M. A., and Done, A. A., 1984
Responses of Grain Sorghum to Varying Irrigation Frequency in the Ord Irrigation Area 2. Evapotranspiration, Water Use Efficiency and Root Distribution of Different Cultivars.
Aust J Agric Res v35 pp31-42

Nakano, M., Amemiya, Y., and Fujii, K., 1986
Saturated and Unsaturated Hydraulic Conductivities of Swelling Clays.
Soil Sci v141 pp1-6

Neuman, S. P., 1976
Wetting Front Pressure Head in the Infiltration Model of Green and Ampt.
Water Res Res v12 pp564-566

Newman, E. I., 1976
Water Relations: in Plant Structure, Function and Adaptation (Ed. Hall, M. A.)
Macmillan pp157-196

Nielsen, D. R., Biggar, J. W., and Erh, K. T., 1973
Spatial Variability of Field-Measured Soil-Water Properties.
Hilgardia v42 pp215-259

Nielsen, D. R., Genuchten, M. th van., and Biggar, J. W., 1986
Water Flow and Solute Transport Processes in the Unsaturated Zone: in Trends in Hydrology (Special Supplement).
Water Res Res v22 89S-108S

Noordwijk, M. van., Floris, J., and Jager, A. de., 1985
Sampling Schemes for Estimating Root Density Distribution in Cropped Fields.
Neth J Agric Sci v33 pp241-262

Nye, P. H., and Tinker, P. B., 1977
Solute Movement in the Soil-Root System.
Blackwell 342pp

Olson, K. R., 1985
Characterization of Pore-Size Distributions Within Soils by Mercury Intrusion and Water Release Methods.
Soil Sci v139 pp400-404

Omoti, V., and Wild, A., 1979
Use of Fluorescent Dyes to Mark the Pathways of Solute Movement Through Soils Under Leaching Conditions 2. Field Experiments.
Soil Sci v128 pp98-104

Onishchenko, V. G., 1986
Hysteretic Relations Between Soil Moisture Tension and

the Moisture Content and their Generalized Description.
Sov Soil Sci v18 pp107-114

Pearson, C. J., and Jacobs, B. C., 1985
Root Distribution in Space and Time in *Trifolium subterraneum*.
Aust J Agric Res v36 pp601-614

Pearson, R. W., Ratliff, L. F., and Taylor, H. M., 1970
Effect of Soil Temperature, Strength and pH on Cotton Seedling Root Elongation.
Agron J pp243-246

Penman, H. L., 1967
Evaporation from Forests: in Forest Hydrology (Eds Sopper, W. E., and Lull, H. W.).
Pergamon pp373-380

Petersen, G. W., Cunningham, R. L., and Matelski, R. P., 1968a
Moisture Characteristics of Pennsylvania Soils 1. Moisture Retention as Related to Texture.
Soil Sci Soc Am Proc v32 pp271-275

Petersen, G. W., Cunningham, R. L., and Matelski, R. P., 1968b
Moisture Characteristics of Pennsylvania Soils 2. Soil Factors Affecting Moisture Retention Within a Textural Class.
Soil Sci Soc Am Proc v32 pp866-870

Philip, J. R., 1957a
The Theory of Infiltration 1. The Infiltration Equation and its Solutions.
Soil Sci v83 pp345-357

Philip, J. R., 1957b
The Theory of Infiltration 2. The Profile at Infinity.
Soil Sci v83 pp435-448

Philip, J. R., 1957c
The Theory of Infiltration 3. Moisture Profiles and Relation to Experiment.
Soil Sci v84 pp163-178

Philip, J. R., 1957d
The Theory of Infiltration 4. Sorptivity and Algebraic Infiltration Equations.
Soil Sci v84 pp257-264

Philip, J. R., 1957e
The Theory of Infiltration 5. The Influence of Initial Moisture Content.
Soil Sci v84 pp329-339

Philip, J. R., 1958a
The Theory of Infiltration 6. Effect of Water Depth over Soil.
Soil Sci v85 pp278-286

Philip, J. R., 1958b
The Theory of Infiltration 7.
Soil Sci v85 pp333-337

Proffitt, A. P. B., Berliner, P. R., and Oosterhuis, D. M., 1985
A Comparative Study of Root Distribution and Water Extraction Efficiency by Wheat Grown Under High- and Low-Frequency Irrigation.
Agron J v77 pp655-662

Protopas, A. L., and Bras, R. L., 1988
State Space Dynamic Hydrological Modelling of Soil Crop Climate Interactions.
Water Res Res v24 pp1765-1779

Raudkivi, A. J., 1979
Hydrology: An Advanced Introduction to Hydrological Processes and Modelling.
Pergamon Press

Rawls, W. J., and Brakensiek, D. L., 1982
Estimating Soil Water Retention from Soil Properties.
Trans ASCE J Irrig Drain Div v108 pp166-171

Rawls, W. J., Brakensiek, D.L., and Saxton, K. E., 1982
Estimation of Soil Water Properties.
Trans ASAE v25 pp1316-1328

Rawls, W. J., Brakensiek, D. L., and Soni, B., 1983
Agricultural Management Effects on Soil Water Processes 1. Soil Water Retention and Green and Ampt Infiltration Parameters.
Trans ASAE v26 pp1747-1752

Rawson, H. M., Begg, J. E., and Woodward, R. G., 1977
The Effect of Atmospheric Humidity on Photosynthesis, Transpiration and Water Use Efficiency of Leaves of Several Plants.
Planta v134 pp5-10

Reeve, M. J., and Hall, D. G. M., 1978
Shrinkage in Clayey Subsoils of Contrasting Structure.
J Soil Sci v29 pp315-323

Reeve, M. J., Hall, D. G. M., and Bullock, P., 1980
The Effects of Soil Composition and Environmental Factors on the Shrinkage of Some Clayey British Soils.
J Soil Sci v31 pp429-442

Reid, J. B., and Hutchison, B., 1986
Soil and Plant Resistances to Water Uptake by *Vicia faba* L.
Plant Soil v92 pp431-441

Reynolds, E. R. C., 1967
The Hydrological Cycle as Affected by Vegetation Differences.
J Inst Wat Eng v21 pp322-330

Richards, L. A., 1931
Capillary Conduction of Liquids Through Porous Mediums.
Physics v1 pp318-333

Rijtema, P. E., 1965
An Analysis of Actual Evapotranspiration.
Cent Agric Publ, Wageningen. 107pp

Ritchie, J. T., 1972
Model for Predicting Evaporation from a Row Crop with Incomplete Cover.
Water Res Res v8 pp1204-1213

Ritchie, J. T., and Adams, J. E., 1974
Field Measurement of Evaporation from Soil Shrinkage Cracks.
Soil Sci Soc Am Proc v38 pp131-134

Robinson, D., and Rorison, I. H., 1985
Quantitative Analysis of the Relationships Between Root Distribution and Nitrogen Uptake from Soil by Two Grass Species.
J Soil Sci v36 pp71-85

Rogowski, A. S., 1971
Watershed Physics: Model of Soil Moisture Characteristic.
Water Res Res v7 pp1575-1582

Russel, R. S., 1977
Plant Root Systems: Their Function and Interaction with the Soil.
McGraw-Hill

Rutter, A. J., 1975
The Hydrological Cycle in Vegetation: in Vegetation and the Atmosphere (Ed Monteith, J. L.).
Academic Press v1 pp111-154

Saxton, K. E., 1983
Soil Water Hydrology: Simulation for Water Balance Computations: in New Approaches in Water Balance Computations.
Proc Hamburg Workshop IAHS Publ. No. 148 pp1-13

Saxton, K. E., Johnson, H. P., and Shaw, R. H., 1974
Modelling Evapotranspiration and Soil Moisture.
Trans ASAE v17 pp673-677

Schafer, W. M., and Singer, M. J., 1976
Influences of Physical and Mineralogical Properties on Swelling of Soils in Yolo County.
Soil Sci Soc Am J v40 pp557-562

Schuh, W. M., and Sweeney, M. D., 1986
Particle-Size Distribution Method for Estimating Unsaturated Hydraulic Conductivity of Sandy Soils.
Soil Sci v142 pp247-254

Schulze, E. -D., and Kuppers, M., 1979

Short Term and Long Term Effects of Plant Water Deficits on Stomatal Response to Humidity in *Corylus avellana* L.
Planta v146 pp319-326

Schulze, E. -D., Lange, O. L., Buschbom, U., Kappen, L., and Evenari, M., 1972
Stomatal Responses to Changes in Humidity in Plants Growing in the Desert.
Planta v108 pp259-270

Schumm, S. A., and Lusby, G. C., 1963
Seasonal Variation of Infiltration Capacity and Runoff on Hillslopes in Western Colarado.
J Geophys Res v68 pp3655-3666

Scott, G. J. T., Webster, R., and Nortcliff, S., 1986
An Analysis of Crack Pattern in Clay Soil: Its Density and Orientation.
J Soil Sci v37 pp653-668

Scotter, D. R., 1978
Preferential Solute Movement Through Larger Soil Voids 1. Some Computations Using Simple Theory.
Aust J Soil Res v16 pp257-267

Shalhevet, J., Mantell, A., Bielorai, H., and Shimshi, D., 1976
Irrigation of Field and Orchard Crops Under Semi-Arid Conditions.
International Irrig. Inf. Centre, Israel. 124pp

Sheriff, D. W., 1977
The Effect of Humidity on Water Uptake by, and Viscous Flow Resistance of, Excised Leaves of a Number of Species: Physiological and Anatomical Observations.
J Exp Bot v28 pp1399-1407

Skaggs, R. W., Huggins, L. E., Monke, E. J., and Foster, G. R., 1969
Experimental Evaluation of Infiltration Equations.
Trans ASAE v12 pp822-828

Smettem, K. R. J., 1986
Analysis of Water Flow from Cylindrical Macropores.
Soil Sci Soc Am J v50 pp1139-1142

Soon, Y. K., 1988
Root Distribution of, and Water Uptake by, Field Grown Barley in Black Solod.
Can J Soil Sci v68 pp425-432

Specht, R. L., 1957
Dark Island Heath (Ninety Mile Plain, South Australia) 4. Soil Moisture Patterns Produced by Rainfall Interception and Stemflow.
Aust J Bot v5 pp137-150

Staple, W. J., 1965
Evaluation of Flow Parameters.

Dept En Mine Res, Can. Proc Hydrol Symp No. 6 pp81-96

Stern, P. H., 1979
Small Scale Irrigation: A Manual of Low-Cost Water Technology.
Inter Tech Publ & Inter Irrig Inf Centre 152pp

Stewart, J. I., Misra, R. D., and Pruitt, W. O., 1975
Irrigation of Corn and Grain Sorghum with a Deficient Water Supply.
Trans ASCE v18 pp270-280

Stewart, J. I., and Hagan, R. M., 1969
Predicting Effects of Water Storage on Crop Yield.
J. Irrig. Drain. Div. v95 pp91-104

Stroosnijder, L., Keulen, H. van., and Vachaud, G., 1972
Water Movement in Layered Soils 2. Experimental Confirmation of a Simulation Model.
Neth J Agric Sci v20 pp67-72

Swatzendruber, D., 1968
The Applicability of Darcy's Law.
Soil Sci Soc Am Proc v32 pp11-18

Szeicz, G., Bavel, C. H. M. van., and Takami, S., 1973
Stomatal Factor in the Water Use and Dry Matter Production by Sorghum.
Agri Meteorol v12 pp361-389

Tackett, J. L., and Pearson, R. W., 1965
Some Characteristics of Soil Crusts Formed by Simulated Rainfall.
Soil Sci v99 pp407-413

Talsma, T., 1970
Hysteresis in Two Sands and the Independant Domain Model.
Water Res Res v6 pp964-970

Talsma, T., 1985
Prediction of Hydraulic Conductivity from Soil Water Retention Data.
Soil Sci v140 pp184-188

Tan, C. S., and Fulton, J. M., 1985
Water Uptake and Root Distribution by Corn and Tomato at Different Depths.
Hortscience v20 pp686-688

Tarchitzky, J., Banin, A., Morin, J., and Chen, Y., 1984
Nature, Formation and Effects of Soil Crusts Formed by Water Drop Impact.
Geoderma v33 pp135-155

Tardieu, F., 1988a
Analysis of the Spatial Variability in Maize Root Density 2. Distances Between Roots.
Plant Soil v107 pp267-272

Tardieu, F., 1988b

Analysis of the Spatial Variability of Maize Root Density 3. Effect of Wheel Compaction on Water Extraction.
Plant Soil v109 pp257-262

Taylor, H. M., and Klepper, B., 1973
Rooting Density and Water Extraction Patterns for Corn (*Zea Mays* L.).
Agron J v65 pp965-968

Taylor, H. M., and Klepper, B., 1974
Water Relations of Cotton 1. Root Growth and Water Use as Related to Top Growth and Soil Water Content.
Agron J v66 pp584-588

Taylor, H. M., and Klepper, B., 1975
Water Uptake by Cotton Root Systems: An Examination of Assumptions in the Single Root Model.
Soil Sci v120 pp57-67

Thom, A. S., 1975
Momentum, Mass and Heat Exchange of Plant Communities: Vegetation and the Atmosphere (Ed Monteith, J. L.).
Academic Press v1 pp57-111

Tinker, P. B., 1976
Roots and Water: Transport of Water to Plant Roots in Soil.
Phil Trans Roy Soc Lond Ser B v273 pp445-461

Tompson, A. F. B., and Gray, W. G., 1986a
A Second Order Approach for the Modelling of Dispersive Transport in Porous Media 1. Theoretical Development.
Water Res Res v22 pp591-599

Tompson, A. F. B., and Gray, W. G., 1986b
A Second Order Approach for the Modelling of Dispersive Transport in Porous Media 2. Application to Solute Motion in Pipes and Capillary Tubes.
Water Res Res v22

Topp, C. G., 1969
Soil Water Hysteresis Measured in a Sandy Loam Compared with the Hysteretic Domain Model.
Soil Sci Soc Am Proc v33 pp643-651

Topp, G. C., 1971
Soil Water Hysteresis in Silt Loam and Clay Loam Soils.
Water Res Res v7 pp914-920

Touma, J., Vachaud, G., and Parlange, J. -Y., 1984
Air and Water Flow in a Sealed, Ponded Vertical Soil Column: Experiment and Model.
Soil Sci v137 pp181-187

Tricker, A. S., 1981
Spatial and Temporal Patterns of Infiltration.
Jnl Hydrol v49 pp261-277

Trouse, A. C., 1971
Soil Conditions as they Affect Plant Establishment,

Root Development and Yield (B) Effect of Soil Moisture on Plant Activities in Compaction of Agricultural Soils (Ed Barnes, K. K. et al)
Am Soc Agric Eng pp241-252

Vachaud, G., and Thony, J. -L., 1971
Hysteresis During Infiltration and Redistribution in a Soil Column at Different Initial Water Contents.
Water Res Res v7 pp111-127

Vincent, P. J., and Clarke, J. V., 1982
Dyestuff Penetration in Soils at Vegetation Boundaries: The Effect of the Canopy.
Jnl Hydrol v59 pp149-160

Virgo, K. J., 1981
Observations of Cracking in Somali Vertisols.
Soil Sci v131 pp60-61

Vos, J., and Groenwold, 1986
Root Growth of Potato Crops on a Marine-Clay Soil.
Plant Soil v94 pp17-33

Walley, W. J., 1981
Estimation of Monthly Overland Flow Using a Generalized Rainfall Intensity/Duration Curve.
Unpubl Tech Note, Dept Civ Eng, Aston Uni.

Walley, W. J., 1983
Soil Moisture Models for Irrigation Management.
Proc Ham Symp IAHS Publ. No. 147 pp463-471

Walley, W. J., and Hussein, D. E. D. A., 1982
Development and Testing of a General Purpose Soil Moisture Plant Model.
Hydrol Sci J v27 pp1-17

Watson, K. K., 1959
A Note on the Field Use of Theoretically Derived Infiltration Equation.
J Geophys Res v64 pp1611-1615

Weier, T. E., Stocking, C. R., Barbour, M. G., and Rost, T. L., 1982
Botany 6th Edition.
John Wiley and Son 720pp

Welbank, P. J., Gibb, M. J., Taylor, P. J., and Williams, E. D., 1973
Root Growth of Cereal Crops.
Rep Roth Exp Stn Part 2 pp26-65

White, E. M., 1986
Longevity and Effect of Tillage-Formed Soil Surface Cracks on Water Infiltration.
J Soil Wat Cons v41 pp344-347

Wilson, L. G., and Luthin, J. N., 1963
Effect of Air Flow Ahead of the Wetting Front Infiltration.

Soil Sci v96 pp136-143

Wit, C. T. de., 1958
Transpiration and Crop Yields.
Inst. Biol. Chem. Res. Field Crops 87pp

Wood, H. C., 1982
Neutron Probe Project
Unpubl. Final Yr Project. Univ. Aston UK

Yang, S. J., and Jong, E. de., 1972
Effect of Aerial Environment and Soil Water Potential on the Transpiration and Energy Status of Water in Wheat Plants.
Agron J v61 pp574-578

Yappa, L. G. G., Fritton, D. D., and Willatt, S. T., 1988
Effect of Soil Strength on Root Growth under Different Water Conditions.
Plant Soil v109 pp9-16